Prepared in cooperation with the Southwest Florida Water Management District

Effects of Surface-Water and Groundwater Inflows and Outflows on the Hydrology of the Tsala Apopka Lake Basin in Citrus County, Florida

Scientific Investigations Report 2018–5055

U.S. Department of the Interior
U.S. Geological Survey

Cover. Top: Shinn Ditch. Bottom left: Lake Henderson. Bottom right: Moccasin Slough. Photos by William S. McBride.

Effects of Surface-Water and Groundwater Inflows and Outflows on the Hydrology of the Tsala Apopka Lake Basin in Citrus County, Florida

By Nicasio Sepúlveda, Mark Fulkerson, Ron Basso, and Patrick J. Ryan

Prepared in cooperation with the Southwest Florida Water Management District

Scientific Investigations Report 2018–5055

U.S. Department of the Interior
U.S. Geological Survey

U.S. Department of the Interior
RYAN K. ZINKE, Secretary

U.S. Geological Survey
James F. Reilly II, Director

U.S. Geological Survey, Reston, Virginia: 2018

For more information on the USGS—the Federal source for science about the Earth, its natural and living resources, natural hazards, and the environment—visit https://www.usgs.gov or call 1–888–ASK–USGS.

For an overview of USGS information products, including maps, imagery, and publications, visit https://store.usgs.gov.

Any use of trade, firm, or product names is for descriptive purposes only and does not imply endorsement by the U.S. Government.

Although this information product, for the most part, is in the public domain, it also may contain copyrighted materials as noted in the text. Permission to reproduce copyrighted items must be secured from the copyright owner.

Suggested citation:
Sepúlveda, N., Fulkerson, M., Basso, R., and Ryan, P.J., 2018, Effects of surface-water and groundwater inflows and outflows on the hydrology of the Tsala Apopka Lake Basin in Citrus County, Florida: U.S. Geological Survey Scientific Investigations Report 2018–5055, 137 p., https://doi.org/10.3133/sir20185055.

ISSN 2328-0328 (online)

Contents

Abstract 1
Introduction 2
Purpose and Scope 2
Approach 2
Hydrologic Setting 4
Hydrogeology 6
Conceptual Flow System 8
Infiltration, Runoff, and Recharge 8
Regional Groundwater Flow 16
Rainfall and Evapotranspiration 19
Groundwater Pumping 19
Surface-Water and Groundwater Exchange 21
Summary of Model Results 23
Simulation of Hydrologic Changes Effected by Variations in the Hydrologic System 25
Simulating Changes in Rainfall Rates 27
Simulating Projected Increases in Groundwater Pumping Rates for 2025 and 2035 32
Simulating No Flow Through the Tsala Apopka Lake Pool Structures 44
Simulating the Removal of Inglis Dam and Inglis Bypass Spillway 53
Model Limitations 53
Summary and Conclusions 57
References Cited 58
Appendix 1. Model Construction and Calibration 60

Figures

1. Map showing the study area in west-central Florida, including the areal extent of the pools in the Tsala Apopka Lake Basin 3
2. Map showing the main pools, location of flow control structures, and lakes in the Tsala Apopka Lake Basin 5
3. Map showing the areal extent and spatial distribution of physiographic regions in the active flow model area 7
4. Chart showing relation between stratigraphic units, hydrogeologic units, and model layers in the Tsala Apopka Lake Basin 9
5. Map showing the land-surface altitude in the active flow model area 10
6. Map showing the altitude of the bottom of the surficial aquifer in the active flow model area 11
7. Map showing the thickness of the upper confining unit where present in the active flow model area 12
8. Map showing the altitude of the bottom of the upper confining unit where present in the active flow model area 13
9. Map showing the thickness of the Upper Floridan aquifer in the active flow model area 14
10. Map showing the altitude of the bottom of the active flow model area 15
11. Schematic diagram showing hydrologic features and flow processes that occur in the shallow part of the hydrologic flow system 16

12. Map showing the estimated altitude of the potentiometric surface of the Upper Floridan aquifer in the active flow model area, May 2010 hydrologic conditions 17
13. Map showing location of Upper Floridan aquifer springs simulated in the active flow model area 18
14. Map of spatial distribution of total rainfall for 2004 calculated from Next Generation Weather Radar Data in the active flow model area 20
15. Map of spatial distribution of reference evapotranspiration for 2004, calculated from Geostationary Operational Environmental Satellite data, in the active flow model area 22
16. Map of spatial distribution of total estimated actual evapotranspiration for 2004 in the active flow model area 24
17. Map of locations where groundwater pumping rates in 2004 in the active flow model area were greater or equal to 0.1 million gallons per day 26
18. Map showing location of flow and gage height streamflow-gaging stations along the Withlacoochee River and in the Tsala Apopka Lake Basin 28
19. Graph of simulated stage at Floral City pool under the RAIND and RAINI scenarios, and net daily flow through Floral City pool structures, for the 2004–12 period.....31
20. Graph of simulated stage at Inverness pool under the RAIND and RAINI scenarios, and net daily flow through Inverness pool structures, for the 2004–12 period.....31
21. Graph of simulated stage at Hernando pool under the RAIND and RAINI scenarios, and net daily flow through Hernando pool structures, for the 2004–12 period.....32
22. Map of calibrated water-table altitudes, averaged over 2004–12 hydrologic conditions, in the active flow model area.....33
23. Map of calibrated heads in the Upper Floridan aquifer, averaged over 2004–12 hydrologic conditions, in the active flow model area.....34
24. Map of simulated water-table altitudes in the active flow model area under the RAIND scenario minus calibrated altitudes for average 2004–12 hydrologic conditions.....35
25. Map of simulated heads in the Upper Floridan aquifer in the active flow model area under the RAIND scenario minus calibrated heads for average 2004–12 hydrologic conditions.....36
26. Map of simulated water-table altitudes in the active flow model area under the RAINI scenario minus calibrated altitudes for 2004–12 hydrologic conditions 37
27. Map of simulated heads in the Upper Floridan aquifer in the active flow model area under the RAINI scenario minus calibrated heads for average 2004–12 hydrologic conditions.....38
28. Graph of simulated stage at Floral City pool under the P2025 and P2035 scenarios, and net daily flow through Floral City pool structures, for the 2004–12 period.....43
29. Graph of simulated stage at Inverness pool under the P2025 and P2035 scenarios, and net daily flow through Inverness pool structures, for the 2004–12 period.....43
30. Graph of simulated stage at Hernando pool under the P2025 and P2035 scenarios, and net daily flow through Hernando pool structures, for the 2004–12 period.....44
31. Map of simulated water-table altitudes in the active flow model area under the P2025 scenario minus HSIMU altitudes.....45
32. Map of simulated heads in the Upper Floridan aquifer in the active flow model area under the P2025 scenario minus HSIMU heads.....46

33. Map of simulated water-table altitudes in the active flow model area under the P2035 scenario minus HSIMU altitudes 47
34. Map of simulated heads in the Upper Floridan aquifer in the active flow model area under the P2035 scenario minus HSIMU heads 48
35. Graph of simulated stage at Floral City pool under the NFCS scenario, and average daily rainfall over lake cells, for the 2004–12 period 49
36. Graph of simulated stage at Inverness pool under the NFCS scenario, and average daily rainfall over lake cells, for the 2004–12 period 49
37. Graph of simulated stage at Hernando pool under the NFCS scenario, and average daily rainfall over lake cells, for the 2004–12 period 50
38. Map of simulated water-table altitudes in the active flow model area under the NFCS scenario minus HSIMU altitudes 51
39. Map of simulated heads in the Upper Floridan aquifer in the active flow model area under the NFCS scenario minus HSIMU heads 52
40. Graph of simulated stage at Lake Rousseau under the NING scenario, and net daily flow through Lake Rousseau structures, 2004 to 2012 53
41. Map of simulated water-table altitudes in the active flow model area under the NING scenario minus HSIMU altitudes 54
42. Map of simulated heads in the Upper Floridan aquifer in the active flow model area under the NING scenario minus HSIMU heads 55

Tables

1. Average annual rainfall per year over active land-surface areas in the flow model 21
2. Monthly average actual to reference evapotranspiration ratios for generalized land covers in the model area 23
3. Average annual reference and estimated actual evapotranspiration rates in the active flow model area 25
4. Groundwater pumping rates from the Upper Floridan aquifer in the active flow model area, per year and per water-use category 27
5. Surface-water station name, identification number, location, type, and average measured streamflow for the 2004 to 2012 period 29
6. Lake or pool name, water-surface area, drainage area, and average measured lake or pool stage for the 2004 to 2012 period 29
7. Projected groundwater pumping rates per county for 2025 and 2035 in the active flow model area 30
8. Description of scenarios simulated using the calibrated surface-water/groundwater flow model 30
9. Simulated changes in pool stage caused by decreases and increases in rainfall from the calibrated model 30
10. Average simulated spring flows, from all stress periods from 2004 to 2012, for each spring and each simulated scenario 39
11. Average simulated streamflows and stream stages over the 2004 to 2012 period at selected streamflow-gaging stations and for each simulated scenario 41
12. Simulated annual inflows and outflows in the model area under scenarios RAINI and RAIND from 2004 to 2012 42
13. Simulated changes in pool stage caused by not allowing flow through the Tsala Apopka Lake structures 50

Conversion Factors

[inch/pound to International System of Units]

Multiply	By	To obtain
	Length	
inch (in.)	2.54	centimeter (cm)
inch (in.)	25.4	millimeter (mm)
foot (ft)	0.3048	meter (m)
mile (mi)	1.609	kilometer (km)
	Area	
square mile (mi^2)	2.590	square kilometer (km^2)
	Flow rate	
cubic foot per second (ft^3/s)	0.02832	cubic meter per second (m^3/s)
million gallons per day (Mgal/d)	0.04381	cubic meter per second (m^3/s)
inch per year (in/yr)	25.4	millimeter per year (mm/yr)
	Infiltration Rate	
inch per day (in/d)	25.4	millimeter per day (mm/d)
	Hydraulic conductivity	
foot per day (ft/d)	0.3048	meter per day (m/d)
	Transmissivity*	
foot squared per day (ft^2/d)	0.09290	meter squared per day (m^2/d)
	Specific Storage	
foot per day per foot [(ft/d)/ft]	1	meter per day per meter
inch per year per foot [(in/yr)/ft]	83.33	millimeter per year per meter [(mm/yr)/m]

Datum

Vertical coordinate information is referenced to the North American Vertical Datum of 1988 (NAVD 88).

Horizontal coordinate information is referenced to the North American Datum of 1983 (NAD 83).

Altitude, as used in this report, refers to distance above the vertical datum.

Supplemental Information

Transmissivity: The standard unit for transmissivity is cubic foot per day per square foot times foot of aquifer thickness [(ft^3/d)/ft^2]ft. In this report, the mathematically reduced form, foot squared per day (ft^2/d), is used for convenience.

Abbreviations

AET	actual evapotranspiration
BCF	Block-Centered Flow Package
DRN	MODFLOW-NWT Drain Package
ET	evapotranspiration
GHB	MODFLOW-NWT General Head Package
GIS	geographic information system
GOES	Geostationary Operational Environmental Satellite
HUF	Hydrologic Unit Flow Package
LAK7	MODFLOW-NWT Lake Package
lidar	light detection and ranging
LPF	Layer Property Flow Package
ME	mean error
NEXRAD	next generation radar
NOAA	National Oceanic and Atmospheric Administration
PEST	parameter estimation software
RET	reference evapotranspiration
RIV	River Package
RMSE	root mean square error
SFR2	MODFLOW-NWT Streamflow Routing Package
SURFK	maximum infiltration rate used by UZF1 package
SJRWMD	St. Johns River Water Management District
SRWMD	Suwannee River Water Management District
SWFWMD	Southwest Florida Water Management District
SWR	Surface-Water Routing Package
UPW	Upstream Weighting Package
USGS	U.S. Geological Survey
UZF1	MODFLOW-NWT Unsaturated Zone Flow Package
VKS	saturated vertical hydraulic conductivity of the unsaturated zone

Effects of Surface-Water and Groundwater Inflows and Outflows on the Hydrology of the Tsala Apopka Lake Basin in Citrus County, Florida

By Nicasio Sepúlveda,[1] Mark Fulkerson,[2] Ron Basso,[2] and Patrick J. Ryan[1]

Abstract

The U.S. Geological Survey, in cooperation with the Southwest Florida Water Management District, initiated a study to quantify the inflows and outflows in the Floral City, Inverness, and Hernando pools of the Tsala Apopka Lake Basin in Citrus County, Florida. This study assesses hydrologic changes in pool stages, groundwater levels, spring flows, and streamflows caused by the diversion of streamflow from the Withlacoochee River to the Tsala Apopka Lake Basin through water-control structures. A surface-water/groundwater flow model was developed using hydraulic parameters for lakes, streams, the unsaturated zone, and the underlying surficial and Upper Floridan aquifers estimated using an inverse modeling calibration technique. After calibration, the model was used to assess the relation between inflows and outflows in the Tsala Apopka Lake Basin and changes in pool stages.

Simulation results using the calibrated surface-water/groundwater flow model showed that leakage rates from the pools to the Upper Floridan aquifer were largest at the deep lake cells and that these leakage rates to the Upper Floridan aquifer were the highest in the model area. Downward leakage to the Upper Floridan aquifer occurred beneath most of the extent of the Floral City, Inverness, and Hernando pools. These leakage rates depended on the lakebed leakance and the difference between lake stages and heads in the Upper Floridan aquifer. Leakage rates were higher for the Floral City pool than for the Inverness pool, and higher for the Inverness pool than for the Hernando pool. Lakebed leakance was higher for the Floral City pool than for the Hernando pool, and higher for the Hernando pool than for the Inverness pool.

Simulation results showed that the average recharge rate to the surficial aquifer was 10.3 inches per year for the 2004 to 2012 simulation period. Areas that recharge the surficial aquifer covered about 86 percent of the model area. Simulations identified areas along segments of the Withlacoochee River and within land-surface depressions that receive water from the surficial aquifer. Recharge rates were largest in physiographic regions having a deep water table. Simulated heads in the Upper Floridan aquifer indicated the general flow directions in the active flow model area were from the northeast toward the southwest and then westward toward the coast, and from the southeast toward the northwest and then westward toward the coast, consistent with flow directions inferred from the estimated potentiometric surface map for May 2010. The largest inflow in the water budget of the Upper Floridan aquifer was downward leakage from the overlying hydrogeologic unit. The largest outflow in the water budget of the Upper Floridan aquifer was spring flow.

The calibrated surface-water and groundwater flow model was used to simulate hydrologic scenarios that included changes in rainfall rates, projected increases in groundwater pumping rates for 2025 and 2035, no flow for the 2004–12 period through the eight water-control structures in the Tsala Apopka Lake Basin, and the removal of the Inglis Dam and the Inglis Bypass Spillway on Lake Rousseau. Scenario simulation results were compared to annual average calibrated water levels and flows from 2004 to 2012. Simulated declines in the Tsala Apopka Lake pool stages under the 10-percent lower rainfall scenario were about 0.8, 0.3, and 1.3 feet (ft) for the Floral City, Inverness, and Hernando pools, respectively. Simulated groundwater levels under the same scenario declined up to 5.4 ft in the surficial aquifer and up to 2.9 ft in the Upper Floridan aquifer. Under the projected increases in groundwater pumping rates for 2035 that represented an increase of 36 percent from average 2004 to 2012 pumping rates, the simulated declines in the Floral City, Inverness, and Hernando pool stages were, in downstream order, 0.02, 0.06, and 0.04 ft. The largest drawdown under the projected increases in groundwater pumping rates for 2035 was 2.1 ft in the surficial aquifer and about 1.8 ft in the Upper Floridan aquifer. A scenario of decreased rainfall by 10 percent caused

[1]U.S. Geological Survey.

[2]Southwest Florida Water Management District, Brooksville, Fla.

greater declines in water levels and pool stages than projected increases in groundwater pumping rates. The simulation with no flow through the eight Tsala Apopka Lake water-control structures resulted in simulated declines in average pool stage of 1.8, 1.9, and 0.5 ft in the Floral City, Inverness, and Hernando pools, respectively. The simulated removal of the two water-control structures in Lake Rousseau caused flow to increase at Rainbow Springs by 28 cubic feet per second, an increase of 4.7 percent from the average calibrated flow for 2004 to 2012.

Introduction

The Tsala Apopka Lake Basin in Citrus County, Florida (fig. 1), is a hydrologic feature composed of lakes and ponds interconnected by wetlands and swamps, and interspersed with woodlands and low-density residential areas. Water levels throughout the Tsala Apopka Lake Basin are managed by the Southwest Florida Water Management District (SWFWMD) to balance recreation and navigation with flood protection using a series of water-control structures. Natural water loss by evapotranspiration (ET) and a strong hydraulic connection between surface water and groundwater in the area (HydroGeoLogic, 2013; McBride and others, 2017) cause a daily decrease in lake levels that is only offset by rainfall or river inflows.

Although increased water conservation and slower population growth have caused groundwater use to decline over the last 10 years in Citrus County, its population is anticipated to continue growing (Citrus County, 1997) and thereby increase the demand for water supply (Citrus County Geographic Resources and Community Planning Division, 2013), which is primarily from groundwater sources (Citrus County Board of County Commissioners, 2017). Stresses to the groundwater system from increased groundwater pumping rates could locally lower the water table, which may result in lower water levels in the Tsala Apopka Lake Basin's lakes, rivers, and wetlands. To more efficiently manage lake levels in the basin, the interaction between the surface-water and groundwater must be evaluated, as well as how management activities affect the hydrologic system.

To address the need to evaluate the hydrologic system in the Tsala Apopka Lake Basin, the U.S. Geological Survey (USGS), in cooperation with the SWFWMD, began a study in 2008 to (1) estimate the water budget for the Tsala Apopka Lake Basin, (2) evaluate the hydraulic connection between the Tsala Apopka Lake Basin and underlying Upper Floridan aquifer, and (3) assess the effects of potential changes in hydrologic inflows and outflows, such as rainfall changes, structural operations/diversions, and projected increases in groundwater pumping rates, on the hydrology of the Tsala Apopka Lake Basin. As part of this study, an analytical water budget was developed for the Tsala Apopka Lake Basin (McBride and others, 2017).

Purpose and Scope

The purpose of this report is to present an evaluation of (1) the effects of changes in the inflows and outflows on the hydrology of the Tsala Apopka Lake Basin and (2) the hydraulic connection between the basin and the underlying Floridan aquifer. To this end, the report documents the use of a surface-water/groundwater flow model of the Tsala Apopka Lake Basin to evaluate (1) fluxes between the lakes and groundwater for various hydrologic conditions; and (2) the effects of rainfall rates, changes in flows through the structures, and groundwater pumping rates on the hydrology of the Tsala Apopka Lake Basin.

This report documents the simulated water exchanges (1) between the lakes and the surficial aquifer, (2) between the surficial aquifer and the upper confining unit, (3) between the upper confining unit and the confined Upper Floridan aquifer, and (4) between Tsala Apopka Lake and the unconfined Upper Floridan aquifer. Results of simulated lake stages, water levels in the surficial and Upper Floridan aquifers, spring flows, and streamflows are presented for scenarios that represent changes in surface-water and groundwater inflows and outflows in the Tsala Apopka Lake Basin. Model limitations are discussed to illustrate appropriate use of the model. Model construction, calibration, and fit to observed conditions are described in Appendix 1. Datasets for the calibrated model and scenarios discussed herein are provided in Sepúlveda (2018).

Approach

A surface-water/groundwater flow model was developed using MODFLOW-NWT and associated packages (Appendix 1) to simulate historical lake stages, water levels in the surficial and Upper Floridan aquifers, spring flows, and streamflows. Model scenarios were constructed to simulate hydrologic impacts on the Tsala Apopka Lake Basin caused by (1) changes in rainfall, (2) increases in groundwater pumping rates, (3) changes in flows through the water-control structures located in the Tsala Apopka Lake Basin, and (4) the removal of a water-control structure outside the Tsala Apopka Lake Basin. The numerical model accounts for surface-water flow, groundwater flow, groundwater pumping rates, the partitioning of rainfall into infiltration and surface runoff, ET, the routing of infiltration in the unsaturated zone and the resulting recharge to the surficial aquifer, and recharge and discharge from lakes and streams. The model was initially calibrated using hydrologic data collected during 2004, and the resulting estimated parameters were then refined to simulate historical hydrologic conditions for the 2004 to 2012 period.

The surface-water/groundwater flow model presented in this report draws from previous studies to (1) estimate annual water budget flows, (2) refine the distribution of hydraulic parameters from existing models that include the Tsala Apopka Lake Basin (Sepúlveda, 2002; HydroGeoLogic, 2013), (3) quantify the flows between the pools in Tsala Apopka Lake

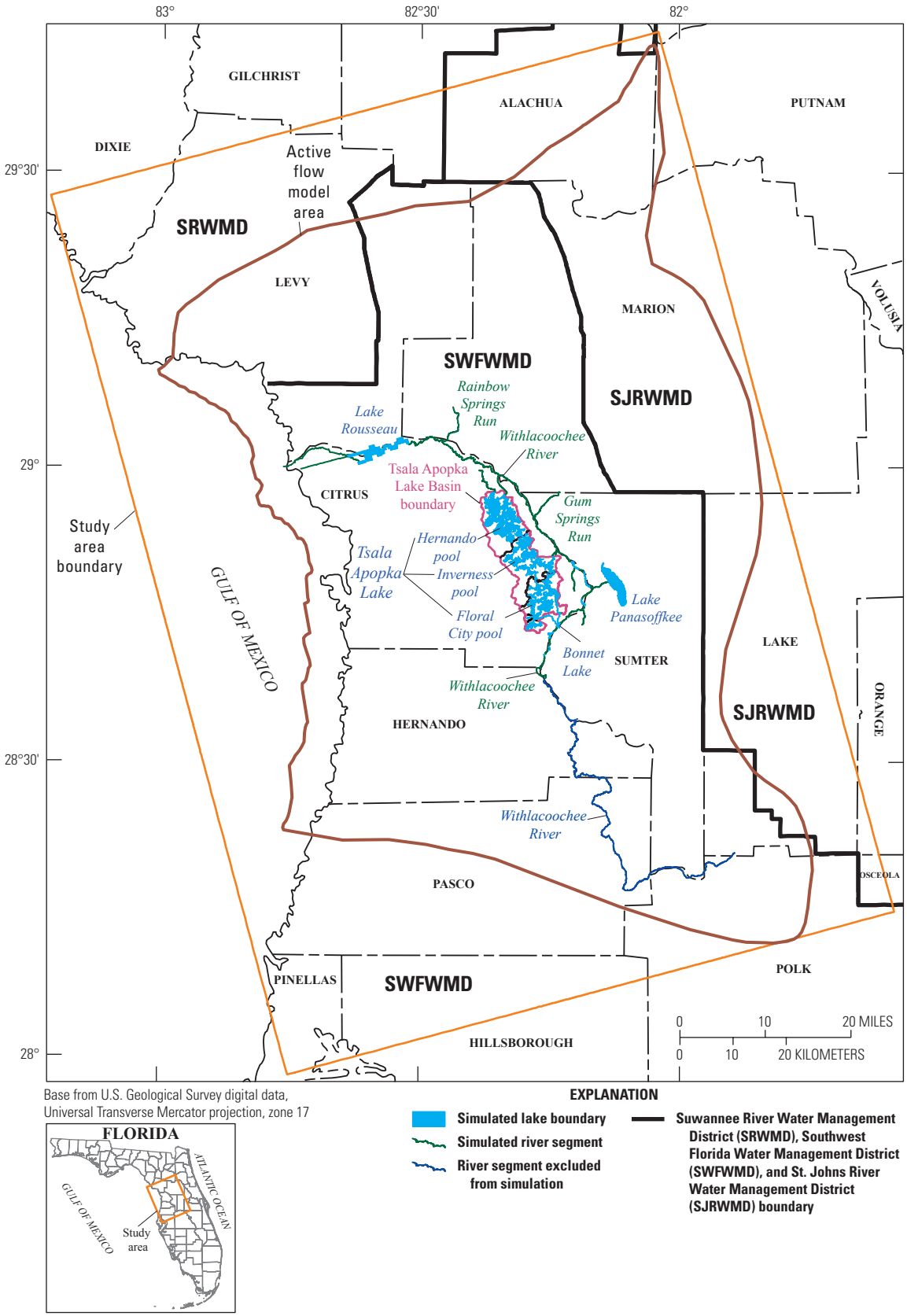

Figure 1. Study area in west-central Florida, including the areal extent of the pools in the Tsala Apopka Lake Basin.

and the underlying aquifer, and (4) consolidate the model calibration strategies using an inverse modeling approach.

The model was used to simulate (1) changes in lake stages when no flow through the structures was allowed, (2) the effects of changes in rainfall rates and increases in groundwater pumping rates on lake stages and spring flows, and (3) the effects that removing a water-control structure on the Withlacoochee River has on the flow of a spring located upstream. The model is designed to capture annual trends in lake stages, spring flows, and water levels during the 2004 to 2012 calibration period. The higher model grid resolution used near the Tsala Apopka Lake Basin, compared to the coarser grid resolution farther away, limits the model's capability to accurately assess the effects of changes in rainfall and increases in groundwater pumping rates on the flow system distal to the Tsala Apopka Lake Basin. Uncertainty in the spatial distribution of recharge and hydraulic conductivity results in a corresponding uncertainty in the simulated stages, heads, and flows.

McBride and others (2017) derived annual water budgets for the Tsala Apopka Lake Basin that served as general guidelines to develop a numerical tool that simulates flows between the Tsala Apopka Lake Basin and the surficial aquifer. McBride and others (2017) delineated the Tsala Apopka Lake Basin as the extent of the flooded area at the maximum stage of the lake in 2004–12 plus 0.5 foot (ft) additional land elevation, which is a different delineation of the Tsala Apopka Lake Basin than used in this report, where all areas with surface runoff draining to Tsala Apopka Lake were considered part of the Tsala Apopka Lake Basin. Leakage rates calculated by McBride and others (2017) were based on a control volume that included both inundated and non-inundated areas of the lake pools, while lake pools in this study refer to the open water-surface lake area only. McBride and others (2017) showed that rainfall is the largest water inflow, that evapotranspiration is the largest water outflow in the Tsala Apopka Lake Basin, and also estimated the potential maximum and minimum downward leakage rates from Tsala Apopka Lake to the underlying aquifer. Their leakage rate estimates were used as general guidelines to simulate the hydraulic interaction between Tsala Apopka Lake and the underlying aquifer.

Although there are model limitations in the conceptualization of the spatial and temporal resolution of rainfall and the spatial resolution of hydraulic parameters to accurately represent field conditions, the model simulations can be used to better understand how to manage water resources by analyzing the results of scenarios that could be costly or impossible to implement. A better understanding of the hydrologic system can be achieved by analyzing how (1) changes in flows through structures affect leakage rate changes from a lake to the underlying aquifer; (2) changes in downward leakage from a lake to the underlying aquifer affect spring flows along the coast of Citrus and Hernando Counties; and (3) increases in projected groundwater pumping rates affect lake stages.

Hydrologic Setting

The Tsala Apopka Lake Basin is divided into pools based on the location of structures that control south-to-north, downgradient flow (fig. 2). The three main pools of Tsala Apopka Lake are Floral City, Inverness, and Hernando. The smaller pools of Lake Consuella and Bradley Lake, although part of the Tsala Apopka Lake Basin, are at times hydraulically separated from Tsala Apopka Lake by additional water-control structures. Channels, including both man-made canals and natural sloughs, along with the water-control structures are used by SWFWMD to help manage the stage and flow of water through the Tsala Apopka Lake pools. The SWFWMD maintains, in downstream order and from south to north, a higher stage in the Floral City pool than in the Inverness pool and a higher stage in the Inverness pool than in the Hernando pool. These different pool stages correspond to the natural topography and development of homes and businesses along the lakeshores, which are also highest around the Floral City pool and lowest around the Hernando pool.

The Floral City, Inverness, and Hernando pools lose water by means of downward leakage to the surficial aquifer, ET, and downstream flows through water-control structures. Lake stages decline when these outflows exceed available inflows to the pools, unless balanced by rainfall. Target pool stages aimed to meet navigation and flood prevention requirements are based on the adopted minimum and guidance levels for Tsala Apopka Lake (SWFWMD, 2007). Inflows from the Withlacoochee River can occur when its stage is higher than that of the Floral City pool. These inflows are split between each pool through operation of the water-control structures according to SWFWMD's operational guidelines. If stages in the Tsala Apopka pools reach their target levels and additional uncontrolled inflow (rainfall) occurs, the structures are also used to release flow from the lakes back to the Withlacoochee River to help prevent flooding. When river inflows are not available, and lake levels are at or below their target levels, the structures are closed to conserve water in the pools. Floral City pool stage has ranged from 35.85 to 43.48 ft, during the 2004–12 period, when structures have been opened to divert flow from the Withlacoochee River to the Floral City pool. During the 2004–12 period, Inverness pool stage ranged from 34.16 to 40.02 ft when structures were opened to allow water to flow from the Floral City pool into the Inverness pool, and the Hernando pool stage ranged from 33.18 to 38.97 ft, when structures were opened to allow water to flow from the Inverness pool into the Hernando pool.

Inflow from the Withlacoochee River into the Floral City pool occurs through the Orange State and Leslie Heifner canals and is controlled by the Floral City and Leslie Heifner structures (fig. 2). Downstream flow from the Floral City pool to the Inverness pool is controlled by the Moccasin Slough and the Golf Course structures (fig. 2). Water flowing through the Golf Course structure is directed to the Inverness pool through the Golf Course canal. Water flowing through the Moccasin Slough structure enters the shallow pool area (marsh) of the

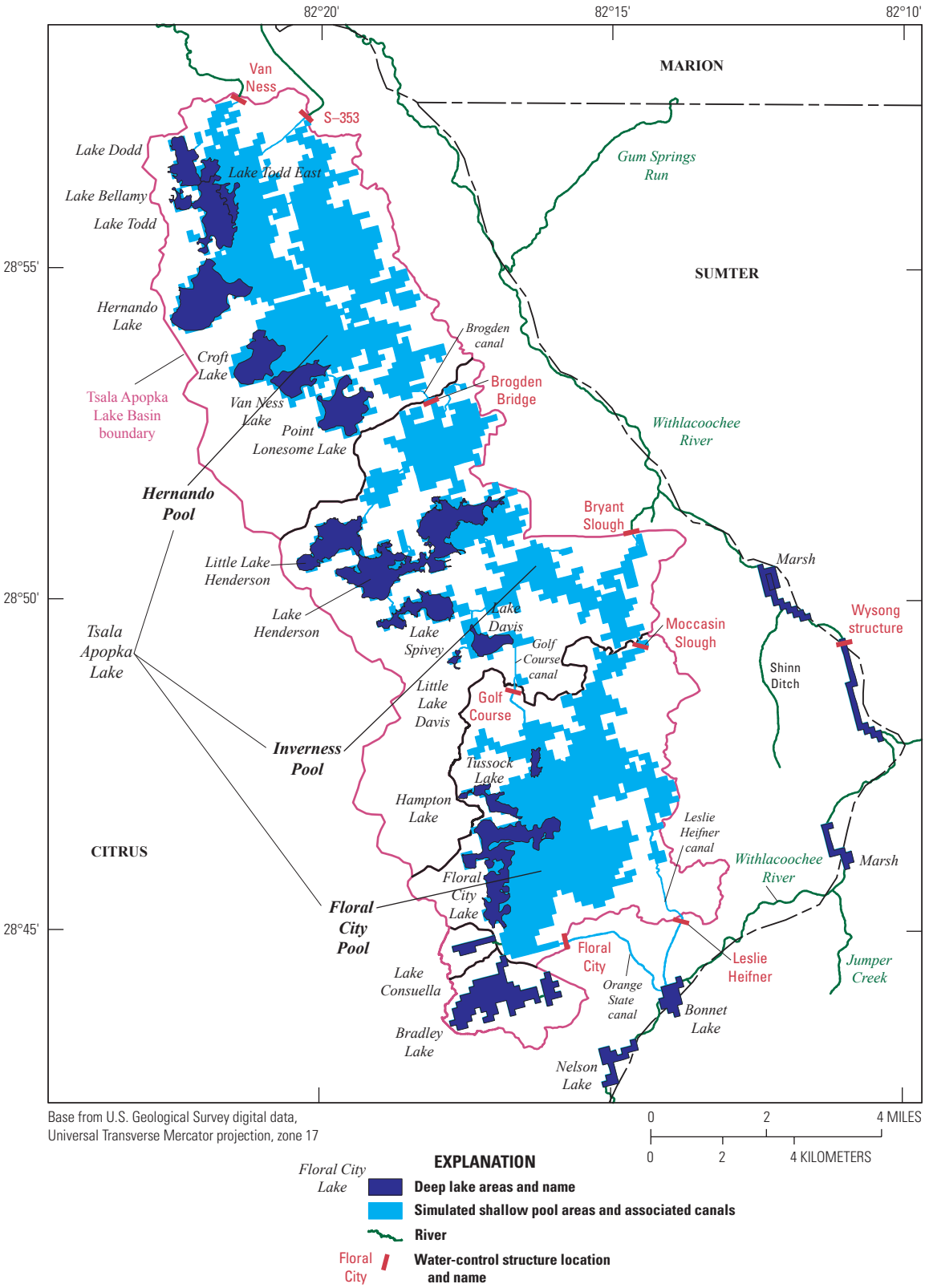

Figure 2. Main pools, location of flow control structures, and lakes in the Tsala Apopka Lake Basin.

Inverness pool (fig. 2). The Brogden Bridge structure is the primary means of controlling flow from the Inverness pool to the Hernando pool. If water levels permit, the Bryant Slough structure is available to discharge excess water from the Inverness pool to the Withlacoochee River. Flow out of the Hernando pool is controlled through the S–353 or Van Ness structure. When water levels in the Hernando pool reach target levels, the Van Ness structure is opened to discharge flow to wetlands and recharge the underlying aquifer. The Van Ness structure is limited in its ability to prevent flooding in the Hernando pool because of the downstream conveyance and available wetland storage. The only flood-control structure in the Tsala Apopka Lake Basin is the S–353 structure, which is used to help maintain target water levels in the Hernando Pool and to release excess water back to the Withlacoochee River.

Several lakes within each of the three main pools have a deeper bottom than the shallow pool areas. For example, Floral City, Hampton, and Tussock Lakes (fig. 2) are the deep lakes in the Floral City pool. The total water-surface area, including deep lakes and shallow pool areas, of the Hernando pool is the largest of the three pools and that of the Floral City pool is the smallest. The lake stage in any pool quickly equilibrates throughout the entire pool area, making it the same for the deep lakes and the shallow pool areas, when water levels are high enough to connect the lakes to the shallow areas. When water levels are low, isolated pools can be present in the shallow pool areas when they are not connected to the deep lakes.

Water in the Withlacoochee River generally flows northward east of the Tsala Apopka Lake Basin (fig. 1) and then westward into the Gulf of Mexico. The Withlacoochee River recharges the underlying surficial aquifer when the river stage is above the water table, common in sections of the river upstream of Bonnet Lake based on stage data. The aquifer discharges to the Withlacoochee River when the river stage is below the water table, which is more prevalent downstream from Bonnet Lake (fig. 1).

Although they are hydraulically connected, Tsala Apopka Lake and the underlying aquifer system have typically been studied as separate resources. Interactions between groundwater and surface water in the study area result in a single active flow system. Previous studies (Sepúlveda, 2002; HydroGeoLogic, 2013; McBride and others, 2017) indicate that a strong hydraulic connection exists through numerous karst features that facilitate the exchange of water between the surface and the underlying Upper Floridan aquifer. This hydraulic connection creates a challenge for water managers to maintain desirable lake stages in the three main pools of Tsala Apopka Lake. Periods of low rainfall or increased withdrawals from projected population growth may place additional stress on the groundwater system by lowering the water table, likely resulting in lower water levels in the basin's lakes, rivers, and wetlands. Reliable data characterizing the hydraulic connection between the lakes and wetlands and the underlying aquifer are scarce. A better assessment of flows between Tsala Apopka Lake and the underlying aquifer could provide a better understanding of the overall interaction of inflows and outflows between the surface water and groundwater of Tsala Apopka Lake. Such an assessment could benefit from estimates of (1) the lakebed leakance and thickness in each pool, (2) the spatial distribution of differences between lake stage and the head in the underlying aquifer, (3) the spatial distribution of actual evapotranspiration (AET) rates, and (4) the coupling of surface-water flow and groundwater flow.

The physiographic regions in the model area, classified by White (1970) on the basis of natural features and land-surface altitude gradients, strongly influence the hydrology of the Tsala Apopka Lake Basin by affecting the time required for water infiltration to recharge the surficial or the Upper Floridan aquifer and the spatial pattern of that recharge. The Tsala Apopka Lake Basin is located in the Tsala Apopka Plain, which is east of the Brooksville Ridge and west of the Western Valley (fig. 3). The Brooksville Ridge, Cotton Plant Ridge, Fairfield Hills, Ocala Hill, and Sumter Upland physiographic regions are characterized by higher land surface altitudes than the surrounding regions and an unsaturated zone thickness, or depth to water-table altitude, greater than 50 ft. A thick unsaturated zone generally results in lower evapotranspiration and, therefore, higher recharge rates than physiographic regions having a water table near land surface. The Central Valley, Coastal Swamps, North Gulf Coastal Lowlands, Tsala Apopka Plain, and Western Valley (fig. 3) physiographic regions are characterized by lower land surface altitude than the surrounding regions and an unsaturated zone of generally less than 20 ft thick, where infiltration reaches the water table faster than in regions having a thicker unsaturated zone. Although groundwater recharge in the Tsala Apopka Plain occurs faster than in the adjacent area to the west where the Brooksville Ridge is located, shallow water-table areas with small storage receive less recharge, generate higher surface runoff, and lose more water to ET than deep water-table areas.

Physiographic regions including ridges, uplands, and hills (regions 1, 4, 6, 7, 8, 10–12 in fig. 3) generally recharge the surficial aquifer, whereas coastal swamps and lowlands (regions 3 and 9 in fig. 3) are mainly discharge areas. The surficial aquifer in the Tsala Apopka Lake Basin is recharged through vertical leakage from the lakebeds and through rainfall infiltration in areas away from the lakes. In addition to this spatial difference in recharge to the surficial aquifer, temporal differences in recharge to the surficial aquifer occur west of the Tsala Apopka Lake Basin, where the unsaturated zone in the Brooksville Ridge is thicker than that in the Tsala Apopka Plain or the Western Valley, causing infiltration in the Brooksville Ridge to reach the surficial aquifer at a later time but at a higher magnitude than in physiographic regions to the east.

Hydrogeology

Designation for the hydrogeologic units in the Tsala Apopka Lake Basin follows the regional delineation of Miller (1986). The regional hydrogeologic units in the Tsala Apopka

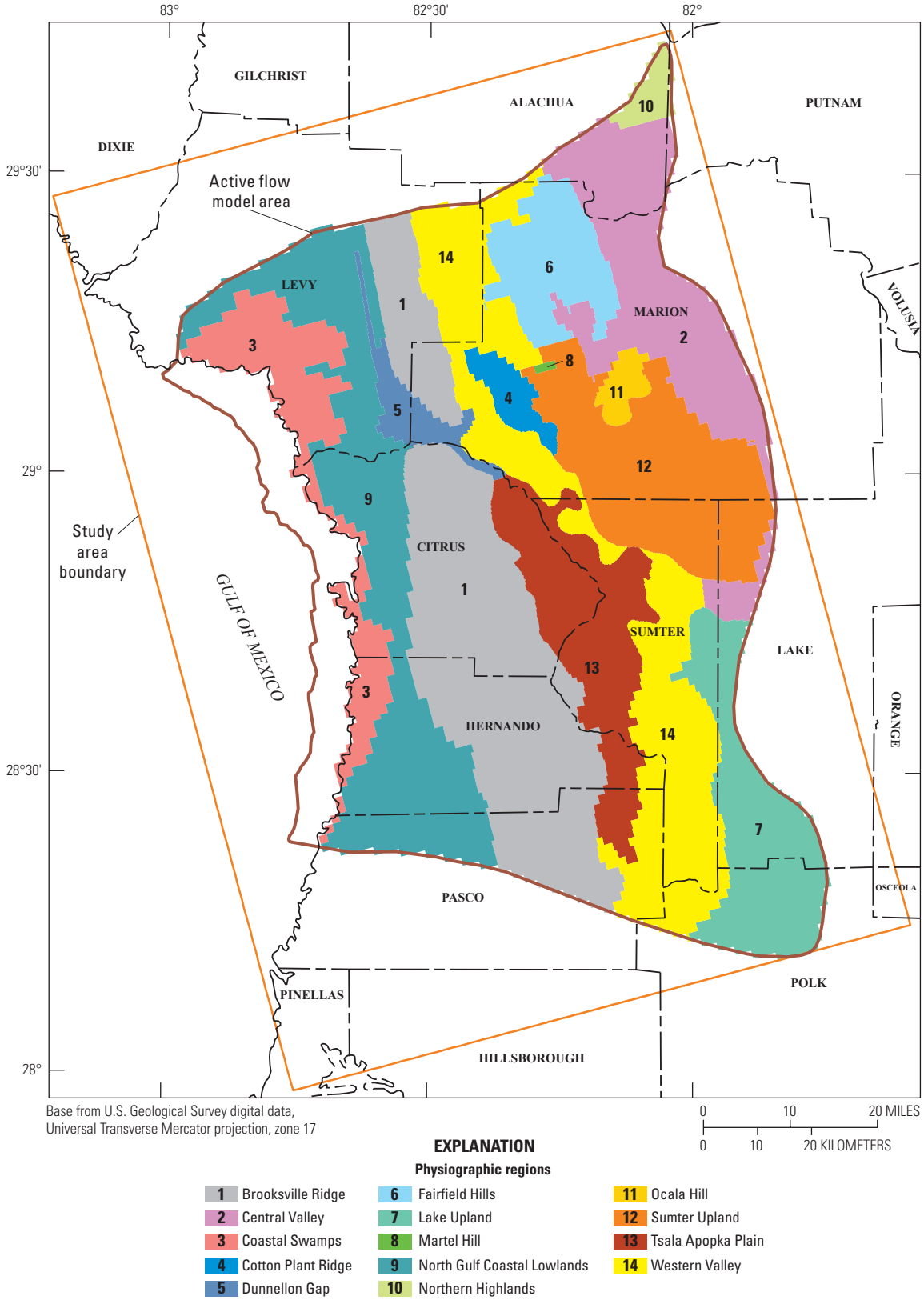

Figure 3. Areal extent and spatial distribution of physiographic regions in the active flow model area.

Lake Basin consist of the surficial aquifer, the upper confining unit, and the Upper Floridan aquifer. The surficial aquifer consists of Holocene undifferentiated, unconfined sediments of Pleistocene to Pliocene age. At land surface, and extending several tens of feet deep, are generally fine-grained quartz sands that grade into clayey sand just above the contact with limestone. A thin, sometimes absent, sandy clay layer forms the upper confining unit and overlies the limestone units of the Upper Floridan aquifer. In general, a regionally extensive surficial aquifer is not present, because the clay confining unit is thin, discontinuous, and breached by numerous karst features. Because of this geology, the Upper Floridan aquifer is unconfined over most of the area. In this unconfined setting, high infiltration soils and generally deep water-table conditions exist, with Upper Floridan aquifer water levels ranging from 10 ft to more than 50 ft below land surface except near the Withlacoochee River and Tsala Apopka Lake.

The upper confining unit, where present, consists of Miocene clay, sand, and Tertiary dolomite. The Upper Floridan aquifer consists of stratigraphic units that include the Suwannee Limestone, the Ocala Limestone, and the Avon Park Formation (fig. 4). The upper surfaces and thicknesses of the hydrogeologic units were mapped using the interpretations and data from the Northern District Model developed for the SWFWMD (HydroGeoLogic, 2013). McBride and others (2017) and HydroGeoLogic (2013) provide a more detailed description of the hydrogeology of the Tsala Apopka Lake Basin.

Land-surface altitude ranges from about -2 to 276 ft NAVD 88 (fig. 5) over the study area and was determined using light detection and ranging (lidar) data (5- by 5-ft pixels) collected under contract by the SWFWMD. These lidar data (Florida Department of Environmental Protection, 2018) were used to develop a digital model of land-surface altitude for the entire study area. Bathymetric data were collected from the open-water lakes, wetlands, and canals of Tsala Apopka Lake and incorporated within the digital model of land-surface altitude to characterize true ground altitudes below water. The processed digital model of land-surface altitude is available from SWFWMD upon request, because the large size of the file prevents the model from being permanently available online.

The altitude of the bottom of the surficial aquifer, which coincides with the top of the Upper Floridan aquifer in areas where the Upper Floridan aquifer is unconfined; ranges from about -102 to 182 ft (fig. 6). The altitude of the bottom of the surficial aquifer decreases from the southeastern and south-central sections of the active flow model area to the coastline of the Gulf of Mexico, and from the northeastern and north-central sections to the Levy County coastline.

A laterally continuous upper confining unit is present in the southern, eastern, and northeastern parts of the model area and ranges in thickness from about 9 to 192 ft (fig. 7). The upper confining unit covers 922 square miles (mi^2) of the 4,535 mi^2 extent of the Upper Floridan aquifer within the model area, making the Upper Floridan aquifer unconfined in over 80 percent of the active flow model area. The upper confining unit, absent in the Tsala Apopka Lake Basin, is the thickest in the northeastern, north-central, and southern sections of the model area. Where the upper confining unit is absent or where the thin, discontinuous clays are dissected by numerous karst openings, the surficial sands directly overlie the Upper Floridan aquifer. The altitude of the bottom of the upper confining unit ranges from about -109 to 125 ft (fig. 8). The bottom of the upper confining unit is highest in the southern section of the model area.

The Upper Floridan aquifer is the thickest and most productive hydrogeologic unit in the Tsala Apopka Lake Basin. The thickness of the Upper Floridan aquifer ranges from about 431 ft in the northeastern section to about 1,006 ft in the southeastern section of the model area (fig. 9), generally increasing in thickness from north to south within the model area. The middle confining unit underlying the Upper Floridan aquifer limits the underlying vertical flow to and from the Upper Floridan aquifer throughout the study area (HydroGeoLogic, 2013). The altitude of the bottom of the Upper Floridan aquifer slopes down from north to south (fig. 10) and from the northeastern to the west-central coastal section. The altitudes of the top and bottom of the Upper Floridan aquifer were obtained from the USGS database for the peninsular Florida groundwater flow model developed by Sepúlveda (2002).

Conceptual Flow System

In the study area, water enters the hydrologic system through rainfall, stream inflows from south and east of the study area, and groundwater inflows from east and northeast of the study area. Rainfall may infiltrate the land surface or become runoff that drains into streams or lakes. Water leaves the hydrologic system through evapotranspiration, surface-water flow into the Gulf of Mexico, and groundwater flow through the western boundary of the study area. Water is exchanged between the surface-water system and groundwater system. Surface water recharges the groundwater system by means of (1) downward leakage through the bottoms of lakes and stream reaches along the Withlacoochee River, (2) infiltration of rainfall, and (3) infiltration of return water from irrigation or septic systems. Groundwater discharges primarily (1) into stream reaches along the Withlacoochee River, (2) from wells, (3) from ET, and (4) from springs between the lakes and the gulf coast.

Infiltration, Runoff, and Recharge

One type of runoff in the Tsala Apopka Lake Basin is generated where the water table is at or near land surface, which allows a larger percentage of rainfall to become runoff compared to areas where the water table is deep. Another type of runoff is generated when the rainfall rate exceeds the infiltration rate of soil. Rainfall is partitioned at land surface into surface runoff and infiltration outside the borders of streams and lakes. Surface runoff enters lakes and streams from the surrounding drainage areas (fig. 11).

<table>
<tr><th>System</th><th colspan="2">Series / Epoch</th><th>Stratigraphic unit</th><th>Lithology</th><th>Hydrogeologic unit (Model layer)</th></tr>
<tr><td rowspan="2">Quaternary</td><td colspan="2">Holocene</td><td rowspan="2">Undifferentiated Quaternary sediments</td><td rowspan="2">Fine sand; interbedded clay, shell, limestone</td><td rowspan="4">Surficial aquifer (Layer 1 - lakes and surficial aquifer where upper confining unit exists; Layer 2 - surficial aquifer where upper confining unit does not exist)</td></tr>
<tr><td colspan="2">Pleistocene</td></tr>
<tr><td rowspan="6">Tertiary</td><td colspan="2">Pliocene</td><td colspan="2">Undifferentiated Tertiary/Quaternary sediments</td><td>Phosphatic sands, clays</td></tr>
<tr><td rowspan="3">Miocene</td><td>Upper</td><td colspan="2" rowspan="3">Hawthorn Group (undifferentiated)</td><td rowspan="3">Clay, sand, dolomite</td><td rowspan="3">Upper confining unit (Layer 2 - where this unit exists)</td></tr>
<tr><td>Middle</td><td>Coosawhatchie Formation (Hawthorn Group)</td></tr>
<tr><td>Lower</td></tr>
<tr><td colspan="2">Oligocene</td><td>Suwannee Limestone</td><td>Limestone, sandy limestone, fossiliferous</td><td rowspan="3">Upper Floridan aquifer (Layer 3)</td></tr>
<tr><td rowspan="2">Eocene</td><td>Upper</td><td>Ocala Limestone</td><td>Limestone, chalky, foraminiferal, dolomitic near bottom</td></tr>
<tr><td>Middle</td><td>Avon Park Formation</td><td>Limestone, porous, granular to chalky, fossiliferous; crystalline dolomite</td></tr>
</table>

Figure 4. Relation between stratigraphic units, hydrogeologic units, and model layers in the Tsala Apopka Lake Basin (modified from McBride and others, 2017).

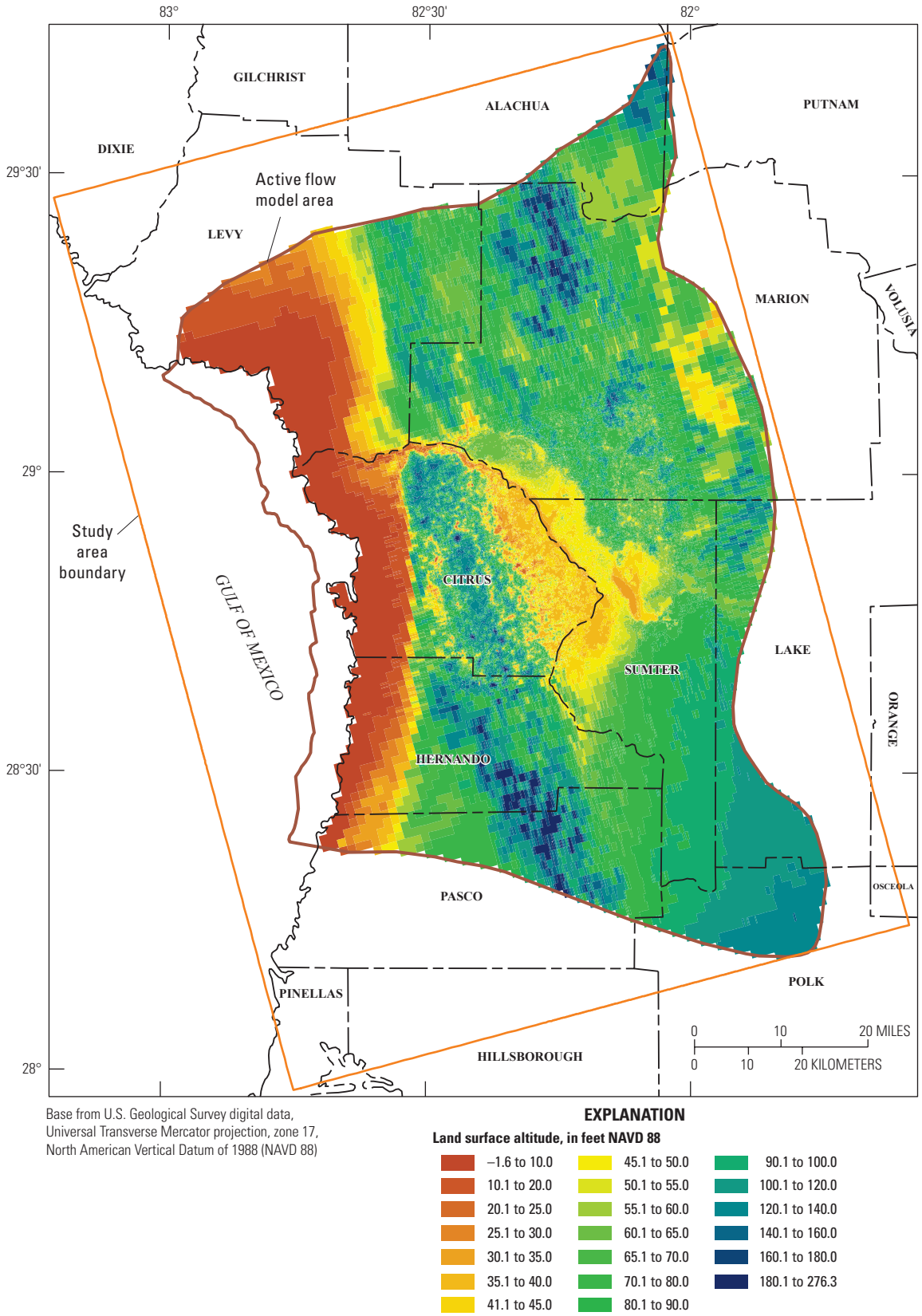

Base from U.S. Geological Survey digital data, Universal Transverse Mercator projection, zone 17, North American Vertical Datum of 1988 (NAVD 88)

Figure 5. Land-surface altitude in the active flow model area.

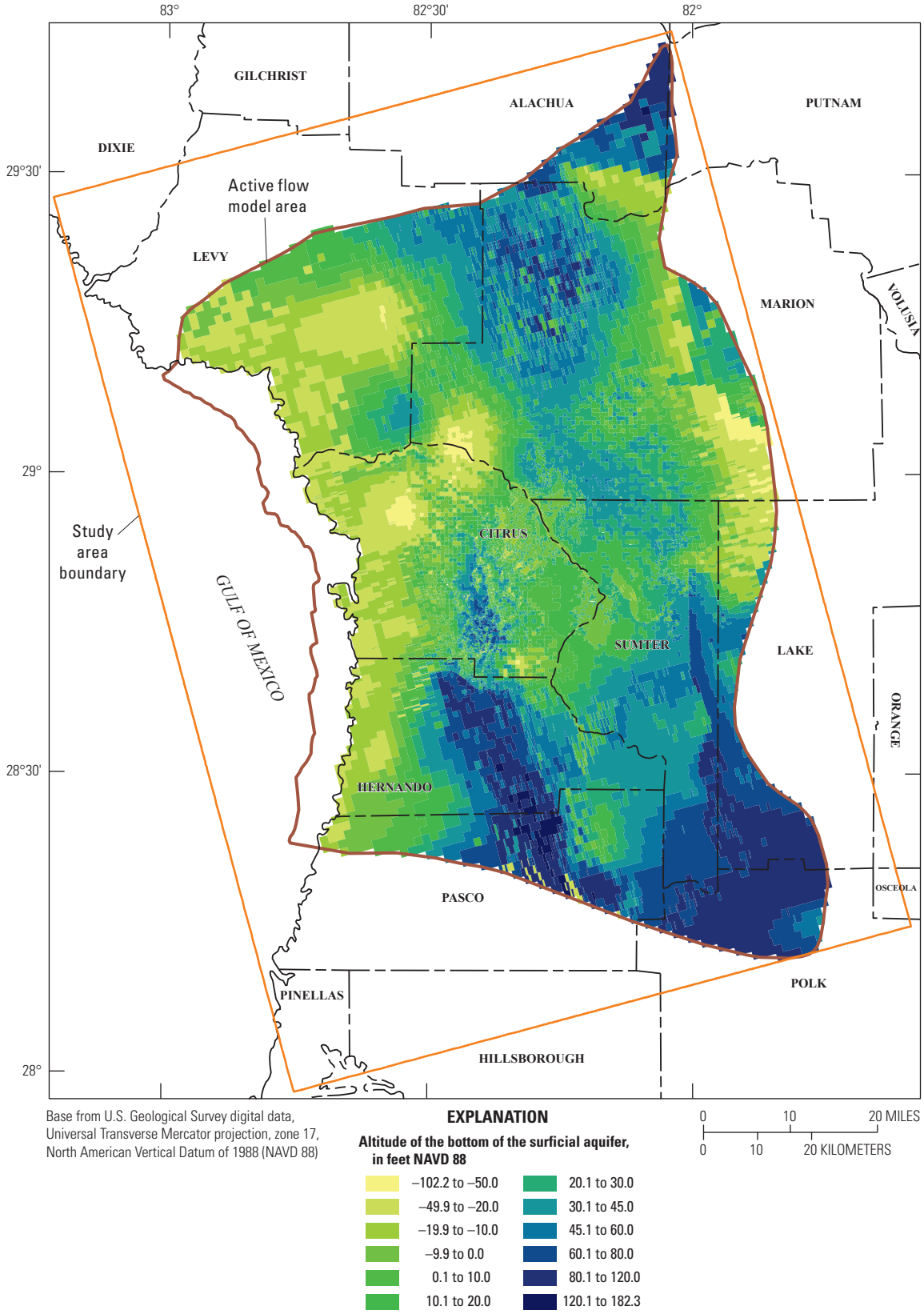

Figure 6. Altitude of the bottom of the surficial aquifer in the active flow model area.

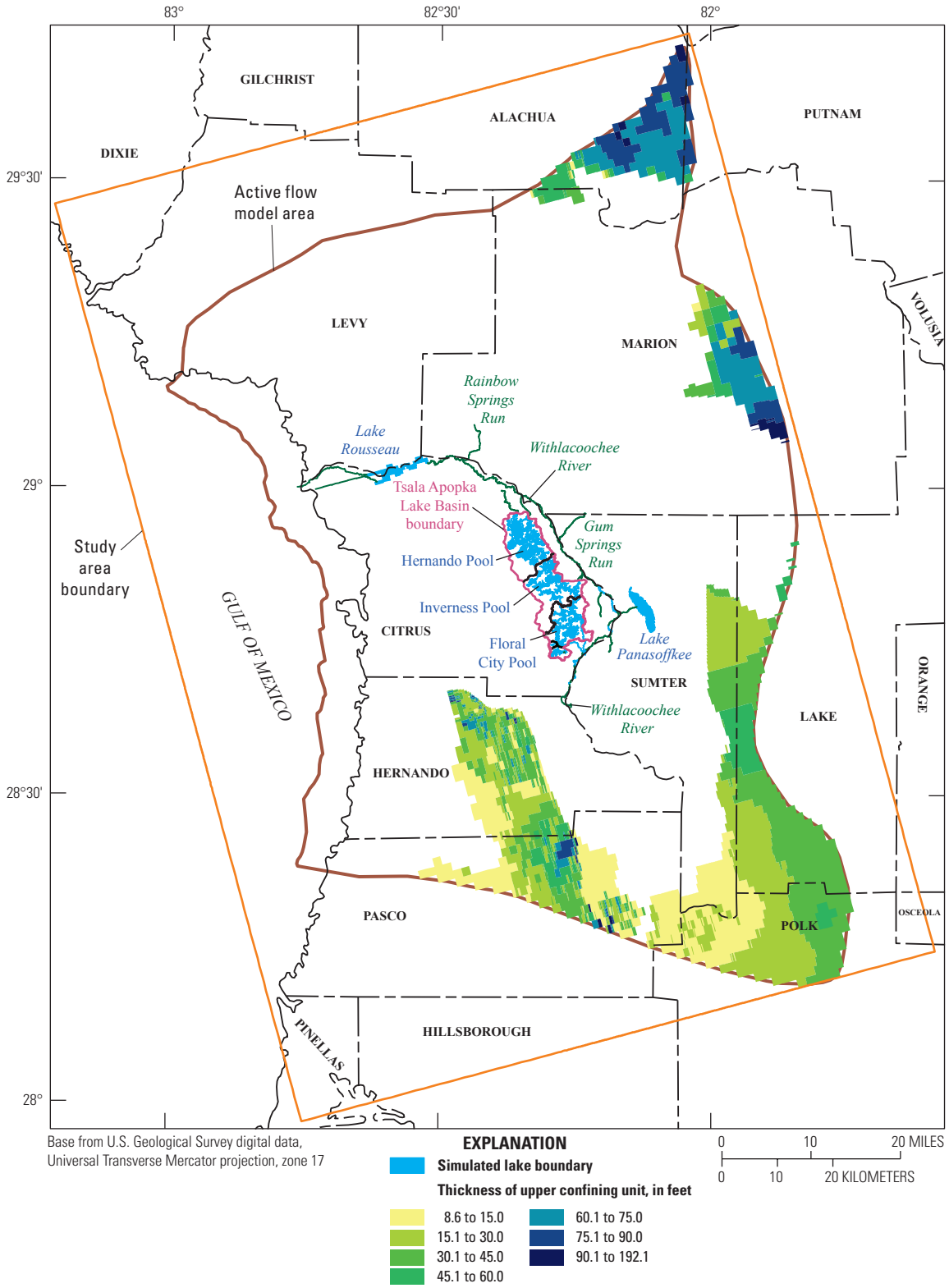

Figure 7. Thickness of the upper confining unit where present in the active flow model area.

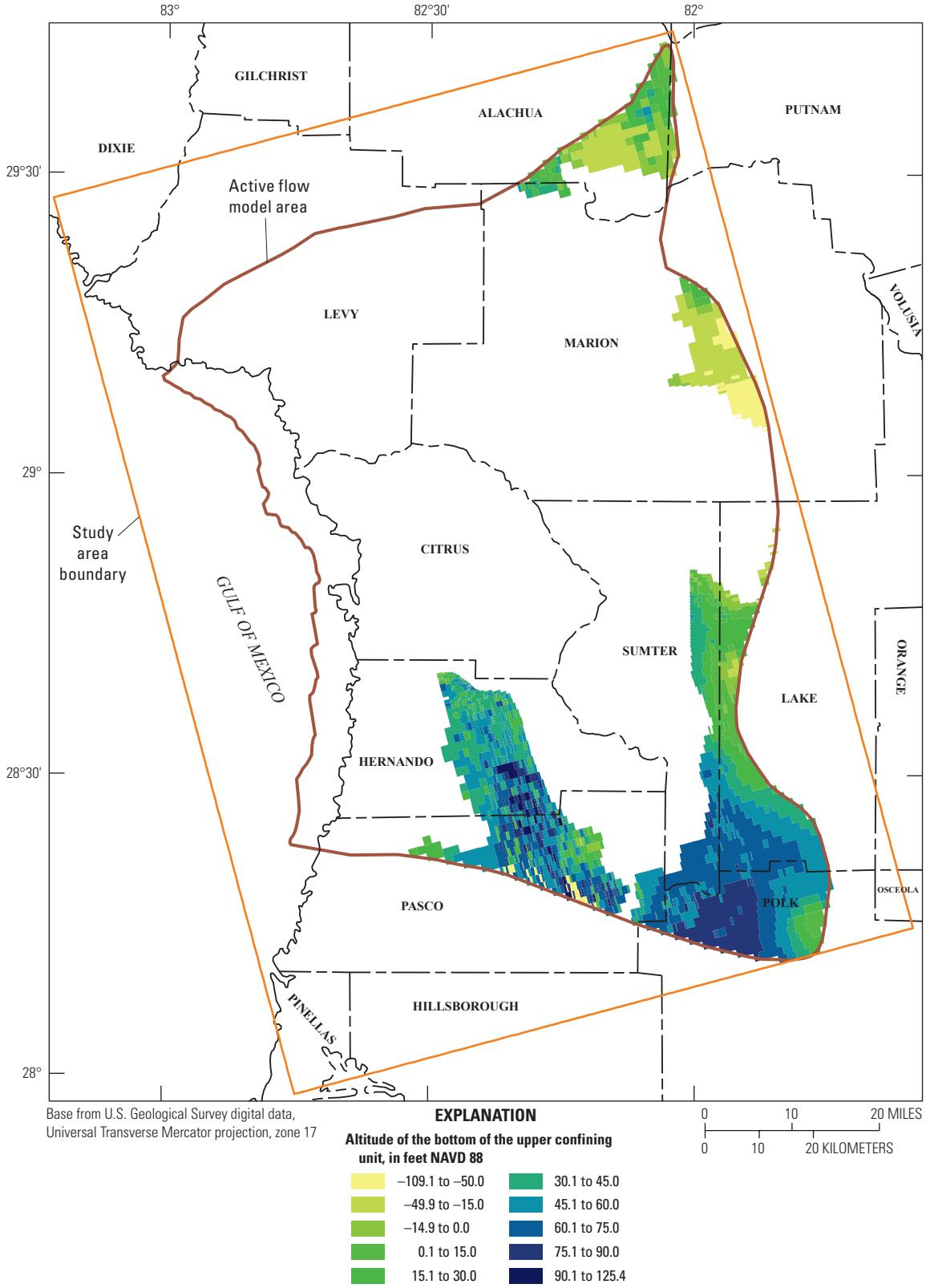

Figure 8. Altitude of the bottom of the upper confining unit where present in the active flow model area.

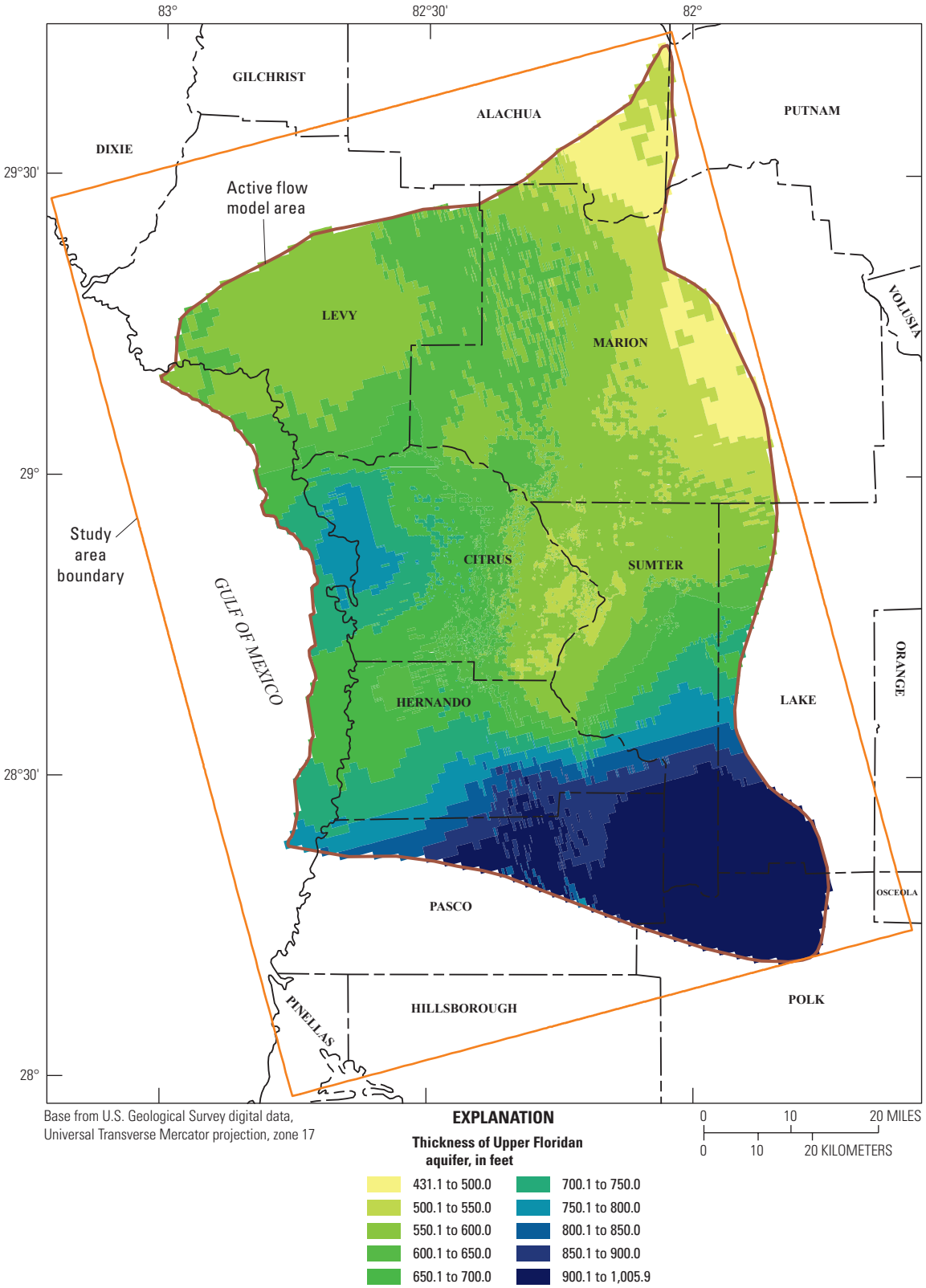

Figure 9. Thickness of the Upper Floridan aquifer in the active flow model area.

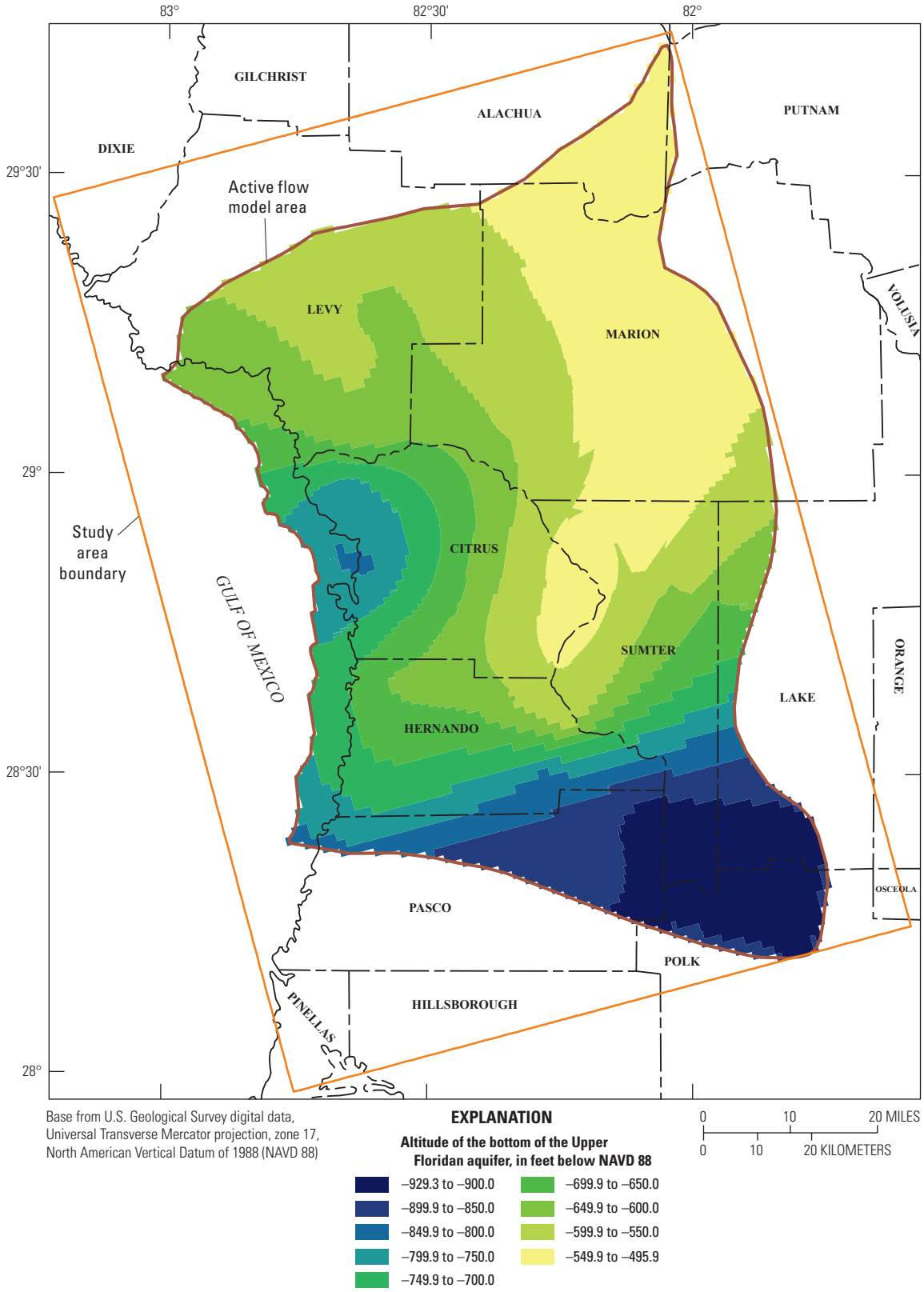

Figure 10. Altitude of the bottom of the active flow model area.

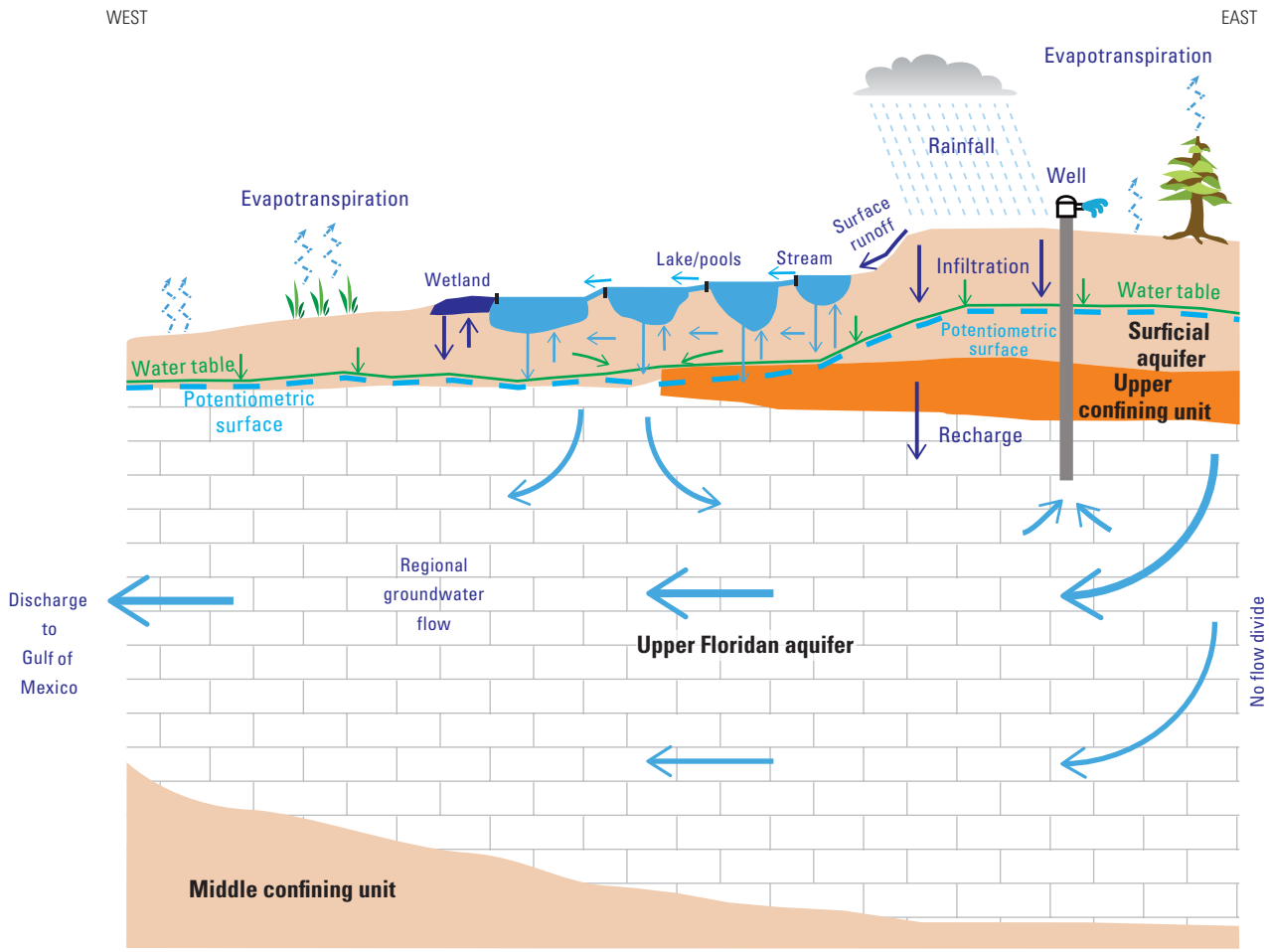

Figure 11. Hydrologic features and flow processes that occur in the shallow part of the hydrologic flow system.

After rainfall infiltrates into the unsaturated zone, ET removes water from the unsaturated zone (fig. 11), and water that is not evaporated or transpired is routed to the water table with a time lag that depends on the thickness of the unsaturated zone. Leakage from streams, lakes, and wetlands enters the surficial aquifer through the streambeds, lakebeds, or unsaturated zone when the stream, lake, or wetland stage is higher than the surrounding water table (fig. 11). Recharge and discharge areas of the Upper Floridan aquifer are determined by the directionality of the difference between the water-table altitude and the head in the Upper Floridan aquifer. Water is removed from the groundwater system through groundwater pumping, discharge to streams and lakes, ET, and spring flows.

Regional Groundwater Flow

The altitude of the potentiometric surface of the Upper Floridan aquifer was estimated for May 2010 hydrologic conditions (Kinnaman and Dixon, 2011). In the Tsala Apopka Lake Basin, the altitude of this surface ranged from near sea level to 120 ft (fig. 12), and was highest near the southeast section of the model area. The altitude of the potentiometric surface was lowest in discharge areas along the Gulf of Mexico. Groundwater in the Upper Floridan aquifer flows from the northeast toward the southwest and then west toward the coast, and from the southeast toward the northwest and then west toward the coast (fig. 12). Groundwater flows from the central parts of the model area to the coastal areas, in part, discharging to coastal Citrus and Hernando Counties (fig. 12); these coastal areas are characterized by high hydraulic conductivity in the Upper Floridan aquifer (Sepúlveda, 2002; HydroGeoLogic, 2013). The general flow pattern described here for May 2010 has been observed in potentiometric surface maps generated for the Upper Floridan aquifer in the model area for other time periods from measured heads at wells (HydroGeoLogic, 2013).

Groundwater flows from the central to coastal areas, discharging to numerous springs located near the coast and as diffuse leakage along the coast throughout the model area (fig. 13). The springs in the study area with the most complete flow measurement records during 2004 to 2012 are Silver (spring number 5 in fig. 13), Rainbow (7–11 in fig. 13), Gum (35–38 in fig. 13), Homosassa (43 in fig. 13), SE Fork Homosassa (46 in fig. 13), Chassahowitzka (57–58 in fig. 13), and Weeki Wachee Springs (81–82 in fig. 13). Silver Springs, Rainbow Springs, Weeki Wachee Springs, the Homosassa

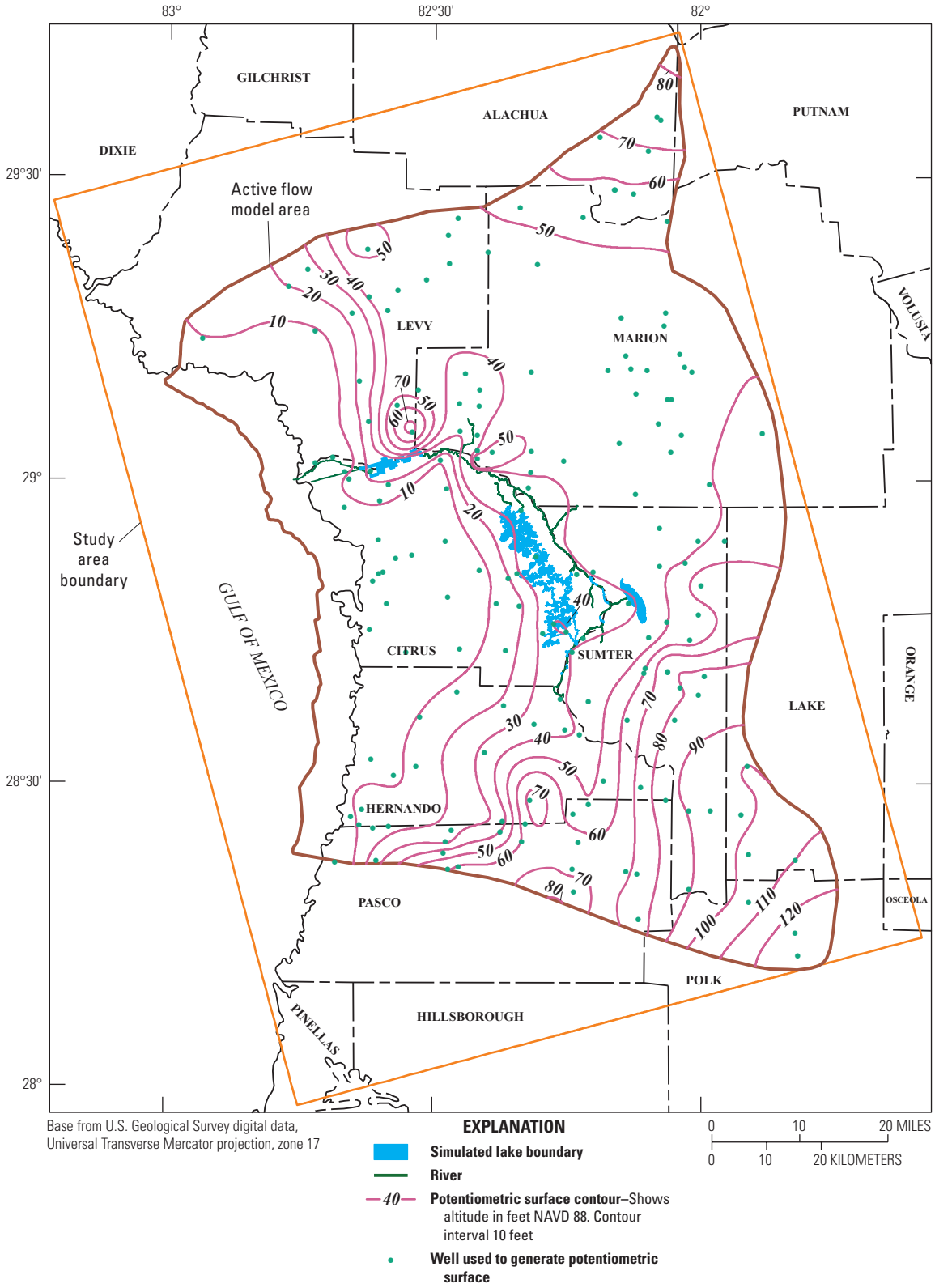

Figure 12. Estimated altitude of the potentiometric surface of the Upper Floridan aquifer in the active flow model area, May 2010 hydrologic conditions (modified from Kinnaman and Dixon, 2011).

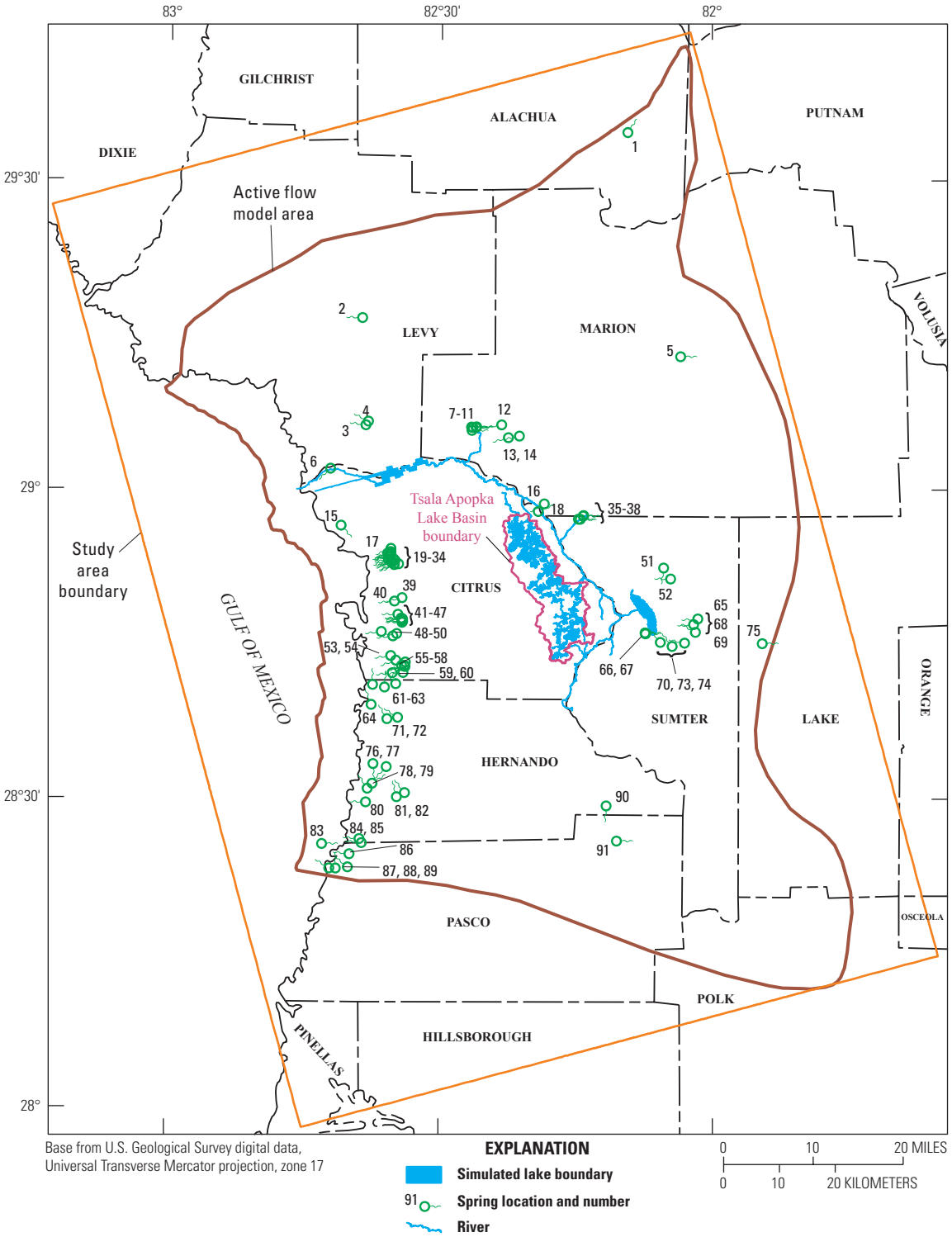

Figure 13. Location of Upper Floridan aquifer springs simulated in the active flow model area.

group, and the Chassahowitzka group are first magnitude springs, having flows equal or larger than 100 cubic feet per second (ft^3/s), whereas Gum Springs are second magnitude springs, having flows equal to or larger than 10 ft^3/s and less than 100 ft^3/s (Scott and others, 2004). Not all of the water from the Upper Floridan aquifer near the coast is discharged to coastal springs; some water is discharged to the Gulf of Mexico.

Rainfall and Evapotranspiration

Rainfall has been estimated to be the greatest annual water inflow to the hydrologic system in the model area (McBride and others, 2017). The spatial and temporal distributions of rainfall in the study area during 2004 to 2012 were obtained from National Oceanic and Atmospheric Administration (NOAA) Next Generation Weather Radar (NEXRAD) data. The methodology used to calculate the spatial distribution of NEXRAD rainfall data was presented by Hoblit and others (2003). The 2004 rainfall totals from NEXRAD varied from about 43 to 76 inches (in.) over the active flow model area (fig. 14). Rainfall totals for 2004 were lowest along the coastline and in the east-central section of the model area. Annual rainfall was averaged over the active flow model areas each year from 2004 to 2012. These annual averages show that rainfall was highest in 2004 and lowest in 2006 (table 1).

The greatest annual water loss in the model area, as documented by McBride and others (2017), occurs as ET. The USGS provides State-wide daily reference evapotranspiration (RET) coverage, at a 2-kilometer (1.24-mile) pixel resolution, computed from satellite and ground-based data (U.S. Geological Survey, 2016). The spatial variation in total RET for 2004 ranged from about 44 to 53 in.; rates generally decrease with increasing latitude and from the coastline to the northeast (fig. 15). RET was used to estimate actual ET, or AET, at sites across Florida using available measurements of RET and AET (Sepúlveda and others, 2012). The availability of these two measurements for various land cover types can be used to calculate AET to RET (or vegetation) ratios, which are used to approximate AET from RET rates for similar land cover types. Field data collected at the ET stations used to calculate AET represented a range of environmental settings, from dry areas having well-drained, sandy soils and a relatively deep water table to wetlands having poorly drained soils. Although the ET stations of Tiger Bay, Duda Farms, Blue Cypress Marsh, Reedy Lake, Lake Wales Ridge, and Orlando had unequal periods of record and were outside the study area, these ET stations provided data from areas characterized by, respectively, forest, grass, marsh, open water surface, ridge, and urban environments (Sumner, 2006; O'Reilly, 2007; Sumner and others, 2017; Sumner, 2017a, b; U.S. Geological Survey, 2017), allowing the calculation of monthly average AET to RET ratios (table 2). These ratios indicate that lakes had the largest AET to RET ratio (1.1760 in August, table 2) and ridge areas had the lowest (0.4523 in January, table 2), which agrees with the findings by McBride and others (2017). This result is expected, because a lake surface evaporation rate is typically close to the RET rate, whereas ridges are characterized by deep water tables and rapid infiltration rates that limit AET.

ET losses in the unsaturated zone and in groundwater were computed using the MODFLOW-NWT Unsaturated Zone Flow (UZF1) Package (Niswonger and others, 2006). Within this simulation framework, the simulated AET varies with water availability in the subsurface, in contrast with the AET/RET ratio approach, described in the previous paragraph, that ignores the impacts of water availability on AET. Sanford and Selnick (2013) estimated, using a water-budget method and linear regressions, that the average annual AET rate for Citrus County, based on data from 1971 to 2000, ranged from 31.9 to 35.4 in. Estimated AET rates, derived from AET/RET ratios shown in table 2, and water budget-based estimates of AET calculated by Sanford and Selnick (2013) for the study area were used as guidelines in Appendix 1 to validate the model-simulated AET.

The model area was spatially classified into generalized land covers as shown in McBride and others (2017, fig. 32) and Sepúlveda (2018). The AET to RET ratios estimated on the basis of land covers (table 2) were used as guidelines to estimate the RET multiplier used to calculate the input ET to the UZF1 Package (Niswonger and others, 2006). AET rates ranged from about 29 to 56 in. for 2004 (fig. 16). The spatial distribution of AET rates for 2004 mimics the delineation of physiographic regions (figs. 3, 16). Brooksville Ridge, Sumter Upland, and Fairfields Hills (fig. 3) are the most areally extensive physiographic regions in the study area and were assigned a "land cover" of ridge. The AET in 2004 for these three physiographic regions ranged from about 29 to 34 in. (fig. 16). Lakes and marshes together account for about 68 percent of the land area in the Tsala Apopka Lake Basin (McBride and others, 2017). AET in 2004 for these two physiographic regions ranged from 46 to 56 in. Average annual RET rates from 2004 to 2012 ranged from 50 to 57 inches per year (in/yr), a range difference of 7 in/yr (table 3). Average annual AET rates for the same 9-year period ranged from 35 to 40 in/yr (table 3).

Groundwater Pumping

Water supply needs in the study area are met by pumping from the Upper Floridan aquifer. Groundwater pumping rates from wells located in the SWFWMD area of the model were provided by SWFWMD (Robert Peterson, Southwest Florida Water Management District, written commun., 2014). All domestic self-supplied water-use data and groundwater pumping rates from wells located in the Suwannee River Water Management District (SRWMD) and St. Johns River Water Management District (SJRWMD) areas of the active flow model were provided by SWFWMD (Kevin Vought, Southwest Florida Water Management District, written commun., 2016).

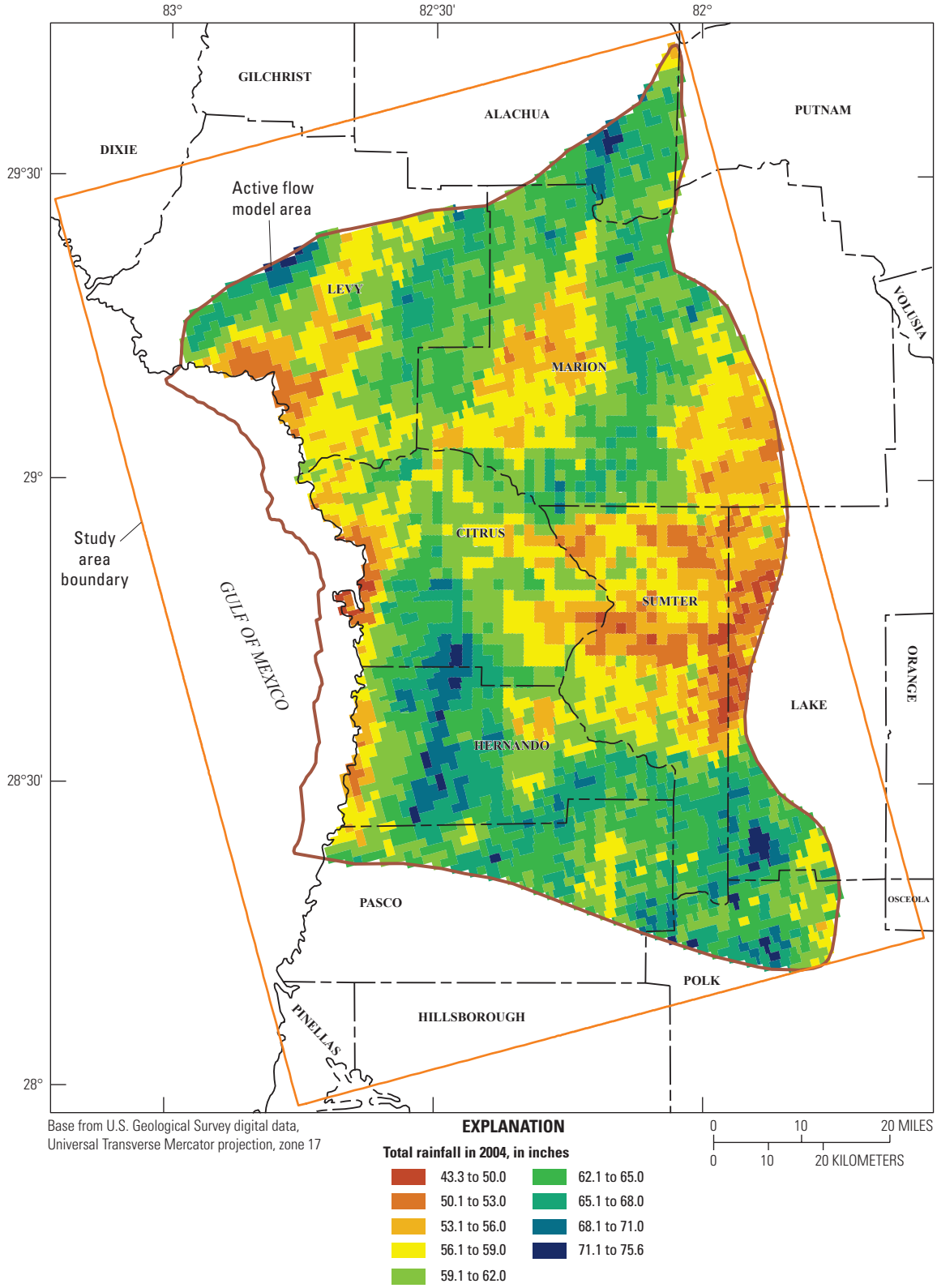

Figure 14. Spatial distribution of total rainfall for 2004 calculated from Next Generation Weather Radar Data (NEXRAD) in the active flow model area.

Table 1. Average annual rainfall per year over active land-surface areas in the flow model.

[RAIN, average rainfall, in inches. Ave, average rainfall over 2004 to 2012 period]

Year	RAIN
2004	59.47
2005	59.34
2006	38.25
2007	47.70
2008	54.43
2009	52.18
2010	51.01
2011	47.78
2012	55.48
Ave	**51.74**

The highest groundwater pumping rates in 2004 were in southwest Hernando County, northwest Pasco County, northeast Sumter County, central and south-central Marion County, and to a lesser degree, in central Citrus County (fig. 17). Most of these larger pumping rates are from public water-supply production wells. On average, about 207 million gallons per day (Mgal/d) were withdrawn from the Upper Floridan aquifer in the study area in the 2004–12 period (table 4). In comparison, the average AET rate of about 37 in/yr for 2004–12 (table 3), when applied to the surficial aquifer flow model area of 4,003 mi^2, is equivalent to about 7,050 Mgal/d, making groundwater pumping rates from the Upper Floridan aquifer in 2004–12 about 3 percent of the AET losses for the same period. Public water supply was the largest use category during the 2004–12 period, followed by agricultural irrigation and domestic self-supplied uses. Pumping rates were mostly highest during the years of lowest rainfall (tables 1 and 4).

Surface-Water and Groundwater Exchange

Stream stage, streamflow, lake stage, and groundwater-level data can be used to determine the direction of flow between the surface-water system and groundwater system. Streamflow is affected by (1) surficial aquifer discharge to stream segments through the streambed, (2) leakage from stream segments to the surficial aquifer, (3) surface runoff from the stream drainage area, and (4) ET losses in the stream channel. Lake stage is controlled by (1) surficial aquifer discharge to the lake through the lakebed, (2) leakage from the lake to the surficial aquifer, (3) surface runoff from the lake drainage area, (4) ET losses at the lake's water surface, and (5) inflows and outflows through the structures. Streamflow and lake stages fluctuate over time depending on the magnitude of these flow processes that occur in the shallow part of the hydrologic flow system.

Within the study area, streamflows and gage heights along the Withlacoochee River and in the Tsala Apopka Lake Basin are reported by 24 streamflow-gaging stations, 11 of which measure gage heights only, 11 report both streamflows and gage heights, and the remaining 2 report streamflows only (fig. 18; table 5; U.S. Geological Survey, 2017; SWFWMD, 2017). Of these 24 stations, 8 are at water-control structures within the pools of the Tsala Apopka Lake Basin, with gages that report both upstream and downstream gage heights, and 3 are outside the basin and report streamflow and gage height. Of all gages inside the pools, only station 02312975 (S–353) measures both streamflow (until 2011) and gage height; the remaining stations measure only gage height. Stations 02312975 and SW 740884 (Bryant Slough Structure) are located at the only two structures inside the Tsala Apopka Lake pools that could discharge water back to the Withlacoochee River. The three flow-control structures outside the Tsala Apopka Lake Basin are located at the Wysong-Coogler Water Conservation structure (referred to hereafter as the Wysong structure in this report), the Inglis Bypass Spillway, and the Inglis Dam (fig. 18). The last two structures are outlets from Lake Rousseau. Two tributaries to the Withlacoochee River discharge mostly spring flow, (1) Gum Springs Run, where the flow from Gum Springs is discharged, shown as spring numbers 35–38 in figure 13; and (2) Rainbow River, (fig. 18) where the flow from Rainbow Springs is discharged, shown as spring numbers 7–14 in figure 13.

A comparison of the average measured streamflows for the Withlacoochee River at Nobleton (station 02312558) and Withlacoochee River near Pineola (station 02312598) from 2004 to 2012 indicates that the Withlacoochee River loses water to the Upper Floridan aquifer between the stations (table 5, fig. 18). Even though the periods of record are different for these two stations, it was consistently observed that during dry hydrologic conditions, streamflow at the Nobleton station was greater than that at Pineola, whereas during wet hydrologic conditions, the reverse was observed. This suggests that (1) the water table between these two gaging stations is lower than the river stage during dry conditions and (2) the water table is higher than the river stage during wet conditions. This dry period decrease in Withlacoochee River streamflow is not observed between any other two consecutive gaging stations, suggesting that the riverbed between these two gaging stations is leakier than elsewhere in the Withlacoochee River.

There are several lake features modeled in the study area. Some segments of the Withlacoochee River are wider than 500 ft and are conceptually considered lakes because of their large water storage capacity. The three pools in Tsala Apopka Lake, Lake Panasoffkee, the pool on the upstream side of the Wysong structure, and Lake Rousseau (figs. 2, 18) are the lakes in the study area for which measured stage data were available. The 2004 to 2012 averages of measured lake stages (table 6) reveal that (1) the average Tsala Apopka Lake pool stages decreased downstream from south to north by more

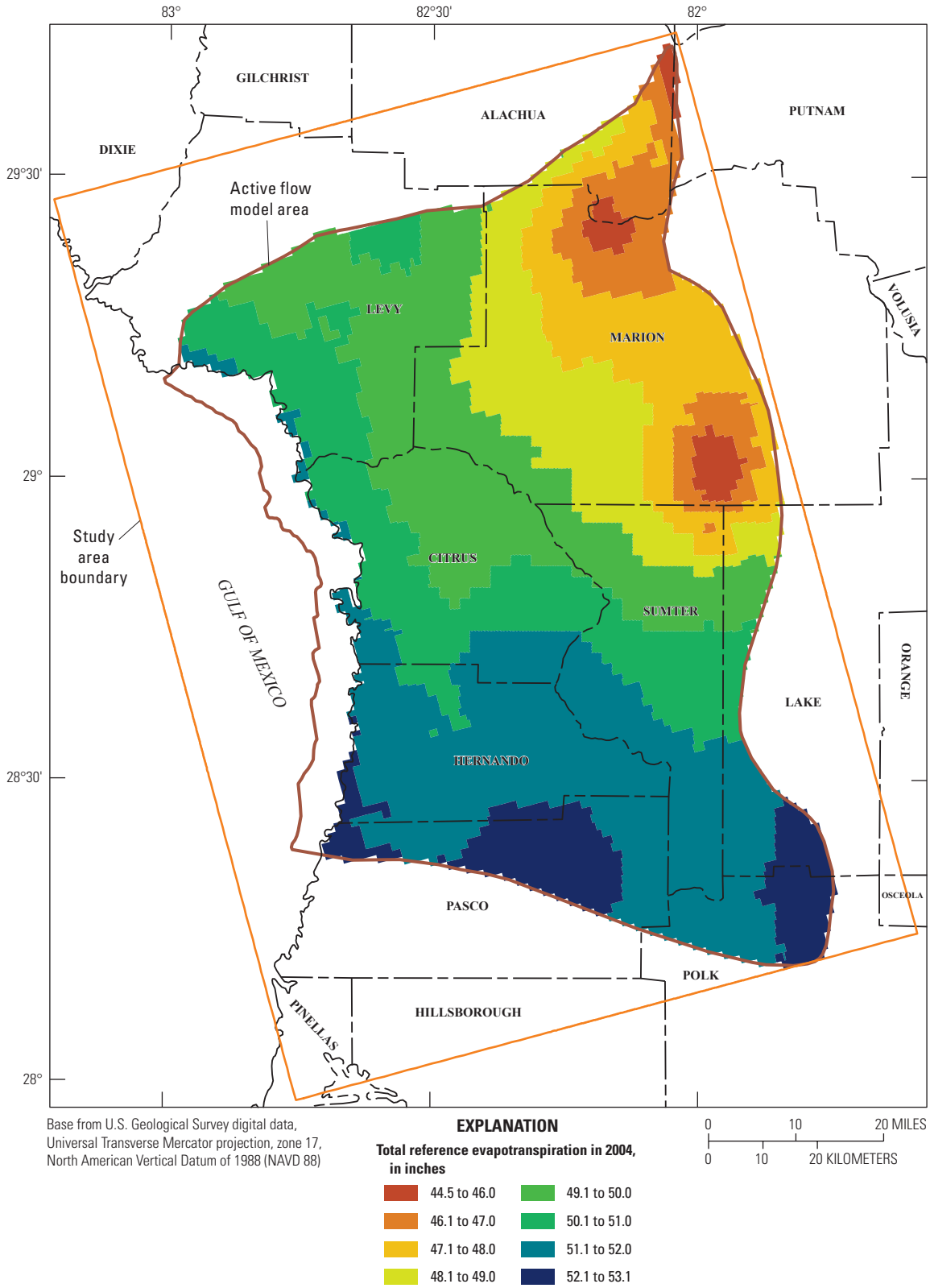

Figure 15. Spatial distribution of reference evapotranspiration for 2004, calculated from Geostationary Operational Environmental Satellite (GOES) data, in the active flow model area.

Table 2. Monthly average actual to reference evapotranspiration ratios for generalized land covers in the model area.

[Forest, grass, marsh, lake, ridge, and urban represent the land cover that prevails at each evapotranspiration (ET) station. Ave, monthly average actual evapotranspiration to reference evapotranspiration (AET/RET) ratios at ET station; POR, period of record of ET station when reference ET (RET) and actual ET (AET) were measured, in month/year (MM/YY) format]

Month	Forest	Grass	Marsh	Lake	Ridge	Urban
January	0.7616	0.6356	0.7790	0.9335	0.4523	0.7584
February	0.7442	0.6453	0.8604	0.9550	0.4762	0.6936
March	0.7542	0.6264	0.9619	1.0278	0.5282	0.5915
April	0.6736	0.6465	0.9294	1.0543	0.5519	0.5385
May	0.6699	0.4590	0.9692	1.0744	0.6194	0.5419
June	0.6258	0.6434	1.0208	1.1016	0.7832	0.6741
July	0.7640	0.8365	0.9701	1.1195	0.7889	0.6920
August	0.8309	0.8846	0.9504	1.1760	0.8186	0.7423
September	0.8142	0.9241	0.9268	1.1415	0.7334	0.6680
October	0.8434	0.8481	0.9769	1.1469	0.6250	0.7302
November	0.9187	0.7769	0.8902	1.0970	0.4891	0.7424
December	0.7764	0.7503	0.7937	1.0420	0.5272	0.7476
Ave	**0.7647**	**0.7231**	**0.9191**	**1.0725**	**0.6161**	**0.6767**
ET station	Tiger Bay	Duda Farms	Blue Cypress	Reedy Lake	Lake Wales Ridge	Orlando
POR	01/98–12/99	06/00–01/03	04/02–09/03	01/02–12/11	09/93–08/94	02/09–08/12

than 1 ft from one pool to the next, (2) the average difference in lake stage between Lake Panasoffkee and the upstream side of the Wysong structure was about 0.9 ft (table 6), and (3) the average water-surface slope in the Withlacoochee River between the downstream side of the Wysong structure and the upstream end of Lake Rousseau was about 5.5×10^{-5} ft/ft (0.29 ft/mi), derived from table 6 data and a stream length between these two points of about 190,300 ft. The effect that the Wysong structure has on changing water-surface slopes in the Withlacoochee River can be estimated from the average stage at the structure, average stream stages, and the stream lengths between specific points in the Withlacoochee River. The 2004 to 2012 average water-surface slope between the Withlacoochee River at Nobleton (station 02312558, fig. 18) and the upstream end of the Wysong structure was about 1.8×10^{-5} ft/ft (0.09 ft/mi), derived from an average stream stage of 38.72 ft at the Nobleton station, an average lake stage of 37.19 ft at the Wysong structure (table 6), and a stream length between these two points of about 85,500 ft. Without considering the Wysong structure, the water-surface altitude in the Withlacoochee River would be expected to decrease in the downstream direction similar to the rate at which land-surface altitudes decline downstream. Because of the Wysong structure, the downstream water-surface slope in the Withlacoochee River downstream from the Wysong structure is about three times higher than that upstream from Wysong structure, as a result of the water stored at the pool generated by the Wysong structure.

The annual water budget flows for the Floral City pool calculated by McBride and others (2017) showed that the annual average leakage rate to the underlying Upper Floridan aquifer, over the 2004 to 2012 period, was 7 in/yr. The study by McBride and others (2017) showed that upward leakage, from the Upper Floridan aquifer to the Tsala Apopka Lake pools, rarely occurred.

Summary of Model Results

Surface-water/groundwater flow model results showed that the largest leakage rates per unit area from the Tsala Apopka Lake pools to the Upper Floridan aquifer were at the deep lake cells and that these leakage rates were higher per unit area than any recharge rates to the Upper Floridan aquifer in the model area in 2004 (fig. 1.23). Downward leakage rates to the surficial aquifer occurred beneath most of the extent of the Floral City, Inverness, and Hernando pools. Leakage rates were higher for the Floral City pool than the Inverness pool, and higher for the Inverness pool than the Hernando pool; however, lakebed leakance was higher for the Floral City pool than the Hernando pool, and higher for the Hernando pool than the Inverness pool.

Model results showed that the annual recharge rate over the active flow model area to the surficial aquifer was 9.8 in/yr in 2004, the annual average for the 2004 to 2012 simulation period was 10.3 in/yr, and annual averages ranged from 3.8 in/yr in 2006 to 14.2 in 2005 (table 1.6). Areas that recharge the surficial aquifer cover about 86 percent of the model area. Most of the discharge areas were simulated near the coast, along segments of the Withlacoochee River downstream from the Wysong structure (fig. 18), in

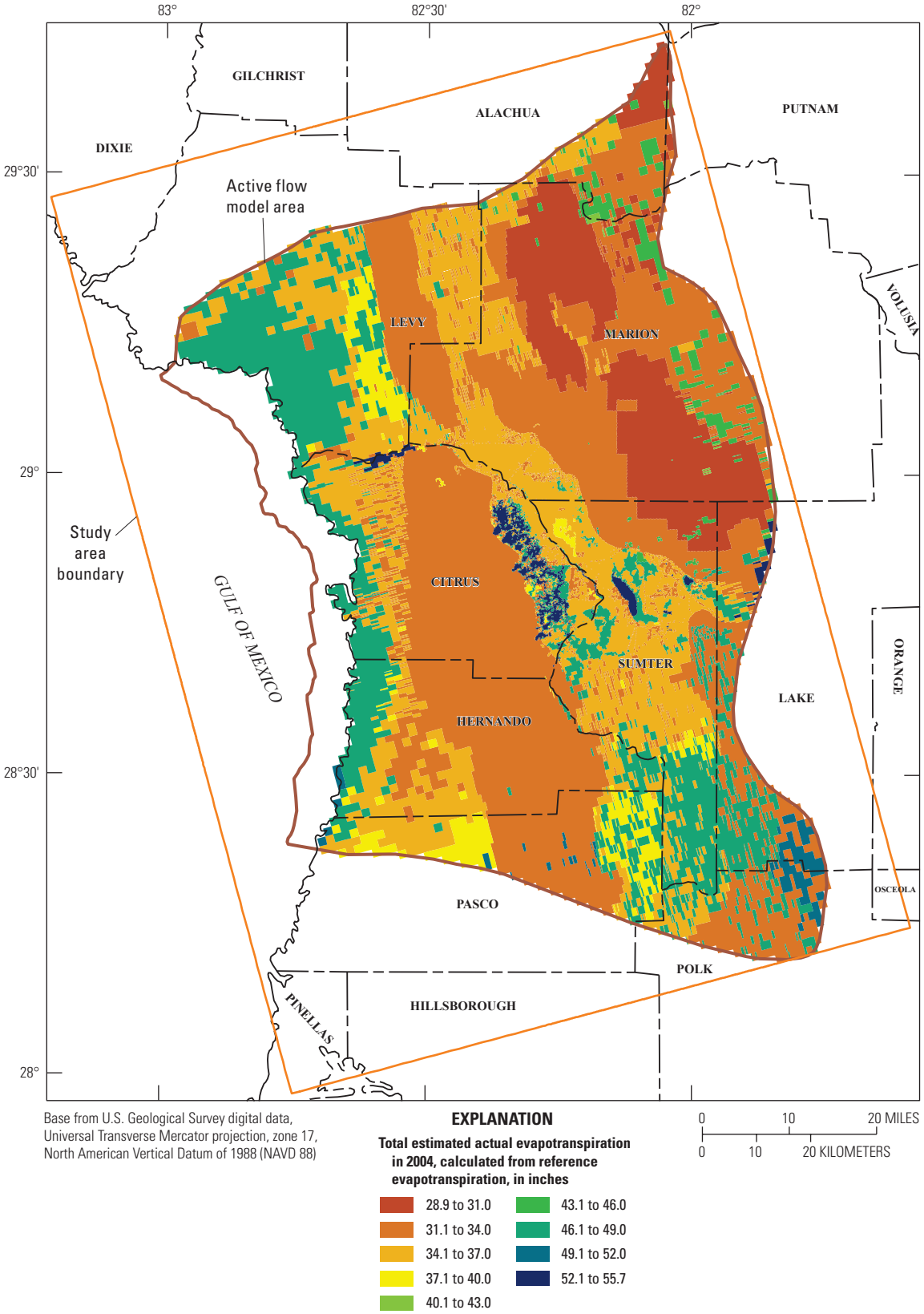

Figure 16. Spatial distribution of total estimated actual evapotranspiration for 2004 in the active flow model area.

Table 3. Average annual reference and estimated actual evapotranspiration rates in the active flow model area.

[AveRET, average reference evapotranspiration over active flow model areas, in inches; AveAET, average estimated actual evapotranspiration over active flow model areas, in inches; Ave, annual average evapotranspiration for the 2004 to 2012 period]

Year	AveRET	AveAET
2004	49.64	34.94
2005	51.37	36.38
2006	57.35	40.45
2007	55.47	39.17
2008	53.81	37.84
2009	54.80	38.70
2010	53.16	37.77
2011	54.15	38.26
2012	51.51	36.29
Ave	**53.47**	**37.76**

areas south and northeast of Lake Panasoffkee, and in the southeastern part of the model area. These discharge areas are characterized by diffuse upward leakage from the Upper Floridan aquifer to the water table. Simulated leakage rates from the Floral City pool to the underlying Upper Floridan aquifer averaged 15.3 in/yr over the 2004 to 2012 period, a rate slightly more than twice the one estimated by McBride and others (2017). The reason for this leakage rate difference is that the pool area considered in the development of the model is half the area considered by McBride and others (2017), because they considered inundated as well as non-inundated areas to be part of their control volume.

The 9-year transient simulation yielded pool stage, head, spring flow, and streamflow residuals that met the calibration criteria listed in the Calibration Targets section in Appendix 1 for the 2004–12 simulation period. The total annual average simulated evapotranspiration (ET) rate was 33.6 in/yr, with 23.1 in/yr of ET from the unsaturated zone, 7.3 in/yr from groundwater, 2.7 in/yr from surface leakage assumed to evaporate after filling land depressions, and 0.5 in/yr from simulated ET in lakes and streams, scaled over the area of all active cells. Total simulated ET ranged from about 31 in/yr during 2006 to 40 in/yr during 2005. The average annual ET from lakes and streams of 0.5 in/yr was calculated based on the ET (averaging 56.4 in/yr) from the nearly 40 mi^2 of lakes and streams distributed over the 4,535 mi^2 of active flow model area.

Annual average flows leaving the Upper Floridan aquifer were, during the 9-year simulation period, (1) 0.47 in/yr through the lateral boundary cells, (2) 1.02 in/yr of groundwater withdrawal rate, (3) 7.64 in/yr in spring flow, and (4) 0.15 in/yr in surface leakage. These outflows were balanced by the annual average inflows entering the Upper Floridan aquifer: (1) 8.44 in/yr of downward leakage rate, whether from the surficial aquifer or the upper confining unit, and (2) 0.84 in/yr of routed recharge rate through the unsaturated zone to the Upper Floridan aquifer. There were no net storage changes in the Upper Floridan aquifer in the 9-year simulation period.

The simulated initial heads in January 2004 in the Upper Floridan aquifer (fig. 1.26) showed that the general flow directions in the model area are from the northeast toward the southwest and then westward toward the coast, and from the southeast toward the northwest and then westward toward the coast, consistent with the potentiometric surface developed using water levels measured in wells during May 2010 (fig. 12). Concerning the water budget of the Upper Floridan aquifer, the largest inflow was downward leakage from the overlying hydrogeologic unit and the largest outflow was total spring flow (table 1.16). Model results indicate that small downward hydraulic gradients between the surficial and Upper Floridan aquifers were simulated, consistent with observations at nested wells screened in these aquifers.

The timing of simulated spring flow peaks at the largest springs in the model area (Silver, Rainbow, Gum, Homosassa, SE Fork Homosassa, Chassahowitzka, and Weeki Wachee Springs, numbers 5, 7–11, 35–38, 43, 46, 57–58, and 81–82, fig. 13) agreed well with the timing of the measured spring flow peaks (figs. 1.49 to 1.55). Simulated spring flow hydrograph peaks generally underestimate measured spring flow peaks during large rainfall events. These spring flow underestimations are probably due to the inclusion, in the field spring flow measurements, of the surface runoff component in the spring run or channel, which increases as the magnitude of the rainfall event increases. Average simulated spring flows during the 9-year simulation period (2004 to 2012) were within 10 percent of the measured flows larger than or equal to 10 ft^3/s (first and second magnitude springs), and within 20 percent of measured flows less than 10 ft^3/s, for all springs with more than 20 flow measurements. The average simulated streamflows and stages in the Withlacoochee River were less than 20 and 10 percent of the measured streamflows and stages, respectively (table 1.12). Surface-water storage in small land-surface depressions was not represented in the model, and this resulted in an overestimation of streamflows and stream stages during large rainfall events.

Simulation of Hydrologic Changes Effected by Variations in the Hydrologic System

The surface-water/groundwater flow model described in Appendix 1 was used to simulate the effects that specified changes to the hydrologic system of the Tsala Apopka Lake Basin and adjacent areas would have on lake stages, groundwater levels, spring flows, and streamflows. Simulated changes to the calibrated model included (1) decreasing and increasing rainfall by 10 percent (referred to as scenarios

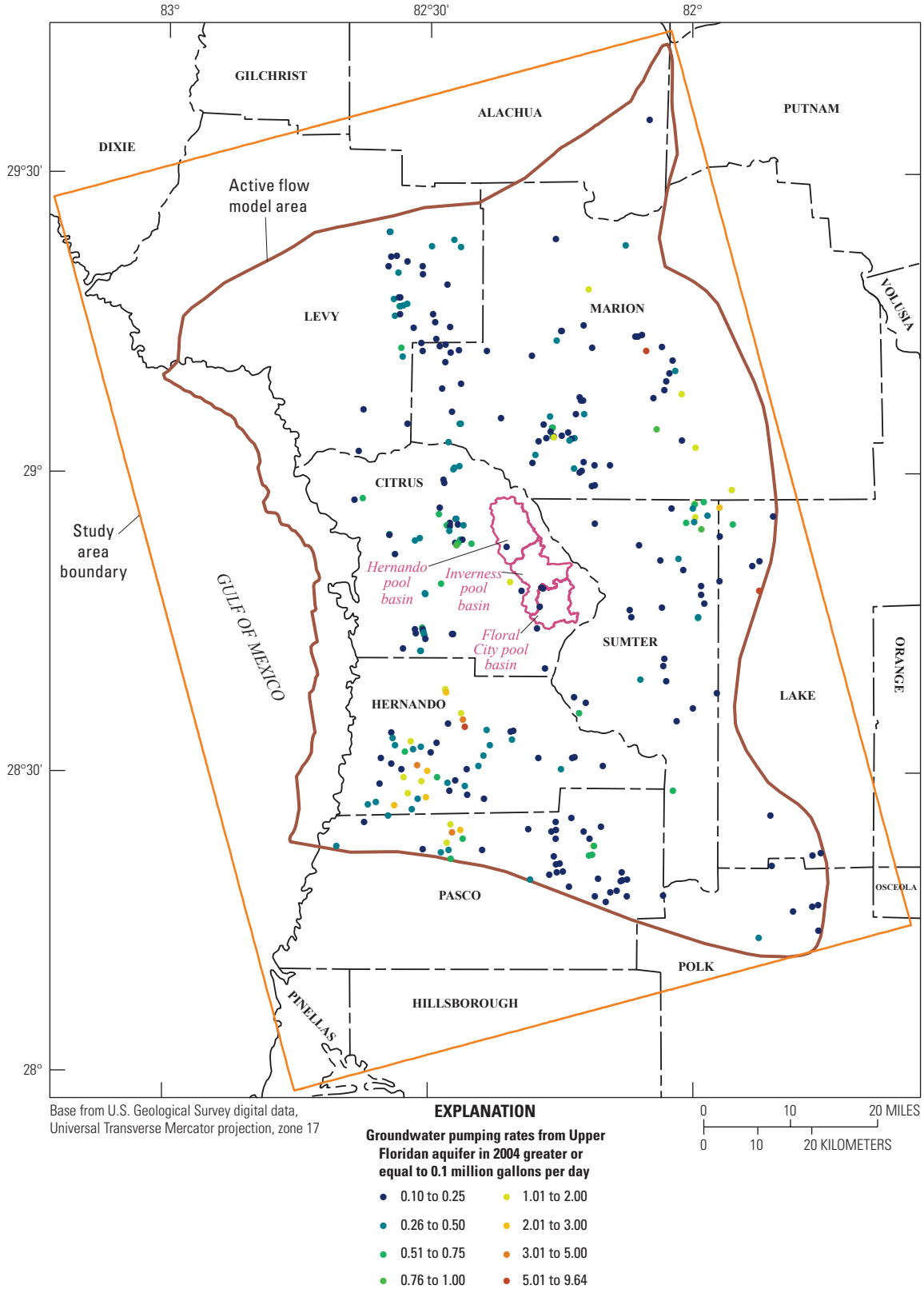

Figure 17. Locations where groundwater pumping rates in 2004 in the active flow model area were greater or equal to 0.1 million gallons per day. All groundwater pumping occurred from the Upper Floridan aquifer.

Table 4. Groundwater pumping rates from the Upper Floridan aquifer in the active flow model area, per year and per water-use category.

[All pumping rates are in million gallons per day. PWS, public water supply; AGR, agricultural irrigation; MIN, mining; REC, recreational; IND, industrial and commercial; DSS, domestic self-supply; TOT, total annual pumping; Ave, average pumping rates for the 2004 to 2012 period]

Year	PWS	AGR	MIN	REC	IND	DSS	TOT
2004	104.081	46.600	12.237	15.827	10.576	18.516	207.837
2005	109.586	29.047	13.291	12.382	16.628	20.416	201.350
2006	125.533	51.084	11.731	15.596	10.669	26.354	240.967
2007	115.556	46.319	9.156	20.434	11.215	24.045	226.725
2008	114.787	36.293	4.683	21.689	11.617	26.878	215.947
2009	104.062	45.253	3.325	15.904	8.081	35.871	212.496
2010	95.939	41.272	3.510	16.013	8.890	29.178	194.802
2011	97.904	34.476	4.952	16.450	8.098	18.457	180.337
2012	93.805	40.058	0.150	15.453	9.157	25.382	184.005
Ave	**106.806**	**41.156**	**7.004**	**16.639**	**10.548**	**25.011**	**207.163**

RAIND and RAINI, respectively); (2) using projected increases in groundwater pumping rates for 2025 and 2035 (table 7, Kevin Vought, Southwest Florida Water Management District, written commun., 2016; Sepúlveda, 2018) relative to average rates for the 2004 to 2012 period (referred to as scenarios P2025 and P2035, respectively); (3) simulating no flow through all eight water-control structures (fig. 2) in the Tsala Apopka Lake Basin (referred to as scenario NFCS); and (4) simulating the removal of both water-control structures, the Inglis Dam and Inglis Bypass Spillway (fig. 18), on Lake Rousseau (referred to as scenario NING). Simulated Tsala Apopka pool stages and flows from these scenarios (table 8) were compared to pool stages and flows for the historical period using the base case model described in Appendix 1 and referred to as scenario HSIMU from this point on.

Simulating Changes in Rainfall Rates

To evaluate the effects of decreases and increases in rainfall on lake stages, groundwater levels, spring flows, and streamflows, scenarios were simulated to represent a 10-percent decrease (RAIND) and a 10-percent increase in rainfall (RAINI). The rate of 10 percent was an arbitrary but common benchmark. Scenarios RAIND and RAINI were simulated by multiplying the daily rainfall rates, used for calibration from 2004 to 2012, by 0.9 and 1.1, respectively.

Simulation results of scenario RAINI show that a 10-percent increase in rainfall resulted in downstream-increasing pool stage reactions, from the Floral City pool to the Hernando pool (table 9). The drainage areas also increase downstream: the Floral City pool is the smallest with 17.44 mi^2; the Inverness pool has a drainage area of 18.97 mi^2; and the Hernando pool is the largest with 21.74 mi^2 (table 6). Thus, the surface-runoff volume being drained to each pool from each rainfall event increases downstream. The furthest upstream pool, Floral City, had an annual average increase in stage of 0.93 ft (11.16 in., fig. 19) over the 9-year simulation period; the rainfall was increased by an annual average of 5.09 in. over the pool area from HSIMU. The next pool downstream, Inverness, had an annual average increase in stage of 1.23 ft (14.76 in., fig. 20); the average annual rainfall was increased by 5.04 in. over the pool area from HSIMU. The furthest downstream pool, Hernando, had an annual average increase in stage of 1.49 ft (17.88 in., fig. 21); the average annual rainfall was increased by 5.22 in. over the pool area from HSIMU (table 9). The increase in rainfall applied to the model area depended on the applied rainfall rate for each grid cell, which varied from one cell to another and from one stress period to another. As expected, decreased rainfall to Tsala Apopka Lake pools decreased stages and increased rainfall to Tsala Apopka Lake pools increased stages (figs. 19-21).

Simulation results of scenario RAIND show that a 10-percent decrease in rainfall resulted in pool stage decreases in the Floral City pool and Hernando pool with smaller decreases in the Inverness pool (table 9). Floral City pool had an annual average decrease in stage of 0.84 ft (10.08 in., fig. 19) over the 9-year simulation period when the rainfall was decreased by an annual average of 5.09 in. from HSIMU. Inverness pool had an annual average decrease in stage of 0.34 ft (4.08 in., fig. 20) when the average annual rainfall was decreased by 5.04 in. from HSIMU. The Hernando pool had an annual average decrease in stage of 1.28 ft (15.36 in., fig. 21) when average annual rainfall was decreased by 5.22 in. from HSIMU (table 9). The reason for the small decrease in the Inverness pool stage in scenario RAIND, compared to scenario HSIMU and during the 2006 drought, was that this pool was within 0.1 ft of being dry during 2006, reducing the downward leakage from Inverness pool to the Upper Floridan aquifer.

To summarize simulation results, as rainfall rates increase, exceeding infiltration rates of the topsoil, larger increases in pool stages occur progressively downstream because larger surface runoff volumes are generated from larger drainage areas. Similarly, pool stages decrease downstream during droughts, when rainfall rates are below average.

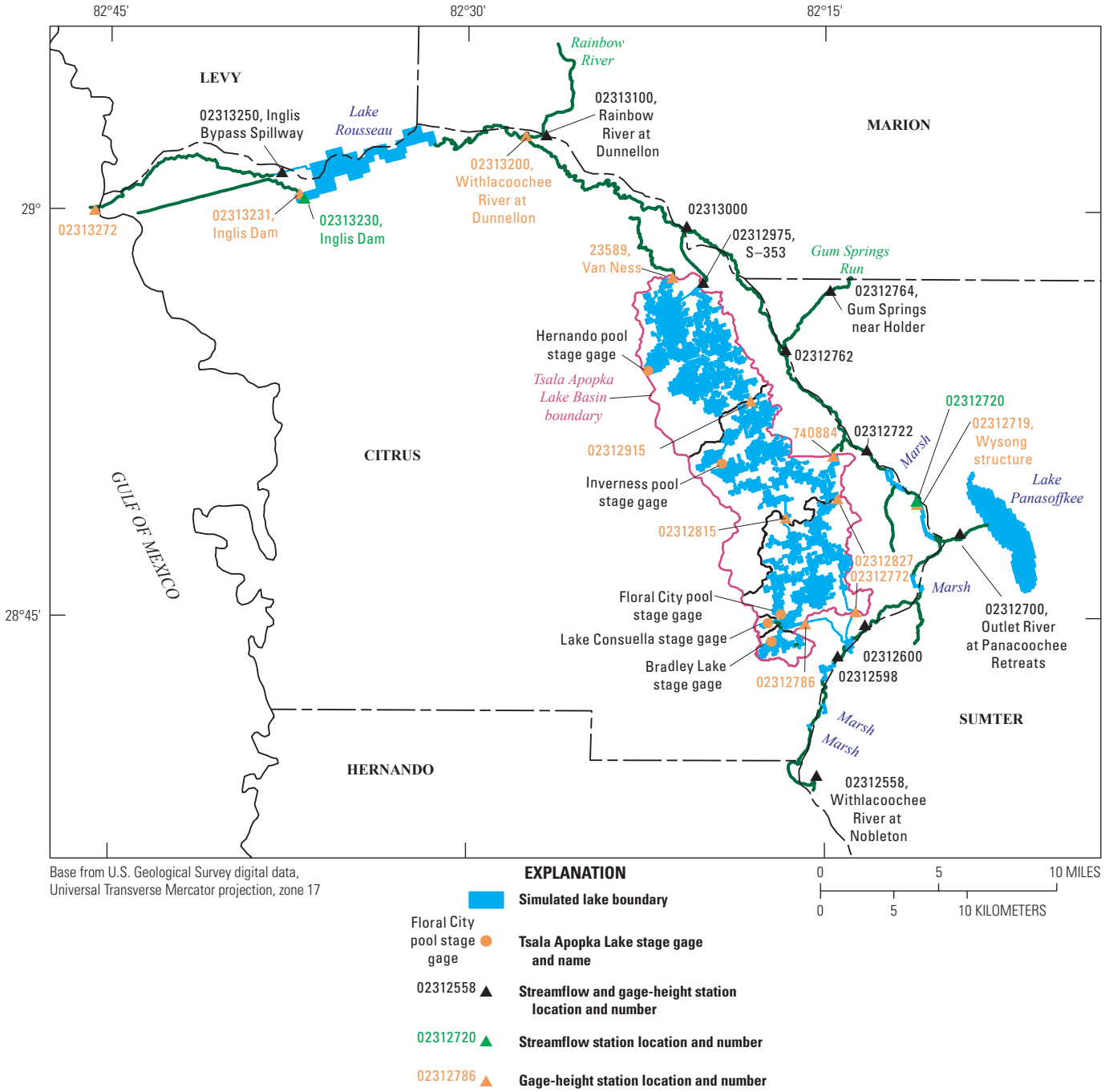

Figure 18. Location of flow and gage height streamflow-gaging stations along the Withlacoochee River and in the Tsala Apopka Lake Basin.

The average annual water levels in the surficial and Upper Floridan aquifers, calculated from the hydrologic conditions in the calibration scenario HSIMU (figs. 22, 23), were used to compare simulated water-level results from all scenarios. Simulation results from scenarios RAIND and RAINI indicate that the range of water-level fluctuations in the surficial aquifer is larger than the range of Upper Floridan aquifer head fluctuations caused by changes in rainfall (figs. 24–27). Simulated groundwater levels under scenario RAIND declined up to 5.4 ft in the surficial aquifer and up to 2.9 ft in the Upper Floridan aquifer. A decrease in rainfall (scenario RAIND) caused the largest drop in water levels in the surficial and Upper Floridan aquifers in the area near the Levy, Marion, and Citrus County lines, and across the eastern half of Hernando County and central part of Sumter County (figs. 24, 25). Water-level responses to changes in rainfall were greatest in the area near the Levy, Marion, and Citrus County lines. The areas where the largest water-level increases were caused by increases in rainfall, in both the water table and Upper Floridan aquifer, coincided with the areas where the largest drops in water levels occurred when rainfall was decreased (figs. 26, 27).

Table 5. Surface-water station name, identification number, location, type, and average measured streamflow for the 2004 to 2012 period.

[GAGEID, gage identification number; XSP, YSP, spring coordinates in State Plane projection, North American Datum of 1983, Florida west 0902 (Snyder, 1983), in feet; SEGNO, segment number of gage location; RCHNO, reach number of gage location in stream segment; AveFlow, average measured flow at station for the 2004–12 period, in cubic feet per second; NA, not applicable; SW, Southwest Florida Water Management District identification number. WR, Withlacoochee River. F, streamflow gaging station; GH, gage height station, whether stream or pool gage height. Streamflow measurements at station 02313200 began after 2012]

Surface-water station name	GAGEID	XSP	YSP	Gage type	SEGNO	RCHNO	AveFlow
WR at Nobleton	02312558	573607	1567099	F, GH	1	1	246.7
WR near Pineola	02312598	578588	1595940	F, GH	4	1	146.3
Leslie Heifner Canal near Floral City	02312772	582523	1606808	GH	9	1	NA
Floral City Structure	02312786	571791	1604360	GH	10	1	NA
Golf Course Structure	02312815	567253	1627836	GH	11	1	NA
Moccasin Slough Structure	02312827	578769	1631957	GH	12	1	NA
Bryant Slough Structure	SW 740884	578010	1642106	GH	13	1	NA
Brogden Bridge Structure	02312915	559357	1654190	GH	14	1	NA
S-353 Structure	02312975/SW 23594	548383	1680128	F, GH	15	1	2.8
Van Ness Structure	SW 23589	541987	1681629	GH	16	1	NA
WR near Floral City	02312600	585594	1602926	F, GH	17	6	214.9
Outlet River at Panacoochee Retreats	02312700	607184	1623602	F, GH	21	14	109.9
WR above Wysong structure	02312719	597491	1631876	GH	22	1	NA
WR at Wysong structure	02312720	597257	1632252	F	23	1	358.2
WR near Rutland	02312722	585433	1642437	F, GH	25	13	256.2
WR near Inverness	02312762	566651	1664534	F, GH	29	61	417.4
Gum Springs near Holder	02312764	577522	1678686	F, GH	30	16	88.6
WR near Holder	02313000	544442	1692337	F, GH	34	1	555.7
Rainbow River at Dunnellon	02313100	513136	1714572	F, GH	35	30	594.3
WR at Dunnellon	02313200	507675	1713172	GH	36	7	NA
WR at Inglis Dam	02313230	459126	1700127	F	37	1	238.0
WR below Inglis Dam	02313231	458553	1700388	GH	38	1	NA
WR Inglis Bypass Spillway	02313250	452484	1704554	F, GH	40	1	901.3
WR at Chambers near Yankeetown	02313272	411317	1697374	GH	40	15	NA

Table 6. Lake or pool name, water-surface area, drainage area, and average measured lake or pool stage for the 2004 to 2012 period.

[Average pool stage is in feet (ft) above the North American Vertical Datum of 1988 (NAVD 88). mi^2, square mile]

Name	Water-surface area (mi^2)	Average stage, 2004–12 (ft)	Drainage area (mi^2)
Floral City Pool	6.56	38.35	17.44
Inverness Pool	7.35	36.62	18.97
Hernando Pool	11.29	35.43	21.74
Lake Panasoffkee	5.07	38.05	23.29
Withlacoochee River at Wysong structure	0.22	37.19	2.81
Lake Rousseau	4.62	26.68	16.84

The average simulated annual spring flow from scenario HSIMU was 2,393 ft^3/s from all 91 springs and considering all 3,288 stress periods, and the average simulated annual spring flows under scenarios RAIND and RAINI were 2,263 and 2,512 ft^3/s, respectively (table 10). These flows indicate that a change in rainfall of 10 percent (1,622 ft^3/s) resulted in a reduction in simulated spring flow of about 5.4 percent (130 ft^3/s) under scenario RAIND and an increase of about 5.0 percent (119 ft^3/s) under scenario RAINI. The largest spring flow changes occurred in first magnitude springs.

The average simulated streamflow from scenario HSIMU, calculated from the simulated streamflow at the 12 streamflow-gaging stations in the Withlacoochee River and its tributaries (table 11), was 327 ft^3/s, and the simulated streamflows under scenarios RAIND and RAINI were 319 and 330 ft^3/s, respectively. These simulated streamflows represent a flow decrease of 2.4 percent under scenario RAIND and an increase of about 1 percent under scenario RAINI (table 11), mainly because changes in precipitation affected only streamflows

Table 7. Projected groundwater pumping rates per county for 2025 and 2035 in the active flow model area.

[All pumping rates are in million gallons per day and from the Upper Floridan aquifer. SIMAVE, average groundwater pumping rate for the 2004–12 simulation period; 2025RAT, 2035RAT, multipliers; 2025, total groundwater pumping rate by county for 2025, equal to SIMAVE times 2025RAT; 2035, total groundwater pumping rate by county for 2035; equal to SIMAVE times 2035RAT; SWFWMD, applies to county section in Southwest Florida Water Management District; SJRWMD, applies to county section in St. Johns River Water Management District; NA, not applicable; PERINC, percentage increase in groundwater pumping rate relative to total SIMAVE]

County	SIMAVE	2025RAT	2035RAT	2025	2035
Alachua	0.591	1.284	1.567	0.759	0.927
Citrus	31.078	1.146	1.276	35.615	39.656
Hernando	44.467	1.153	1.288	51.270	57.273
Lake (SWFWMD)	1.235	0.822	0.700	1.015	0.864
Lake (SJRWMD)	7.937	1.071	1.142	8.501	9.064
Levy	11.048	1.074	1.159	11.866	12.805
Marion (SWFWMD)	25.527	1.261	1.510	32.189	38.545
Marion (SJRWMD)	23.230	1.268	1.536	29.455	35.681
Pasco	30.933	1.152	1.283	35.634	39.687
Polk	2.793	1.127	1.214	3.148	3.391
Sumter	28.325	1.292	1.546	36.596	43.790
Total	**207.163**	**NA**	**NA**	**246.049**	**281.683**
PERINC	NA	NA	NA	18.770	35.971

Table 8. Description of scenarios simulated using the calibrated surface-water/groundwater flow model.

Scenario name	Scenario description
HSIMU	Historical simulation for the 2004 to 2012 period used to calibrate heads and flows in the Tsala Apopka Lake Basin model and presented in Appendix 1.
RAIND	Decrease rainfall by 10 percent over the entire model area and for the 2004 to 2012 period. All other inflows and outflows used in the calibrated model remain the same.
RAINI	Increase rainfall by 10 percent over the entire model area and for the 2004 to 2012 period. All other inflows and outflows used in the calibrated model remain the same.
P2025	Replace the withdrawal data used by the Well Package in the calibrated model with the withdrawal data representing the predicted groundwater pumping rates for 2025. All other inflows and outflows used in the calibrated model remain the same.
P2035	Replace the withdrawal data used by the Well Package in the calibrated model with the withdrawal data representing the predicted groundwater pumping rates for 2035. All other inflows and outflows used in the calibrated model remain the same.
NFCS	Simulate the removal of the eight water-control structures in the Tsala Apopka Lake Basin, including both river diversions that allow water into the Floral City pool and the internal structures.
NING	Simulate the removal of the Inglis Dam and the Inglis Bypass Spillway on Lake Rousseau and reconnect the Lower Withlacoochee River.

Table 9. Simulated changes in pool stage caused by decreases and increases in rainfall from the calibrated model.

[RAIN, annual average of rainfall rates over all pool cells, the first number is the rainfall rate for scenario RAIND, the second number is the average for the calibration period of 2004 to 2012, and the third number is the rainfall rate for scenario RAINI, all three rates are in inches per year; DIFF_RAIN, differences from the average of rainfall rates used in the calibration run, the first number is the 10 percent decrease in rainfall (negative) and the second number is the 10 percent increase in rainfall (positive), both rates are in inches per year; STAGE_R, simulated average pool stage for the corresponding rainfall rates in RAIN, specified in feet NAVD 88; DIFF_ft, DIFF_in, differences from the average pool stage for the calibration period, the first number is the simulated drop in pool stage corresponding to scenario RAIND (negative number) and the second number is the simulated rise in pool stage corresponding to scenario RAINI (positive number), in feet and in inches, respectively]

Descriptor	Floral City pool	Inverness pool	Hernando pool
RAIN	45.85, 50.94, 56.03	45.32, 50.36, 55.40	46.99, 52.21, 57.43
DIFF_RAIN	-5.09, 5.09	-5.04, 5.04	-5.22, 5.22
STAGE_R	37.76, 38.60, 39.53	36.51, 36.85, 38.08	34.06, 35.34, 36.83
DIFF_ft	-0.84, 0.93	-0.34, 1.23	-1.28, 1.49
DIFF_in	-10.08, 11.16	-4.08, 14.76	-15.36, 17.88

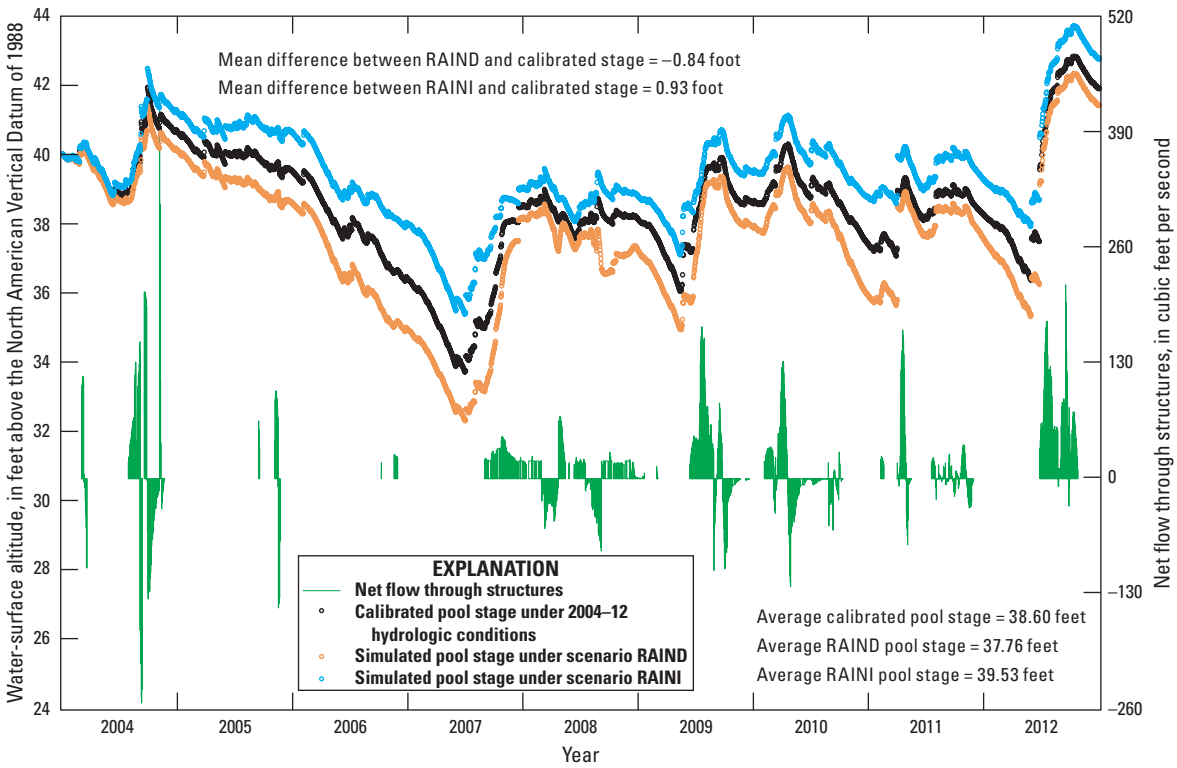

Figure 19. Simulated stage at Floral City pool under the RAIND and RAINI scenarios, and net daily flow through Floral City pool structures, for the 2004–12 period.

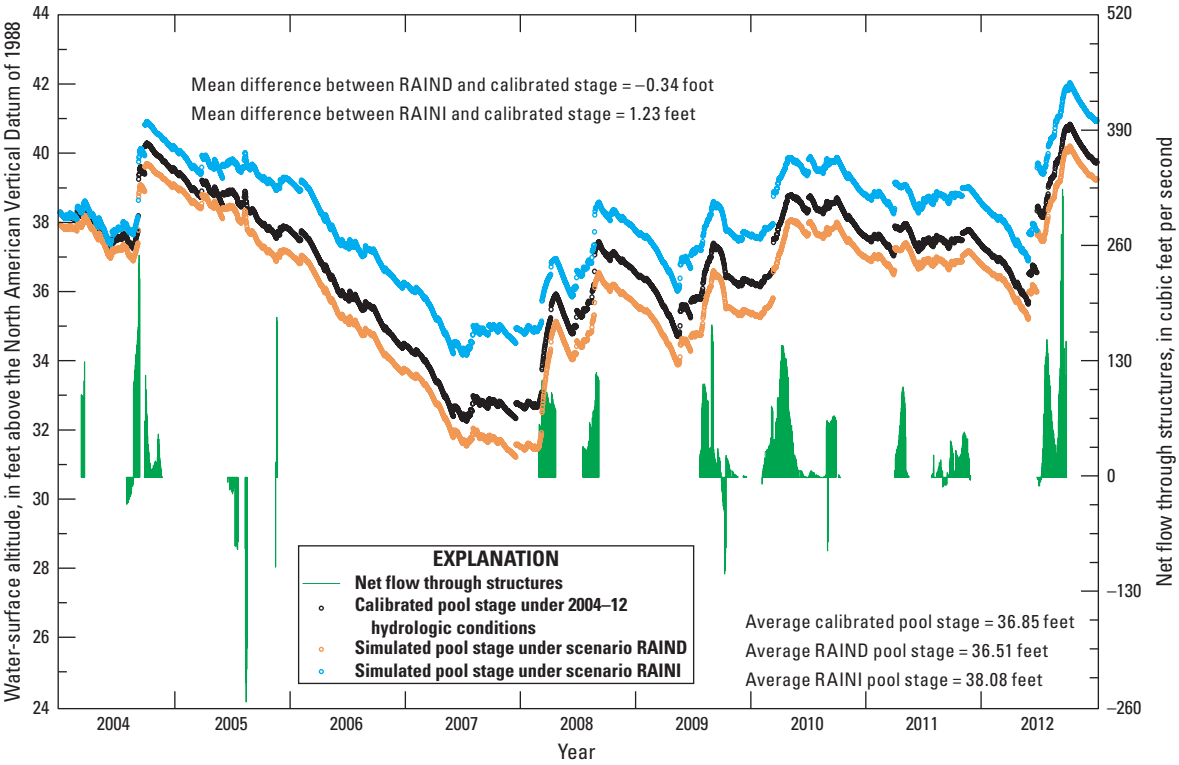

Figure 20. Simulated stage at Inverness pool under the RAIND and RAINI scenarios, and net daily flow through Inverness pool structures, for the 2004–12 period.

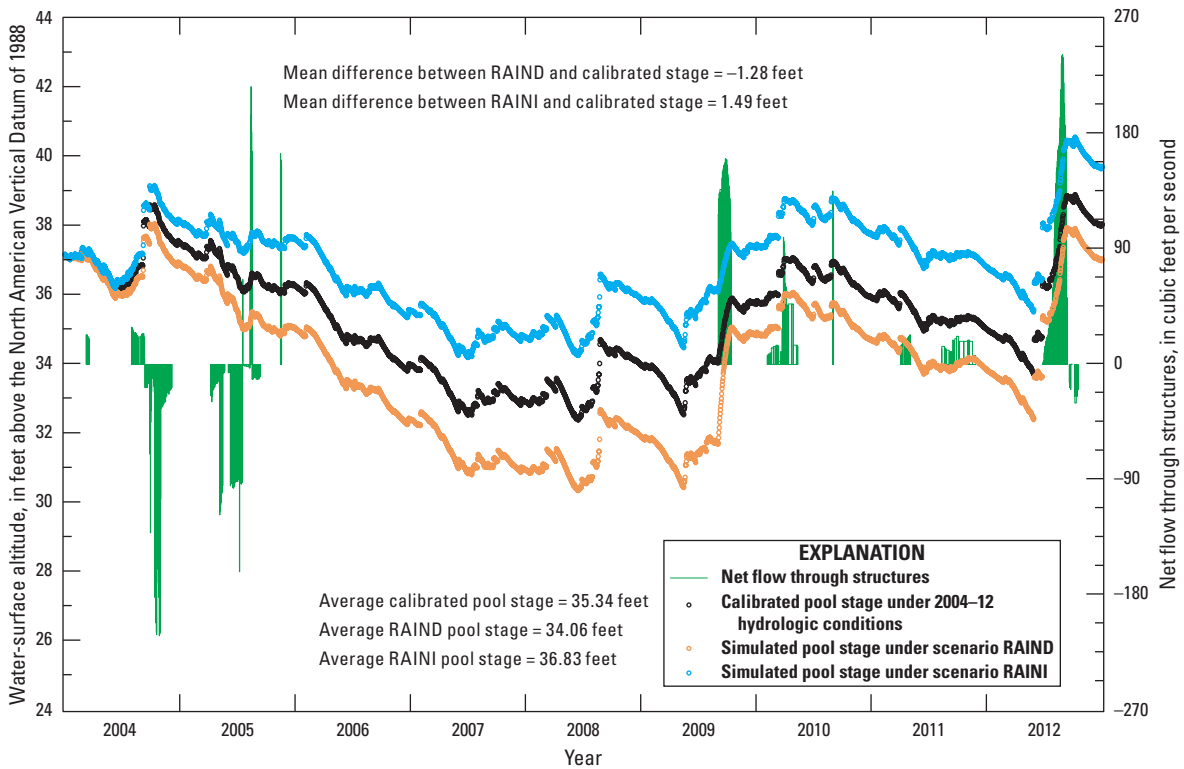

Figure 21. Simulated stage at Hernando pool under the RAIND and RAINI scenarios, and net daily flow through Hernando pool structures, for the 2004–12 period.

just downstream of where the inflows were specified in the model. Measured flows at streamflow-gaging stations 02312558, 02312700, 02312764, and 02313100, or along corresponding stream segments 1, 21, 30, and 35 (tables 5 and 11, fig. 18, fig. 1.3) were specified in both RAIND and RAINI scenarios. Changes in simulated streamflow from changes in precipitation were limited to stations where flows were actively simulated, mostly stations 02312598, 02312600, 02312722, 02312762, and 02313000. The average streamflow at these stations represented a flow decrease of about 52 ft^3/s under scenario RAIND and an increase of about 30 ft^3/s under scenario RAINI (table 11).

Water budgets for the control volume of all model layers were calculated for scenarios RAIND and RAINI to indicate the distribution of decreased or increased rainfall relative to the calibration scenario HSIMU. The additional 5.17 in/yr of annual average rainfall simulated under scenario RAINI, when compared to scenario HSIMU, caused (1) an increase of 1.97 in/yr in runoff discharged to cells draining outside the simulated lakes and streams, (2) an increase of 1.75 in/yr of ET losses, including surface leakage, (3) an increase in outflow through the general-head boundary cells of 0.78 in/yr, (4) an increase of 0.38 in/yr in spring flow, (5) an increase of 0.27 in/yr in net storage, and (6) an increase of 0.02 in/yr in streamflow (table 12).

The decrease of 5.17 in/yr of annual average rainfall simulated under scenario RAIND, when compared to scenario HSIMU, caused (1) a decrease of 1.75 in/yr in runoff discharged to cells draining outside the simulated lakes and streams; (2) a decrease of 1.72 in/yr of ET losses, including surface leakage; (3) a decrease in outflow through the general-head boundary cells of 0.85 in/yr; (4) a decrease of 0.41 in/yr in spring flow; (5) a decrease of 0.35 in/yr in net storage; and (6) a decrease of 0.09 in/yr in streamflow (table 12).

Simulating Projected Increases in Groundwater Pumping Rates for 2025 and 2035

To evaluate the effects of projected increases in groundwater pumping, scenarios P2025 and P2035 were executed by increasing all groundwater pumping rates in scenario HSIMU by factors that varied by county, representing the estimated population increases for the years 2025 and 2035 (table 7; Vibhava Srivastava, Southwest Florida Water Management District, written commun., 2017). The decreases in simulated pool stages, from the calibrated model, under scenario P2035 were 0.02 ft for the Floral City pool, 0.06 ft for Inverness pool, and 0.04 ft for Hernando pool (figs. 28–30); decreases in pool stages under scenario P2025 were half of those simulated under scenario P2035. These small declines in simulated pool stage indicate that the projected groundwater pumping rates for 2025 and 2035 in and near the Tsala Apopka Lake Basin were not sufficient to substantively affect the pool stages in the Tsala Apopka Lake Basin, a likely outcome considering that groundwater pumping activity was lower (fig. 17) in and near the Tsala Apopka Lake Basin than away from it.

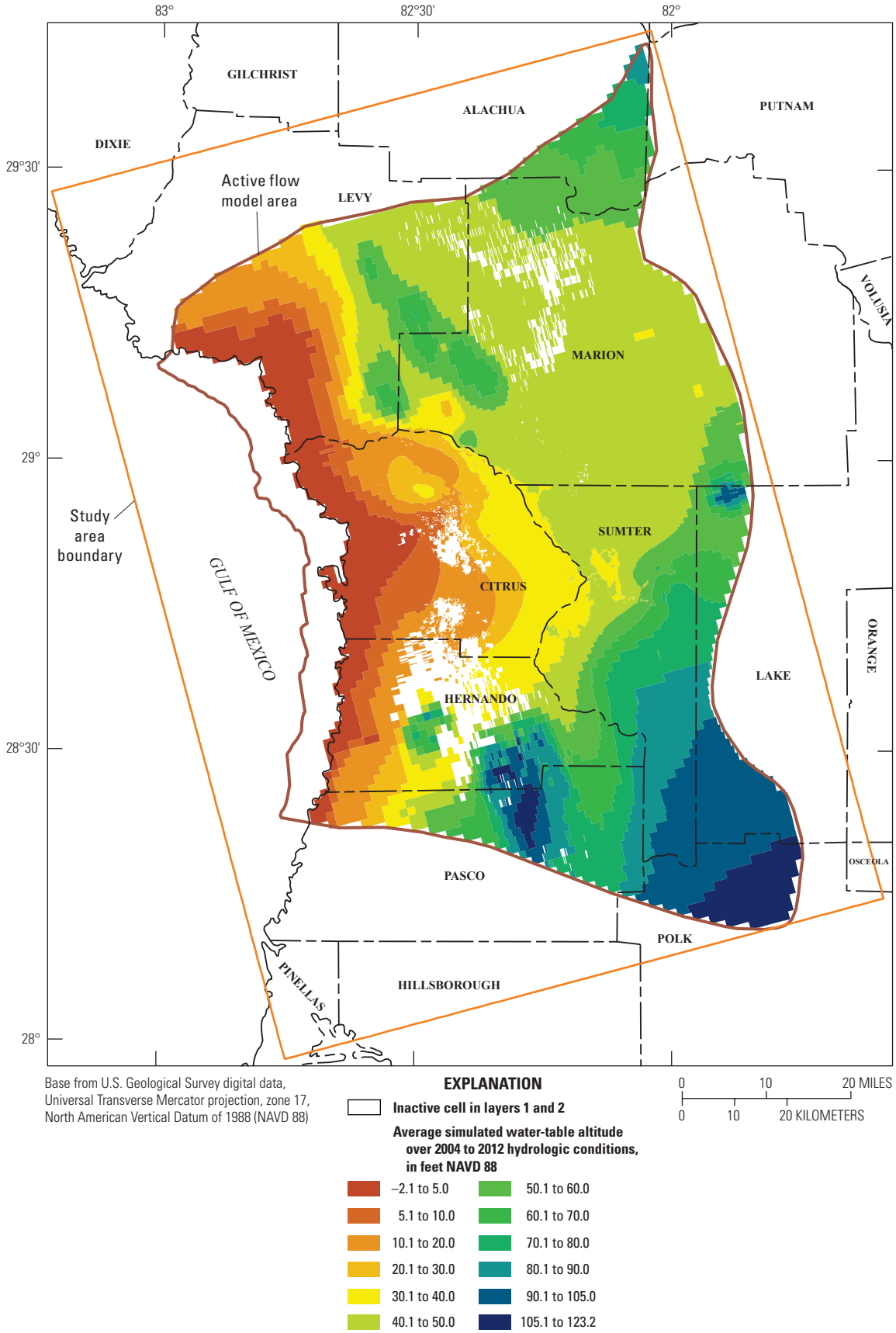

Figure 22. Calibrated water-table altitudes, averaged over 2004–12 hydrologic conditions, in the active flow model area.

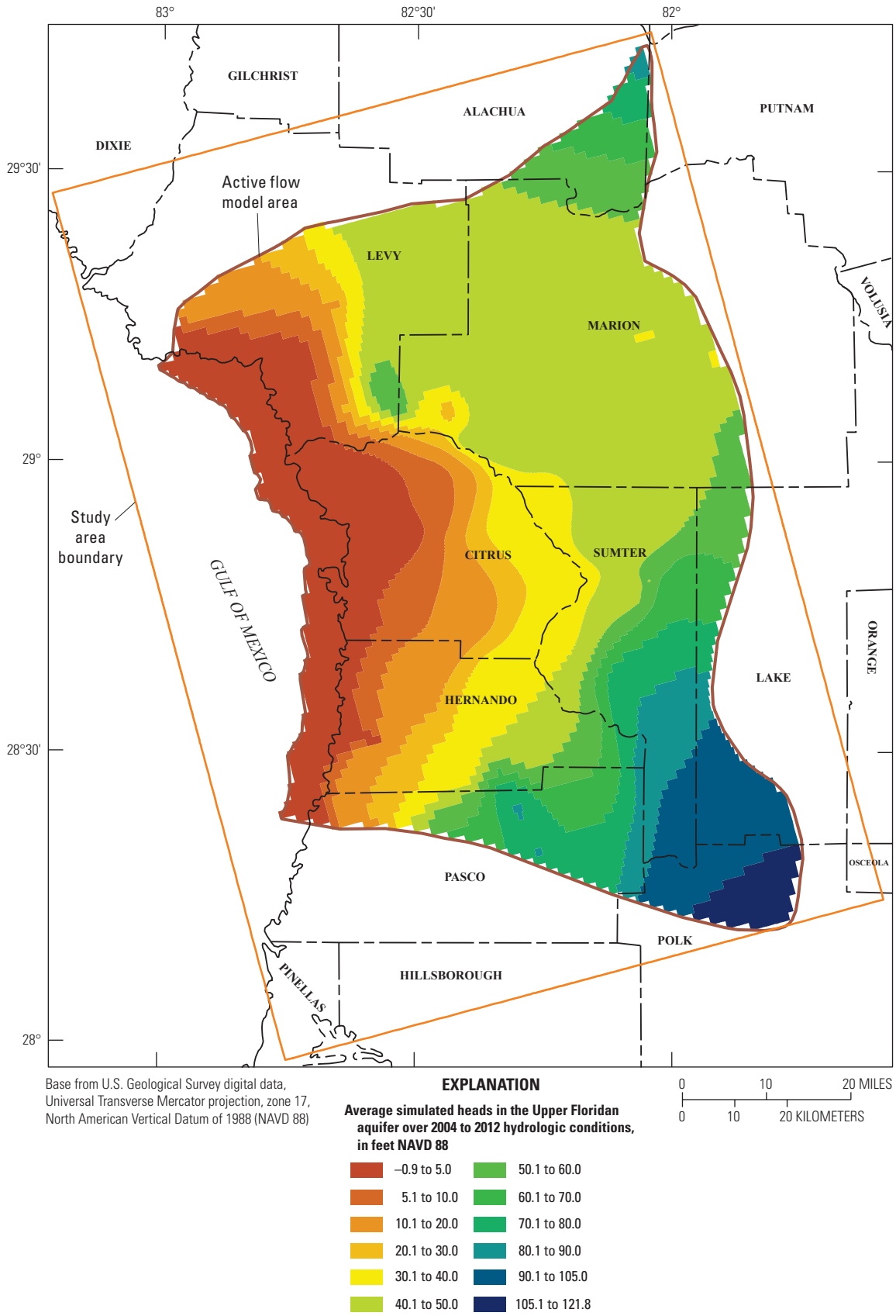

Figure 23. Calibrated heads in the Upper Floridan aquifer, averaged over 2004–12 hydrologic conditions, in the active flow model area.

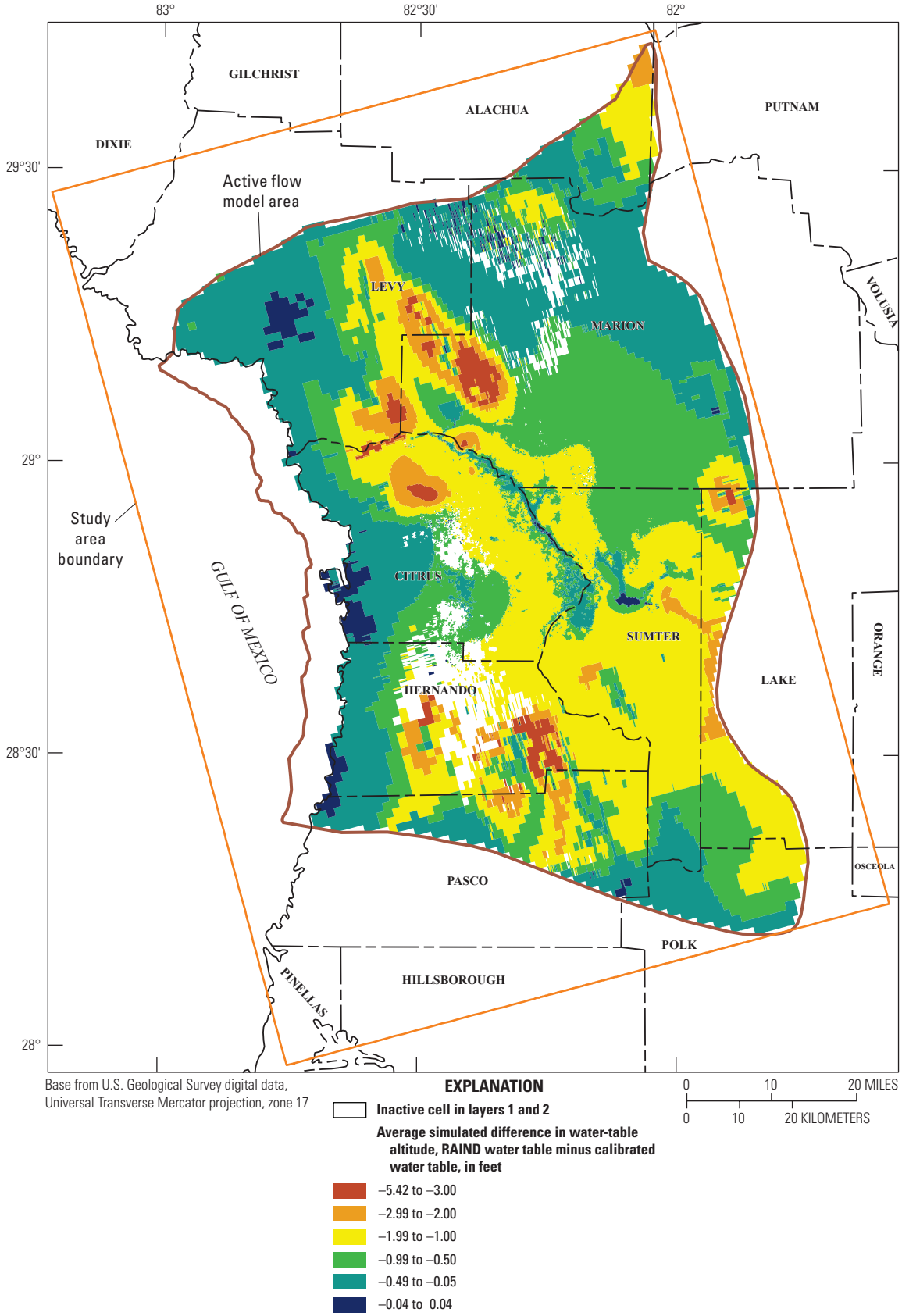

Figure 24. Simulated water-table altitudes in the active flow model area under the RAIND scenario minus calibrated altitudes for average 2004–12 hydrologic conditions.

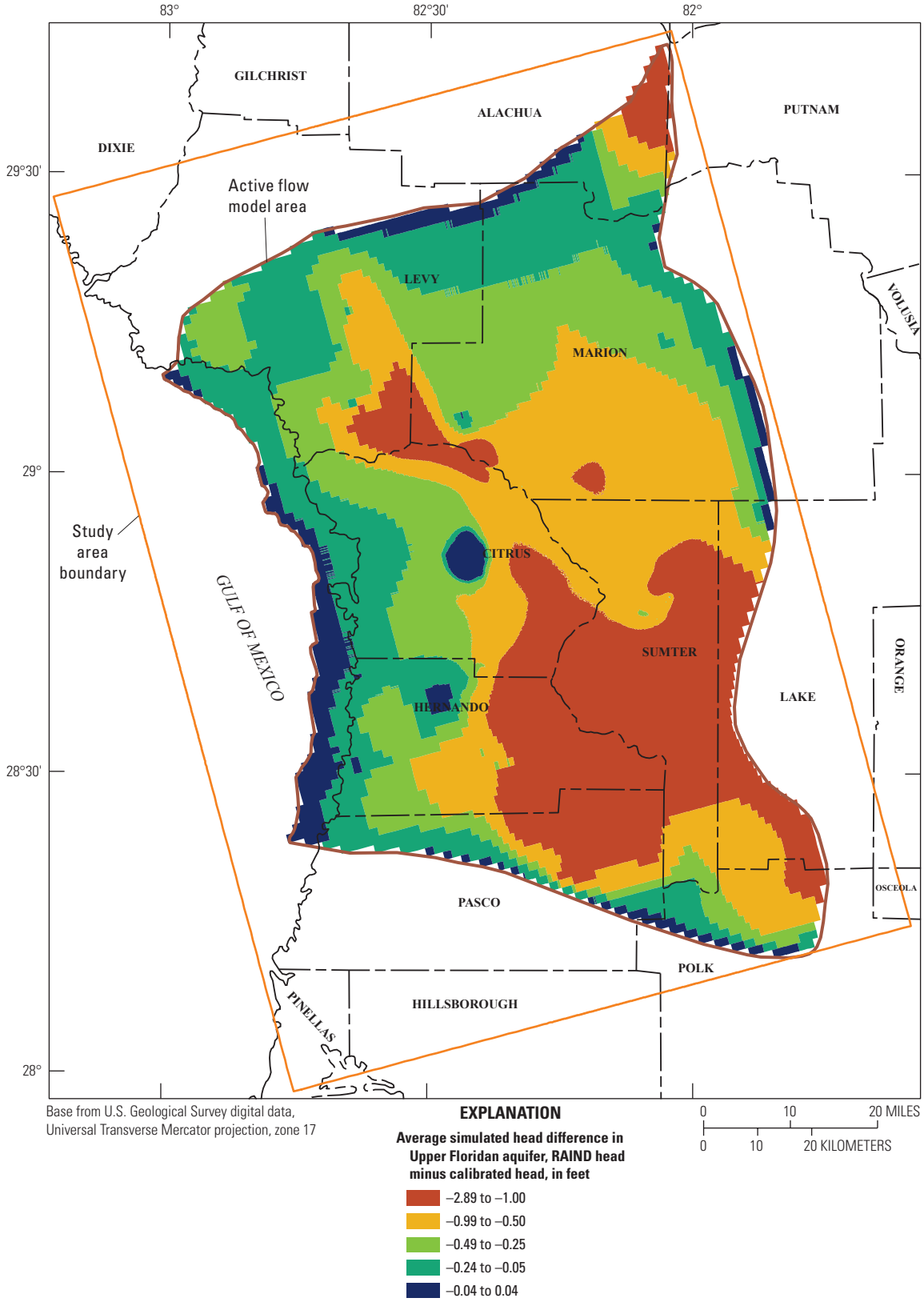

Figure 25. Simulated heads in the Upper Floridan aquifer in the active flow model area under the RAIND scenario minus calibrated heads for average 2004–12 hydrologic conditions.

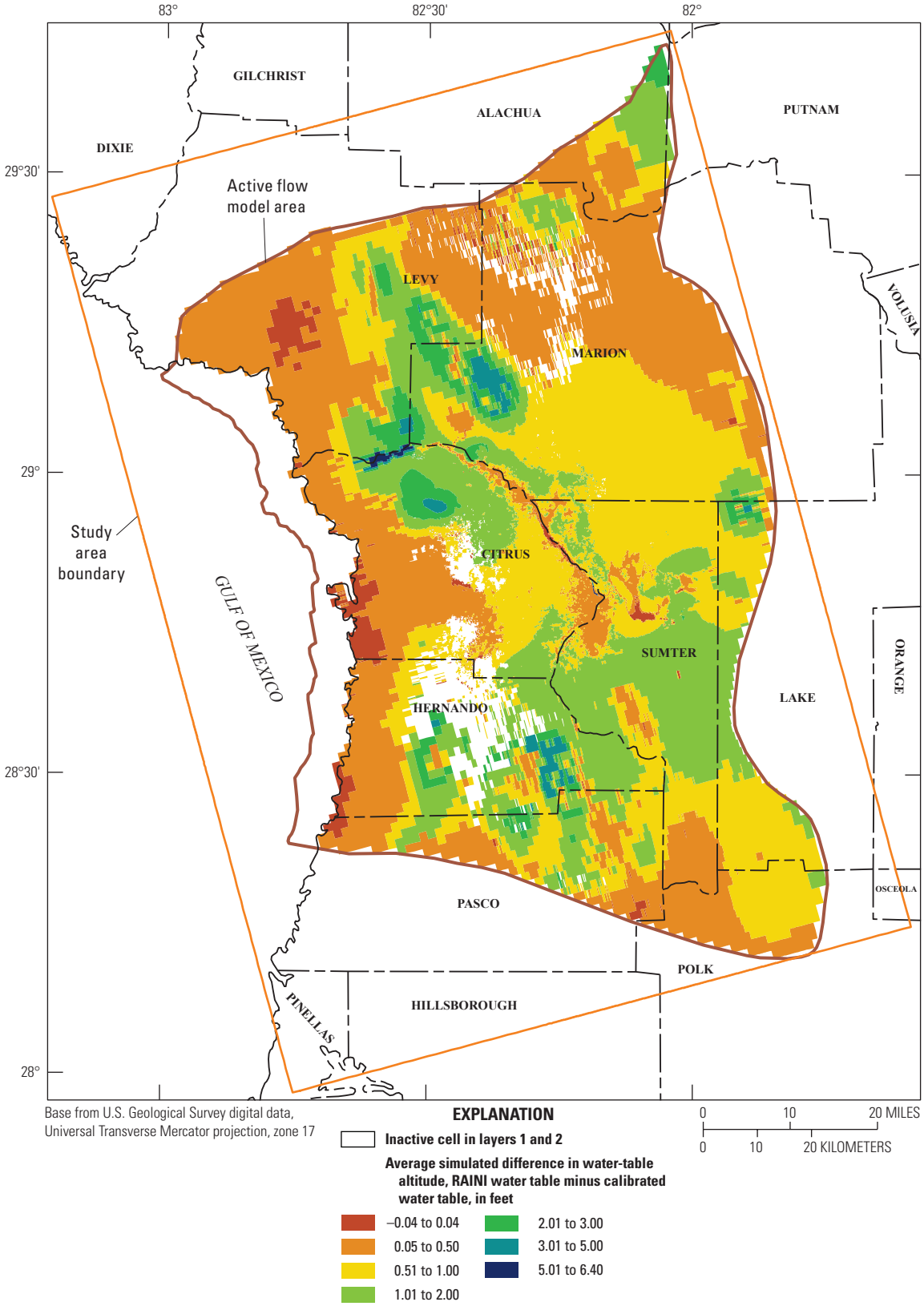

Figure 26. Simulated water-table altitudes in the active flow model area under the RAINI scenario minus calibrated altitudes for 2004–12 hydrologic conditions.

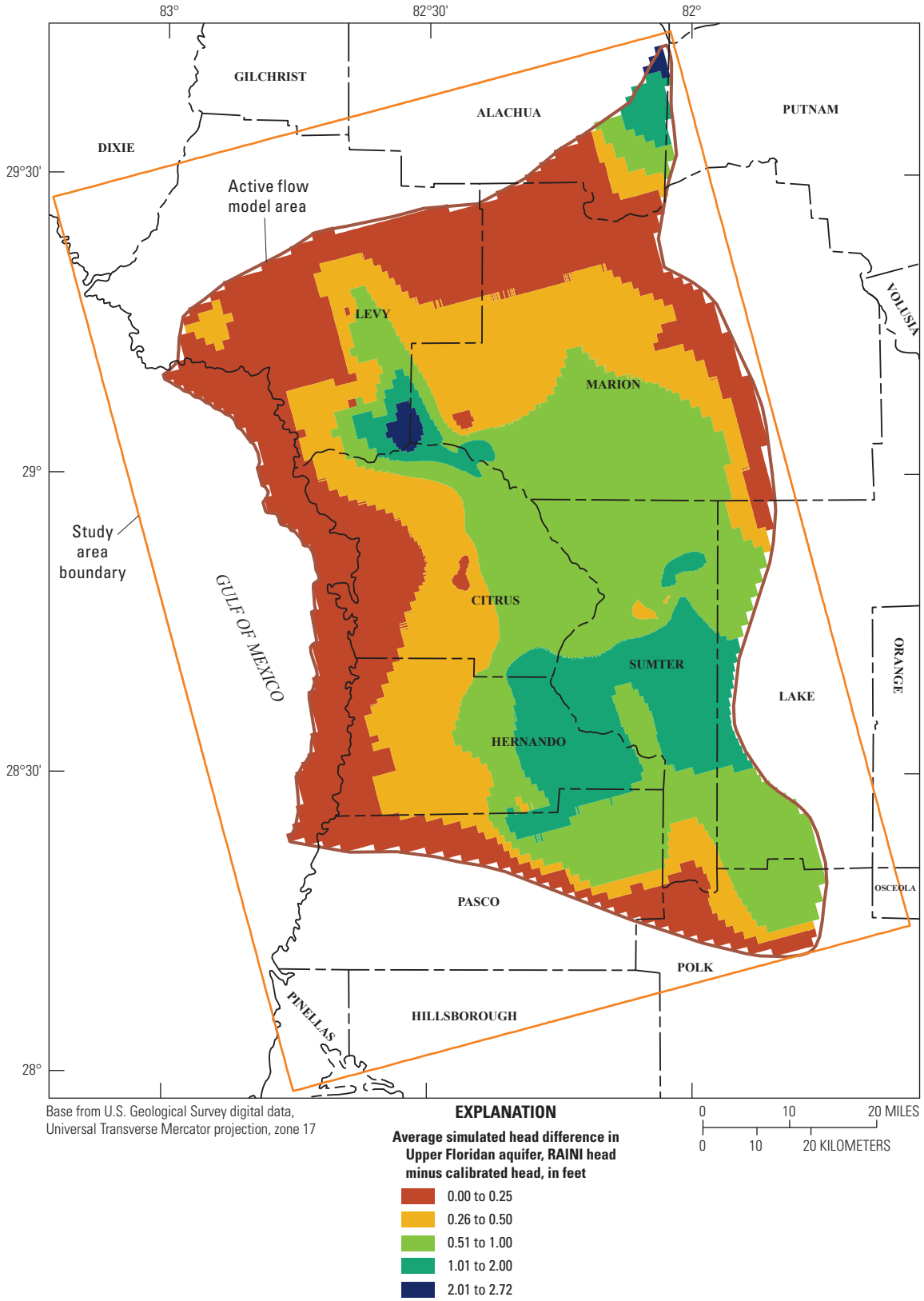

Figure 27. Simulated heads in the Upper Floridan aquifer in the active flow model area under the RAINI scenario minus calibrated heads for average 2004–12 hydrologic conditions.

Table 10. Average simulated spring flows, from all stress periods from 2004 to 2012, for each spring and each simulated scenario.

[All flow rates are in cubic feet per second. SRPNO, spring number from table 1.5; HSIMU, average spring flow simulated with calibrated model, over all stress periods from 2004 to 2012; RAIND, RAINI, spring flows from scenarios simulating rainfall rate decreases and increases, respectively; P2025, P2035, spring flows from scenarios simulating groundwater pumping projections for 2025 and 2035, respectively; NFCS, spring flows from simulating scenario of no flow through structures in the Tsala Apopka Lake Basin; NING, spring flows from simulating the removal of Inglis Dam and Inglis Bypass Spillway; Total, total average spring flow from all 91 springs]

SPRNO	HSIMU	RAIND	RAINI	P2025	P2035	NFCS	NING
1	3.7	3.1	4.2	3.6	3.6	3.7	3.7
2	28.5	27.3	29.6	28.5	28.5	28.5	28.5
3	2.2	1.8	2.5	2.2	2.2	2.2	2.2
4	0.4	0.2	0.5	0.4	0.4	0.4	0.4
5	492.2	468.9	513.7	488.4	484.7	492.0	491.6
6	3.0	2.7	3.3	3.0	3.0	3.0	3.0
7	221.2	216.2	225.9	220.6	220.0	221.2	230.7
8	320.8	315.4	325.8	320.1	319.5	320.8	332.7
9	13.7	12.6	14.9	13.6	13.4	13.7	16.0
10	28.6	27.2	30.0	28.5	28.3	28.6	31.7
11	13.5	12.4	14.5	13.4	13.2	13.5	14.8
12	7.2	6.9	7.4	7.1	7.1	7.2	4.3
13	6.7	6.4	6.9	6.6	6.6	6.7	5.6
14	4.9	4.7	5.1	4.9	4.8	4.9	4.4
15	3.8	3.6	3.9	3.8	3.8	3.8	3.8
16	3.8	3.3	4.2	3.7	3.7	3.7	3.7
17	1.3	1.1	1.4	1.3	1.3	1.3	1.3
18	5.9	5.3	6.3	5.8	5.8	5.8	5.8
19	6.3	6.1	6.5	6.3	6.3	6.3	6.3
20	4.0	3.8	4.1	3.9	3.9	3.9	3.9
21	2.3	2.2	2.4	2.3	2.3	2.3	2.3
22	4.1	4.0	4.2	4.1	4.1	4.1	4.1
23	1.5	1.4	1.6	1.5	1.5	1.5	1.5
24	4.1	4.0	4.2	4.1	4.1	4.1	4.1
25	413.9	388.5	437.8	411.5	409.3	412.8	412.2
26	12.2	11.9	12.4	12.1	12.1	12.1	12.1
27	4.0	3.8	4.2	4.0	4.0	4.0	4.0
28	4.5	4.3	4.7	4.5	4.5	4.5	4.5
29	4.1	3.8	4.4	4.1	4.0	4.1	4.1
30	2.2	2.0	2.3	2.1	2.1	2.2	2.2
31	2.1	2.0	2.2	2.1	2.1	2.1	2.1
32	2.2	2.1	2.3	2.2	2.2	2.2	2.2
33	2.1	2.0	2.3	2.1	2.1	2.1	2.1
34	2.2	2.1	2.4	2.2	2.2	2.2	2.2
35	38.0	34.6	40.8	37.7	37.4	37.8	37.9
36	7.6	6.9	8.2	7.5	7.4	7.5	7.6
37	7.6	6.9	8.3	7.6	7.5	7.6	7.6
38	14.8	13.3	16.0	14.6	14.5	14.7	14.7
39	83.7	73.2	93.2	82.8	81.8	83.3	83.3
40	12.3	11.9	12.6	12.2	12.2	12.3	12.3
41	4.1	3.9	4.2	4.1	4.0	4.1	4.1
42	4.1	3.9	4.3	4.1	4.1	4.1	4.1
43	85.4	81.6	88.8	85.1	84.8	85.3	85.3
44	5.0	4.6	5.3	4.9	4.9	5.0	5.0
45	4.1	3.8	4.4	4.1	4.1	4.1	4.1
46	59.2	54.1	63.8	58.8	58.3	59.0	59.1
47	4.6	4.4	4.8	4.6	4.6	4.6	4.6

Table 10. Average simulated spring flows, from all stress periods from 2004 to 2012, for each spring and each simulated scenario.—Continued

[All flow rates are in cubic feet per second. SRPNO, spring number from table 1.5; HSIMU, average spring flow simulated with calibrated model, over all stress periods from 2004 to 2012; RAIND, RAINI, spring flows from scenarios simulating rainfall rate decreases and increases, respectively; P2025, P2035, spring flows from scenarios simulating groundwater pumping projections for 2025 and 2035, respectively; NFCS, spring flows from simulating scenario of no flow through structures in the Tsala Apopka Lake Basin; NING, spring flows from simulating the removal of Inglis Dam and Inglis Bypass Spillway; Total, total average spring flow from all 91 springs]

SPRNO	HSIMU	RAIND	RAINI	P2025	P2035	NFCS	NING
48	3.7	3.5	3.8	3.7	3.6	3.7	3.7
49	7.2	6.2	8.1	7.1	7.0	7.2	7.2
50	2.8	2.6	3.0	2.8	2.8	2.8	2.8
51	3.1	2.4	3.7	3.0	2.9	3.1	3.1
52	3.4	2.6	4.0	3.3	3.2	3.4	3.4
53	10.7	10.2	11.1	10.7	10.6	10.7	10.7
54	0.3	0.3	0.3	0.3	0.3	0.3	0.3
55	4.1	3.9	4.2	4.1	4.1	4.1	4.1
56	36.2	35.0	37.2	36.1	36.0	36.2	36.2
57	16.9	12.4	20.8	16.4	16.0	16.7	16.8
58	38.4	33.8	42.5	38.0	37.6	38.3	38.3
59	2.1	2.0	2.2	2.1	2.1	2.1	2.1
60	3.1	2.8	3.3	3.1	3.0	3.1	3.1
61	6.8	6.4	7.1	6.7	6.7	6.8	6.8
62	7.3	6.9	7.6	7.2	7.2	7.3	7.3
63	6.1	5.7	6.3	6.0	6.0	6.1	6.1
64	16.8	15.8	17.6	16.7	16.6	16.7	16.7
65	5.4	4.8	5.9	5.3	5.3	5.4	5.4
66	3.4	2.8	3.9	3.4	3.3	3.4	3.4
67	3.4	2.7	3.9	3.3	3.3	3.3	3.4
68	0.9	0.5	1.3	0.9	0.8	0.9	0.9
69	1.3	1.1	1.4	1.3	1.3	1.3	1.3
70	3.3	3.0	3.6	3.3	3.3	3.3	3.3
71	4.4	4.0	4.7	4.3	4.3	4.4	4.4
72	4.2	3.8	4.5	4.1	4.1	4.1	4.1
73	1.3	1.1	1.4	1.3	1.3	1.3	1.3
74	7.2	6.2	8.0	7.1	7.0	7.2	7.2
75	2.3	0.8	6.2	2.0	1.7	2.3	2.3
76	5.1	4.8	5.4	5.1	5.1	5.1	5.1
77	19.3	17.9	20.4	19.1	19.0	19.2	19.2
78	3.4	3.3	3.5	3.4	3.4	3.4	3.4
79	5.3	4.9	5.6	5.3	5.2	5.3	5.3
80	12.4	11.9	12.9	12.4	12.3	12.4	12.4
81	43.5	42.1	44.6	43.1	42.9	43.4	43.4
82	115.0	111.7	118.0	114.1	113.3	114.9	115.0
83	4.3	4.2	4.3	4.3	4.2	4.3	4.3
84	0.6	0.6	0.6	0.6	0.6	0.6	0.6
85	1.3	1.2	1.3	1.2	1.2	1.2	1.2
86	2.8	2.7	2.9	2.8	2.8	2.8	2.8
87	2.6	2.6	2.6	2.6	2.6	2.6	2.6
88	3.2	3.0	3.4	3.2	3.2	3.2	3.2
89	2.7	2.6	2.8	2.7	2.6	2.7	2.7
90	1.0	0.3	2.2	0.9	0.8	1.0	1.0
91	0.5	0.1	1.2	0.4	0.4	0.5	0.5
Total	**2,392.8**	**2,263.4**	**2,512.1**	**2,377.5**	**2,363.3**	**2,389.0**	**2,412.2**

Table 11. Average simulated streamflows and stream stages over the 2004 to 2012 period at selected streamflow-gaging stations and for each simulated scenario.

[All flow rates are in cubic feet per second. All stages are in feet above the North American Vertical Datum of 1988 (NAVD 88). GAGEID, streamflow-gaging station number listed in table 5; AVSST and AVSFL, average stream stage and streamflow from scenario HSIMU, 2004 to 2012; RAIND, RAINI, stream stages and flows from scenarios simulating rainfall rate decreases and increases, respectively; P2025, P2035, stream stages and flows from scenarios simulating groundwater pumping for 2025 and 2035, respectively; NFCS, stream stages and flows from scenario simulating no flow through structures; NING, stream stages and flows from scenario simulating the removal of Inglis Dam and Inglis Bypass Spillway; Ave, average calculated for all stream gages]

Stream stages							
GAGEID	**AVSST**	**RAIND**	**RAINI**	**P2025**	**P2035**	**NFCS**	**NING**
02312558	38.69	38.69	38.69	38.69	38.69	38.69	38.69
02312598	38.59	38.58	38.60	38.59	38.59	38.59	38.59
02312600	38.42	38.40	38.44	38.42	38.42	38.47	38.42
02312700	37.61	37.59	37.63	37.61	37.61	37.61	37.61
02312719	37.20	37.14	37.20	37.20	37.20	37.20	37.20
02312722	33.96	33.92	33.96	33.96	33.96	33.96	33.96
02312762	33.46	33.37	33.47	33.46	33.46	33.46	33.46
02312764	40.04	40.04	40.05	40.04	40.04	40.04	40.04
02313000	28.35	28.23	28.39	28.35	28.34	28.34	28.35
02313100	27.31	27.30	27.31	27.31	27.31	27.31	27.31
02313200	27.13	27.05	27.17	27.13	27.13	27.13	27.13
02313231	0.31	0.30	0.31	0.31	0.31	0.31	2.77
Ave	**31.76**	**31.72**	**31.77**	**31.76**	**31.76**	**31.76**	**31.96**

Streamflows							
GAGEID	**AVSFL**	**RAIND**	**RAINI**	**P2025**	**P2035**	**NFCS**	**NING**
02312558	245.04	244.99	245.10	245.04	245.04	245.04	245.04
02312598	162.30	159.93	165.65	162.24	162.21	162.26	162.29
02312600	223.58	219.77	228.82	223.49	223.42	244.73	223.57
02312700	106.86	104.31	109.29	106.81	106.76	106.84	106.85
02312720	345.76	332.07	345.47	345.76	345.75	345.76	345.76
02312722	239.94	223.86	242.58	239.85	239.78	239.88	239.93
02312762	358.92	340.58	365.35	358.77	358.65	358.70	358.90
02312764	76.89	76.29	77.67	76.87	76.86	76.88	76.89
02313000	455.80	431.19	470.18	455.52	455.27	452.67	455.75
02313100	618.08	616.90	619.47	618.07	618.06	618.08	617.97
02313230	195.57	193.12	195.66	195.57	195.57	195.56	733.16
02313250	900.05	879.44	900.11	900.05	900.05	900.06	371.76
Ave	**327.40**	**318.54**	**330.45**	**327.34**	**327.29**	**328.87**	**328.16**

Table 12. Simulated annual inflows and outflows in the model area under scenarios RAINI and RAIND from 2004 to 2012.

[All linear volumetric flow rates are total annual rates, in inches per year, averaged over all active cells in the model area for scenarios RAINI and RAIND. RAINI, RAIND, total annual rainfall over land surface areas that are active in the flow model; STORI, STORD, combined flow rates from storage to/from the model layers; GWW3, groundwater withdrawals from the Upper Floridan aquifer; DRAIN3I, DRAIN3D, total spring flow from the Upper Floridan aquifer; GHBI, GHBD, net flow through the lateral boundaries of the model layers; STRM, sum of stream flow specified as inflow at stream segment 1, reach 1, specified runoff along stream segment 30 (fig. 1.3) equal to the simulated flow from Gum Springs, and specified runoff along stream segment 35 (fig. 1.3) equal to the simulated flow from Rainbow Springs; STRM_I, STRM_D, sum of simulated stream flows leaving the model area through stream segments 33, 38, 40, and 42 (fig. 1.3); SLEAKI, SLEAKD, surface leakage occurring at land surface depressions from the model layers; ET_I, ET_D, sum of evapotranspiration loss rate in the unsaturated zone, groundwater, and lakes; ROFF_I, ROFF_D, surface runoff simulated at active grid cells that do not drain to a simulated lake or stream; Ave, average for the 2004 to 2012 simulation period; HSIMUI, HSIMUD, rate differences between calibrated scenario HSIMU and scenarios RAINI and RAIND; Negative values indicate outflows, whereas positive values indicate inflows. Water balance in the model area is calculated from the equations RAINI+STORI+GWW3+DRAIN3I+GHBI+STRM+STRM_I+SLEAKI+ET_I+ROFF_I=0 and RAIND+STORD+GWW3+DRAIN3D+GHBD+STRM+STRM_D+SLEAKD+ET_D+ROFF_D=0]

Water Budget for Scenario RAINI										
Year	**RAINI**	**STORI**	**GWW3**	**DRAIN3I**	**GHBI**	**STRM**	**STRM_I**	**SLEAKI**	**ET_I**	**ROFF_I**
2004	65.42	-2.32	-1.03	-8.27	1.63	4.57	-5.84	-4.77	-31.02	-18.37
2005	65.27	-4.68	-0.99	-9.57	0.04	4.14	-5.18	-5.75	-35.75	-7.54
2006	42.08	7.38	-1.19	-8.15	-1.27	2.67	-3.13	-2.04	-30.88	-5.46
2007	52.47	0.29	-1.12	-7.19	-1.79	2.15	-2.42	-1.86	-32.05	-8.49
2008	59.87	-2.14	-1.07	-8.10	-1.70	2.33	-3.10	-3.11	-31.12	-11.87
2009	57.40	-1.29	-1.05	-7.91	-1.78	2.60	-3.10	-3.12	-31.84	-9.91
2010	56.11	1.53	-0.96	-8.51	-1.95	3.01	-3.75	-4.15	-32.80	-8.52
2011	52.56	1.71	-0.89	-7.27	-2.32	2.38	-2.63	-2.62	-31.67	-9.25
2012	61.03	-2.15	-0.91	-7.20	-0.98	3.05	-3.63	-3.36	-30.23	-15.62
Ave	**56.91**	**-0.19**	**-1.02**	**-8.02**	**-1.13**	**2.99**	**-3.64**	**-3.41**	**-31.93**	**-10.56**
HSIMUI	**5.17**	**0.27**	**0.00**	**0.38**	**0.78**	**0.00**	**0.02**	**0.71**	**1.04**	**1.97**

Water Budget for Scenario RAIND										
Year	**RAIND**	**STORD**	**GWW3**	**DRAIN3D**	**GHBD**	**STRM**	**STRM_D**	**SLEAKD**	**ET_D**	**ROFF_D**
2004	53.52	0.47	-1.03	-7.87	2.55	4.57	-5.76	-3.53	-29.91	-13.01
2005	53.41	-2.74	-0.99	-8.71	1.92	4.14	-5.02	-3.56	-34.28	-4.16
2006	34.43	7.17	-1.19	-7.40	0.20	2.67	-3.03	-1.31	-28.02	-3.51
2007	42.93	1.12	-1.12	-6.46	-0.24	2.15	-2.34	-1.11	-29.67	-5.26
2008	48.99	-2.08	-1.07	-7.19	0.13	2.33	-2.94	-1.70	-28.90	-7.57
2009	46.96	-1.09	-1.05	-7.08	-0.01	2.60	-2.98	-1.73	-29.35	-6.27
2010	45.91	1.04	-0.96	-7.54	0.00	3.01	-3.58	-2.35	-30.52	-5.01
2011	43.00	1.88	-0.89	-6.45	-0.78	2.38	-2.57	-1.63	-29.20	-5.73
2012	49.93	-1.90	-0.91	-6.35	0.71	3.05	-3.52	-1.95	-28.04	-11.03
Ave	**46.57**	**0.43**	**-1.02**	**-7.23**	**0.50**	**2.99**	**-3.53**	**-2.10**	**-29.77**	**-6.84**
HSIMUD	**-5.17**	**-0.35**	**0.00**	**-0.41**	**-0.85**	**0.00**	**-0.09**	**-0.60**	**-1.12**	**-1.75**

Simulated increases in groundwater pumping rates for 2025 and 2035 in northeast Pasco County caused the largest drawdowns in the surficial and Upper Floridan aquifers when compared to scenario HSIMU (figs. 31–34). Drawdowns in the surficial aquifer were caused by downward leakage induced by groundwater pumping from the Upper Floridan aquifer. The largest simulated water-level declines under scenario P2025 were 1.9 ft in the surficial aquifer and 1.7 ft in the Upper Floridan aquifer (figs. 31, 32). The largest declines under scenario P2035 were 2.1 ft in the surficial aquifer and 1.8 ft in the Upper Floridan aquifer (figs. 33, 34). Declines in rainfall of 10 percent caused greater declines in water levels and pool stages near the Tsala Apopka Lake Basin than projected increases in groundwater pumping rates for 2025 and 2035.

The average simulated annual spring flow under scenarios P2025 and P2035 scenarios, considering all 3,288 stress periods, were 2,378 and 2,363 ft^3/s, respectively, compared to the simulated flow of 2,393 ft^3/s under

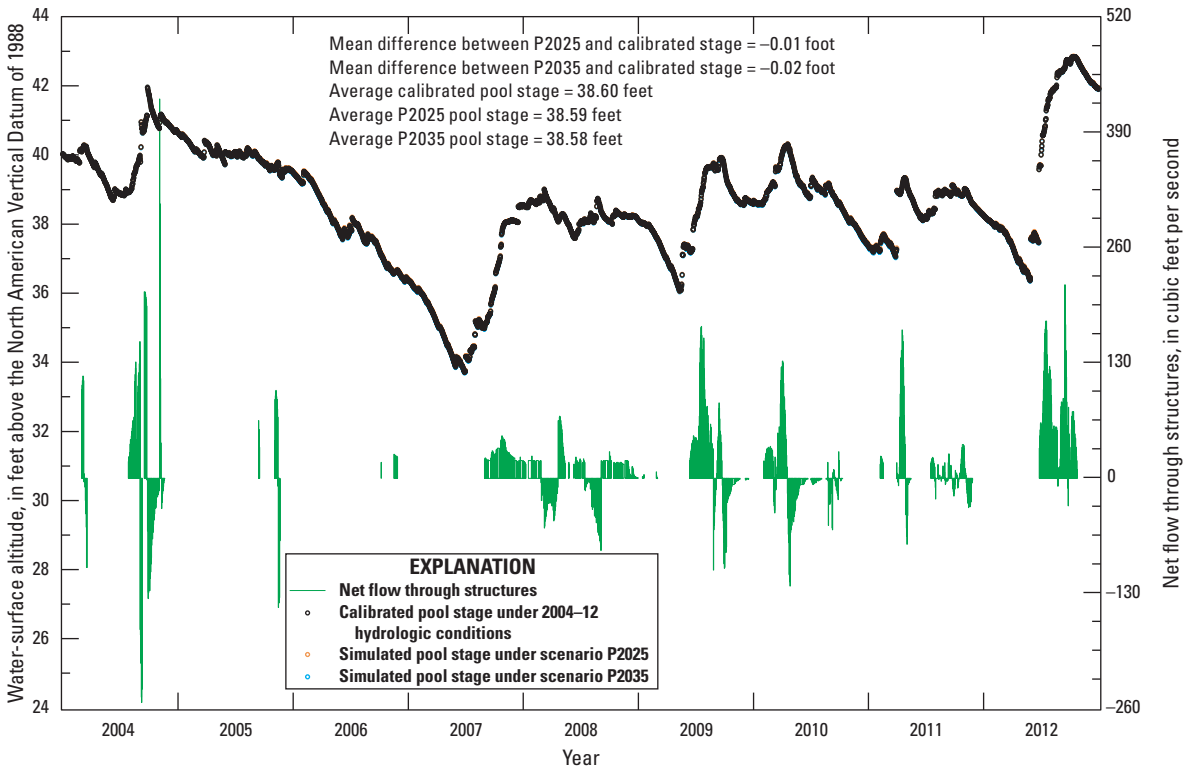

Figure 28. Simulated stage at Floral City pool under the P2025 and P2035 scenarios, and net daily flow through Floral City pool structures, for the 2004–12 period. The simulated pool stages for both scenarios are indistinguishable from the calibrated pool stage.

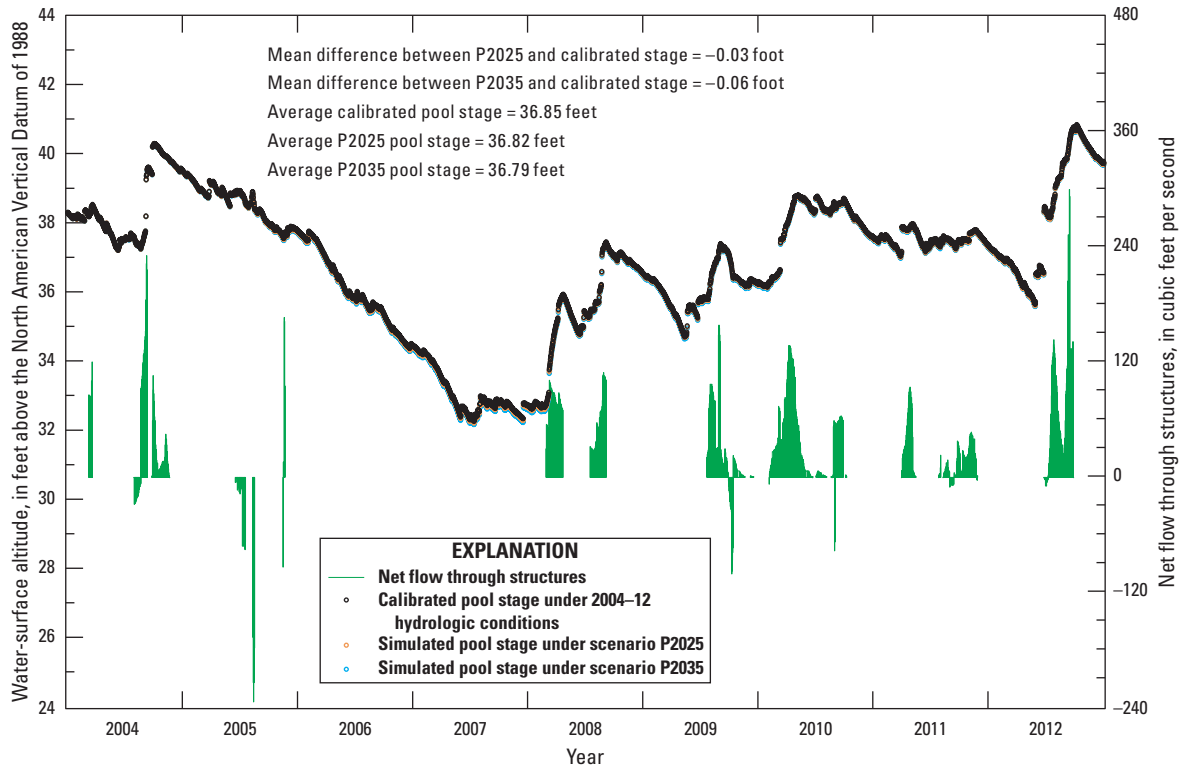

Figure 29. Simulated stage at Inverness pool under the P2025 and P2035 scenarios, and net daily flow through Inverness pool structures, for the 2004–12 period. The simulated pool stages for both scenarios are indistinguishable from the calibrated pool stage.

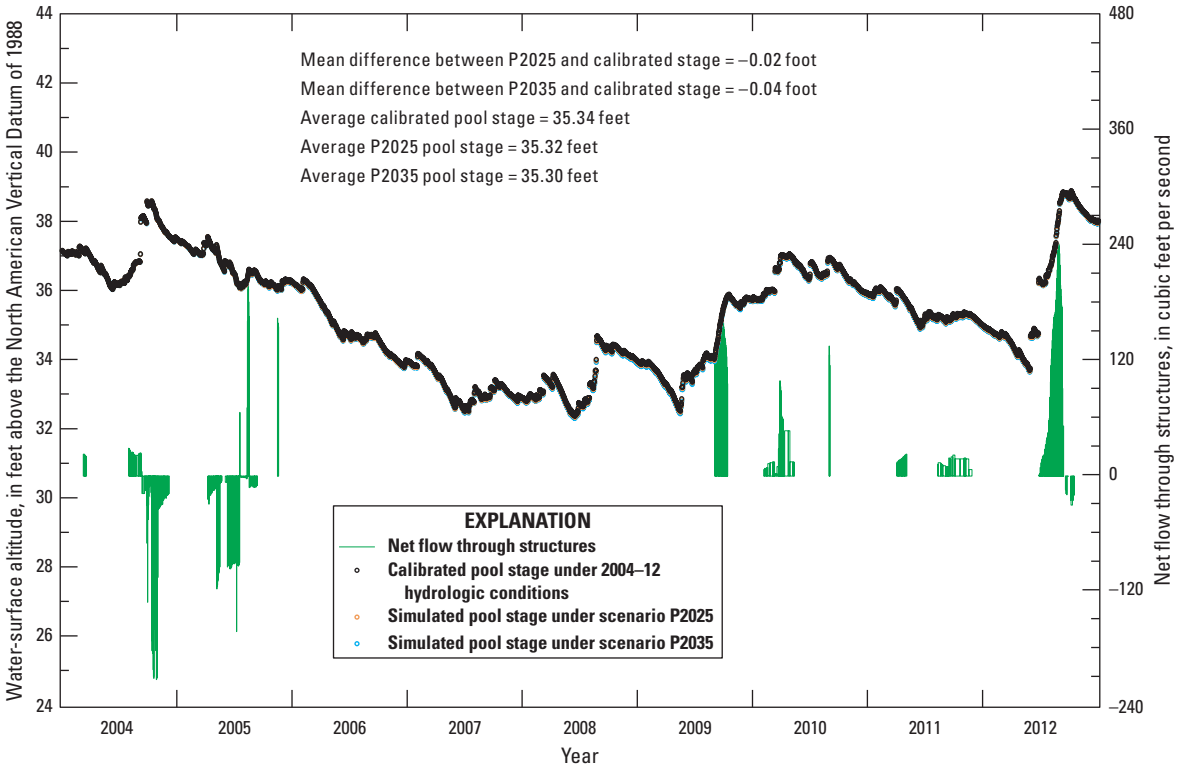

Figure 30. Simulated stage at Hernando pool under the P2025 and P2035 scenarios, and net daily flow through Hernando pool structures, for the 2004–12 period. The simulated pool stages for both scenarios are indistinguishable from the calibrated pool stage.

scenario HSIMU (table 10). These flows indicate that an increase in groundwater pumping rates of about 19 percent (scenario P2025), from the pumping rates in the calibrated model, caused simulated spring flow to decrease 0.6 percent and an increase in groundwater pumping of about 36 percent (scenario P2035) caused simulated spring flow to decrease 1.2 percent (tables 7, 10). Differences between the annual average simulated streamflow at stream reaches with streamflow-gaging stations in the Withlacoochee River and its tributaries from scenario HSIMU and flows simulated under scenario P2025 or P2035 were about 0.1 ft^3/s (table 11).

Simulating No Flow Through the Tsala Apopka Lake Pool Structures

Scenario NFCS was simulated to evaluate the effects of not allowing surface-water flow through the eight water-control structures in the Tsala Apopka Lake Basin for the 2004–12 period. Scenario NFCS isolates the interaction between rainfall and lakebed leakance, because under this scenario, no surface-water exchange occurs between any Tsala Apopka Lake pools. Compared to annual average simulated pool stages from the calibrated model HSIMU average declines in pool stage of 1.80, 1.91, and 0.51 ft (21.60, 22.92, and 6.12 in.) were simulated in the Floral City, Inverness, and Hernando pools, respectively under scenario NFCS (figs. 35–37). The largest stage decline occurred in the Inverness pool, because this pool had the largest simulated decrease in net surface-water flow, from a net annual average of 10 ft^3/s of inflow during scenario HSIMU to no flow under NFCS (table 13). Similarly, the largest simulated decreases in pool stages under scenario NFCS, compared to the simulated stages from scenario HSIMU, occurred at times when the net inflows in the simulation were the highest (figs. 28–30).

As the head difference between each pool and underlying aquifer increases, the downward leakage from the pool also increases. With less recharge from leakage, water levels in the surficial aquifer decreased in the Tsala Apopka Lake Basin under NFCS compared to scenario HSIMU. The largest decrease in water levels in the surficial aquifer under NFCS was about 2 ft (fig. 38). Heads in the Upper Floridan aquifer under NFCS decreased by at most 0.2 ft (fig. 39), less than water levels in the surficial aquifer, because the Upper Floridan has a much larger horizontal hydraulic conductivity than the surficial aquifer (figs. 1.31, 1.33). The impact of NFCS was limited to the Tsala Apopka Lake Basin and to a small distance away from the basin (figs. 38, 39).

The simulated daily average total spring flow under scenario NFCS was nearly the same as that for scenario HSIMU (table 10). A negligible (0.13 percent) drop in simulated daily average total spring flow, from 2,393 ft^3/s for scenario HSIMU to 2,389 ft^3/s for scenario NFCS (table 10), indicates that the changes in pool stages generated by not allowing water to flow through the structures of the Tsala Apopka Lake Basin were such that no substantive net changes

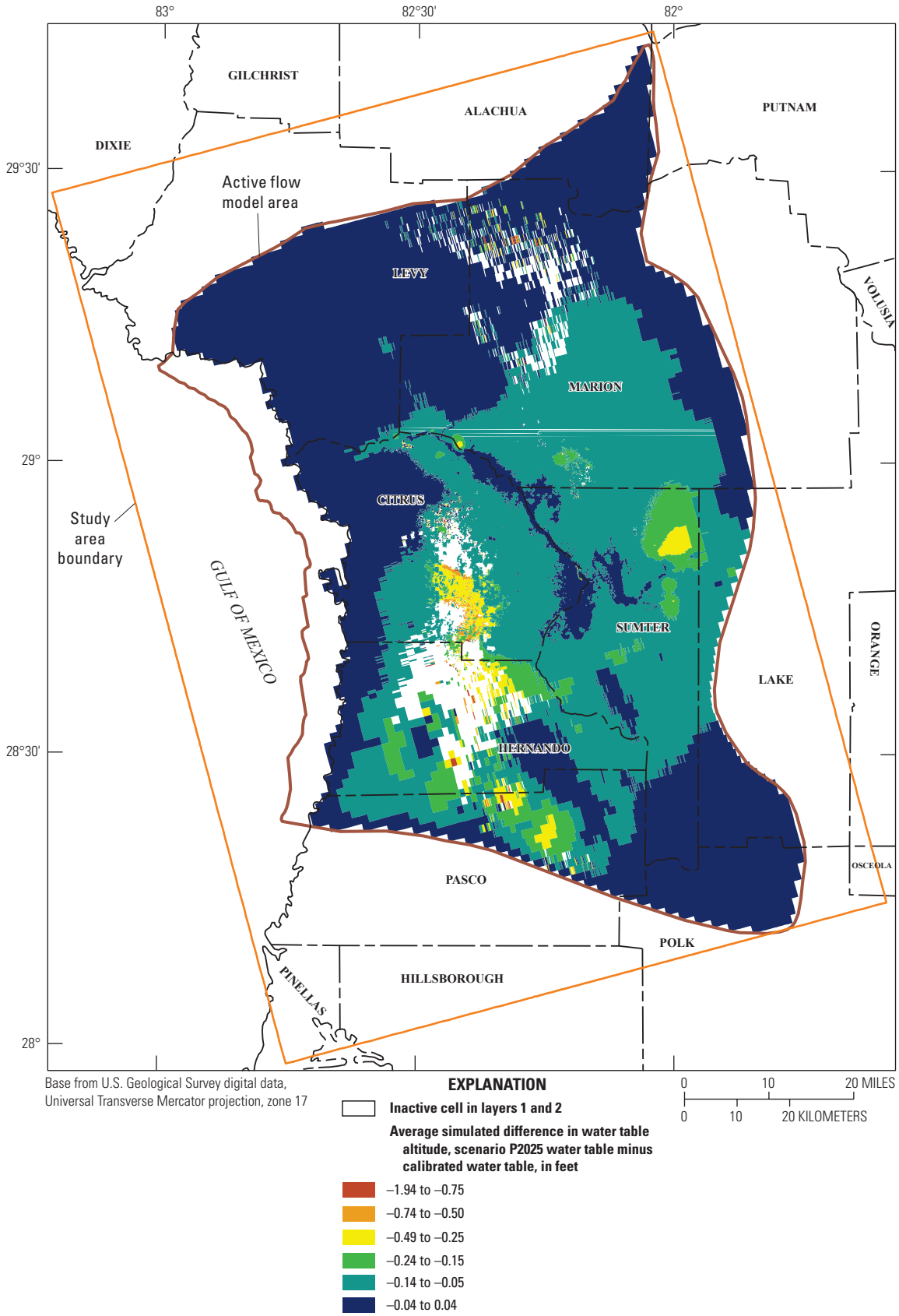

Figure 31. Simulated water-table altitudes in the active flow model area under the P2025 scenario minus HSIMU altitudes.

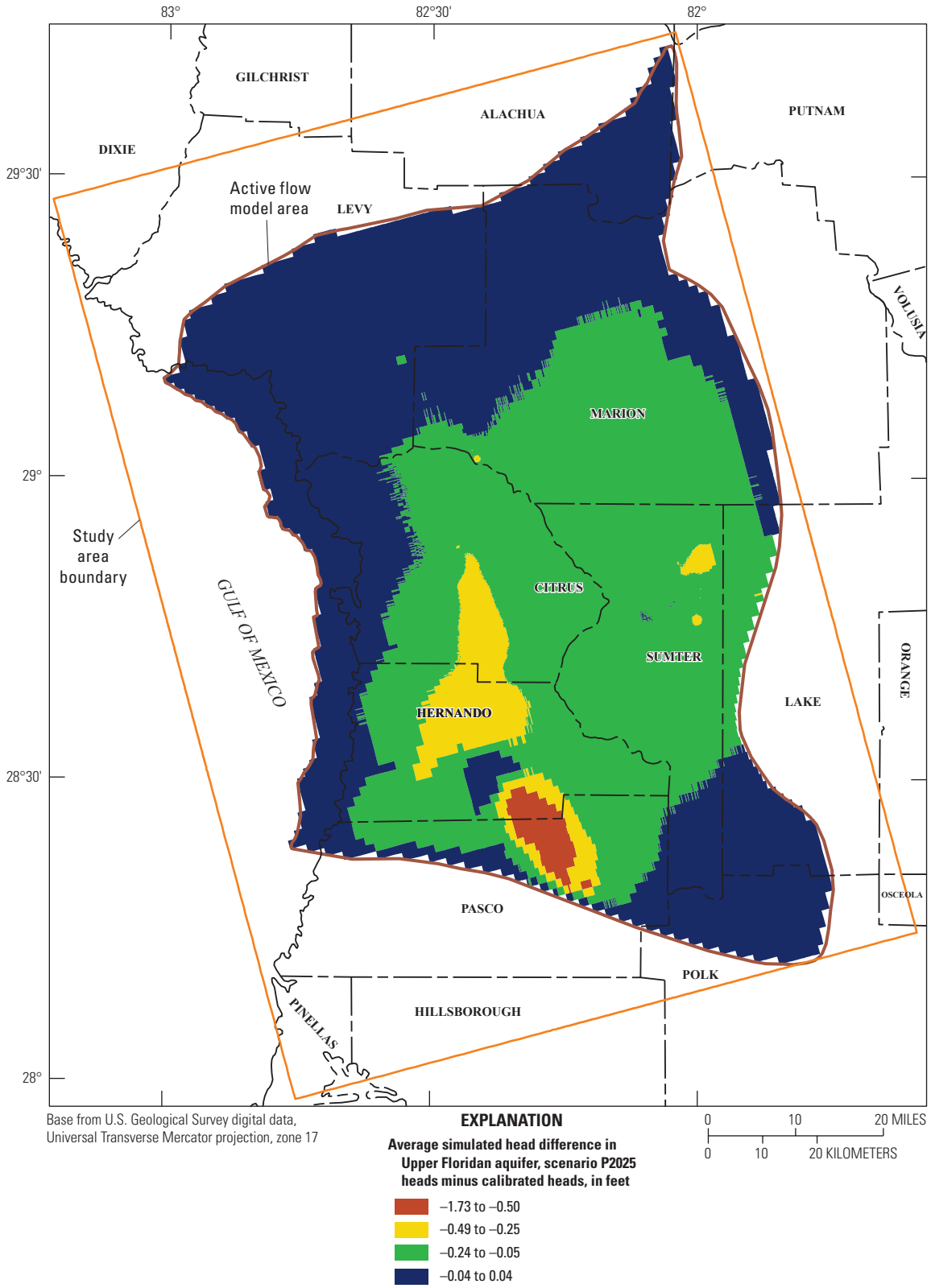

Figure 32. Simulated heads in the Upper Floridan aquifer in the active flow model area under the P2025 scenario minus HSIMU heads.

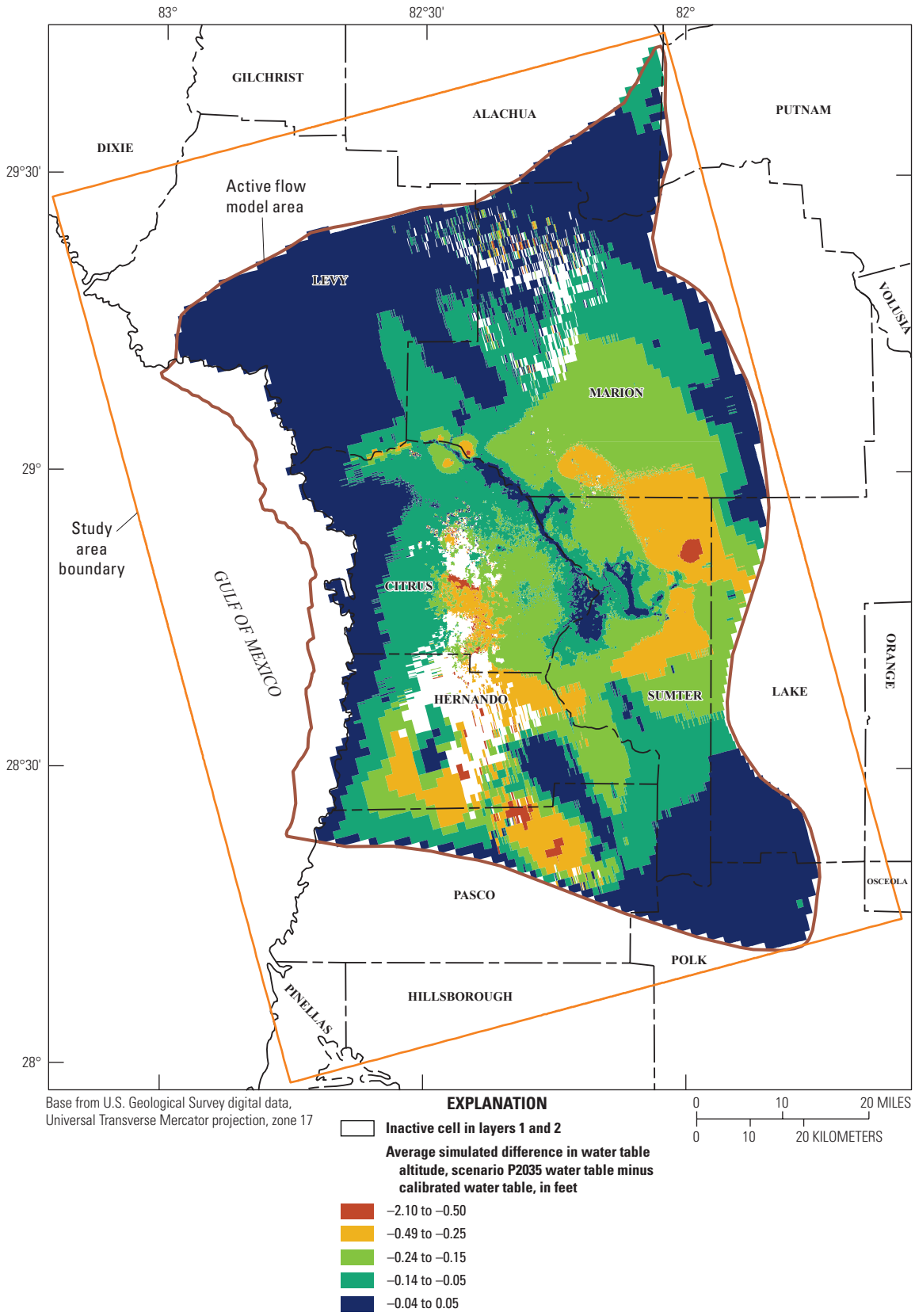

Figure 33. Simulated water-table altitudes in the active flow model area under the P2035 scenario minus HSIMU altitudes.

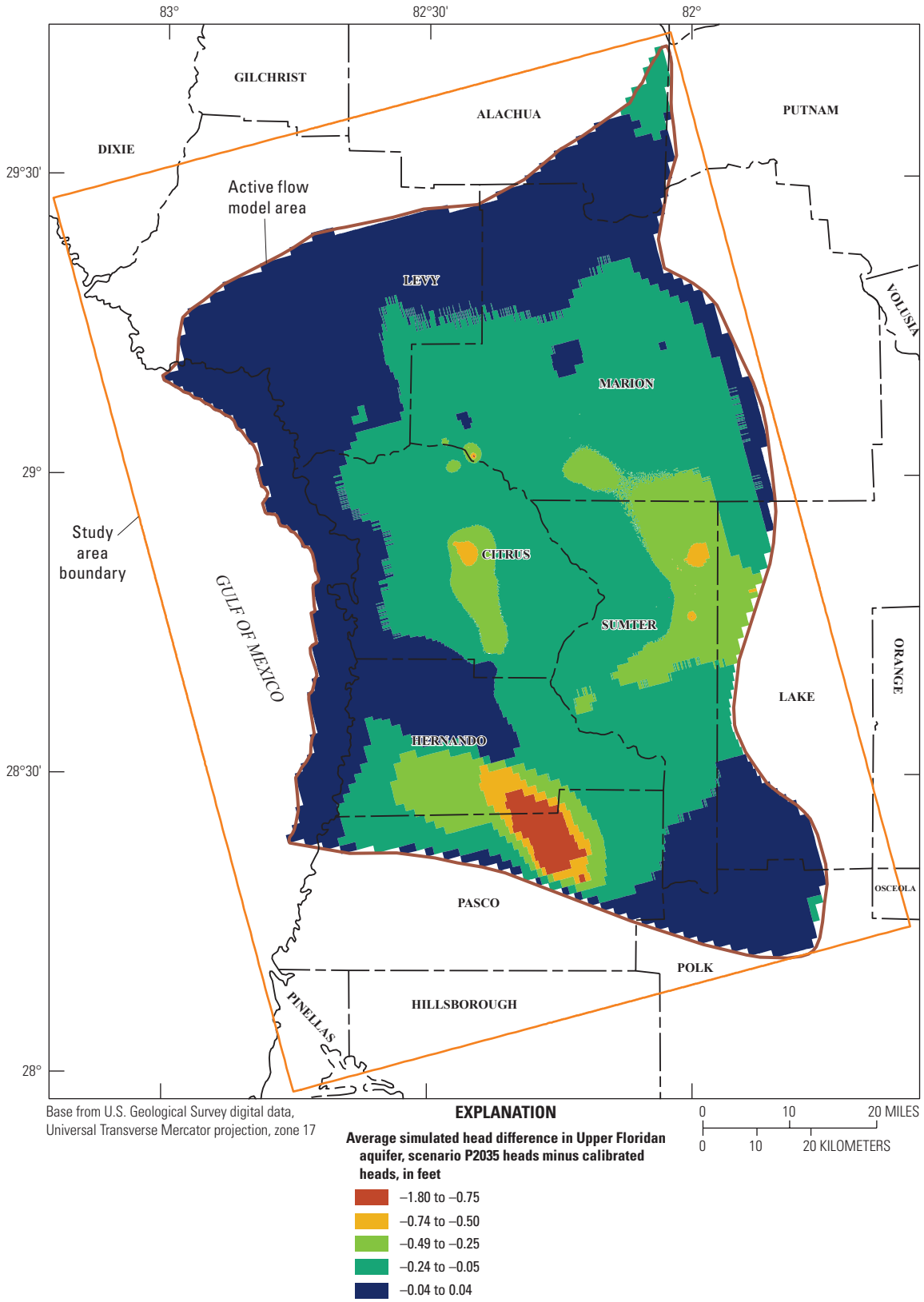

Figure 34. Simulated heads in the Upper Floridan aquifer in the active flow model area under the P2035 scenario minus HSIMU heads.

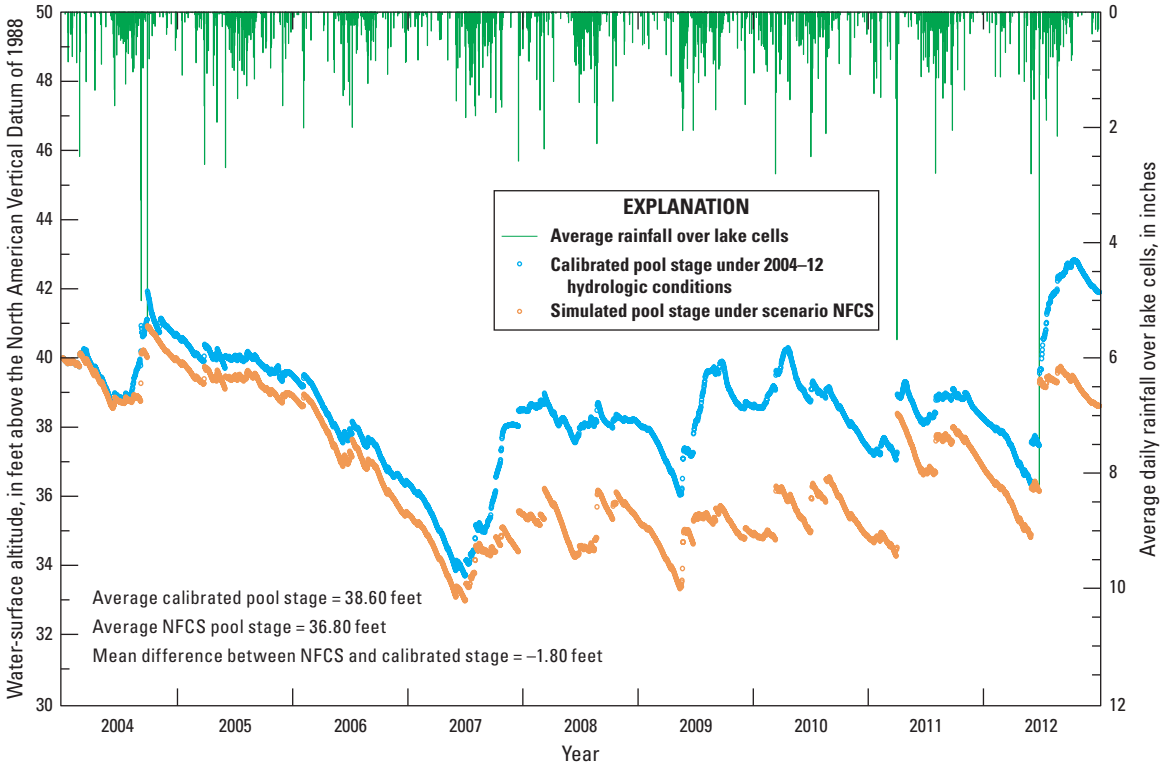

Figure 35. Simulated stage at Floral City pool under the NFCS scenario, and average daily rainfall over lake cells, for the 2004–12 period.

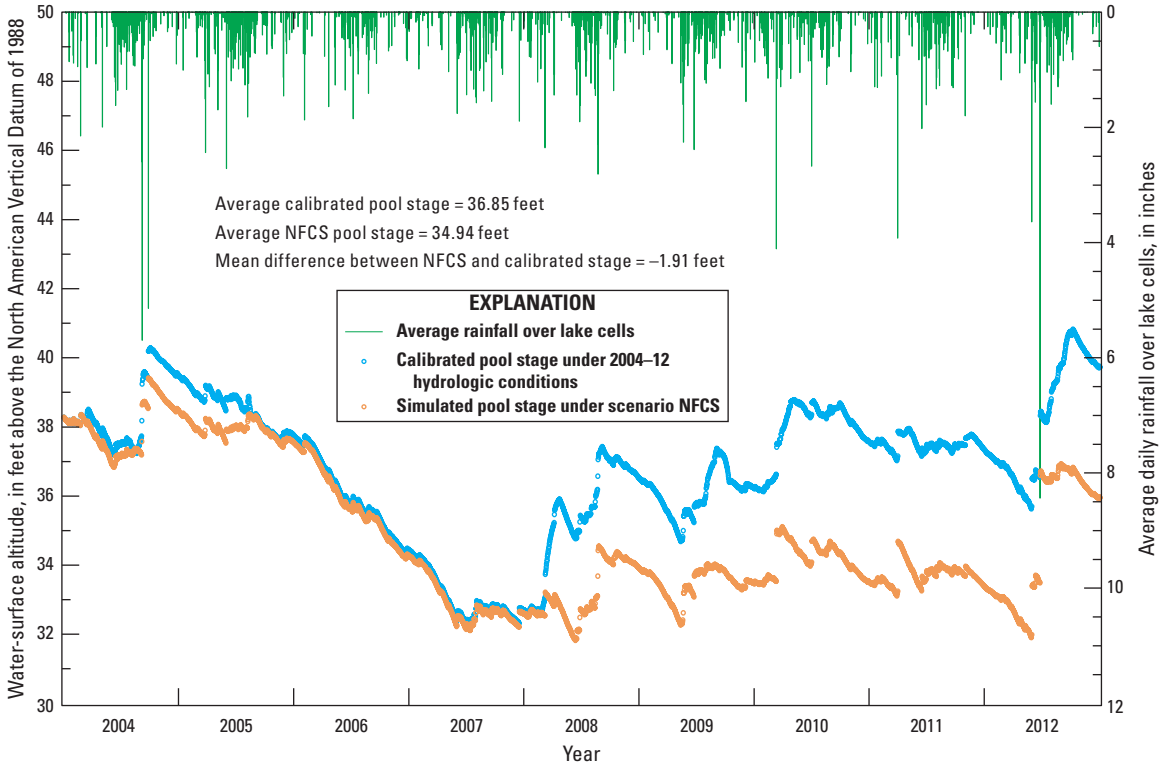

Figure 36. Simulated stage at Inverness pool under the NFCS scenario, and average daily rainfall over lake cells, for the 2004–12 period.

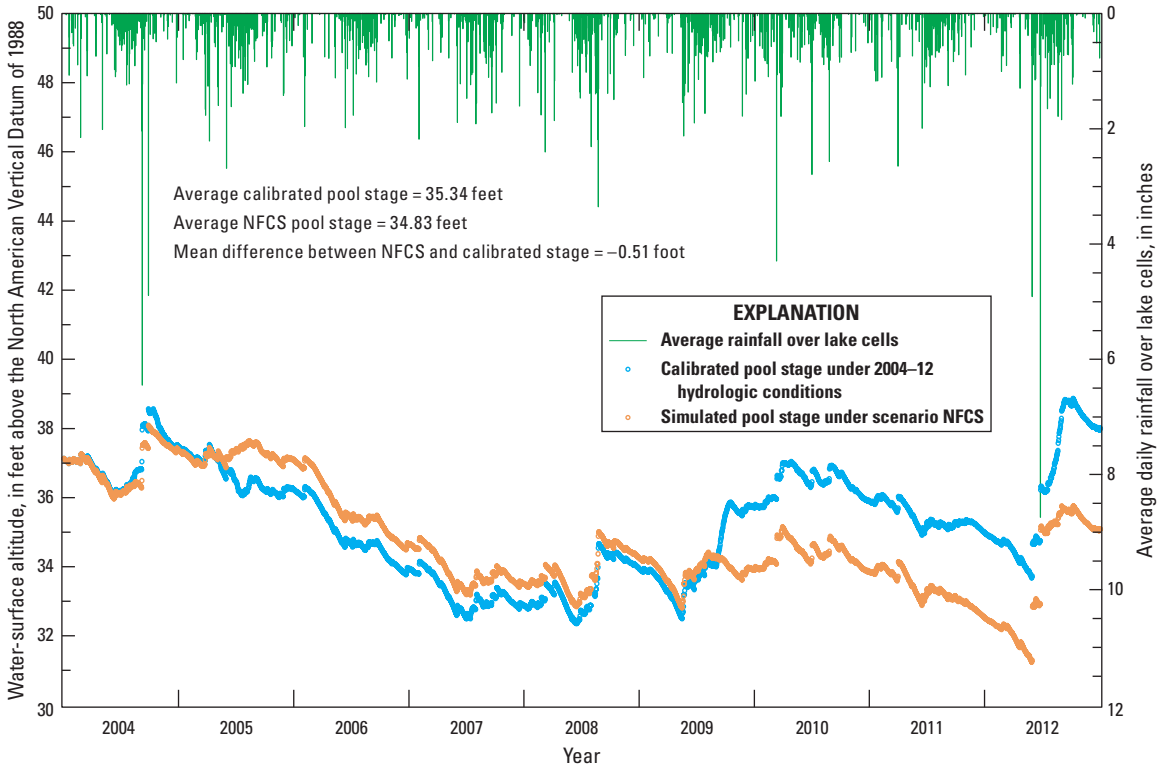

Figure 37. Simulated stage at Hernando pool under the NFCS scenario, and average daily rainfall over lake cells, for the 2004–12 period.

Table 13. Simulated changes in pool stage caused by not allowing flow through the Tsala Apopka Lake structures.

[NSWF, annual average net surface-water flow through the corresponding structures for each pool from calibrated model, 2004 to 2012, in cubic feet per second; DIFF_F, net flow through structures in each pool under scenario NFCS, in cubic feet per second; STAGE_CAL, simulated annual average pool stage from the calibration run, 2004 to 2012, in feet above the North American Datum of 1988 (NAVD 88); STAGE_NFCS, simulated annual average pool stage from scenario NFCS, 2004 to 2012, in feet above NAVD 88; DIFF_ft, DIFF_in, differences between the annual average pool stage for the calibration period and that from scenario NFCS, in feet and in inches, respectively, with negative numbers indicating a stage drop from calibration and positive numbers indicating a stage rise]

Descriptor	Floral City pool	Inverness pool	Hernando pool
NSWF	4.63	10.04	3.73
DIFF_F	0.00	0.00	0.00
STAGE_CAL	38.60	36.85	35.34
STAGE_NFCS	36.80	34.94	34.83
DIFF_ft	-1.80	-1.91	-0.51
DIFF_in	-21.60	-22.92	-6.12

in Upper Floridan aquifer heads were produced. A mix of small increases and decreases in Upper Floridan aquifer heads beneath the Tsala Apopka Lake Basin, caused by the small increases or decreases in downward leakage to the aquifer, resulted in no substantive net increase or decrease in spring flow.

The main difference in simulated streamflow under NFCS was an increase of about 21 ft^3/s, or 9.4 percent increase relative to scenario HSIMU, in daily average flow at the Withlacoochee River near Floral City (table 11, station 02312600 in fig. 18). Stream segment 17 in the Withlacoochee River (fig. 1.3, fig. 18) had a daily average increase in simulated streamflow because no flow from the Withlacoochee River was diverted to the Floral City pool under scenario NFCS. The daily average simulated streamflow at the Withlacoochee River near Rutland (table 11, segment 25 in fig. 1.3, station 02312722 in fig. 18), under scenario NFCS, was nearly equal to that from scenario HSIMU. This suggests that the upstream average daily streamflow increase of 21 ft^3/s from scenario NFCS resulted in additional downward leakage to the aquifer through the streambed between stations 02312600 and 02312722, because under both scenarios the outflow at station 02312720 (fig. 18) was the same.

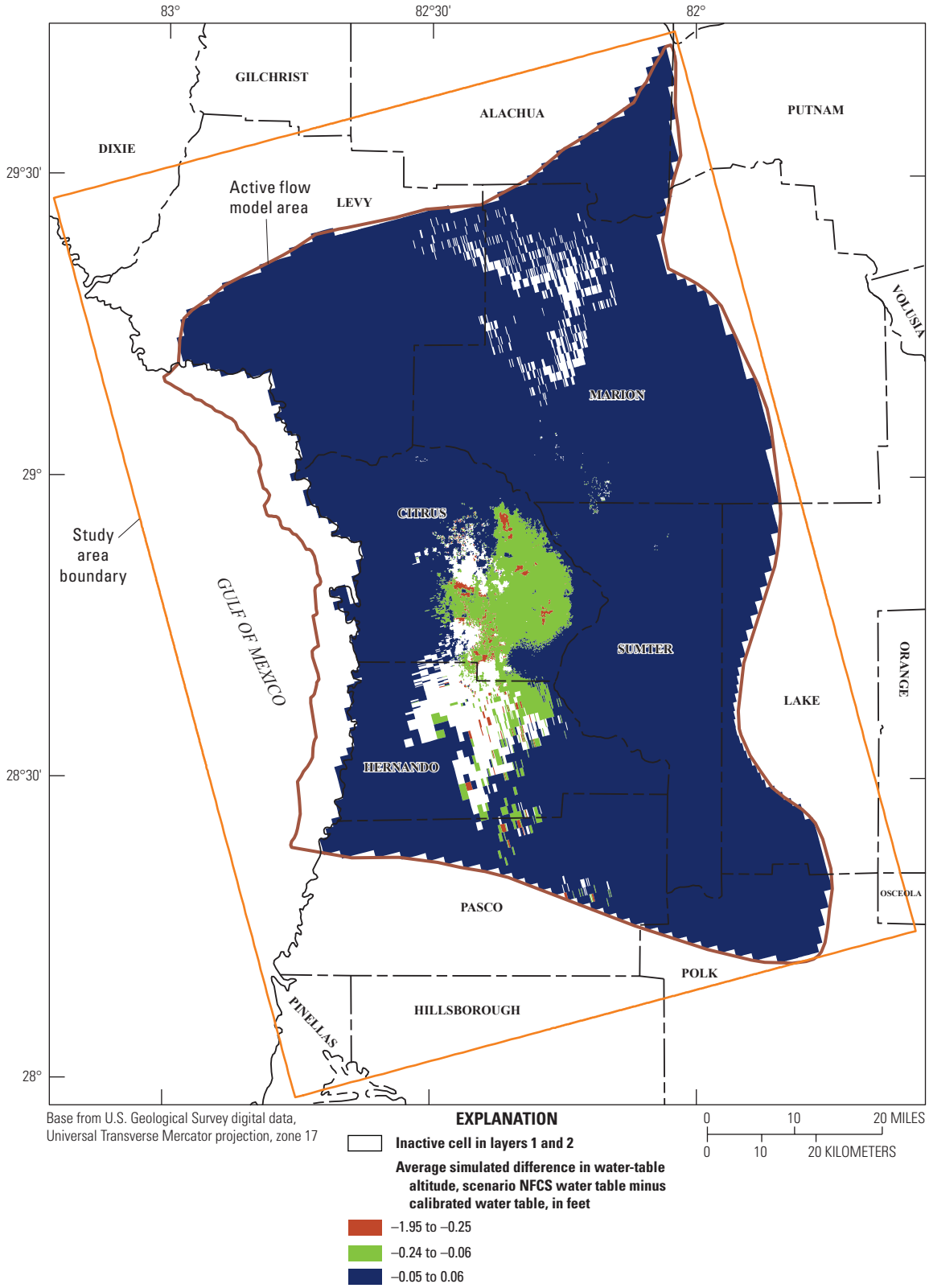

Figure 38. Simulated water-table altitudes in the active flow model area under the NFCS scenario minus HSIMU altitudes.

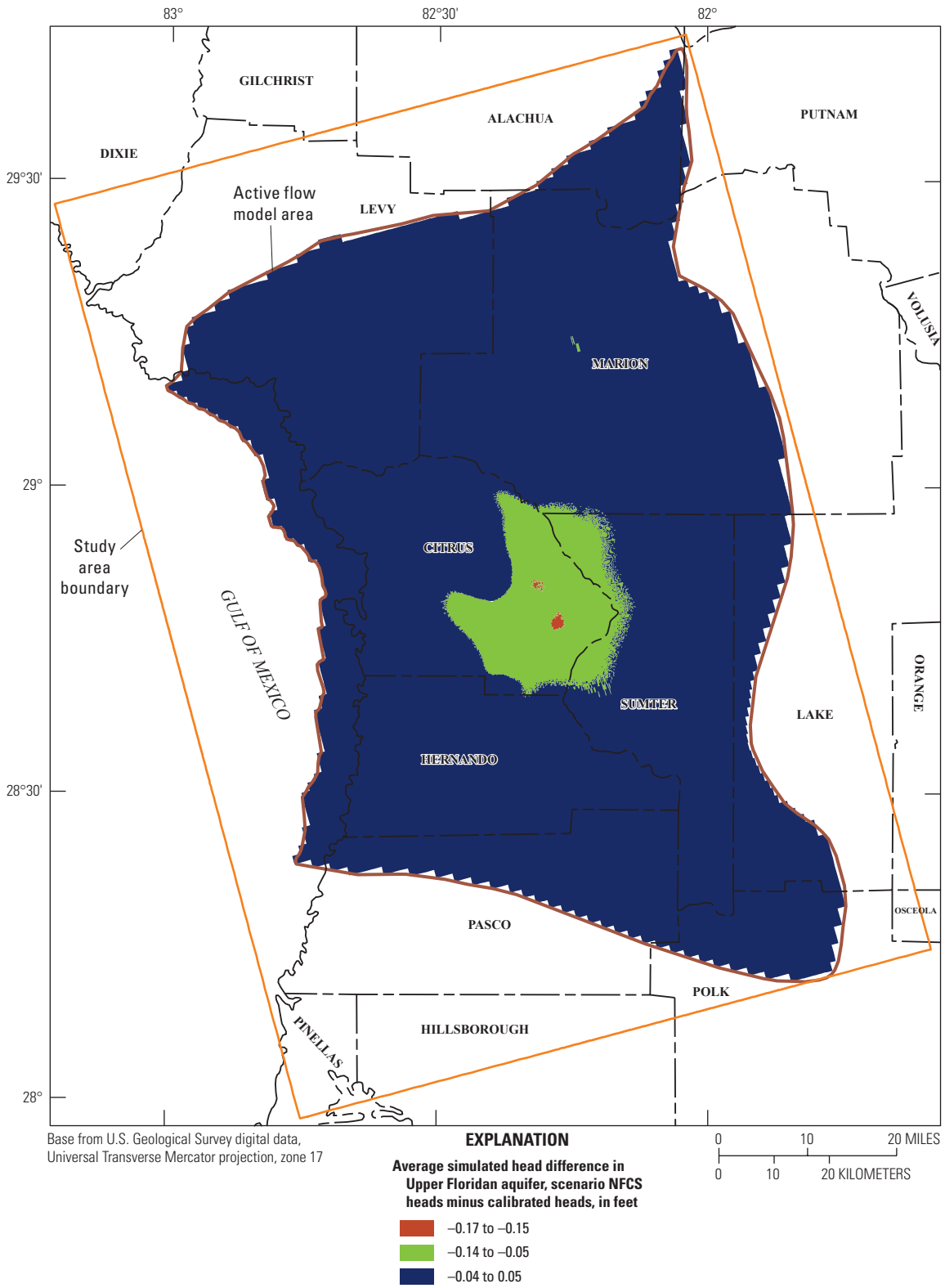

Figure 39. Simulated heads in the Upper Floridan aquifer in the active flow model area under the NFCS scenario minus HSIMU heads.

Simulating the Removal of Inglis Dam and Inglis Bypass Spillway

To evaluate the potential effects that water-control structures in Lake Rousseau have on lake stages, groundwater levels, flow at Rainbow Springs (spring numbers 7–11 in fig. 13), and streamflows, the removal of the Inglis Dam and the Inglis Bypass Spillway (scenario NING) was simulated. This scenario allows free flow from Lake Rousseau to stream segments 38 and 40 from segments 37 and 39, the respective segment numbers for the two structures (fig. 1.3). Simulation results indicated that the annual average stage for Lake Rousseau, during the 2004–12 period, was 11.8 ft lower under scenario NING compared to scenario HSIMU (fig. 40). The implementation of scenario NING caused no detectable stage changes in the Tsala Apopka Lake pools and small stage changes at stations located upstream from Lake Rousseau (table 11).

The largest decline in water levels in the surficial aquifer caused by implementing scenario NING was 4.7 ft and occurred near Lake Rousseau (figs. 1 and 41). The largest decline in heads in the Upper Floridan aquifer was about 1 ft (fig. 42), also near Lake Rousseau. The decline in water levels in the surficial aquifer was caused by a reduction in downward leakage to the aquifer, which also resulted in lower heads in the Upper Floridan aquifer.

Total spring flow increased 19.4 ft^3/s under scenario NING compared to total calibrated spring flow from scenario HSIMU (table 10). In particular, there was an increase in flow at Rainbow Springs (spring numbers 7–11 in table 10) of 28 ft^3/s, an increase of 4.7 percent from scenario HSIMU. The simulated flow at Rainbow Springs increased under scenario NING, because the decline in stage at Lake Rousseau caused a decline in stage along the Rainbow Springs run, which in turn caused an increase in flow to the stream. The small increase in difference between stream stage and head in the Upper Floridan aquifer caused this increase in flow at Rainbow Springs. Combined flow through the Inglis Dam and Inglis Bypass Spillway was 1,096 ft^3/s for scenario HSIMU, compared to 1,105 ft^3/s under scenario NING, as indicated by the combined flow through stations 02313230 and 02313250 (table 11). The increase in streamflow through these streamflow-gaging stations under NING was less than 0.8 percent.

Model Limitations

Surface-water/groundwater flow simulations generally are based on conceptual models that are simplified representations of complex, heterogeneous flow systems. The lack of sufficient measurements to fully describe the spatial and temporal variability of hydrologic conditions and the spatial variability of hydraulic properties throughout the model area often necessitate these simplifications. Approximations of hydraulic properties such as isotropy, spatial uniformity,

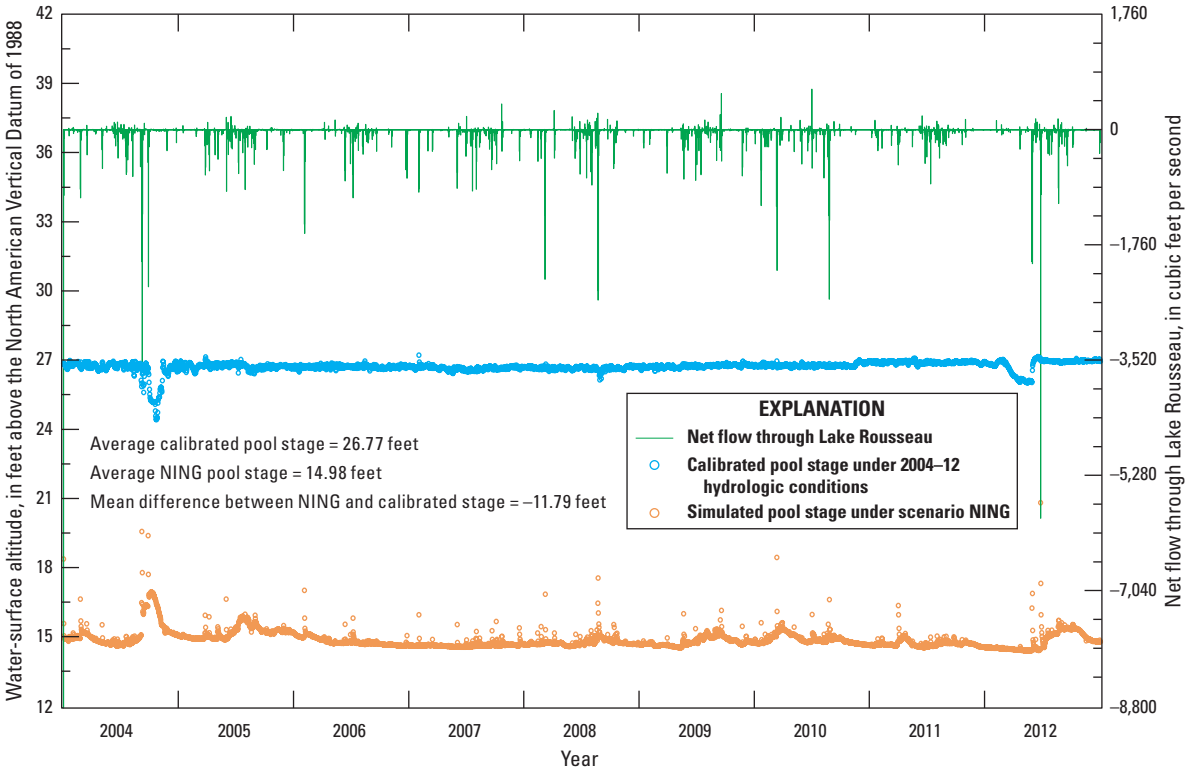

Figure 40. Simulated stage at Lake Rousseau under the NING scenario, and net daily flow through Lake Rousseau structures, 2004 to 2012.

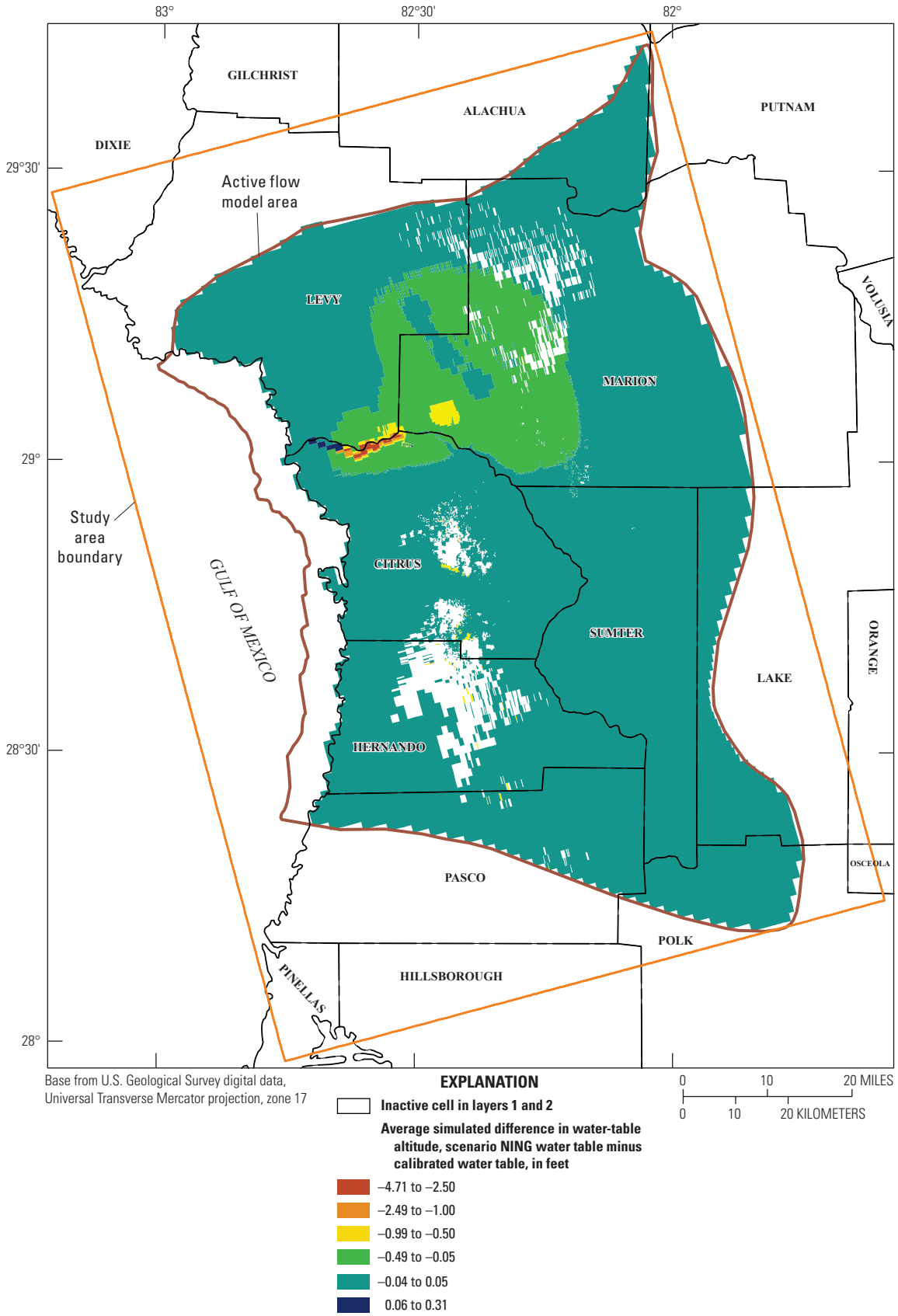

Figure 41. Simulated water-table altitudes in the active flow model area under the NING scenario minus HSIMU altitudes.

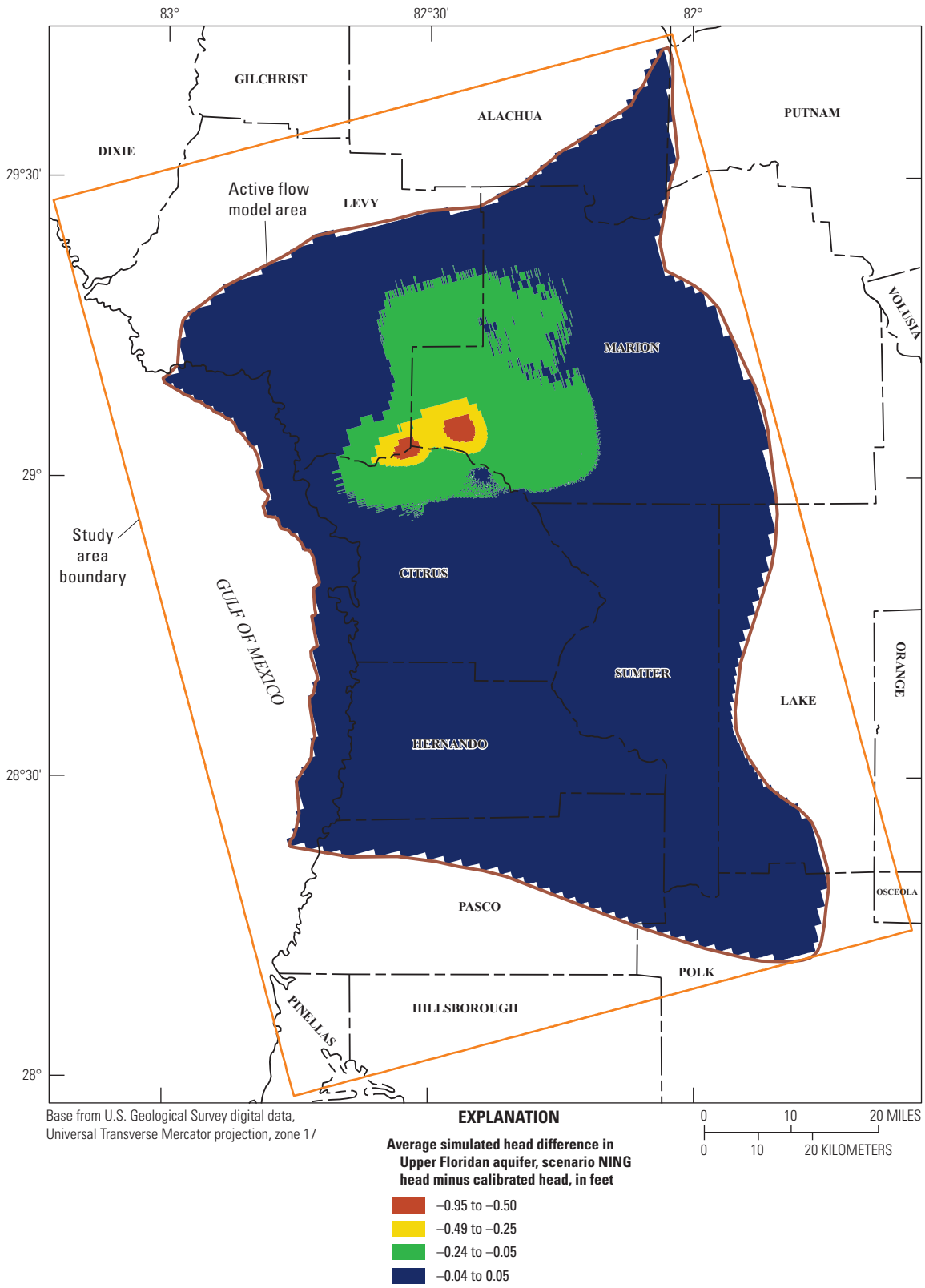

Figure 42. Simulated heads in the Upper Floridan aquifer in the active flow model area under the NING scenario minus HSIMU heads.

and the absence of preferential flow zones are examples of simplified representations that can be sources of error in a flow model. Other examples of simplified representations are the coarseness of the numerical grid model and the inherent limitations on the ET estimates used as input to the UZF1 Package (Niswonger and others, 2006). These simplifications impose limitations on model simulation capabilities and should be considered when interpreting model results. Additional ET stations in the area would eliminate the need to extrapolate AET/RET ratios from stations outside the area.

The feasibility of the model to represent the hydrologic system during the simulation period is limited by the assumptions and simplifications associated with the (1) conceptualization of the flow system; (2) data available to represent the physical properties of the system, as well as observations of system conditions, such as the measured heads, spring flows, lake stages, and streamflows; (3) temporal range of hydrologic and anthropogenic stresses and the spatial scale of the model grid; and (4) equations used as an approximate conceptualization of the flow system. The model was shown to approximate spring flow, streamflow, lake stages, and aquifer heads throughout the wide range of hydrologic stresses and groundwater pumping rates for monthly stress periods from 2004 to 2012, which included dry, wet, and average hydrologic conditions. Nonetheless, there may be some limitations using the model with hydrologic conditions outside the range simulated during model calibration, or to extrapolate groundwater pumping rates greater than those used in the simulation near the boundaries of the model area.

Simplifying the actual flow system with the selected conceptualizations does not invalidate model results, although model results should not be interpreted at scales smaller than the representative grid cell. The groundwater flow equation solved by the model is based on Darcy's Law and the continuity equation when the velocity of groundwater is low and flow is laminar. In karstic terrains, however, it is possible for flow through caverns and solution channels to be turbulent, particularly near pumping wells or springs. It was assumed herein that laminar flow prevailed throughout the model area. It is assumed that discrete karstic conduits within the Upper Floridan aquifer can be represented as a continuum at the spatial scale of the model. On a subregional scale, these are valid approximations when examining average flow and head changes (Kuniansky, 2016).

One model limitation arises from the assumption that surface runoff and (or) surface leakage volumes were not captured in land-surface depressions and instead were added to the nearest stream or lake without being routed over the land surface. Errors may occur when the simulated excess in surface runoff and (or) surface leakage volumes can bias the simulated lake stage, stream stage, and streamflow residuals during large rainfall events. Not all surface runoff volumes generated in a day will arrive at the assigned stream or lake the same day, and some runoff may infiltrate en route to a stream or pond. This simplification is a result of assuming steady flow across the landscape. As a result, there will be errors in the magnitude and timing of the streamflow hydrograph peaks. Simulating transient overland runoff would require a more sophisticated approach, such as the use of the Surface-Water Routing (SWR) Package (Hughes and others, 2012); however, such approaches may not benefit model prediction because of long run times and numerical instability that hampers model calibration.

Although the calibrated hydraulic property maps are within acceptable ranges, it is highly likely that there are other distributions of hydraulic properties that would be reasonable and also fit the calibration criteria. The transient model presented herein addresses the surface water and groundwater interactions by means of a systematic and process-oriented approach in the Tsala Apopka Lake Basin using appropriate and available modeling tools. By providing estimates of hydraulic parameters, this model can be used to generate initial estimates of the hydraulic properties as well as the boundary conditions needed for more local studies.

Specifying flow through the structures in the Tsala Apopka Lake Basin as a user input, instead of actively simulating the flow through the structures based on the differences between upstream and downstream lake stages, can result in bias in the simulated lake stages. This model limitation was observed in the simulated stages for Inverness and Hernando pools. Specified flows through the structures underestimate the actual downstream flow, causing the upstream stage to be overestimated and the downstream stage underestimated. Similarly, overestimated flows through the structures cause upstream stage to be underestimated and the downstream stage to be overestimated. Simulating the water release through hydraulic structures from these lakes, however, can result in model errors that similarly cause model bias. The approach used herein is considered a balance between model complexity and the challenges posed by parameter estimation.

The designation of 6,655 inactive cells in layers 1 and 2 based on numerical convergence challenges uncovered in the model where the overlying unsaturated zone is generally thicker than 70 ft is another model limitation. Perched conditions generated in the unsaturated zone caused water levels in the surficial aquifer to drop below the bottom of the surficial aquifer. The simulation of recharge to the Upper Floridan aquifer was achieved after inactivating these cells in layers 1 and 2 and extending the thickness of the overlying unsaturated zone. To preserve mass balance and model integrity, recharge rates were applied directly to the Upper Floridan aquifer instead of layers 1 or 2 in these inactive areas of the surficial aquifer.

Another assumption of the modeling approach used herein is that backwater effects on streamflow routing through channels can reasonably be neglected. The impacts of a low-gradient landscape on the direction and rate of surface flows can result in deviations from the normal flow condition that was assumed for stream channels in this model. The impacts of structures that generate nearly stagnant flows

upstream of flow control structures was represented using an innovative combination of the MODFLOW-NWT Streamflow Routing (SFR2) and Lake (LAK7) Packages (Niswonger and Prudic, 2006; Merritt and Konikow, 2000). This approach considers both nearly stagnant surface water upstream of control structures and channel flows controlled by channel slope and geometry. This approach greatly enhances model efficiency relative to a more complicated alternative that simulates two-dimensional flows while considering changes in water acceleration that can occur in low-gradient systems.

Recharge rates to the Upper Floridan aquifer from drainage wells in Marion County (Sepúlveda, 2002) were not simulated in this model. The relatively small recharge from these drainage wells (Sepúlveda, 2002) and the large hydraulic conductivity of the Upper Floridan aquifer in Marion County reduce the water-level errors introduced to the model by not simulating recharge from drainage wells.

The use of the relatively wet hydrologic conditions of 2004 to calibrate hydraulic parameters was a model limitation, because model execution times precluded averaging aquifer responses with dry hydrologic conditions like those in 2006. The execution time of more than one day for a forward run of the model limited the calibration of 2004–12 hydrologic conditions to changing parameters based on a trial-and-error approach. The generation of the initial distribution of heads was based on available steady-state packages. Another model limitation is that there are no corresponding steady-state MODFLOW packages for the transient simulation of lake stages, streamflow, or flow in the unsaturated zone. This model limitation in the generation of the initial distribution of heads included the simulation of lake stages as specified heads at lake cells instead of using the LAK7 Package (Merritt and Konikow, 2000), replacing the streamflow routing with the river package, and using the recharge package instead of routing the infiltration in the unsaturated zone (Appendix 1).

Summary and Conclusions

A three-layer, finite-difference, transient surface-water/groundwater flow model of the surficial aquifer, upper confining unit, and Upper Floridan aquifer for the Tsala Apopka Lake Basin in Citrus County, Florida was developed and calibrated to 2004–12 hydrologic conditions. The purpose of developing the model was to (1) evaluate the interaction of inflows and outflows in the Floral City, Inverness, and Hernando pools in the Tsala Apopka Lake Basin; (2) assess the recharge rates to the surficial aquifer from infiltration through the unsaturated zone; and (3) assess the effects that changes in rainfall rates, increases in groundwater pumping rates and the presence of water-control structures have on lake and pool stages, water levels in the surficial and Upper Floridan aquifers, spring flows, and streamflows. The flow model was calibrated using inverse modeling techniques with the automated parameter estimation software (PEST; Doherty, 2013a, b; Doherty and Hunt, 2010) to best replicate lake stages, water levels, spring flows, and streamflows reflecting 2004 conditions. Calibration was refined for 2005 to 2012 conditions using a trial-and-error approach. Hydrologic processes at land surface and in the unsaturated zone were simulated by using MODFLOW-NWT v 1.1.2 with the Lake (LAK7), Streamflow Routing (SFR2), and Unsaturated Zone Flow (UZF1) Packages used to simulate surface and unsaturated zone flows.

A variable size grid consisting of 384 rows and 369 columns, rotated counterclockwise at an angle of 15 degrees with respect to the south to north direction, was assigned hydraulic parameters to produce a three-layer flow model. Flow model layer 1 represented the surficial aquifer where an underlying upper confining unit is present and was also the layer in which lakes were simulated. Flow model layer 2 represented the surficial aquifer where the underlying hydrogeologic unit is the Upper Floridan aquifer and also represented the upper confining unit where present. Flow model layer 3 represented the Upper Floridan aquifer. One lakebed leakance value was assigned per lake and one streambed vertical hydraulic conductivity value was assigned per stream segment, excluding the spillways used at water-control structures located in the Tsala Apopka Lake Basin. The application of an inverse modeling technique identified the specific yield of the surficial aquifer as the most sensitive parameter in the model. Hydraulic conductivity in the Upper Floridan aquifer was highest in areas having a low hydraulic gradient in the potentiometric surface and near Upper Floridan aquifer springs of first and second magnitude.

Calibration criteria for the 2004–12 simulation period were met for pool stages, water levels at wells, spring flows, and streamflows. The annual average simulated evapotranspiration (ET) rate was about 33.6 inches per year (in/yr). Total simulated ET ranged from about 31 in/yr during 2006 to 40 in/yr during 2005. Average net recharge to the surficial aquifer in the active flow model area was about 10.3 in/yr, ranging annually from 3.8 in/yr in 2006 to 14.2 in/yr in 2005.

The annual average groundwater withdrawal rate from the Upper Floridan aquifer, about 1.0 in/yr during the 9-year simulation period, was larger in magnitude than the annual average flow leaving the Upper Floridan aquifer through the lateral boundary cells, which was about 0.5 in/yr. Annual average downward leakage to the Upper Floridan aquifer, 8.4 in/yr, whether from the surficial aquifer or the upper confining unit, was larger in magnitude than the average annual spring flow from the Upper Floridan aquifer, which was 7.6 in/yr.

The magnitude of the increases or decreases in pool stages from the simulation of a 10-percent increase or decrease in rainfall rates was proportional to the drainage area of each pool. Such increases or decreases in pool stages, therefore, were largest in the Hernando pool and smallest in the Floral City pool. Simulated effects on Tsala Apopka Lake pool stages from projected increases in groundwater pumping rates for 2025 and 2035 were negligible. The simulation of no flow

through the eight water-control structures in the Tsala Apopka Lake Basin showed annual average declines in pool stage of 0.99, 1.58, and 0.37 feet at the Floral City, Inverness, and Hernando pools, respectively. The changes in simulated spring flow, under the simulation of no flow through the structures, were found to be very small. The simulation of the removal of both water-control structures in Lake Rousseau, Inglis Dam and the Inglis Bypass Spillway, caused flow to increase at Rainbow Springs by about 10 cubic feet per second, an increase of 1.5 percent from the average calibrated flow for 2004 to 2012.

The capacity of this surface-water/groundwater flow model to represent the Tsala Apopka Lake hydrologic system during the 9-year simulation period is limited by: (1) the assumptions and simplifications associated with the conceptualization of the flow system; (2) the data available to represent the hydrologic conditions of the system, such as head data, spring flow, lake stages, and streamflows; (3) the temporal and spatial discretization of the model; and (4) the equations used in the simulation of each component of the flow system. The model was shown to adequately simulate lake stages, heads in wells, spring flow, and streamflow during dry, wet, and average hydrologic stresses periods from 2004 to 2012. Unknown errors may arise if the model is used to simulate conditions outside the range of those used for calibration, or if groundwater pumping rates are imposed that exceed those used in the simulation near the boundaries of the model area.

References Cited

Citrus County, 1997, Methodologies used in the future land use element, appendix F *of* Citrus County Comprehensive Plan: Citrus County report, accessed January 2017 at https://www.citrusbocc.com/plandev/landdev/comp-plan/appendix-f.pdf.

Citrus County Board of County Commissioners, 2017, FAQ—Drinking water (potable water): Citrus County Board of County Commissioners website, accessed January 2017 at http://www.citrusbocc.com/waterres/utilities/faq-drinking-water.htm.

Citrus County Geographic Resources and Community Planning Division, 2013, Citrus County 10-year water supply facilities work plan: Citrus County Geographic Resources and Community Planning Division report, accessed January 2017 at https://www.citrusbocc.com/plandev/landdev/comp-plan/chapter-5-10-year-plan.pdf.

Doherty, J., 2013a, PEST, Model-independent parameter estimation—User manual (8th ed., with minor revisions): Brisbane, Australia, Watermark Numerical Computing.

Doherty, J., 2013b, Addendum to the PEST manual: Brisbane, Australia, Watermark Numerical Computing.

Doherty, J.E., and Hunt, R.J., 2010, Approaches to highly parameterized inversion—A guide to using PEST for groundwater model calibration: U.S. Geological Survey Scientific Investigations Report 2010–5169, 59 p.

Florida Department of Environmental Protection, 2018, Land Boundary Information System—Web interface, accessed January 23, 2018, at http://ftp.labins.org/LiDAR/.

Hoblit, B.B., Castello, Cris, Liu, Leiji, and Curtis, David, 2003, Creating a seamless map of gage-adjusted radar rainfall estimates for the State of Florida: Proceedings of the EWRI World Water and Environmental Congress, Philadelphia, Pa.

Hughes, J.D., Langevin, C.D., Chartier, K.L., and White, J.T., 2012, Documentation of the Surface-Water Routing (SWR1) Process for modeling surface-water flow with the U.S. Geological Survey Modular Ground-Water Model (MODFLOW-2005): U.S. Geological Survey Techniques and Methods, book 6, chap. A40 (Version 1.0), 113 p., accessed May 26, 2016, at http://pubs.usgs.gov/tm/6a40/.

HydroGeoLogic, 2013, Northern District Groundwater Flow Model, v 4.0: Brooksville, Southwest Florida Water Management District, St Johns Water Management District, Marion County, and the Withlacoochee River Water Supply Authority, 755 p.

Kinnaman, S.L., and Dixon, J.F., 2011, Potentiometric surface of the Upper Floridan aquifer in Florida and parts of Georgia, South Carolina, and Alabama, May–June 2010: U.S. Geological Survey Scientific Investigations Map 3182, 1 sheet.

Kuniansky, E.L., 2016, Simulating groundwater flow in karst aquifers with distributed parameter models— Comparison of porous-equivalent media and hybrid flow approaches: U.S. Geological Survey Scientific Investigations Report 2016–5116, 14 p., accessed May 26, 2017, at http://dx.doi.org/10.3133/sir20165116.

McBride, W.S., Metz, P.A., Ryan, P.J., Fulkerson, Mark, and Downing, H.C., 2017, Groundwater levels, geochemistry, and water budget of the Tsala Apopka Lake system, west-central Florida, 2004–12: U.S. Geological Survey Scientific Investigations Report 2017–5132, 100 p., https://doi.org/10.3133/sir20175132.

Merritt, M.L., and Konikow, L.F., 2000, Documentation of a computer program to simulate lake-aquifer interaction using the MODFLOW ground-water flow model and the MOC3D solute-transport model: U.S. Geological Survey Water-Resources Investigations Report 00–4167, 146 p.

Miller, J.A., 1986, Hydrogeologic framework of the Floridan aquifer system in Florida and parts of Georgia, Alabama, and South Carolina: U.S. Geological Survey Professional Paper 1403–B, 91 p.

Niswonger, R.G., and Prudic, D.E., 2006, Documentation of the Streamflow-Routing (SFR2) Package to include unsaturated flow beneath streams—A modification to SFR1: U.S. Geological Survey Techniques and Methods, book 6, chap. A13, 48 p.

Niswonger, R.G., Prudic, D.E., and Regan, S., 2006, Documentation of the Unsaturated-Zone Flow (UZF1) Package for modeling unsaturated flow between the land surface and the water table with MODFLOW-2005: U.S. Geological Survey Techniques and Methods, book 6, chap. A19, 62 p.

O'Reilly, A.M., 2007, Effects of the temporal variability of evapotranspiration on hydrologic simulation in central Florida: U.S. Geological Survey Scientific Investigations Report 2007–5100, 36 p.

Sanford, W.E., and Selnick, D.L., 2013, Estimation of evapotranspiration across the conterminous United States using a regression with climate and land-cover data: Journal of the American Water Resources Association (JAWRA), v. 49, no. 1, p. 217–230, https://doi.org/10.1111/jawr.12010.

Scott, T.M., Means, G.H., Meegan, R.P., Means, R.C., Upchurch, S.B., Copeland, R.E., Jones, J., Roberts, T, and Willet, A., 2004, Springs of Florida: Florida Geological Survey Bulletin 66, 658 p., accessed June 28, 2016, at http://www.dep.state.fl.us/geology/geologictopics/springs/bulletin66.htm.

Sepúlveda, N., 2002, Simulation of ground-water flow in the intermediate and Floridan aquifer systems in peninsular Florida: U.S. Geological Survey Water-Resources Investigations Report 02–4009, 130 p., accessed June 2, 2016, at http://fl.water.usgs.gov/PDF_files/wri02_4009_sepulveda.pdf.

Sepúlveda, N., 2018, MODFLOW-NWT Data sets for simulation of effects of surface-water and groundwater inflows and outflows on the hydrology of the Tsala Apopka Lake Basin in Citrus County, Florida: U.S. Geological Survey data release, https://doi.org/10.5066/F7QF8RS2.

Sepúlveda, N., Tiedeman, C.R., O'Reilly, A.M., Davis, J.B., and Burger, P., 2012, Groundwater flow and water budget in the surficial and Floridan aquifer systems in east-central Florida: U.S. Geological Survey Scientific Investigations Report 2012–5161, 214 p.

Snyder, J.P., 1983, Map projections used by the U.S. Geological Survey: U.S. Geological Survey Bulletin B–1532, 313 p.

Southwest Florida Water Management District (SWFWMD), 2007, Minimum and guidance levels for Tsala Apopka Lake in Citrus County, Florida: Accessed June 16, 2017, at http://www.swfwmd.state.fl.us/projects/mfl/reports/lakes/tsala_apopka_lake_adopted_mfls_report_17jan2007.pdf.

Southwest Florida Water Management District (SWFWMD), 2017, Hydrologic Data Water Management Information System—Web interface: Accessed January 23, 2018, at http://www.swfwmd.state.fl.us/data/hydrologic/.

Sumner, D.M., 2006, Adequacy of selected evapotranspiration approximations for hydrologic simulation: Journal of the American Water Resources Association, v. 42, no. 3, p. 699–711.

Sumner, D.M., 2017a, Evapotranspiration (ET) at Tiger Bay State Forest site, Volusia County, Florida, January 1, 1998–December 31, 1999: U.S. Geological Survey data release, accessed September 20, 2017, at https://doi.org/10.5066/F7SB447H.

Sumner, D.M., 2017b, Evapotranspiration (ET) at Lake Wales Ridge site, 20-minute data, Orange County, Florida, September 15, 1993–August 27, 1994: U.S. Geological Survey data release, accessed September 20, 2017, at https://doi.org/10.5066/F7PK0DN5.

Sumner, D.M., Hinkle, C.R. and Becker, K.E., 2017, Evapotranspiration (ET) at University of Central Florida urban site, daily data, Orange County, Florida, January 29, 2009–September 27, 2012: U.S. Geological Survey data release, accessed September 20, 2017, at https://doi.org/10.5066/F7JS9NZB.

U.S. Geological Survey, 2016, Evapotranspiration information and data: Caribbean-Florida Water Science Center website, accessed June 29, 2016, at http://fl.water.usgs.gov/et/.

U.S. Geological Survey, 2017, National Water Information System—Web interface: Accessed September 20, 2017, at http://dx.doi.org/10.5066/F7P55KJN.

White, W.A., 1970, The geomorphology of the Florida peninsula: Tallahassee, Florida Geological Survey Bulletin 51, 164 p.

Appendix 1. Model Construction and Calibration

A surface-water/groundwater flow model was developed for the Tsala Apopka Lake Basin in Citrus County, Florida, to simulate the lake stages, streamflows, spring flows, and water levels in the surficial and Upper Floridan aquifers and to simulate changes in water management. The parameters calibrated included lakebed, streambed, and aquifer hydraulic parameters that produced a best-fit simulation to the measured data from 2004 to 2012. The initial distribution of the hydraulic parameters calibrated in this model used the spatial distribution of parameter values in the Northern District Model developed by HydroGeoLogic (2013) for the Tsala Apopka Lake Basin.

The measured pool stages, flows through structures, spring flows, streamflows, and aquifer water levels were used to calibrate the model using a highly parametrized inverse modeling approach. This is an approach for calibrating a model to fit observation data, subject to the limitations associated with numerical grid resolution, lack of measured data, and the fact that some parameters are not selected for adjustment as part of the inverse modeling calibration process.

Simulation Code

The simulation code used to develop the surface-water/groundwater flow model presented here for the Tsala Apopka Lake Basin was MODFLOW-NWT v. 1.1.2 (Niswonger and others, 2011). MODFLOW-NWT, a Newton formulation for MODFLOW-2005, is a standalone computer code modified to solve problems involving drying and rewetting nonlinearities of the unconfined groundwater-flow equation. MODFLOW-NWT requires the Upstream-Weighting (UPW) Package to compute intercell conductances in a manner that handles nonlinearities of cell drying and rewetting more reliably with a continuously varying groundwater head than the discrete approach of drying and rewetting that is used by the Block-Centered Flow (BCF), Layer Property Flow (LPF), or Hydrogeologic-Unit Flow (HUF) Packages.

Specific packages used for the sole purpose of developing this model were the Lake Package (LAK7; Merritt and Konikow, 2000) with modifications to improve convergence (Prudic and Niswonger, 2006), the Streamflow Routing Package (SFR2; Niswonger and Prudic, 2006), and the Unsaturated Zone Flow Package (UZF1; Niswonger and others, 2006). The reader is referred to http://water.usgs.gov/ogw/modflow-nwt/MODFLOW-NWT-Guide/index.html?beginners_guide_to_modflow.htm for detailed guidelines of the input files these and other packages require. The UZF1 Package was used to simulate the interaction of the groundwater flow system with the surface environment, including rainfall, calculation of infiltration and surface runoff, and evapotranspiration (ET). The LAK7 Package was used to (1) simulate the lake stages considering streamflows leaving or entering a lake, seepage to or from the surficial aquifer, surface runoff that drains to a lake, ET losses, specified flows through the water-control structures, and (2) represent the backwater parts of the channels that had water-control structures. The SFR2 Package simulates streamflow and stream stage considering upstream flows, seepage to or from the surficial aquifer, surface runoff that drains to a stream, and ET losses.

Extent and Discretization

The study area was divided into active and inactive flow model areas. The study area was extended beyond the model area so that data would be available just outside the active model boundary. Inactive flow model areas are far enough from the Tsala Apopka Lake Basin to avoid lateral boundary effects on the pool stages. The active flow model area spans approximately 4,535 square miles (mi^2) in west-central Florida, including Citrus, Hernando, and Sumter Counties, parts of Alachua, Lake, Levy, Marion, Pasco, Polk, and Putnam Counties, and those parts of the Gulf of Mexico that receive groundwater discharge from the Upper Floridan aquifer (fig. 1). The boundaries of the active flow model area were delineated along sections where flow perpendicular to these boundaries was minimal (inferred based on the configuration of potentiometric maps) so that no-flow lateral boundary conditions could be used without incurring substantial errors. The northern, eastern, and southern boundaries of the active flow model conform to the boundaries of what has been identified as the Northern West-Central Florida Groundwater Basin (HydroGeoLogic, 2013).

The active flow model domain was horizontally discretized into a variable grid with cells ranging from a finest resolution of 500 by 500 feet (ft) in the Tsala Apopka Lake Basin, near the center of the model grid, to a coarsest resolution of 5,000 by 5,000 ft in the four corners of the model grid (fig. 1.1). Cells having the finest resolution in the grid span an area of about 790 mi^2 and are contiguous. The model area was discretized into three layers, 384 rows, and 369 columns. The number of active cells varied by layer: there were 8,678 active cells in layer 1 (853 mi^2), which represents the surficial aquifer where this unit is underlain by the upper confining unit; 3,775 inactive cells in layer 1 used as lake cells (38 mi^2); 114,650 active cells in layer 2 (4,003 mi^2), which represents either the surficial aquifer where the upper confining unit is absent or the upper confining unit where this unit is present; and 126,695 active cells in layer 3 (about 4,535 mi^2), which represents the Upper Floridan aquifer. There are 1,615 cells in the Gulf of Mexico, near the western boundary, that are active only in layer 3. In addition, there are 6,655 cells, active on layer 3, where infiltration is routed through the thickness of layers 1 and 2, until infiltration recharges layer 3, with the additional time delay caused by the additional routing over the thicknesses of layers 1 and 2.

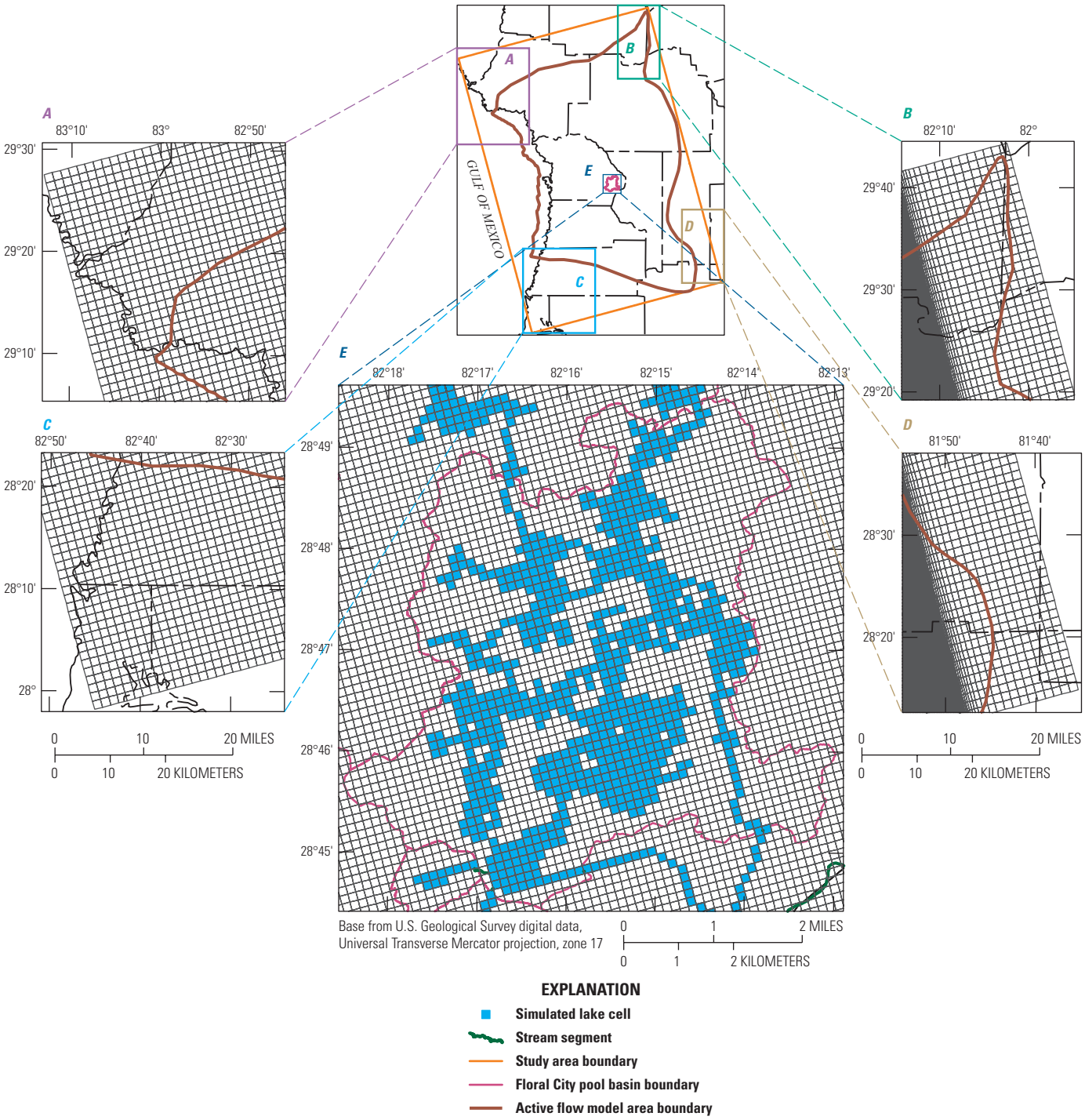

Figure 1.1 Expanded view of the spatially-variable grid used to develop the surface-water/groundwater flow model for the Tsala Apopka Lake Basin and adjacent areas, showing grid-cell sizes in, *A*, Levy County near the northwest corner, *B*, Alachua County near the northeast corner, *C*, Pinellas County near the southwest corner, *D*, Polk County near the southeast corner, and in the, *E*, Floral City pool in Citrus County.

This time delay caused perched conditions in the unsaturated zone and water levels in the surficial aquifer drop below the bottom of the aquifer from a delayed recharge in a thick unsaturated zone. These perched conditions caused a lack of convergence to a head solution when a dry cell in layer 2 receives a large recharge at the top of the cell. To avoid this lack of convergence, in the final version of the model, these 6,655 cells were simulated as inactive in layers 1 and 2, but recharge was applied directly to the Upper Floridan aquifer, and the thickness of the unsaturated zone for these cells was extended to include the thicknesses of layers 1 and 2. Recharge to the Upper Floridan aquifer at these 6,655 cells was simulated by applying recharge from the unsaturated zone to the highest active cell in each vertical column, which was accomplished by assigning the value of 3 to NUZTOP in the UZF1 Package (Niswonger and others, 2006).

The numerical grid is rotated 15 degrees counterclockwise from the south to north direction using the State Plane coordinates of the model grid corners. The rotation, in degrees, is the inverse tangent of the rise divided by the run, calculated from the differences in XSP and YSP coordinates of the northwest and northeast corners (table 1.1). The orientation of the rotated grid is approximately parallel to the main direction of the surface-water flow.

Four of the 15 lakes in the model area are sections of the Withlacoochee River simulated as lakes, because the stream width is greater than or equal to the width of a grid cell (lakes 1, 2, 11, 14, fig. 1.2). All 15 lakes were simulated in 3,775 cells from the numerical grid. Lake cells are grid cells having at least 50 percent of their surface area occupied by a lake. Lake cells were treated as inactive cells in layer 1 by setting the grid-cell condition (IBOUND) array entry to zero and setting the layer thickness equal to zero. Lake cells are located away from the active cells in layer 1 where the surficial aquifer is underlain by the upper confining unit (fig. 7). The bathymetry of the lakes, marshes, and canals was determined from light detection and ranging (lidar) data collected by Southwest Florida Water Management District (SWFWMD) and used to refine the model of digital land-surface altitude that in turn was used to generate the relation between stage, water surface area, and lake volume at each of the 15 lakes in the model area.

Table 1.1. Geographical information system coordinates of the corners of the flow model grid.

[XSP and YSP coordinates refer to State Plane projection, North American Datum 1983, Florida west 0902, in feet (Snyder, 1983)]

Grid corner	XSP	YSP
Northwest	268582.82	1865027.10
Northeast	643190.10	1965402.82
Southwest	413993.06	1322348.72
Southeast	788600.35	1422724.44

Simulated streams in the model area were divided into 43 stream segments; each segment begins or ends at a confluence or at a lake inlet (fig. 1.3). The confluence of two segments must be the beginning of another stream segment. The 43 stream segments in the model area were further divided into stream reaches and are connected to the active cells in layer 2. For this flow model, a stream reach is defined as the length of a stream contained within a single cell. The location of water-control structures (fig. 2) are indicated by stream segments 9–16, 22, 37, and 39 (fig. 1.3). The water-control structures were treated as 10-ft-long flow spillways, where flow leaving a lake and entering either another lake or a stream segment was specified. Stream segments consisting of only one reach were used to represent each of the water-control structures. The bathymetry of the stream reaches was also obtained from the model of digital land-surface altitude developed from the lidar data collected by SWFWMD. The altitude of the top of the streambed, used by the model as one of the factors that determines the surface-water flow entering the downstream stream reach, was assigned from the digital model of land-surface altitude.

The simulation period of January 2004 to December 2012 was discretized into daily time steps. A total of 3,288 days were simulated for this 9-year period. The inverse modeling calibration period was from January to December 2004. Additional model calibration for the entire simulation period, from 2004 to 2012, was achieved by trial and error.

Calibration Approach

The flow model was calibrated using automated parameter estimation software (PEST; Doherty, 2013a, b) with highly parametrized inverse modeling techniques (Doherty and Hunt, 2010). Model parameters were calibrated using pool stages, spring flows, aquifer heads, and streamflows measured during 2004. A steady-state run for January 2004 average hydrologic conditions prior to the start of the calibration period was used to produce initial conditions, reducing the effects of unknown initial heads on model results. The calibration was refined by using a trial-and-error approach to quantitatively match simulated lake stages, spring flows, streamflows, and groundwater heads to measured values during 2005–12 when hydrologic conditions were sometimes substantially different from those of 2004.

The subregional transient Northern District model that encompasses the Tsala Apopka Lake Basin and beyond was developed by HydroGeoLogic (2013) for SWFWMD to assess the effects of current and future groundwater pumping rates on groundwater flow and surface-water flows and levels. The spatial distribution of the calibrated hydraulic parameters from the Northern District Model provides an initial distribution of parameters for a subregional study like the one presented herein as well as a basic understanding of conceptual flow in the Tsala Apopka Lake Basin.

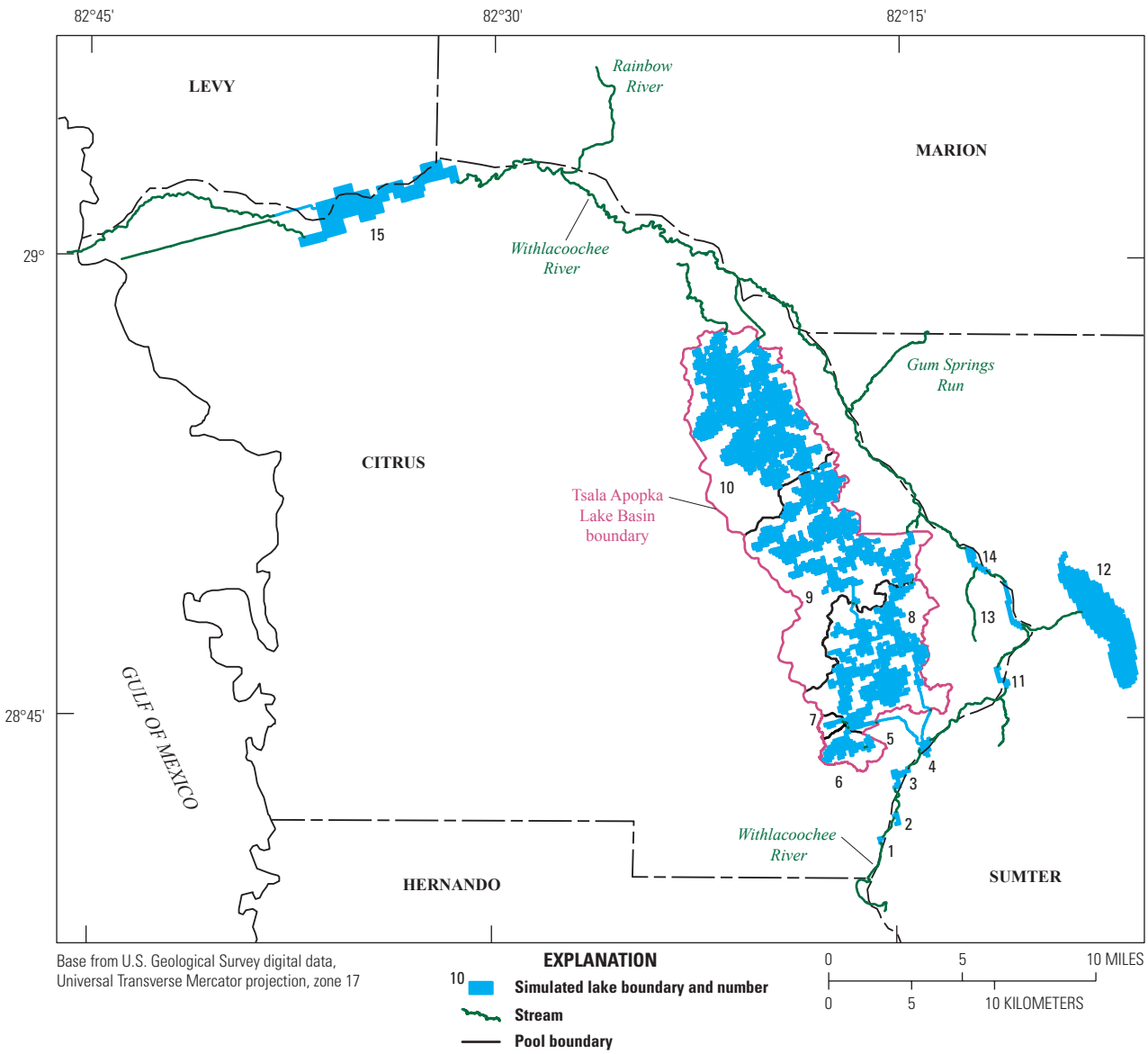

Figure 1.2 Lake network in the active flow model area.

Model Parameterization

The parameters estimated were the horizontal hydraulic conductivity values of the surficial aquifer, upper confining unit, and Upper Floridan aquifer; the vertical hydraulic conductivity values of the surficial aquifer and upper confining unit; the specific storage values of the upper confining unit and Upper Floridan aquifer; the specific yield of the surficial aquifer; the lakebed leakance values of the 15 lakes; the streambed vertical hydraulic conductivity values; the vertical anisotropy of the Upper Floridan aquifer, and multipliers relating reference evapotranspiration (RET) to the UZF1 Package evapotranspiration demand rates (Niswonger and others, 2006). Parameters that were assigned values (not estimated) were the saturated vertical hydraulic conductivity in the unsaturated zone, the initial and residual soil water content, the hydraulic conductivity of the topsoil, Manning's n, the water-surface slope in streams, and the thickness of the streambed or lakebed.

A smooth spatial distribution of a hydraulic property was estimated using the pilot-points method over all or part of a model layer by spatially interpolating from values at specific points distributed at grid cells. The inverse modeling code PEST (Doherty, 2013a, b) was used to estimate parameters in the model area and includes a suite of programs that facilitates the use of the pilot-points method (Doherty, 2008). Pilot points were placed at model grid cells distributed in the region where a smooth parameter distribution was to be estimated. Parameter values at some or all pilot points were estimated at all iterations of the nonlinear regression, and parameter values at all model cells in the region were interpolated from the values at the pilot points. In this way, parameter values

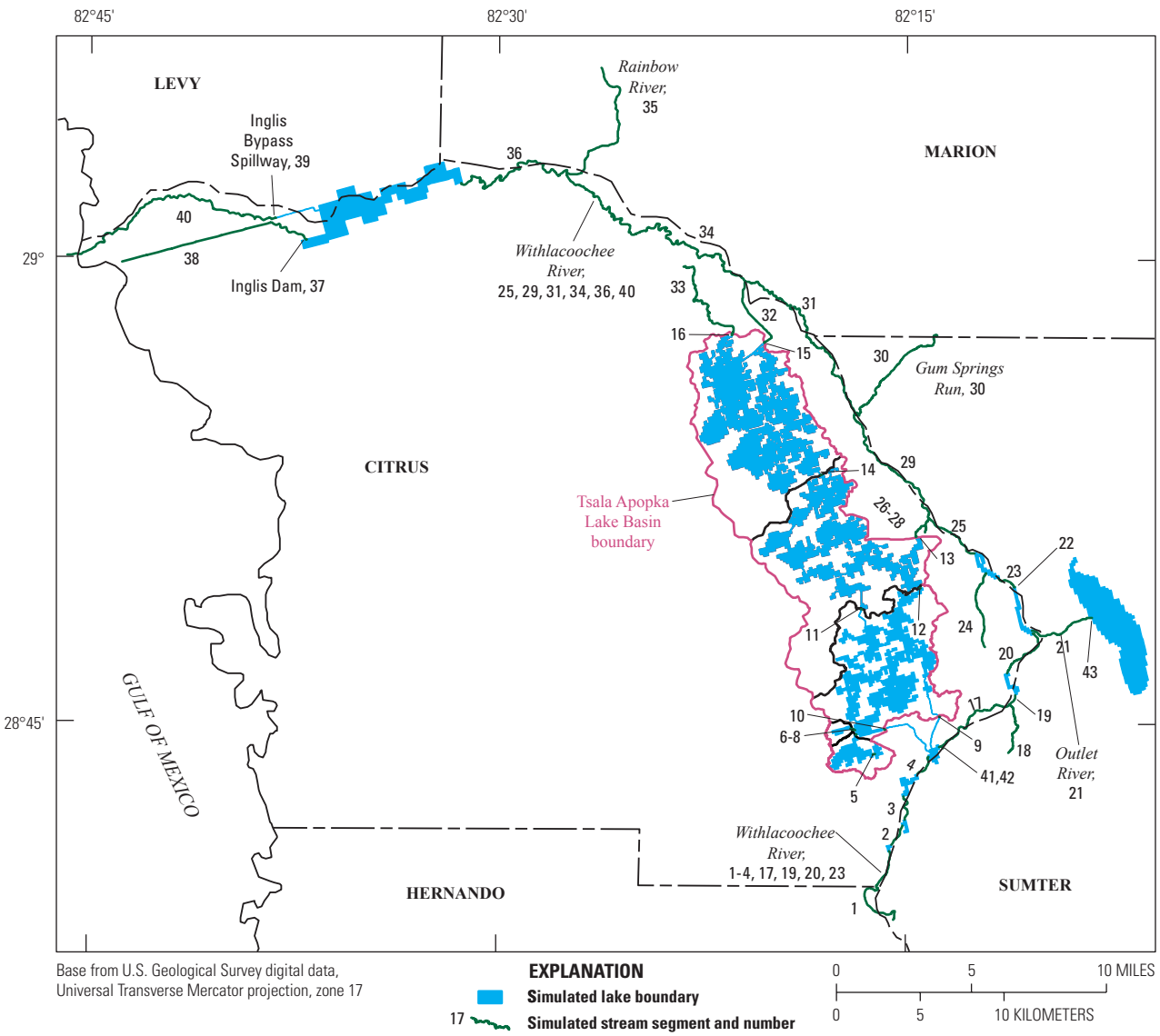

Figure 1.3 Stream network in the active flow model area and the tributaries of the Withlacoochee River.

at all cells were estimated, but the computational expense of calculating parameter sensitivities was limited to the pilot-point parameter locations. An irregular distribution of 227 unique pilot points (Doherty, 2013a) was used to parameterize hydraulic properties in the model (fig. 1.4). Pilot points generally extend beyond the active flow model areas to avoid extrapolating near the model boundaries. The pilot points were not spatially distributed regularly, because the grid cells varied in size (fig. 1.1).

Model parameters were defined to represent the distribution of horizontal (Kh) and vertical (Kv) hydraulic conductivity for the three model layers. Generally, Kh and Kv are represented as spatially variable in layers where the calibration observations are sensitive to these aquifer properties and field data indicate spatial variability, and as spatially uniform in layers where calibration observations are not sensitive to aquifer properties and field data provide little or no information about spatial variability. Layer 1, where the surficial aquifer is underlain by the upper confining unit (fig. 7), has 104 pilot points (fig. 1.4) each for Kh and Kv, for a total of 208 parameters in layer 1. Layer 2, composed of the surficial aquifer where this unit is underlain by the Upper Floridan aquifer and of the upper confining unit, where this unit is present, has 227 pilot points each (fig. 1.4) for Kh and Kv, for a total of 454 parameters in layer 2. Layer 3, simulating the Upper Floridan aquifer, was represented with 227 pilot points for Kh. In layer 3, Kv is represented by one parameter, a single value for vertical anisotropy ($\alpha = Kh/Kv$). MODFLOW-NWT internally calculates Kv (from Kh/α) using the spatially variable Kh for layer 3.

Three parameters were used to represent storage in the model: the first parameter represents specific yield in layer 1

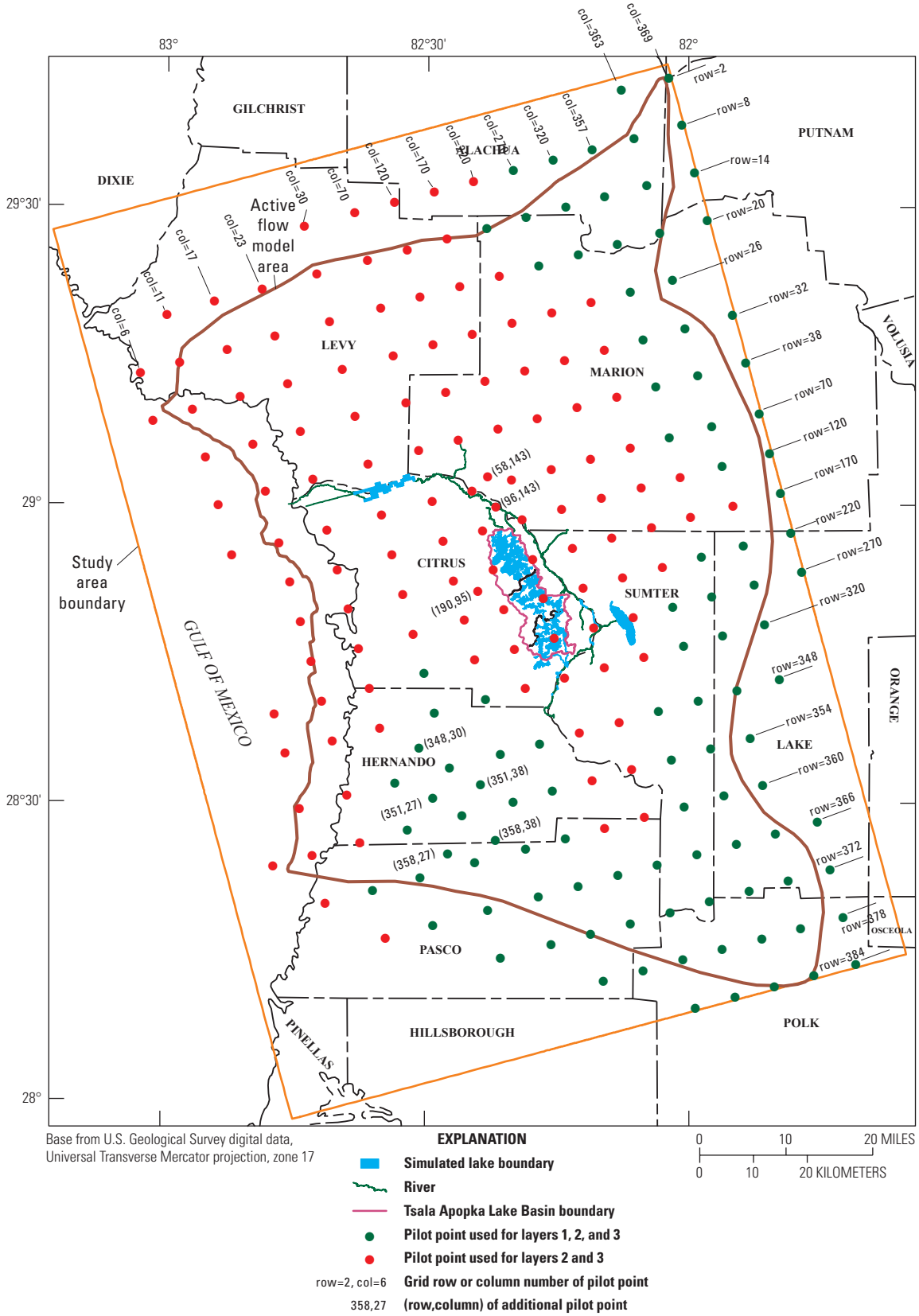

Figure 1.4 Location of pilot points used in the model layers.

where the surficial aquifer overlies the upper confining unit and in layer 2 where the surficial aquifer overlies the Upper Floridan aquifer, the second parameter represents specific storage in the upper confining unit, and the third parameter represents specific storage in the Upper Floridan aquifer. The parameter representation of specific yield for the surficial aquifer in layers 1 and 2 and specific storage for the upper confining unit and Upper Floridan aquifer was guided by the need to avoid introducing more parameters into the model, because storage values cannot be easily distinguished between grid cells representing fine sands and limestone. A single parameter value was used to simulate specific yield where the surficial aquifer is present in layer 1 or 2 to eliminate determining spatial variations in soil density and void ratios in various sand deposits. Similarly, the lack of data on the spatial variability of specific storage within the upper confining unit and Upper Floridan aquifer led to the assumption of one uniform value for the upper confining unit and another value for the Upper Floridan aquifer (layer 3).

The vertical flow between the lake and the underlying aquifer depends on the lakebed leakance. Each of the 15 lakes was calibrated with its own lakebed leakance, adding 15 lakebed leakance parameters to the model. Lake stages become more sensitive to lakebed leakances as the difference between lake stage and water-table altitude becomes large; similarly, as lakebed leakances become large, the differences between water-table altitude and lake stage become small and model results become insensitive to additional increases in lakebed leakances.

The hydraulic connection between the water table and the river is dictated by the vertical hydraulic conductivity of the streambed. Of the 43 stream segments in the model, 11 segments (9 to 16, 22, 37, and 39) simulate structure spillways (fig. 1.3). Because these spillways are simulated as water-control structures, no hydraulic connection with the underlying surficial aquifer is represented and no parameters requiring calibration are contributed. Stream segments 17, 41, and 42 were grouped, as were stream segments 21 and 43 (fig. 1.3), and streambed vertical hydraulic conductivity was a constant for each group. Stream segment 41 is the outlet of lake number 4, and segment 42 is used to discharge water into the neighboring marsh during high streamflows, thereby representing a low river bank. Stream segment 43 simulates the outlet of lake number 12 as a spillway (figs. 1.2, 1.3). Thus, 29 parameters were used to simulate the vertical hydraulic conductivity of streambeds. The model contains a total of 937 parameters for calibration, counting Kh and Kv at pilot points, specific yield, specific storage, lakebed leakances, and vertical hydraulic conductivity of the streambed.

Wherever regional-scale variability of Kh or Kv was represented using the pilot point method, an irregularly-spaced grid of regional pilot points was placed over the extent of the model area in each layer. An exponential variogram, recommended by Doherty and Hunt (2010), was used for the kriging procedure to interpolate Kh or Kv values for all model cells in a given layer using the variogram $\gamma(h)$ defined by

$$\gamma(h) = C_0\left[1-\exp(-h/a)\right] , \qquad (1.1)$$

where

C_0 is the sill (the constant value the variogram model approaches asymptotically at large distances h);

h is the separation distance between points; and

a is a parameter defined by the value that makes the range of distances equal to $3a$, which is also set equal to the distance h where the variogram reaches 95 percent of the sill.

For the regional variogram, the value of a was set to 35,000 ft, about 1.4 times the average pilot point separation distance. This is consistent with the recommendation of Doherty and Hunt (2010) that the value of a should be set equal to 1 to 2 times the pilot point separation distance. Ordinary kriging, in which the mean of the interpolated values is not specified *a priori*, is used for interpolation of the pilot points.

Conductance values for the 91 springs in the active model area were taken from the Northern District Model (HydroGeoLogic, 2013). All 91 springs emanate from the Upper Floridan aquifer. Initial estimates of spring pool altitudes were also taken from the Northern District Model; however, pool altitudes for springs influenced by tides were taken from U.S. Geological Survey (USGS) and SWFWMD databases.

The surface runoff and groundwater discharge to land surface calculated by the UZF1 Package at each cell is distributed based on the specified subbasin delineation for lakes and streams. These subbasins were generated using (1) the delineation of drainage basins (fig. 1.5) to determine the destination of the surface runoff, and (2) the lidar data to estimate drainage directions within each delineated drainage basin. Surface leakage, generally simulated at land-surface depressions, represents spring discharge and is enhanced by applied infiltration. Surface leakage should not always be directed to a lake or stream, because these surficial runoff volumes generally have to fill the land surface depressions before any runoff drains to surface-water bodies. The subbasin delineation of surface leakage cells and the corresponding stream segment where runoff is routed were adjusted as part of the manual component of model calibration.

Water levels below extinction depth are not subject to ET. The extinction depths used in the simulation of ET losses were developed by combining (1) the classification of generalized soils and land use types made from SWFWMD geographic information system (GIS) databases, and (2) the results of a lab study by Shah and others (2007) (table 1.2). Extinction depth values ranged from 6.00 to 7.55 ft.

Calibration Targets

Data used to calibrate the model for transient conditions for 2004 hydrologic conditions were the measured heads at observation wells, measured spring flows, measured lake stages, and measured streamflows. For the 2004–12 period,

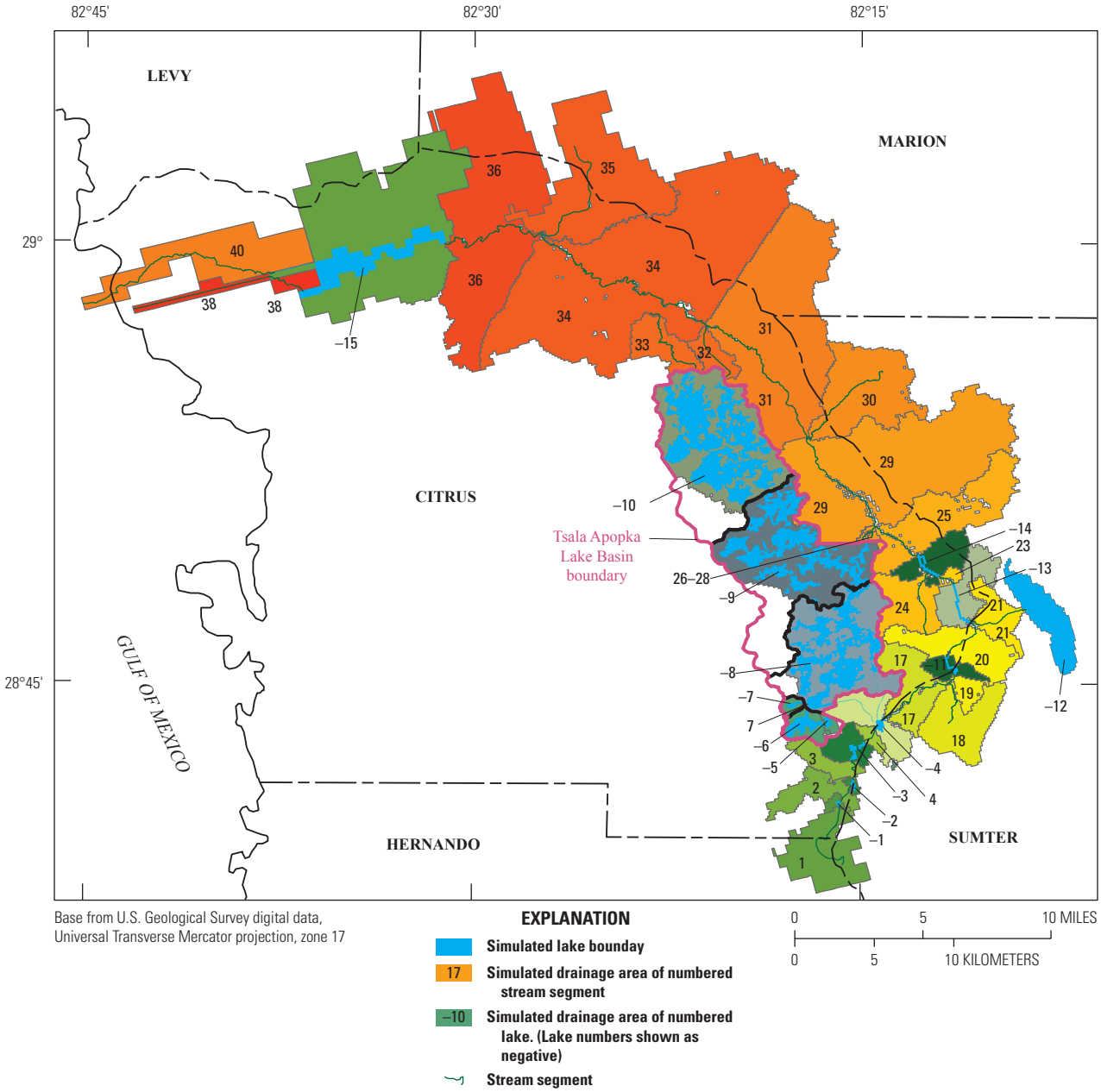

Figure 1.5 Stream and lake basins where surface runoff from excess infiltration and groundwater discharge to land surface are routed. Positive numbers indicate areas draining to stream segments and negative numbers indicate areas draining to lakes.

Table 1.2. Extinction depth values, in feet, used based on generalized soil and land cover types.

[Extinction depths, in feet, were taken from values derived by Shah and others (2007)]

Soil	Grass	Urban	Forest
Sand	6.00	7.55	7.55
Loamy sand	6.50	7.55	7.55
Sandy loam	7.55	7.55	7.55
Sandy clay loam	7.55	7.55	7.55
Sandy clay	7.55	7.55	7.55

calibration criteria for observed head and flow data were established on the basis of the average residuals calculated over the period of record. Residuals were calculated as simulated minus measured head, stage, or flow at each well, lake, spring, or streamflow-gaging station.

The calibration criterion for lake stage was selected on the basis of uncertainty in rainfall and flow through the control structures. The calibration goal was an average absolute value residual for each lake stage of less than 1 ft, calculated for each lake over the 9-year simulation period (2004–12).

To qualify the level of calibration of the simulated water levels at wells, residuals were assumed to be normally distributed, $N(\mu \approx 0, \sigma)$, with a mean μ as close as possible

to zero to minimize bias in the distribution of water-level residuals and with a dimensionless ratio of standard deviation σ divided by the range of the water-level measurements less than 0.1 (Kuniansky and others, 2003). The calibration of simulated water levels continued until residuals were close to satisfying the requirement that the minimum number of water-level residuals falling under each of the intervals [-0.75 σ, 0.75 σ], [-1.5 σ, 1.5 σ], and [-2.25 σ, 2.25 σ] were at least 55, 87, and 98 percent (http://onlinestatbook.com/2/calculators/normal_dist.html) of the total number of sites with water-level measurements, respectively.

The calibration criterion for spring flows with at least 20 flow measurements during the 9-year simulation period was to simulate spring flow within 10 percent of the measured flows larger than or equal to 10 cubic feet per second (ft^3/s), and within 20 percent of measured flows less than 10 ft^3/s. Springs with flows greater or equal to 10 ft^3/s account for about 90 percent of total spring flow. About 90 percent of the springs without measured flows during the 2004–12 period had flows estimated by the Northern District Model (HydroGeoLogic, 2013), and many of these were less than 10 ft^3/s. The calibration goal for these small springs with less than 20 flow measurements was to simulate most spring flows within 50 percent of the flow estimated by the Northern District Model.

The calibration criterion for streamflows (or for stream stages) was that the average simulated streamflow (or simulated stream stage) at a streamflow-gaging station was within 20 percent (or within 10 percent for stream stage) of the average measured streamflow (or stream stage). These calibration criteria considered that surface leakage volumes generated at land-surface depressions generally result in the overestimation of surface runoff flows. Surface leakage volumes entering land-surface depressions (whether ponds or ridges) should be identified and removed from the model area. The model limitation of not capturing some surface runoff in land-surface depressions but instead adding such surface leakage volumes to lakes and streams results in the overestimation of simulated surface-water flow during large rainfall events when actual surface runoff only drains from depressions to lakes or streams after these depressions are filled.

Measured Lake Stages

Only 8 of the 15 lakes simulated in the model had measured stage data. These lakes are the three main pools of Tsala Apopka Lake (Floral City, Inverness, and Hernando), Bradley Lake, Lake Consuella, Lake Panasoffkee, the pool on the upstream side of the Wysong structure, and Lake Rousseau (table 1.3). Stage data from Bradley Lake and Lake Consuella were not used for calibration. January 2004 initial stages at these lakes were obtained from the measured data; initial data for the remaining nine ungaged lakes were interpolated from either measured stages at streamflow-gaging stations along the Withlacoochee River or were estimated from measured pool stages in Tsala Apopka Lake. Lakes 1, 2, and 11 were simulated on the basis of the fact that the widths

Table 1.3. Lake name, number, water-surface area, drainage area, and number of grid cells covered by lake.

[All cells in lakes 2 to 14 are 500- by 500-ft grid cells except for connecting channels, which are considered to be part of the extended lake. Initial lake stage is in feet above the North American Vertical Datum of 1988 (NAVD 88). ft, foot; mi^2, square mile; WR, Withlacoochee River]

Name	Lake number	Initial lake stage, Jan. 1, 2004 (ft)	Lake area (mi^2)	Drainage area (mi^2)	Number of cells covered by lake
WR Marsh 1	1	39.28	0.0309	0.2915	3
WR Marsh 2	2	39.19	0.0628	0.2087	7
Nelson Lake	3	39.11	0.1883	0.6838	21
Bonnet Lake	4	39.06	0.2376	2.8179	53
Lake East of Bradley Lake	5	39.94	0.1076	0.5813	12
Bradley Lake	6	39.94	0.7443	1.9919	83
Lake Consuella	7	39.94	0.0986	0.5996	11
Floral City Pool Lakes	8	40.04	6.5600	17.4379	757
Inverness Pool Lakes	9	38.32	7.3518	18.9735	850
Hernando Pool Lakes	10	37.18	11.2868	21.7388	1,279
WR Marsh 3	11	38.51	0.1255	1.1936	14
Lake Panasoffkee	12	38.79	5.0666	23.2876	565
Withlacoochee River at Wysong structure	13	38.29	0.2152	2.8128	24
WR Marsh 4	14	34.62	0.2063	0.9407	23
Lake Rousseau	15	26.91	4.6212	16.8405	73

of the Withlacoochee River cells were about the same as that of the grid cells at these locations. All but two of these lakes (1 and 15) were composed of uniform lake cells measuring 500 by 500 ft, the highest grid resolution in the flow model.

Measured Groundwater Levels

Measured water-table altitudes from 52 surficial aquifer wells and measured heads from 167 Upper Floridan aquifer wells were used for calibration (table 1.4, figs. 1.6, 1.7). The spatial distribution of the Upper Floridan aquifer wells covered most of the flow model domain, but the surficial aquifer well locations are limited to the southern and central parts of the model area. The lack of water-level data from surficial aquifer wells prevents a thorough calibration of the hydraulic parameters in the surficial aquifer, which is a model limitation. In areas without surficial aquifer wells, the only parameters affecting calibration of the surficial aquifer parameters are the aquifer stresses caused by groundwater pumping and, where applicable, the existence of Upper Floridan aquifer springs or wells.

Nested pairs of surficial and Upper Floridan aquifer wells inside each of the three Tsala Apopka Lake pool drainage areas had measured water levels that allow the calculation of the vertical hydraulic gradient between these two hydrogeologic units. These well pairs, written as pairs of well identification numbers for the hydrogeologic units (surficial aquifer, Upper Floridan aquifer) each well taps, are (759564, 759565) east of the Floral City pool basin, (781078, 781081) west of the Inverness pool basin, (759560, 759562) east of the Inverness pool basin, (775485, 775484) west of the Hernando pool basin, and (759552, 759559) east of the Hernando pool basin (table 1.4, figs. 1.6, 1.7). Measured water levels at these wells became available after they were drilled in 2011 or later. The model calibration needed additional estimated water-level data at these wells to guide the calibration of lakebed leakances with reliable vertical hydraulic gradients between the surficial and Upper Floridan aquifers in the Tsala Apopka Lake Basin. To generate the necessary estimated water levels in the surficial aquifer and heads in the Upper Floridan aquifer, a linear regression was developed from measured water levels in and near the Tsala Apopka Lake Basin. All measured water levels in 2004 and 2012 and in the vicinity of the Tsala Apopka Lake Basin were used in this linear regression. Regression coefficients α and β were determined from a set of measured water levels for each corresponding day in 2004 and 2012, denoted by h_{2004} and h_{2012}. Water levels not measured in 2004 could then be calculated from measured water levels in 2012 from the equation

$$h_{2004} = \alpha h_{2012} + \beta. \tag{1.2}$$

Water levels from all well pairs listed earlier were available except for surficial aquifer well 781089, which was dry during the entire period of record. Linear regression coefficients α and β in equation 1.2 were determined separately for the surficial aquifer and Upper Floridan aquifer wells for every day of 2004; the lowest correlation coefficient was 0.98. The average residuals between the predicted h_{2004} from equation 1.2 and the measured heads at surficial and Upper Floridan aquifers were 2.05 and 3.62 ft, an assessment of the head approximation error introduced by using the regressed heads at the nested wells. Equation 1.2 provided estimated water levels for 2004 in both the surficial and Upper Floridan aquifer wells in all the nested wells having 2012 water-level data. Calibration runs were performed with and without the inclusion of the interpolated water levels at these wells, and the residuals in stage and water-level data in the Tsala Apopka Lake Basin were lower when the interpolated water levels were used in the calibration, suggesting an improvement in the estimation of hydraulic properties in the Tsala Apopka Lake Basin. No interpolated heads were used to calculate the overall mean residual from calibration.

Measured Spring Flows

All springs simulated by the Northern District Model and inside the Tsala Apopka Lake Basin were simulated in the active flow model developed here. Groups of springs contributing flow to a measurement site were grouped to compare measured and simulated spring flows. A total of 91 springs were simulated in the model (fig. 13), including 82 spring groups (table 1.5). Spring group numbers 5, 7, 31, 36, 39, 50, and 73 had the longest period of record. These spring groups (Silver, Rainbow, Gum, Homosassa, SE Fork Homosassa, Chassahowitzka, and Weeki Wachee Springs) influenced calibration the most because of their comprehensive measured spring-flow datasets. Specifically, the number of spring-flow measurements associated with each of these 7 groups far exceeded the few measurements associated with each of the remaining 75 spring groups. The measured spring flow data were primarily used to calibrate the hydraulic parameters near the springs. Spring group numbers 36, 39, and 50 have tide-fluctuating spring pool altitudes, and spring group number 5 has a spring pool altitude that varies because of vegetation along the spring run that impedes the flow. Spring pool altitudes varied on a monthly basis at these 4 spring groups and remained constant at the remaining 78 spring groups.

Measured Streamflows and Stream Stages

Measured streamflows and gage heights at the 24 streamflow-gaging and (or) gage-height stations along the Withlacoochee River and in the Tsala Apopka Lake Basin (table 5, fig. 18) were used to calibrate the surface-water flow component of the model. The calibrated hydraulic parameters of this model component included the vertical hydraulic conductivity of the streambed and the hydraulic conductivity of the topsoil, which affected the seepage between the river and surficial aquifer and partitioned the rainfall into surface runoff and infiltration, respectively.

Table 1.4. Well name, well identification number, model layer tapped by well, well location, and row and column in numerical grid used in the active flow model area.

[Id, well identification number; XSP and YSP coordinates refer to State Plane projection, North American Datum of 1983, Florida west 0902, in feet (Snyder, 1983); Row, Column, location of the well in the numerical grid; AveHd, average head calculated from measured water levels from 2004 to 2012, in feet above the North American Vertical Datum of 1988 (NAVD 88); NOBS, number of days in the 2004 to 2012 period for which water level measurement was available out of 3,288 days; Layer=1 for surficial aquifer well where the underlying upper confining unit exists; Layer=2 for surficial aquifer well where there is no underlying upper confining unit; Layer=3 for Upper Floridan aquifer well; NOBS, number of days in the 2004 to 2012 period for which water level measurement was available; ROMP, Regional Observation and Monitoring-Well Program; SRWMD, Suwannee River Water Management District; FA, Floridan aquifer]

Well name	Id	Layer	XSP	YSP	Row	Column	AveHd	NOBS
ROMP 101 surficial aquifer well	17497	1	680106.38	1498054.38	364	317	97.41	3,005
Green Swamp 2 Wetland surficial	17501	1	672630.88	1474986.25	368	290	97.69	3,239
Green Swamp 1 Wetland surficial	17503	1	673351.62	1464281.00	371	286	98.31	3,250
Green Swamp Bay Wetland surficial	17507	1	671040.25	1486061.00	366	293	98.4	3,288
Green Swamp 3 Wetland surficial	17508	1	678859.94	1469548.12	370	300	100.64	3,268
Eva Shallow	17525	1	712883.12	1470698.75	371	356	110.47	8
Green Swamp Marsh Wetland surficial	17586	1	650582.25	1461512.62	370	241	91.95	3,185
Green Swamp 6 Wetland surficial	17596	1	665503.88	1476115.75	368	277	95.4	3,250
Green Swamp 5 Wetland surficial	17600	1	668700.38	1482860.25	367	287	96.31	3,288
Green Swamp L-11M Shallow	17603	1	649151.69	1453026.25	371	234	89.01	7
Green Swamp 4 Wetland surficial	17726	1	678496.81	1475289.88	369	302	100.49	3,288
BR-2 surficial aquifer well	18328	1	561839.56	1476145.75	362	77	149.62	3,245
Pless Park surficial	18338	1	555508.75	1487570.00	360	71	97.37	3,096
CR 581 North surficial	18341	1	538709.94	1458979.12	365	33	72.05	3,137
BR-3 surficial aquifer well	18869	1	579912.25	1451715.88	368	99	101.25	3,210
San Antonio Park surficial	18886	1	566799.50	1458126.50	366	77	162.91	3,262
Cross Bar 1E Phillips surficial aquifer	20468	1	515790.56	1463539.75	362	27	66.39	3,250
Cross Bar 3E Barthle B surficial aquifer	20472	1	525750.25	1468413.38	362	30	68.14	3,206
Cross Bar SERW Shallow	20511	1	510560.16	1467245.25	362	27	60.96	204
Cross Bar 1W Wolfe surficial aquifer	20529	1	494093.28	1472966.38	360	24	44.36	3,274
Mascotte Shallow surficial aquifer	l_0041	1	683993.81	1527225.62	359	339	98.95	3,046
Eva Tower at Groveland surficial aquifer	l_0872	1	709351.25	1503292.62	365	358	108.3	2,859
Leesburg WWTF at Leesburg surficial aquifer	l_0874	1	679041.62	1605495.88	341	357	80.63	2,315
Green Swamp L-12B Shallow	17607	2	649035.62	1500386.50	362	258	90.62	2
Engle Park surficial	20548	2	455122.41	1476320.38	357	16	13.96	3,212
Spring Hill surficial	20582	2	504887.34	1526472.38	350	29	70.27	3,277
ROMP 97 surficial aquifer well	20840	2	468895.75	1491280.38	355	20	15.68	3,061
ROMP 131 surficial aquifer well	22941	2	478675.00	1818324.88	20	93	45.06	2,888
ROMP 112 surficial aquifer well	23021	2	583149.38	1652910.50	203	210	41.17	3,270
WR-6D surficial aquifer well	23067	2	584282.75	1553234.00	349	160	51.15	1
LP-5 surficial aquifer well	23085	2	626752.06	1605080.12	318	269	42.86	2,477
LP-4 surficial aquifer well	23108	2	615417.81	1614436.12	294	252	43.6	1
LP-6 surficial aquifer well	23148	2	625866.75	1623621.50	282	277	44.62	3,272
Wysong structure surficial	23182	2	597827.12	1632056.38	251	227	38.31	5
Townsen Park surficial	23392	2	568086.06	1568673.00	344	137	36.98	3,247
ROMP 110 surficial aquifer well	23503	2	585851.94	1606728.25	294	191	39	3,288
Brooksville East surficial	23574	2	561325.56	1521343.25	354	99	99.17	3,288
ROMP 116 surficial aquifer well	23596	2	548376.44	1680282.38	132	157	32.7	2,604
Big Jones Creek surficial aquifer well	670310	2	608800.56	1644292.62	233	255	39.43	1,767
Little Jones Creek surficial aquifer well	670312	2	613996.56	1639226.38	246	262	41.9	1,794
Lake Tsala Apopka (Flying Eagle) surficial aquifer	670314	2	573949.69	1631331.88	240	181	38.35	1,285

Table 1.4. Well name, well identification number, model layer tapped by well, well location, and row and column in numerical grid used in the active flow model area.—Continued

[Id, well identification number; XSP and YSP coordinates refer to State Plane projection, North American Datum of 1983, Florida west 0902, in feet (Snyder, 1983); Row, Column, location of the well in the numerical grid; AveHd, average head calculated from measured water levels from 2004 to 2012, in feet above the North American Vertical Datum of 1988 (NAVD 88); NOBS, number of days in the 2004 to 2012 period for which water level measurement was available out of 3,288 days; Layer=1 for surficial aquifer well where the underlying upper confining unit exists; Layer=2 for surficial aquifer well where there is no underlying upper confining unit; Layer=3 for Upper Floridan aquifer well; NOBS, number of days in the 2004 to 2012 period for which water level measurement was available; ROMP, Regional Observation and Monitoring-Well Program; SRWMD, Suwannee River Water Management District; FA, Floridan aquifer]

Well name	Id	Layer	XSP	YSP	Row	Column	AveHd	NOBS
ROMP 100 surficial aquifer well	736736	2	628899.75	1492054.38	363	215	73.66	1,412
Gum Springs surficial aquifer well	751432	2	575305.38	1672711.75	161	205	39.97	1,372
ROMP 102.5 surficial aquifer well	755916	2	621320.00	1569152.38	348	240	66.45	850
Tsala Apopka Lake 2 surficial aquifer well	759552	2	558242.31	1661704.25	173	166	36.57	1,207
Tsala Apopka Lake 6 surficial aquifer well	759560	2	593913.06	1631227.25	251	219	37.69	1,196
Tsala Apopka Lake 4 surficial aquifer well	759564	2	581092.75	1620745.25	264	189	38.66	1,225
Tsala Apopka Lake 1 surficial aquifer well	775485	2	537233.50	1660334.12	165	125	36.07	965
Tsala Apopka Lake 3 surficial aquifer well	781078	2	551813.75	1637432.12	217	141	36.42	965
Well at Carlton Village surficial aquifer	l_0696	2	692766.94	1679035.62	210	364	84.02	2,425
SR 466A at Fruitland Park surficial aquifer	l_0700	2	671281.69	1646498.25	261	358	51.81	2,508
Lake Griffin State Pk at Leesburg surficial aquifer	l_0927	2	688443.81	1643983.88	275	362	56.82	2,441
ROMP 90 Upper Floridan aquifer well	17518	3	610488.88	1463635.88	367	164	66.69	3,284
EVA deep	17526	3	712884.06	1470703.88	371	356	109.36	13
Green Swamp Marsh FA	17589	3	650433.06	1461778.75	370	241	89.58	3,264
ROMP 89 Upper Floridan aquifer	17590	3	643318.00	1462688.88	369	227	89.66	3,276
Green Swamp L-11M deep	17605	3	649151.69	1453030.25	371	234	88.59	7
Green Swamp L-12B deep	17606	3	649035.62	1500386.50	362	258	90.64	2
Withlacoochee State Forest Green Swamp	17608	3	661908.06	1500549.88	363	283	94.27	7
ROMP 88 Upper Floridan aquifer well	17708	3	684689.69	1445671.75	375	298	102.69	3,272
US 98 near Dade City FA	17719	3	618761.12	1435277.75	373	166	77.48	10
ROMP 101 Upper Floridan aquifer	17728	3	680099.94	1498062.38	364	317	96.15	2,951
Weeki 11 deep	18289	3	537040.50	1494201.62	358	39	48.01	318
BR-2 Upper Floridan aquifer well	18326	3	561839.56	1476145.75	362	77	77.24	3,190
PLESS Park FA	18337	3	555505.25	1487568.12	360	71	74.99	3,064
CR 581 North FA	18340	3	538718.94	1458969.25	365	33	68.81	3,179
ROMP 92 (CB-4E) Upper Floridan aquifer well Replacement	18351	3	539746.25	1470832.88	362	35	63.99	3,185
BR-3 Upper Floridan aquifer well	18868	3	579921.25	1451705.75	368	99	73.62	3,282
San Antonio Park FA	18887	3	566710.00	1458116.88	366	77	79.56	3,262
ROMP TR 21-2 Upper Floridan aquifer chloride monitoring	20062	3	465120.00	1643430.25	161	27	1.11	3,282
North LECANTO deep	20075	3	503028.41	1661576.00	145	59	4.01	363
ROMP TR 21-3 Avon Park chloride monitoring	20085	3	473284.47	1651815.00	149	29	2.46	3,280
ROMP TR 20-3 Upper Floridan aquifer well	20120	3	478769.16	1572435.88	305	26	6.33	2,403
ROMP TR 20-2 Upper Floridan aquifer well	20125	3	472108.00	1575229.62	296	25	6.2	2,394
Crystal river deep	20172	3	462983.09	1662638.50	122	28	0.22	2
Cross Bar 1E Phillips Upper Floridan aquifer	20469	3	515799.56	1463539.62	362	27	66.04	3,196
C B 2NE Barthle A North Upper Floridan aquifer	20475	3	526477.12	1485348.00	359	31	46.62	3,101
Cross Bar 1N Finest Farms Upper Floridan aquifer	20481	3	510620.69	1488070.62	357	28	27.47	3,287
Cross Bar 3E Barthle B Upper Floridan aquifer	20507	3	525741.56	1468423.25	362	30	60.85	3,172

Table 1.4. Well name, well identification number, model layer tapped by well, well location, and row and column in numerical grid used in the active flow model area.—Continued

[Id, well identification number; XSP and YSP coordinates refer to State Plane projection, North American Datum of 1983, Florida west 0902, in feet (Snyder, 1983); Row, Column, location of the well in the numerical grid; AveHd, average head calculated from measured water levels from 2004 to 2012, in feet above the North American Vertical Datum of 1988 (NAVD 88); NOBS, number of days in the 2004 to 2012 period for which water level measurement was available out of 3,288 days; Layer=1 for surficial aquifer well where the underlying upper confining unit exists; Layer=2 for surficial aquifer well where there is no underlying upper confining unit; Layer=3 for Upper Floridan aquifer well; NOBS, number of days in the 2004 to 2012 period for which water level measurement was available; ROMP, Regional Observation and Monitoring-Well Program; SRWMD, Suwannee River Water Management District; FA, Floridan aquifer]

Well name	Id	Layer	XSP	YSP	Row	Column	AveHd	NOBS
Cross Bar WRW FA	20521	3	501359.72	1474806.25	360	25	43.02	207
Cross Bar 1W Wolfe Upper Floridan aquifer	20531	3	494102.25	1472956.25	360	24	46.35	3,274
Cross Bar 2W Crews Lake Upper Floridan aquifer	20532	3	482901.47	1470894.00	359	22	24.83	3,272
Cross Bar 1NW Kuka Upper Floridan aquifer	20539	3	502621.88	1488333.88	357	26	27.43	3,280
Masaryktown deep	20541	3	506569.19	1488571.12	357	27	28.22	3,265
ENGLE Park FA	20547	3	455131.44	1476320.25	357	16	13.87	3,184
Spring Hill FA	20581	3	504896.25	1526452.00	350	29	18.24	3,216
Weeki Wachee FA NR Weeki Wachee	20584	3	485088.50	1527070.50	349	25	17.49	269
ROMP TR 19-2 Upper Floridan aquifer chloride monitoring	20690	3	458512.78	1531399.25	346	20	5.61	2,144
Centralia 2 Upper Floridan aquifer well	20720	3	487484.25	1556929.00	338	27	10	2,708
ROMP 107 Upper Floridan aquifer well	20727	3	509763.53	1571846.38	322	33	10.64	3,256
WR-1 Malibar Upper Floridan aquifer well	20732	3	484164.97	1583655.75	286	28	6.9	2,687
ROMP 105 Upper Floridan aquifer well	20754	3	526367.94	1535130.50	349	39	33.21	3,283
C B 2NW Spring Hill 12 Upper Floridan aquifer	20824	3	496952.72	1494901.50	355	25	25.14	3,287
Cross Bar 4N Airport Upper Floridan aquifer	20829	3	510551.72	1507725.25	354	29	27.27	3,239
ROMP 97 Upper Floridan aquifer well	20841	3	468895.81	1491290.12	355	20	15.96	3,263
ROMP TR 18-3 Upper Floridan aquifer well	20846	3	451635.69	1492549.50	354	17	12.26	727
ROMP TR 18-1 Upper Floridan aquifer well	20854	3	452779.12	1501138.75	352	17	14.09	729
C B 2N Masaryktown Canal Upper Floridan aquifer	20868	3	510653.25	1494423.50	356	28	27.19	3,271
ROMP 98 Upper Floridan aquifer well	20878	3	513687.72	1503865.62	355	29	27.82	3,205
WW-4 Weeki Wachee Upper Floridan aquifer well	20893	3	463296.50	1521355.75	349	20	7.68	3,021
Weeki Wachee FA	20922	3	470591.62	1519057.25	349	22	10.03	3,239
ROMP TR 18-2A Upper Floridan aquifer interface well	20937	3	445408.16	1499824.50	352	16	3.7	2,653
Norris Cattle Company FA	20993	3	467792.72	1624495.38	198	27	1.14	2
Lecanto 7 surficial	21006	3	482874.38	1653863.75	150	31	3.82	2
ROMP 113 Upper Floridan aquifer well replacement	21012	3	523687.25	1644370.88	189	90	5.57	2,331
ROMP 108 Upper Floridan aquifer well	21015	3	502154.78	1601567.75	261	33	6.48	3,029
Chassahowitzka 1 deep	21035	3	479318.16	1595587.00	260	27	5.51	3,255
Lecanto 1 FA	21038	3	511456.06	1597440.75	273	42	9.11	2
Homosassa 3 FA	21049	3	469837.81	1610958.75	226	26	3.24	264
ROMP 109 Upper Floridan aquifer well	21053	3	539244.00	1596579.88	289	96	14.82	3,020
ROMP 134 Upper Floridan aquifer well	22929	3	510678.97	1855804.12	15	175	43.91	3,285
Devils Den sink FA	22931	3	504477.88	1844818.88	17	157	44.04	7
Bullock-Huber FA near Williston	22939	3	474662.03	1812901.12	21	83	43.41	7
ROMP TR 124 Upper Floridan aquifer well	22964	3	425085.88	1709226.12	39	23	1.97	2,856
CE 62 Florida Power FA	22966	3	439973.97	1709177.88	40	26	2.94	4

Table 1.4. Well name, well identification number, model layer tapped by well, well location, and row and column in numerical grid used in the active flow model area.—Continued

[Id, well identification number; XSP and YSP coordinates refer to State Plane projection, North American Datum of 1983, Florida west 0902, in feet (Snyder, 1983); Row, Column, location of the well in the numerical grid; AveHd, average head calculated from measured water levels from 2004 to 2012, in feet above the North American Vertical Datum of 1988 (NAVD 88); NOBS, number of days in the 2004 to 2012 period for which water level measurement was available out of 3,288 days; Layer=1 for surficial aquifer well where the underlying upper confining unit exists; Layer=2 for surficial aquifer well where there is no underlying upper confining unit; Layer=3 for Upper Floridan aquifer well; NOBS, number of days in the 2004 to 2012 period for which water level measurement was available; ROMP, Regional Observation and Monitoring-Well Program; SRWMD, Suwannee River Water Management District; FA, Floridan aquifer]

Well name	Id	Layer	XSP	YSP	Row	Column	AveHd	NOBS
ROMP TR 125 Upper Floridan aquifer sulfate monitor	22976	3	435890.12	1711987.00	39	25	2.08	1,038
Tidewater 1 FA	22980	3	473983.06	1743594.88	35	46	53.61	452
CE 5 FA	22984	3	458068.16	1704185.12	44	29	4.81	358
CE 14 Dunnellon deep	23020	3	522264.97	1715956.88	50	125	37.33	2,952
Sumter 13 JC 59 Upper Floridan aquifer replacement	23032	3	591652.75	1643767.50	225	221	39.84	3,251
WR-6D deep Upper Floridan aquifer well	23069	3	584277.62	1553236.12	349	160	45.57	6
Webster City FA	23078	3	640322.00	1554772.00	351	269	80.07	3,266
LP-5 Upper Floridan aquifer well	23086	3	626746.62	1605079.00	318	269	42.96	2,392
LP-4 Upper Floridan aquifer well 120-ft	23109	3	615420.38	1614444.12	294	252	40.43	2,516
ROMP 111 Upper Floridan aquifer well	23115	3	635581.25	1613459.25	307	290	48.48	3,242
Masters Avenue at Wildwood	23135	3	646913.12	1647873.88	246	330	47.51	7
LP-3 Upper Floridan aquifer well	23143	3	607040.50	1624784.38	270	241	38.15	3,196
LP-6 Upper Floridan aquifer well	23147	3	625858.06	1623620.50	282	277	45.99	3,274
Wysong structure UFA	23176	3	597827.12	1632046.25	251	227	39.06	5
LYKES PASCO FA	23207	3	599245.56	1472126.88	365	147	67.63	352
ROMP 119 Upper Floridan aquifer sulfate monitoring	23229	3	580821.00	1705842.88	100	232	42.89	3,008
CE 24 Drake Ranch FA	23236	3	552772.50	1693795.62	109	172	40.08	2
CE 23 Dunnellon FA	23243	3	554135.19	1703205.00	91	180	41.87	6
ROMP 119.5 Upper Floridan aquifer well	23244	3	555530.88	1708352.00	82	185	43.82	2,148
CE 74 FA Observation near Ocala	23245	3	574083.88	1709697.12	89	221	42.4	6
ROMP 121 Avon Park	23250	3	531356.12	1713057.12	60	141	54.57	3,275
CE 22 FA	23253	3	554500.94	1715934.00	67	187	49.15	2
CE 73 Dunnellon Firetower FA	23264	3	531309.88	1715872.00	55	142	53.05	6
CE 13 FA	23274	3	522379.88	1725646.00	41	130	34.38	2
Rainbow Springs FA near Dunnellon	23316	3	511932.09	1728463.12	40	111	30.14	3,269
WR-5 Upper Floridan aquifer well	23335	3	594189.88	1751461.12	39	282	42.41	2,915
ROMP 120 Upper Floridan aquifer well	23349	3	554610.94	1763130.00	35	211	42.19	3,285
Townsen Park Upper Floridan aquifer well	23393	3	568093.12	1568670.00	344	137	37.1	3,247
CE 77 FA	23421	3	499993.84	1710524.88	49	79	14.23	2
CE 88 USGS FA	23426	3	442686.50	1703772.38	42	26	3.37	2
Camp Mining FA	23439	3	530466.81	1673141.12	137	118	20.96	5
Inverness DOT FA	23485	3	545597.94	1643442.38	202	132	29.79	359
ROMP 110 Upper Floridan aquifer well	23500	3	585829.06	1606835.62	294	191	38.83	3,265
WR-6A deep Upper Floridan aquifer well	23516	3	578927.25	1548836.88	349	148	38.45	2,016
ROMP 103 Upper Floridan aquifer well	23534	3	573738.81	1548667.00	349	137	38.48	3,288
WR-6B deep Upper Floridan aquifer well	23542	3	580118.00	1551526.88	349	151	37.68	2,216
WR-2 Upper Floridan aquifer well	23545	3	590222.38	1507870.50	358	148	48.87	2,015
ROMP 99X Upper Floridan aquifer well	23558	3	597787.25	1518240.62	356	168	50.49	3,094
Brooksville East FA	23575	3	561343.19	1521343.12	354	99	41.07	3,268

Table 1.4. Well name, well identification number, model layer tapped by well, well location, and row and column in numerical grid used in the active flow model area.—Continued

[Id, well identification number; XSP and YSP coordinates refer to State Plane projection, North American Datum of 1983, Florida west 0902, in feet (Snyder, 1983); Row, Column, location of the well in the numerical grid; AveHd, average head calculated from measured water levels from 2004 to 2012, in feet above the North American Vertical Datum of 1988 (NAVD 88); NOBS, number of days in the 2004 to 2012 period for which water level measurement was available out of 3,288 days; Layer=1 for surficial aquifer well where the underlying upper confining unit exists; Layer=2 for surficial aquifer well where there is no underlying upper confining unit; Layer=3 for Upper Floridan aquifer well; NOBS, number of days in the 2004 to 2012 period for which water level measurement was available; ROMP, Regional Observation and Monitoring-Well Program; SRWMD, Suwannee River Water Management District; FA, Floridan aquifer]

Well name	Id	Layer	XSP	YSP	Row	Column	AveHd	NOBS
Johnson Pond	23582	3	534541.81	1695086.75	97	138	27.42	3,278
ROMP 116 Upper Floridan aquifer well	23595	3	548372.88	1680280.38	132	157	31.74	3,270
CE 25 Barnhart FA	23616	3	571694.75	1567220.62	345	143	41.47	7
Ferris Packing Company FA	23627	3	561305.81	1606355.25	282	143	32.61	6
Mascotte deep	26390	3	683926.88	1527079.00	359	339	100.05	2
Little Jones Creek Upper Floridan aquifer well	670311	3	614005.50	1639216.25	246	262	42.47	1,794
Lake Tsala Apopka (Flying Eagle) Upper Floridan aquifer well	670313	3	573951.50	1631331.88	240	181	38.17	1,285
Big Jones Creek Upper Floridan aquifer well	670350	3	609814.12	1642049.12	238	255	39.84	1,767
ROMP 129 Upper Floridan aquifer well	670761	3	578398.12	1735971.12	44	243	42.72	2,040
ROMP 117 Upper Floridan aquifer well	704501	3	655673.06	1634475.12	276	340	58.24	787
Trails End Fish Camp FA	713122	3	585683.56	1603440.00	300	189	40.33	5
WSF Perryman Tract FA	713125	3	504046.25	1628493.75	210	44	7.28	2
USGS SR 44 FA	713727	3	581827.94	1642302.62	223	202	37.31	2
ROMP 100 Upper Floridan aquifer well	717345	3	628913.19	1492064.50	363	215	73.86	1,413
ROMP 119.5 Upper Floridan aquifer well	726932	3	553410.81	1707987.12	81	181	44.31	1,347
ROMP 102.5 Upper Floridan aquifer well	738457	3	621307.56	1569157.38	348	240	67.07	878
Fort Cooper Lake Upper Floridan aquifer well	749149	3	558350.06	1626189.38	242	148	23.24	1,273
ROMP 128 Upper Floridan aquifer well	750199	3	517973.66	1737274.25	38	127	33	1,043
ROMP 132 Upper Floridan aquifer well	750867	3	557483.75	1815291.88	25	244	43.23	907
Gum Springs Upper Floridan aquifer well	751429	3	575305.44	1672718.75	161	205	39.88	1,332
ROMP 112 Upper Floridan aquifer well	755810	3	583122.62	1652956.00	203	210	40.12	1,193
Tsala Apopka Lake 2 Upper Floridan aquifer well	759559	3	558245.00	1661710.25	173	166	36.43	1,207
Tsala Apopka Lake 6 Upper Floridan aquifer well	759562	3	593912.19	1631235.38	251	219	38.12	1,194
Tsala Apopka Lake 4 Upper Floridan aquifer well	759565	3	581086.50	1620748.38	264	189	38.57	1,207
Tsala Apopka Lake 1 Upper Floridan aquifer well	775484	3	537233.50	1660334.12	165	125	26.74	927
Tsala Apopka Lake 3 Upper Floridan aquifer well	781081	3	551813.75	1637430.12	217	141	33.45	861
Tsala Apopka Lake 5 Upper Floridan aquifer well	781090	3	562256.62	1611524.25	272	148	29.78	841
Hawthorne Tower Deep FA	a_0071	3	632125.00	1914147.12	10	365	73.8	3,168
Lybass at Phifer FA	a_0420	3	595912.88	1903861.62	10	356	63.92	2,947
Lochloosa Well at Hawthorne FA	a_0421	3	623748.19	1890945.00	14	362	64.14	2,646
Orange Lake Weather Station FA	a_0725	3	615869.81	1869962.62	18	359	53.74	3,253
Bronson High School Upper Floridan aquifer well - SRWMD	bronso	3	474617.78	1812807.25	21	83	42.39	3,233
Circle K Store Upper Floridan aquifer well - SRWMD	circks	3	425114.16	1788574.75	23	27	9.12	102
Crystal Water Upper Floridan aquifer well - SRWMD	crystw	3	447170.28	1799055.50	22	32	23.57	3,154

Table 1.4. Well name, well identification number, model layer tapped by well, well location, and row and column in numerical grid used in the active flow model area.—Continued

[Id, well identification number; XSP and YSP coordinates refer to State Plane projection, North American Datum of 1983, Florida west 0902, in feet (Snyder, 1983); Row, Column, location of the well in the numerical grid; AveHd, average head calculated from measured water levels from 2004 to 2012, in feet above the North American Vertical Datum of 1988 (NAVD 88); NOBS, number of days in the 2004 to 2012 period for which water level measurement was available out of 3,288 days; Layer=1 for surficial aquifer well where the underlying upper confining unit exists; Layer=2 for surficial aquifer well where there is no underlying upper confining unit; Layer=3 for Upper Floridan aquifer well; NOBS, number of days in the 2004 to 2012 period for which water level measurement was available; ROMP, Regional Observation and Monitoring-Well Program; SRWMD, Suwannee River Water Management District; FA, Floridan aquifer]

Well name	Id	Layer	XSP	YSP	Row	Column	AveHd	NOBS
Goethe Upper Floridan aquifer well - SRWMD	goethe	3	457301.69	1808736.88	21	47	45.28	99
College St at Leesburg FA	l_0054	3	690859.31	1627825.88	308	361	62.94	3,142
Eva Deep FA	l_0057	3	712882.31	1470703.75	371	356	108.68	95
Mascotte Deep FA	l_0062	3	683993.81	1527225.62	359	339	98.06	3,082
Eva Tower at Groveland Upper Floridan aquifer	l_0950	3	709356.62	1503316.12	365	358	102.64	1,666
Lebanon Tower Upper Floridan aquifer well - SRWMD	lebant	3	454809.47	1755079.88	31	31	29.58	237
Moss Bluff FA	m_0013	3	693173.75	1726177.50	119	367	50.23	3,084
CE47 at Silver Springs FA	m_0026	3	645878.25	1766585.50	39	360	40.82	3,267
CE36 at Pedro FA	m_0031	3	617804.56	1691058.75	148	296	44.66	2,925
CE39 SR464 FA	m_0037	3	637240.06	1747617.62	48	356	42.01	211
CE79 CR35 FA	m_0038	3	639093.81	1756383.00	42	357	41.8	61
CE45 NE 35 St FA	m_0039	3	629806.69	1777341.12	36	356	41.09	1,824
CE80 SR40 FA	m_0040	3	627267.69	1767089.75	38	352	42.25	661
CE33 SR475B FA	m_0041	3	606970.12	1720428.12	85	291	43.45	1,387
Romp 120 FA	m_0059	3	554590.25	1763159.88	35	211	42.82	2,160
Sparr Replacement FA	m_0063	3	620583.69	1819547.75	28	357	45.68	86
NE 10th St Deep FA	m_0239	3	616641.25	1767908.38	37	334	42.89	484
CE31 Golden Flake Plant FA	m_0321	3	600339.12	1764652.38	37	301	41.87	865
Huff Well at McIntosh FA	m_0367	3	585610.06	1856205.62	19	320	48.9	1,957
Sheriffs Office at Ocala FA	m_0419	3	608408.81	1795805.25	31	332	41.54	2,351
Citra Ranch at Citra FA	m_0443	3	636271.38	1853259.12	22	362	51.89	3,174
Belleview Elem. Sch. at Belleview FA	m_0465	3	638327.75	1715080.38	112	348	44.74	3,154
Lake Weir Middle School at Lady Lake FA	m_0467	3	661405.69	1695582.75	161	359	46.74	3,277
CR 316 at Reddick FA	m_0527	3	599139.31	1830415.12	24	332	45.52	1,398
Rotary Park at Montague FA	m_0528	3	636375.25	1747012.25	49	355	42.2	1,853
Silver River T3 675	m_0685	3	654981.38	1770888.25	39	362	37.94	1,037
Silver River T9 1240	m_0690	3	643531.94	1774257.25	37	360	40.49	1,032
Ocklawaha River T5 320 at SR40	m_0698	3	660923.44	1773378.75	39	363	41.69	758
Otter Creek Waccasassa Upper Floridan aquifer well - SRWMD	otterc	3	420821.97	1824902.75	16	28	26.52	99
Town of Otter Creek Upper Floridan aquifer well - SRWMD	ottert	3	409245.16	1814880.00	17	25	21.39	95
Rosewood Tower Upper Floridan aquifer well - SRWMD	rosewt	3	357633.94	1783870.25	21	14	9.33	3,034

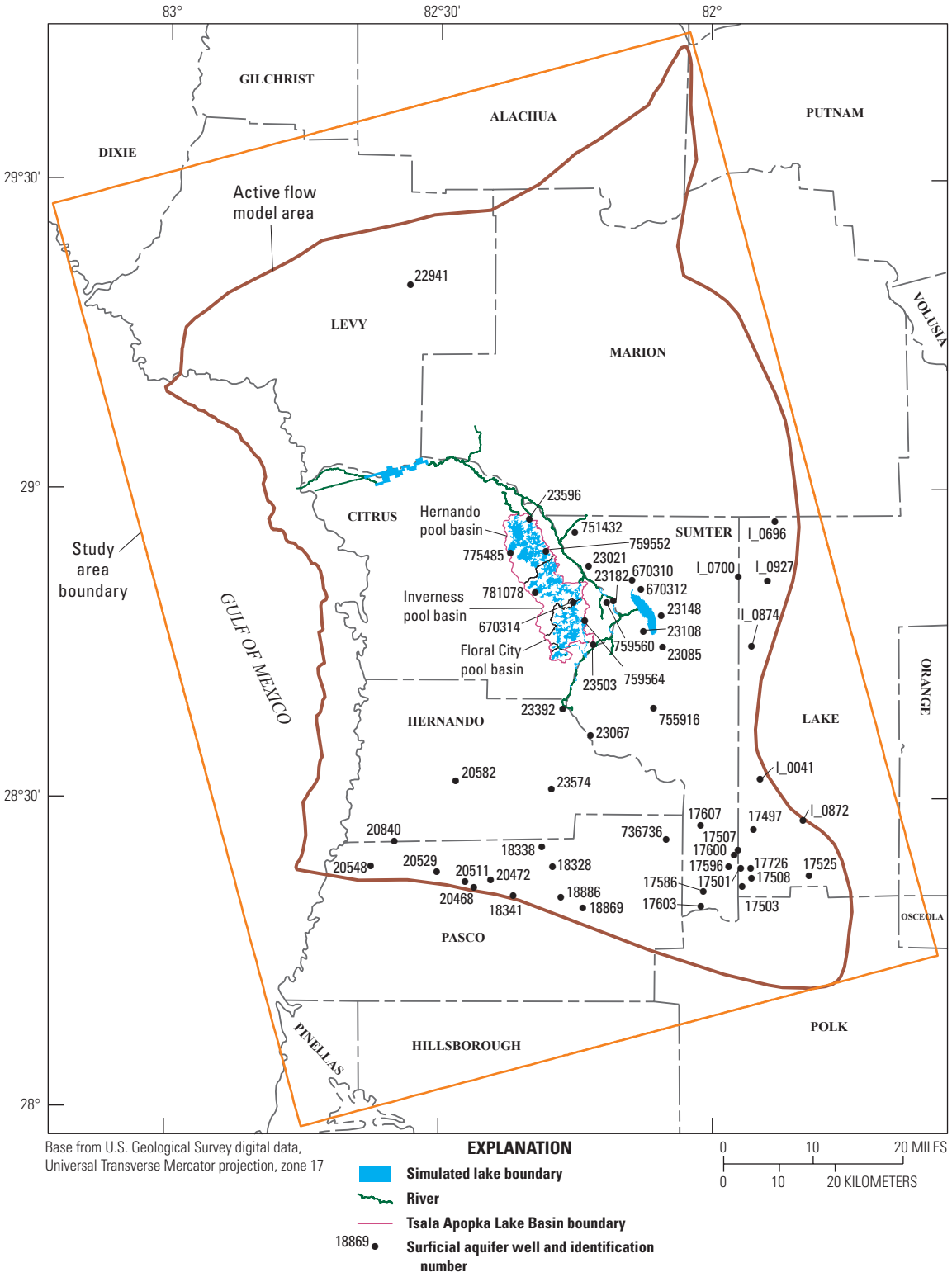

Figure 1.6 Spatial distribution of surficial aquifer wells in the active flow model area.

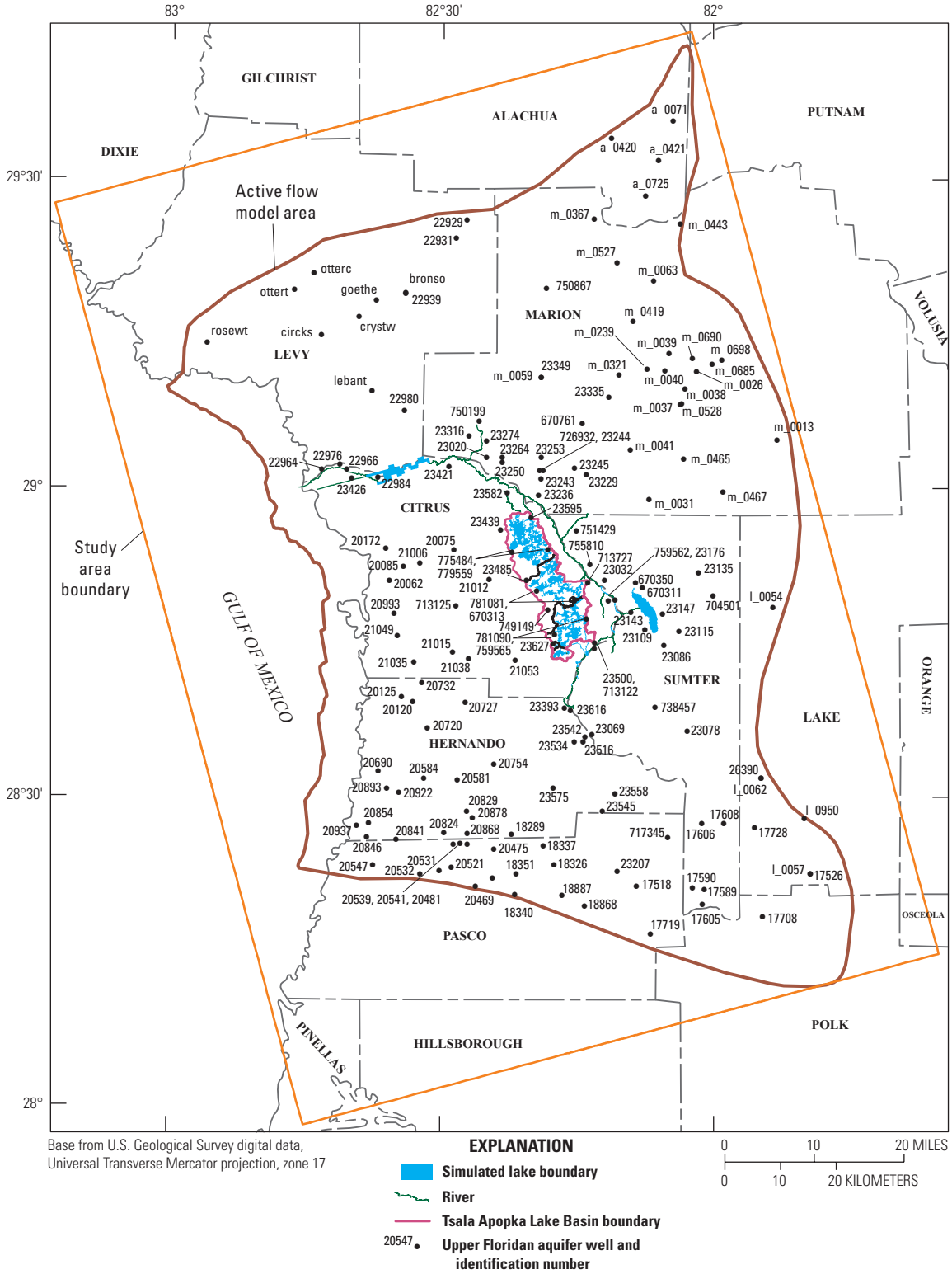

Figure 1.7 Spatial distribution of Upper Floridan aquifer wells in the active flow model area.

Table 1.5. Spring name, number, group number, location, row and column in numerical grid, and spring conductance used in the active flow model area.

[SPRNO, spring number location in figure 13; GRPNO, spring group number that indicates group of spring cells included in the same spring flow measurement; XSP, YSP, spring coordinates in State Plane projection, North American Datum of 1983, Florida west 0902 (Snyder, 1983), in feet; Row, Column, location of well in the numerical grid; COND, spring conductance, in square feet per day]

Spring name	SPRNO	GRPNO	XSP	YSP	Row	Column	COND
Magnesia Springs	1	1	609593	1907380	10	360	84,530
Wekiva Spring	2	2	447025	1798869	23	32	500,000
Big King Spring	3	3	451075	1739195	34	29	200,000
Little King Spring	4	4	449300	1737168	35	29	15,320
Silver Springs near Ocala	5	5	639380	1774913	37	359	25,000,000
Coastie Spring	6	6	428794	1708431	39	23	84,530
Rainbow 5, Spring Bridge Seep North, South	7	7	516830	1731661	39	122	15,000,000
Rainbow 1, 2, 3, 4, Spring Seep 1A, East Seep Waterfall Sp.	8	7	516506	1733823	39	123	15,000,000
Rainbow 6 Spring	9	7	519338	1730300	40	126	2,500,000
Rainbow 7 Spring, Rainbow Cave Spring	10	7	519795	1729894	40	127	2,500,000
Rainbow 8 Spring	11	7	519172	1727307	41	124	1,500,000
Bubbling Spring	12	8	517303	1733365	39	124	300,000
Indian Creek Spring #3, #4	13	9	521738	1730340	40	131	150,000
Indian Creek Spring #1, #2	14	10	522530	1730455	40	133	84,530
Lost Springs	15	11	438687	1674272	87	23	84,530
Wilson Head Spring	16	12	553388	1689081	118	171	84,530
Millers Creek Spring	17	13	463086	1660939	126	28	84,530
Citrus-Blue Spring	18	14	555611	1685289	126	173	84,530
Little Spring, Charles Fish House, Cedar Spring	19	15	465642	1660537	128	28	150,000
Birds Underwater Spring, Pool Springs, Catfish Spring	20	16	465288	1660009	129	28	84,530
Magnolia Circle Spring	21	17	464270	1658235	131	28	84,530
Hunters, Jurassic, Petes Pier Springs Complex	22	18	466571	1658393	132	28	84,510
Moray Springs Complex	23	19	465810	1658085	133	28	84,530
Buzzard Island Spring (Citrus), Paradise Isles Complex	24	20	464731	1656873	134	28	84,530
Crystal River Spring Group, Manatee Sanctuary Spring	25	21	466543	1657018	135	28	29,000,000
Idiots Delight #1, #2, #3, Three Sisters Springs #1, #2, #3	26	22	467448	1656076	137	28	253,620
Parker Island Springs, Banana Island Springs North	27	23	466058	1655234	138	28	150,000
Banana Island Springs Complex, FWS Spring Complex	28	24	465885	1654161	140	28	150,000
Tarpon Hole Spring, Hole #2, Mary Spring, Art Spring	29	25	465789	1653828	141	28	202,100
Lightbourns Ledge	30	26	464404	1652863	142	27	84,530
Daves Quest Springs Complex	31	27	465666	1653289	142	28	84,530
Wynn Court Springs Complex, Black Spring	32	28	464980	1652573	143	27	84,530
Golfview Boathouse Spring	33	29	466750	1652827	143	28	84,530
Sids Spring, Garys Grotto	34	30	464942	1651992	144	27	84,530
Gum Springs Main	35	31	582129	1681351	148	222	433,500
Gum Springs No. 1	36	31	582365	1681563	148	223	84,530
Gum Springs No. 4	37	31	579196	1679430	150	216	84,530
Gum Springs No. 2 and No. 3	38	31	580418	1679582	150	218	169,060
Halls River Head Spring	39	32	470348	1633770	182	28	4,800,000
Halls River #1 Spring	40	33	465979	1632212	183	27	159,900
Bear Spring (Citrus)	41	34	468085	1624685	198	27	84,530
Alligator Spring (Citrus), Banana Spring	42	35	467852	1624196	199	27	84,530
Homosassa #1, #2, #3 Spring, Blue Hole Spring (Citrus)	43	36	467747	1623748	200	26	2,083,000
Pumphouse Spring	44	37	467761	1622716	202	26	180,000
Trotter Main Spring	45	38	468355	1622748	202	27	133,100
SE Fork Head Spring Homosassa	46	39	468705	1622110	204	27	2,216,000

Table 1.5. Spring name, number, group number, location, row and column in numerical grid, and spring conductance used in the active flow model area.—Continued

[SPRNO, spring number location in figure 13; GRPNO, spring group number that indicates group of spring cells included in the same spring flow measurement; XSP, YSP, spring coordinates in State Plane projection, North American Datum of 1983, Florida west 0902 (Snyder, 1983), in feet; Row, Column, location of well in the numerical grid; COND, spring conductance, in square feet per day]

Spring name	SPRNO	GRPNO	XSP	YSP	Row	Column	COND
Bluebird Springs	47	40	470541	1620018	209	27	84,530
Otter Creek Spring	48	41	461359	1613838	216	25	84,530
Hidden River Head Spring, #2, #6 Spring	49	42	468958	1612615	222	26	425,000
Hidden River Spring #7, #8	50	43	468726	1611767	224	26	84,530
Henry Green Spring	51	44	625856	1648775	233	290	67,110
A. Wayne Lee Spring	52	45	628095	1645285	241	292	84,530
Ruth and Potters Creek Spring	53	46	465311	1599319	246	25	260,000
Salt Creek Head Spring (Citrus)	54	47	468782	1596242	254	25	18,440
Lettuce Creek Spring	55	48	471357	1594714	258	26	84,530
Crab Creek Spring	56	49	471541	1593967	259	26	700,000
Chassahowitzka #1, #2 Spring	57	50	471829	1593535	260	26	2,974,000
Chassahowitzka Main 1 Spring	58	50	471467	1593254	261	26	2,974,000
Johnson Creek HeadSpring	59	51	464603	1590036	263	24	84,530
Baird Spring, #2, #3, #4	60	52	470862	1590362	266	25	132,200
Ryles Spring	61	53	459367	1583035	274	23	458,200
Beteejay and Rita Marie Spring	62	54	466523	1584183	276	24	193,400
Blue Run	63	55	463332	1582897	277	24	180,000
Blind Spring, Hernando Unnamed #7	64	56	452638	1572429	291	21	2,400,000
Fenney Spring	65	57	643968	1621742	295	311	600,000
Canal 485A Spring 2	66	58	618490	1612773	299	257	84,210
Canal 485 Spring 5 and Canal 485A Spring 1B	67	59	618680	1612224	300	257	84,530
Sumter-Blue Spring	68	60	641563	1618337	300	305	250,000
Shady Brook Spring 3	69	61	642259	1616193	305	305	18,440
Big Hole Spring (Dead Spring)	70	62	624577	1608739	310	267	54,870
Buford #2 (Hernando)	71	63	464837	1564437	313	23	84,530
Buford HeadSpring (Hernando)	72	64	466752	1563492	316	23	84,530
Shady Brook Spring 4	73	65	629527	1607009	316	275	18,440
Belton's Millpond Spring Group	74	66	636177	1608076	317	289	200,000
Bugg Spring	75	67	687313	1606415	342	359	4,253,000
Mud and Wilderness Spring	76	68	455693	1533727	346	19	300,000
Hernando - Salt Spring	77	69	457437	1531830	346	20	1,500,000
Hospital Hole Spring	78	70	456031	1526120	347	19	104,900
Jenkins Creek Spring	79	71	452552	1523038	348	18	2,000,000
Weeki Preserve Spring	80	72	450714	1514236	349	18	1,000,000
Weeki Wachee Little Spring	81	73	469586	1519832	349	21	1,000,000
Weeki Wachee Main Spring	82	73	472099	1521191	349	22	3,000,000
Jewfish Hole	83	74	428525	1489189	353	12	40,430
Boat Spring	84	75	445176	1491996	353	15	9,724
Magnolia Spring and Gator Spring, Bobhill Spring	85	76	446462	1491033	354	16	31,750
Double Keyhole Spring	86	77	439102	1484261	355	14	84,530
Cedar Island Spring (Pasco)	87	78	428726	1471839	356	11	364,900
Horseshoe Spring	88	79	434346	1477876	356	12	2,000,000
Isabella Spring	89	80	439537	1478133	356	13	150,000
Riverdale Spring	90	81	591295	1509091	358	151	150,000
Dobes Hole Spring	91	82	601629	1490673	362	161	150,000

Model Calibration

The calibration of the Tsala Apopka Lake flow model required modifying the initial input parameters until differences between simulated and measured heads and flows were reduced to meet the calibration targets presented earlier. The modified input parameters included the (1) horizontal and vertical hydraulic conductivity of the surficial aquifer, upper confining unit, and Upper Floridan aquifer; (2) specific yield of the surficial aquifer; (3) specific storage of the upper confining unit and Upper Floridan aquifer; (3) lakebed leakances; (4) streambed vertical hydraulic conductivity; (5) hydraulic conductivity of the topsoil; (6) stream water-surface slope; and (7) initial soil water contents. Calculating the initial set of input parameters required calculating the average hydraulic conductivity for the Upper Floridan aquifer from layers 3 to 5 of the Northern District Model to derive the initial spatial distribution of hydraulic conductivity for the Upper Floridan aquifer layer in the model developed here.

The execution time of a forward simulation of the 2004–12 transient model, with daily time steps, varied from about 20 to 24 hours (depending on input values) using a state-of-the-art computer. This execution time was prohibitively long for the 9-year transient flow model to be used as the basis for parameter estimation through inverse methods. A calibration run that involves (1) seven iterations to achieve the calibration targets, (2) an average 22-hour duration for a forward run time per parameter, (3) the calibration of 937 parameters, (3) a forward and backward run for each parameter, and (4) the average availability of about 400 computer nodes requires a minimum, continuous run time of about 27 days. A run time of this length would have delayed progress in calibrating the model substantially if the calibration required conceptual model changes as part of the calibration adjustments. Limiting calibration to matching measured 2004 head and flow data, and assuming a 1-year forward run averages about 3 hours, the minimum run time to complete seven iterations would be about 7 days, assuming the availability of the same computer equipment and the same number of calibrated parameters. Therefore, inverse modeling techniques were applied to 2004 hydrologic conditions using PEST (Doherty, 2013a, b) to attain this more manageable time duration (about 3 hours) for a calibration run. For this model calibration, the sum of squared weighted residuals objective function to be minimized can be written in terms of 67,450 measurements, including measured spring flows, heads at wells, lake stages, and streamflows:

$$\sum_{i=1}^{N_{SP}}\left(w_{SP}(SP_{S_i}-SP_{M_i})\right)^2+\sum_{i=1}^{N_h}\left(w_h(h_{S_i}-h_{M_i})\right)^2+ \sum_{i=1}^{N_{LS}}\left(w_{LS}\ (LS_{S_i}-LS_{M_i})\right)^2+\sum_{i=1}^{N_{SF}}\left(w_{SF}(SF_{S_i}-SF_{M_i})\right)^2 \quad (1.3)$$

where

SP_{S_i}, SP_{M_i} are the simulated and measured spring flows, where the number of spring- flow measurements $N_{SP}=5{,}945$;

h_{S_i}, h_{M_i} are the simulated and measured water levels, where the number of head measurements at wells $N_h=57{,}173$;

LS_{S_i}, LS_{M_i} are the simulated and measured lake stages, where the number lake-stage measurements $N_{LS}=1{,}464$;

SF_{S_i}, SF_{M_i} are the simulated and measured streamflows, where the number of streamflow measurements $N_{SF}=2{,}868$;

w_{SP} is the weight applied to spring flow measurements, equal to 1.069×10^{-6} / (ft^3/d);

w_h is the weight applied to water-level measurements, equal to 7.251×10^{-2} / ft;

w_{LS} is the weight applied to lake-stage measurements, equal to 0.932 / ft; and

w_{SF} is the weight applied to streamflow measurements, equal to 8×10^{-7} /(ft^3/d).

PEST uses a modified Gauss-Newton nonlinear regression method to estimate parameters that minimize a sum of squared weighted residuals objective function. The weights in equation (1.3) were calculated by PEST to provide an equal contribution to the objective function from each of the four observation types, namely spring flows, heads, pool stages, and streamflows. The units of feet and days were used for each of the measurement types, and because flow rates are substantially larger in magnitude than heads and stages, the PEST-generated weights for flows were correspondingly lower than weights for heads and stages to make the starting contributions to the objective function equal for each of the four measurement types.

Model calibration was achieved by (1) estimating hydraulic parameters using PEST for transient 2004 hydrologic conditions, (2) using results from a forward simulation of the 9-year transient model to guide manual adjustments of parameters of areas where no water levels were measured during 2004, and (3) making required changes to some parameters to reduce residuals in areas either not stressed by 2004 pumping rates or not represented with measured water levels in 2004. These three steps were repeated until simulation results met calibration targets while keeping calibrated parameters within reasonable ranges. Regularization was used to avoid sharp spatial gradients in the spatial distribution of hydraulic parameters.

Boundary Conditions

The main boundary conditions imposed in the active flow model are (1) time-dependent heads at lateral boundary cells using the General Head Boundary (GHB) Package, (2) time-dependent pool altitudes at 4 spring groups and time-independent pool altitudes at 78 spring groups, and

(3) a no-flow condition imposed at the bottom of the Upper Floridan aquifer and at some lateral boundaries of the surficial and Upper Floridan aquifers. Additional boundary conditions implemented in the model area consist of (1) specified flows leaving some lakes through water-control structures, (2) specified rainfall, and (3) specified RET. The LAK7 Package was used to represent backwater pools with water-control structures represented by stream segments in the SFR2 Package. SFR2 segments represent water-control structures using Manning's equation, and the altitude, slope, and width of the segment are parameters that determine the relation between pool depth and outflow. The boundary conditions simulated in the model area are implemented by several MODFLOW-NWT Packages (fig. 1.8).

The model simulates the freshwater flow system using three layers. Model boundaries were selected to approximate the groundwater flow system from potentiometric surface maps as accurately as possible. The estimated potentiometric surface for the Upper Floridan aquifer for January 2004 (fig. 1.9) indicates that there are nonzero flows through some of the lateral boundaries of the model. GHB cells were established at these lateral boundary cells to simulate flows entering and leaving the model area. Head-dependent flow boundary conditions were simulated using the GHB Package and were applied to sections of the lateral boundaries (fig. 1.9) for the surficial and Upper Floridan aquifer layers. The specified heads at the GHB cells were varied monthly for the 2004–12 simulation period. Specified heads used in the GHB Package were interpolated along the lateral boundaries based on measured water levels in wells. Boundary conductance values used in the GHB Package were computed as the product of the horizontal hydraulic conductivity of the model layer for the corresponding cell and the cross-sectional area of the cell, divided by an internode distance specified by the variable numerical grid. Such conceptualization is a common approach for simulating regional flow across model boundaries.

Flows at the 91 springs in the active flow model area (fig. 13) were calibrated using estimated spring pool altitudes. A major component of spring flow is the net aquifer recharge

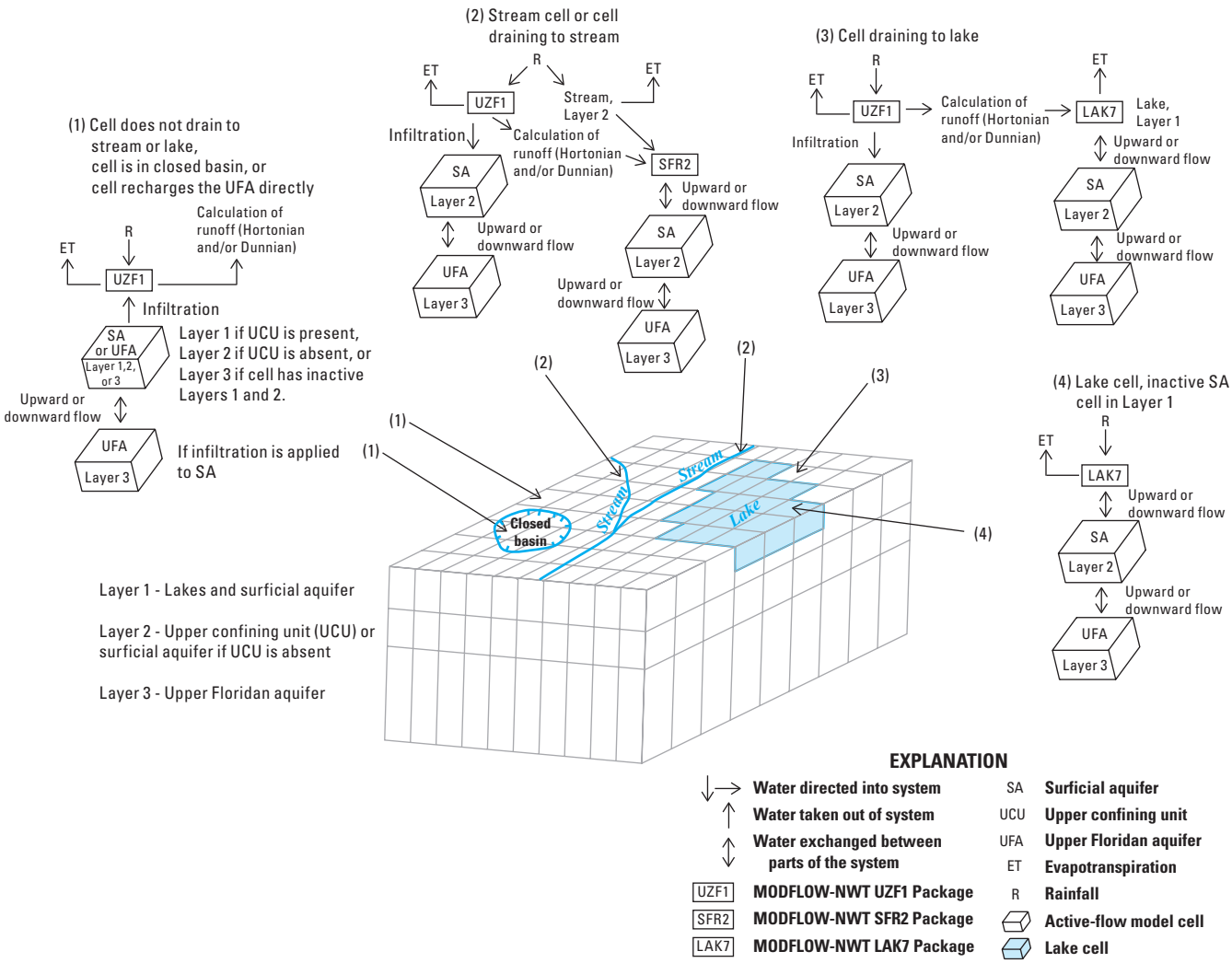

Figure 1.8 Implementation of the conceptual model with flow packages used to develop the surface-water/groundwater model.

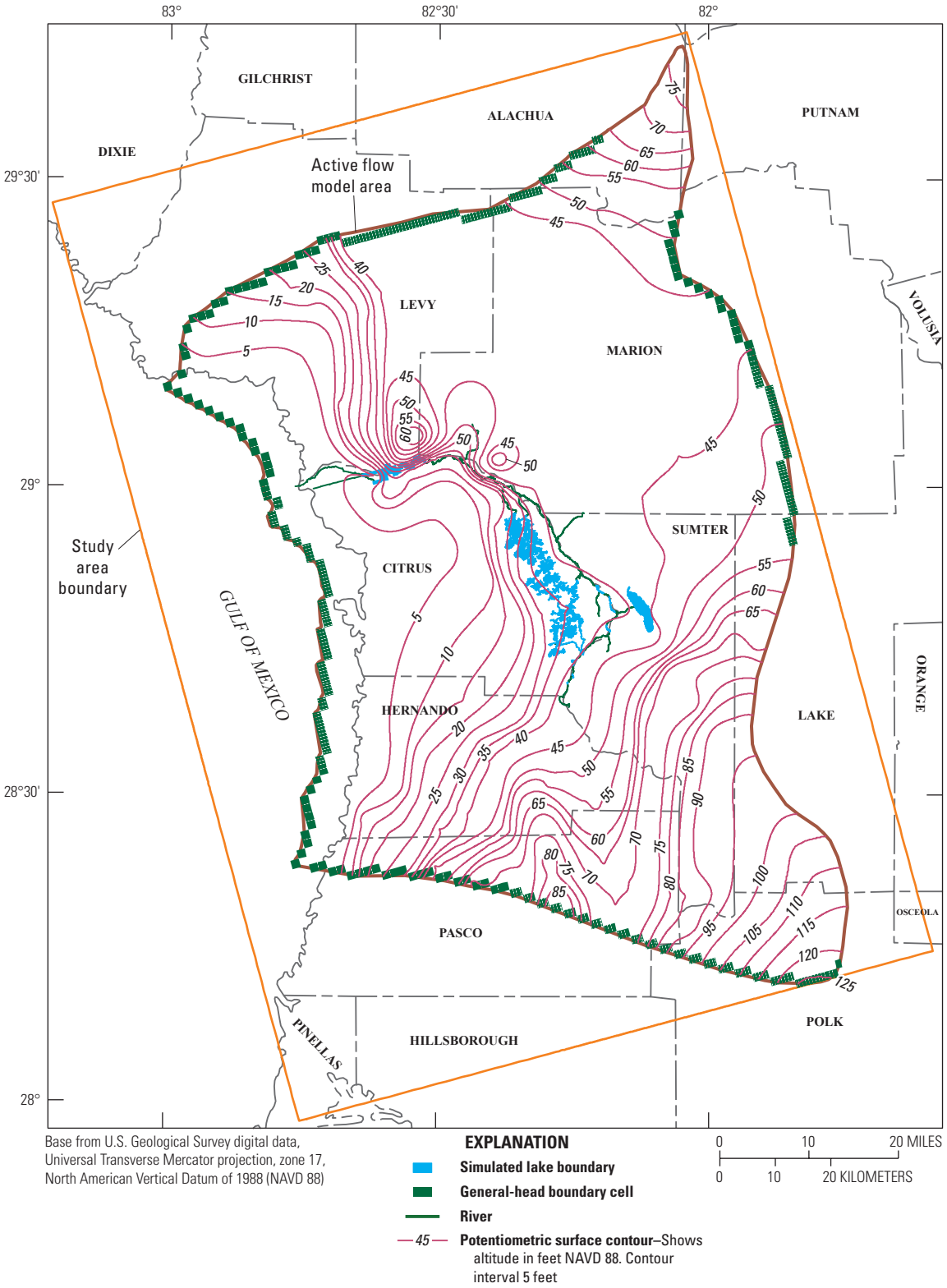

Figure 1.9 Location of grid cells where general-head boundaries were applied and potentiometric surface of the Upper Floridan aquifer for January 2004 conditions.

from rainfall; however, spring response is delayed by aquifer-matrix storage. Higher spring flows are common in late fall after the rainy season, whereas lower flows occur in late spring at the end of the dry season. Spring flows from the Upper Floridan aquifer tend to create depressions in the potentiometric surface, the areal extent and depth of which depends on the magnitude of spring flow and hydraulic parameters of the Upper Floridan aquifer. Parameters in the GHB Package were used to calibrate spring flow by specifying an estimated head at the spring that best represented the spring pool altitude and specifying a conductance value equal to that specified by HydroGeoLogic (2013). The estimated pool altitudes at the springs were varied monthly for the 2004–12 simulation period at four springs where the flow is either influenced by tidal effects or varies according to a time-dependent impedance to flow in the spring run. After spring flow was calibrated, the parameters in the GHB Package were then used to generate the Drain (DRN) Package input file, which allows discharge flow only.

Lakes constitute another boundary condition on the model involving leakage to or from the surficial aquifer through the lakebed material. The water-surface altitudes at the 15 lakes included in the active flow model area (fig. 1.2) were simulated using the LAK7 Package developed by Merritt and Konikow (2000). Initial water-surface altitudes at the lakes were assigned from measured values in January 2004.

Lake stage is calculated according to a water balance equation consisting of sources and sinks, including land-surface runoff, rainfall, ET at the lake's water-surface, and lake-aquifer water exchanges. Parameters that influence water-surface altitudes at lakes are the lakebed leakance and the streambed slope and channel width of the first stream reach of the lake's outlet. The vertical hydraulic conductivity of the lakebed and the difference between water-surface altitude and head determined the lateral and (or) vertical flow to or from the surficial aquifer. The streambed slope of the first stream reach of each lake outlet was adjusted as needed during the calibration of the water-surface altitudes at lakes not affected by water-control structures.

Streamflow routing was performed using the SFR2 Package developed by Niswonger and Prudic (2006). The main streams simulated in the active flow model area were the Withlacoochee River, the Outlet River, Gum Springs Run, and the Rainbow River (fig. 1.3). Initial flow along the uppermost reach of stream segment 1 was specified from measured streamflow data obtained from Withlacoochee River at Nobleton (station 02312558). Additional streamflow was specified as runoff distributed over segment 30 (Gum Springs Run, fig. 1.3) and over segment 35 (Rainbow River, fig. 1.3).

The parameters that determine the magnitude and routing of streamflow are the surface runoff applied to each stream, stream-channel width, streambed slope, streambed thickness, vertical hydraulic conductivity of the streambed, actual ET, rainfall applied to the stream water-surface area, and Manning's dimensionless roughness coefficient. The surface runoff was calculated by the UZF Package for each stream and depended on the rainfall, the drainage area of each stream determined from a digital elevation model from the SWFWMD GIS database, and the infiltration rate of the topsoil. The stream channel width and streambed altitude along cross sections of segment reaches were calculated from the collected lidar data. The lack of data for streambed thickness led to the generalized assumption of a streambed thickness of 5 ft for most stream reaches. Streambeds thicker than the assumed 5 ft would result in a calibrated vertical hydraulic conductivity that is proportionally larger than the previous calibrated value.

Specified Flows in Streamflow Routing

Streamflow routing is initiated at the most upstream point of reach 1 of segment 1, which is near the Withlacoochee River at Nobleton streamflow-gaging station (station 02312558, fig. 18). Measured streamflow at this station (fig. 1.10) was specified as the initial flow for the streamflow routing; average daily streamflow was 246.7 ft^3/s, with flow ranging from 0 to 4,350 ft^3/s during the 2004–12 period.

Flow through the structures in the Tsala Apopka Lake Basin was calculated by the SWFWMD and USGS on the basis of measured upstream and downstream stages, channel geometry, and structure openings. Periodic measured flows by the USGS and SWFWMD were used to calibrate step-backwater calculations by the SWFWMD and rating curves developed by USGS. McBride and others (2017) provide more details about the calculated flows and rating curves used for a submerged orifice, free weir, submerged weir, and free orifice. Differences between the SWFWMD and USGS calculated flows were identified, and when the differences were large, final flows were reconciled by the SWFWMD.

Daily streamflow through the Leslie Heifner and Floral City structures (figs. 1.11, 1.12; stations 02312772 and 02312786, fig. 18) was used to specify the flow diverted from the Withlacoochee River to the Floral City pool. Negative flow at these structures, implying reversed streamflow, occurred at isolated times in minimal quantities and was simulated as Floral City pool withdrawals and as surface runoff draining to Bonnet Lake (fig. 2). Average annual streamflow during the 2004–12 period, through the Leslie Heifner and Floral City structures to the Floral City pool, was 17.53 and 4.80 ft^3/s per day, respectively. Total average streamflow entering the Floral City pool was 22.33 ft^3/s per day. The Leslie Heifner structure was open 908 days during the 2004–12 period (27 percent), and the estimated flow ranged from -35 to 245 ft^3/s. The Floral City structure was open 296 days during the 2004–12 period (9 percent), and the estimated flow ranged from -2 to 140 ft^3/s.

Daily streamflow through the Golf Course and Moccasin Slough structures (figs. 1.13, 1.14; stations 02312815 and 02312827, fig. 18) was estimated by SWFWMD to specify the flow leaving the Floral City pool and entering the Inverness pool. Average annual streamflow during the 2004–12 period,

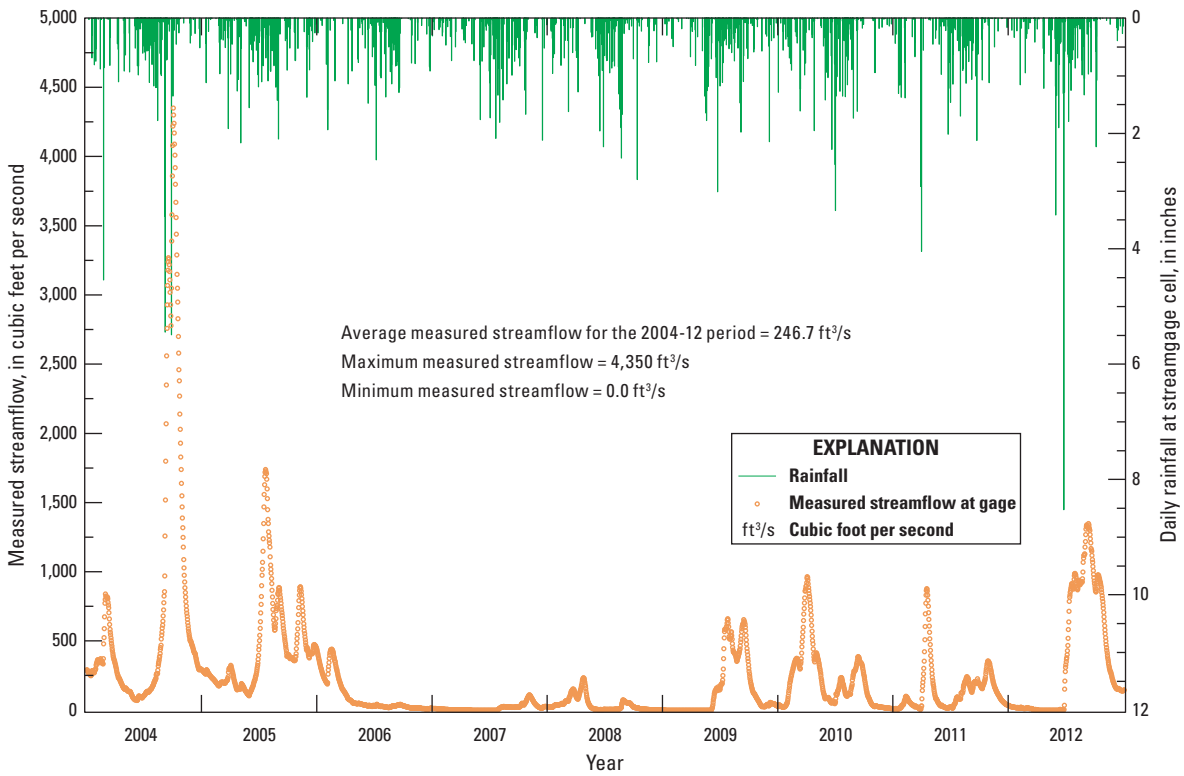

Figure 1.10 Measured flow at the Withlacoochee River at Nobleton streamflow-gaging station 02312558 and daily rainfall at streamgage, for the 2004–12 period.

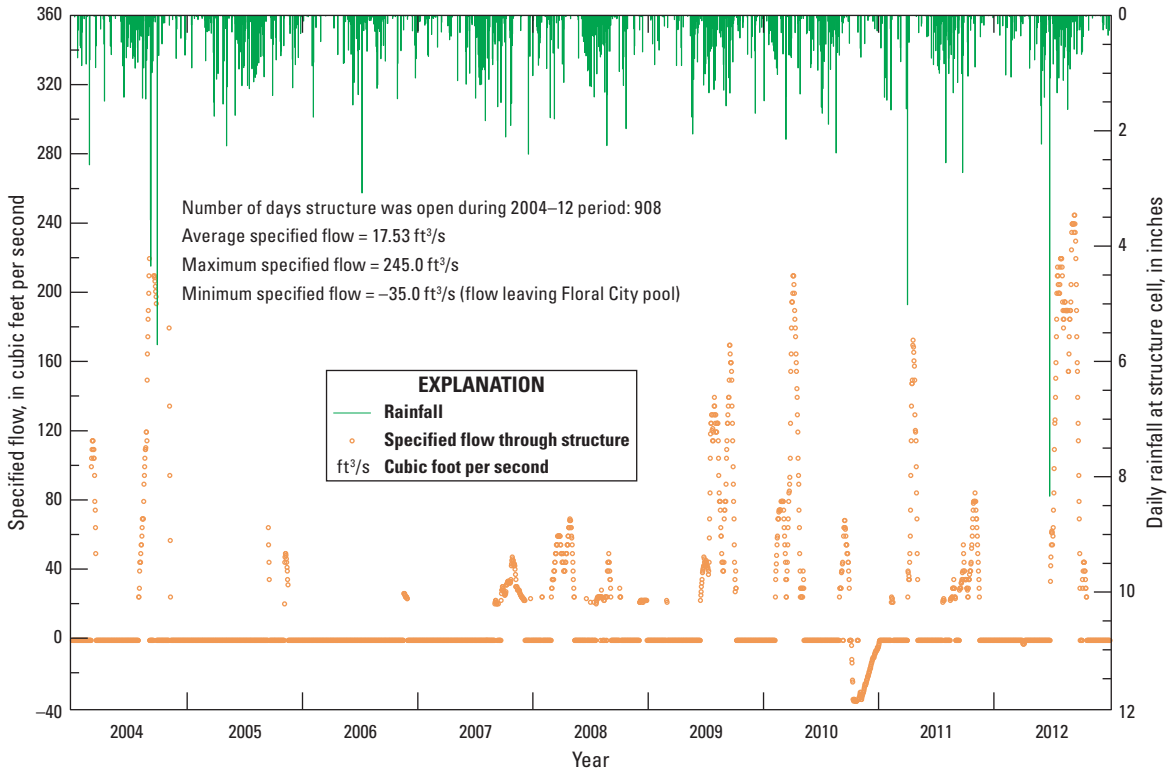

Figure 1.11 Specified flow through the Leslie Heifner structure and daily rainfall at structure cell, for the 2004–12 period.

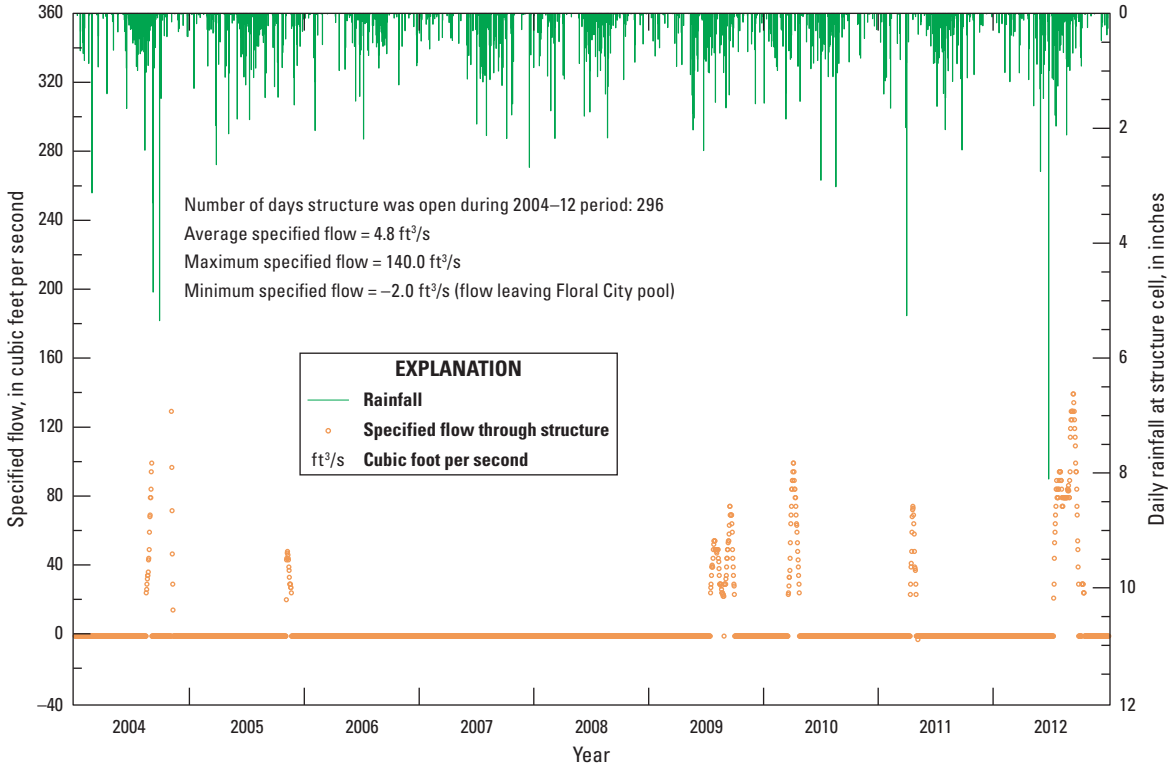

Figure 1.12 Specified flow through the Floral City structure and daily rainfall at structure cell, for the 2004–12 period.

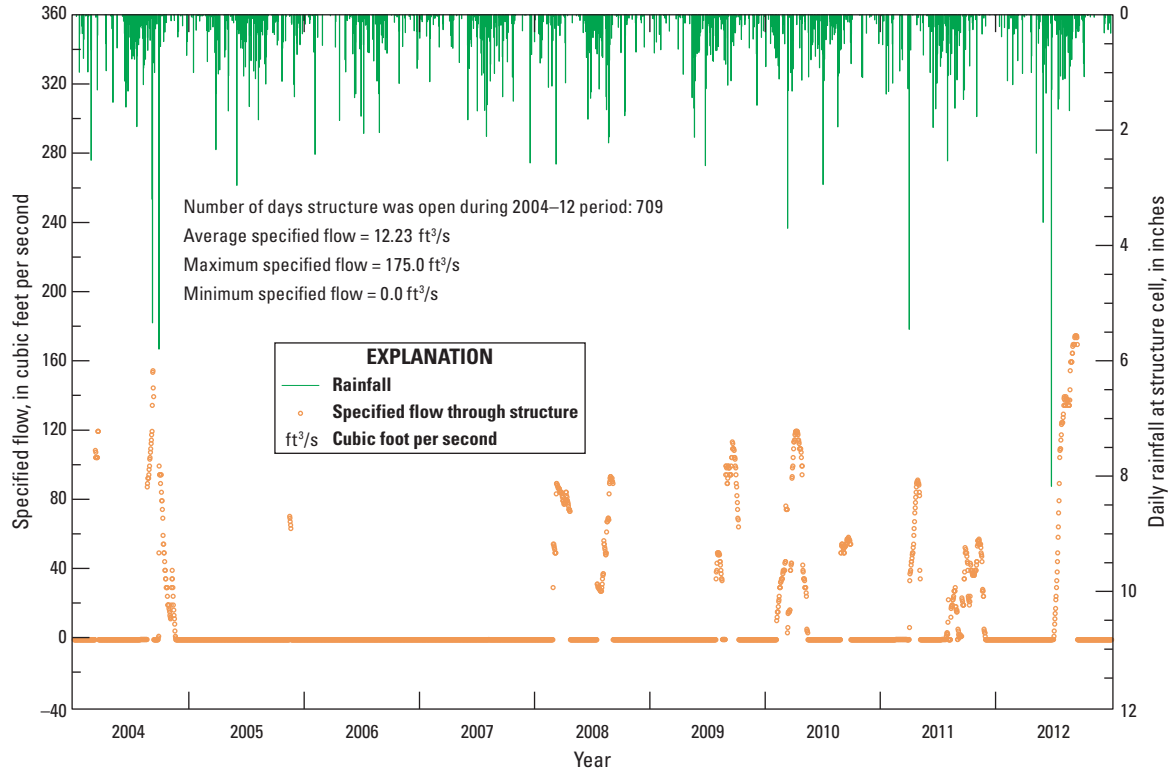

Figure 1.13 Specified flow through the Golf Course structure and daily rainfall at structure cell, for the 2004–12 period.

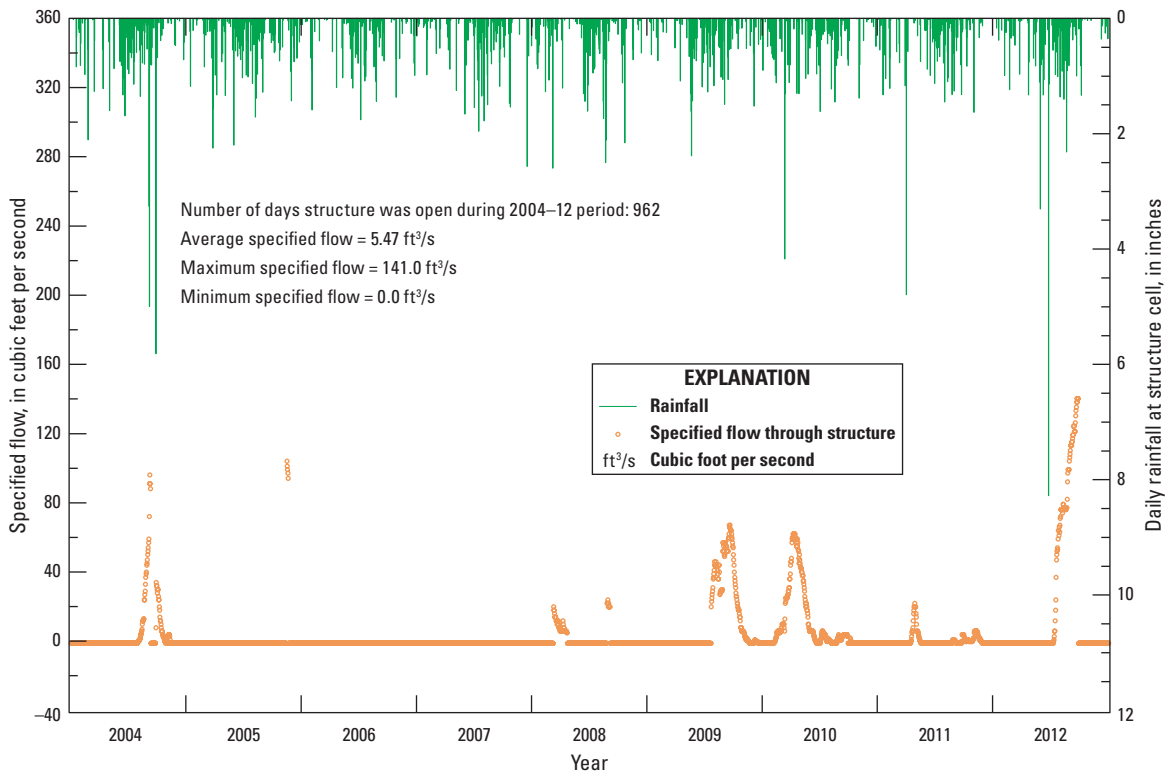

Figure 1.14 Specified flow through the Moccasin Slough structure and daily rainfall at structure cell, for the 2004–12 period.

through the Golf Course and Moccasin Slough structures to the Inverness pool, was 12.23 and 5.47 ft^3/s per day, respectively. Total average streamflow entering the Inverness pool was 17.70 ft^3/s per day. The Golf Course structure was open 709 days during the 2004–12 period (22 percent), and the estimated flow ranged from 0 to 175 ft^3/s. The Moccasin Slough structure was open 962 days during the 2004–12 period (29 percent), and the estimated flow ranged from 0 to 141 ft^3/s. Daily flow through the Bryant Slough structure (fig. 1.15; station 740884, fig. 18) was used to specify the flow that leaves the Inverness pool and is routed to the Withlacoochee River through stream segments 26 and 28 (fig. 1.3). Average annual streamflow during the 2004–12 period, through the Bryant Slough structure and leaving the Inverness pool, was 0.11 ft^3/s per day. The Bryant Slough structure was open 83 days during the 2004–12 period (2.5 percent), and the estimated flow ranged from -9 to 50 ft^3/s. Daily flow through the Brogden Bridge structure (fig. 1.16; station 02312915, fig. 18) was used to specify the flow leaving the Inverness pool and entering the Hernando pool, which averaged 7.66 ft^3/s per day. The Brogden Bridge structure was opened 495 days during the 2004–12 period (15 percent), and the estimated flow ranged from 0 to 241 ft^3/s.

Daily streamflow through the S–353 and Van Ness structures (figs. 1.17, 1.18; stations 02312975 and 23589, fig. 18) was used to specify the flow leaving the Hernando pool. The flow through the S–353 structure enters the Withlacoochee River, and the flow through the Van Ness structure discharges to the north. Average annual outflow during the 2004–12 period, through the S–353 and Van Ness structures, was 2.83 and 1.10 ft^3/s per day, respectively. Total average flow leaving the Hernando pool was 3.93 ft^3/s per day. The S–353 structure was open 166 days during the 2004–12 period (5 percent), and the measured flow ranged from 0 to 218 ft^3/s. The Van Ness structure was opened 228 days during the 2004–12 period (7 percent), and the measured flow ranged from 0 to 100 ft^3/s.

Measured streamflow at the Outlet River at Panacoochee Retreats (station 02312700, fig. 18, fig. 1.19) was used to specify lake outflow at stream segment 43 (fig. 1.3) to calibrate the stage of Lake Panasoffkee (lake 12 in fig. 1.2). The average flow at station 02312700 was 109.9 ft^3/s per day during the 2004–12 period, with streamflow ranging from 0 to 500 ft^3/s (fig. 1.19). Lake stage calibration was achieved by (1) using the tabulated relation between stage, volume, and water-surface area provided as input for each lake, (2) establishing a mass balance of inflows and outflows, and (3) solving for the temporal changes in surface runoff arrival at the lake. The stage calibration of Lake Panasoffkee used a balance of inflows and outflows instead of a direct calibration that involved identifying the areal extent of the cells draining to Lake Panasoffkee. The simpler approach of a mass balance did not require solving the nonlinear surface leakage problem associated with identifying the cells that drain to Lake Panasoffkee.

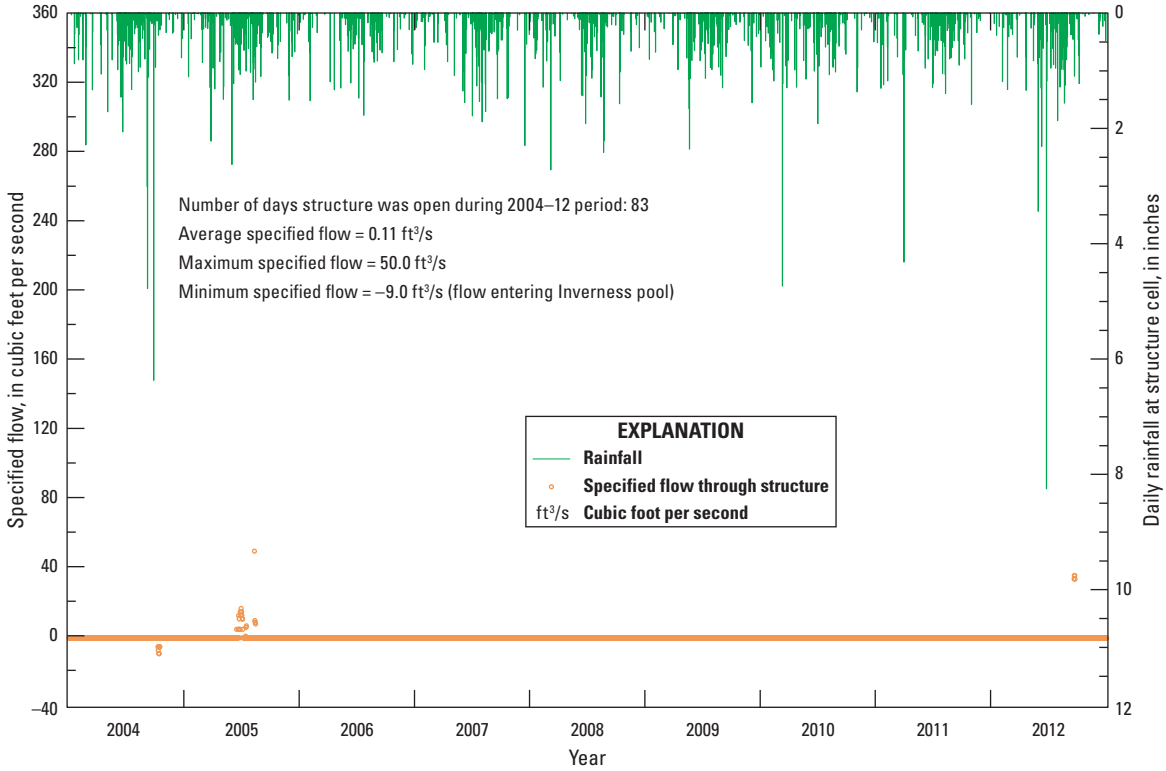

Figure 1.15 Specified flow through the Bryant Slough structure and daily rainfall at structure cell, for the 2004–12 period.

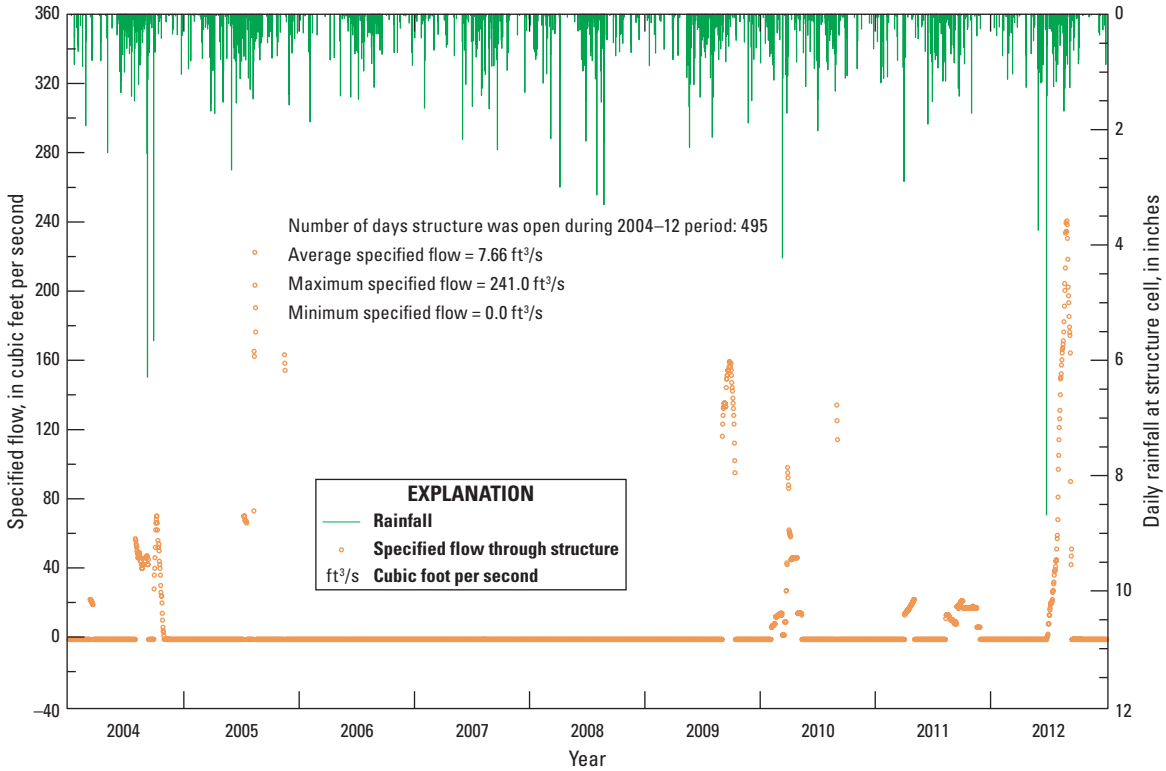

Figure 1.16 Specified flow through the Brogden Bridge structure and daily rainfall at structure cell, for the 2004–12 period.

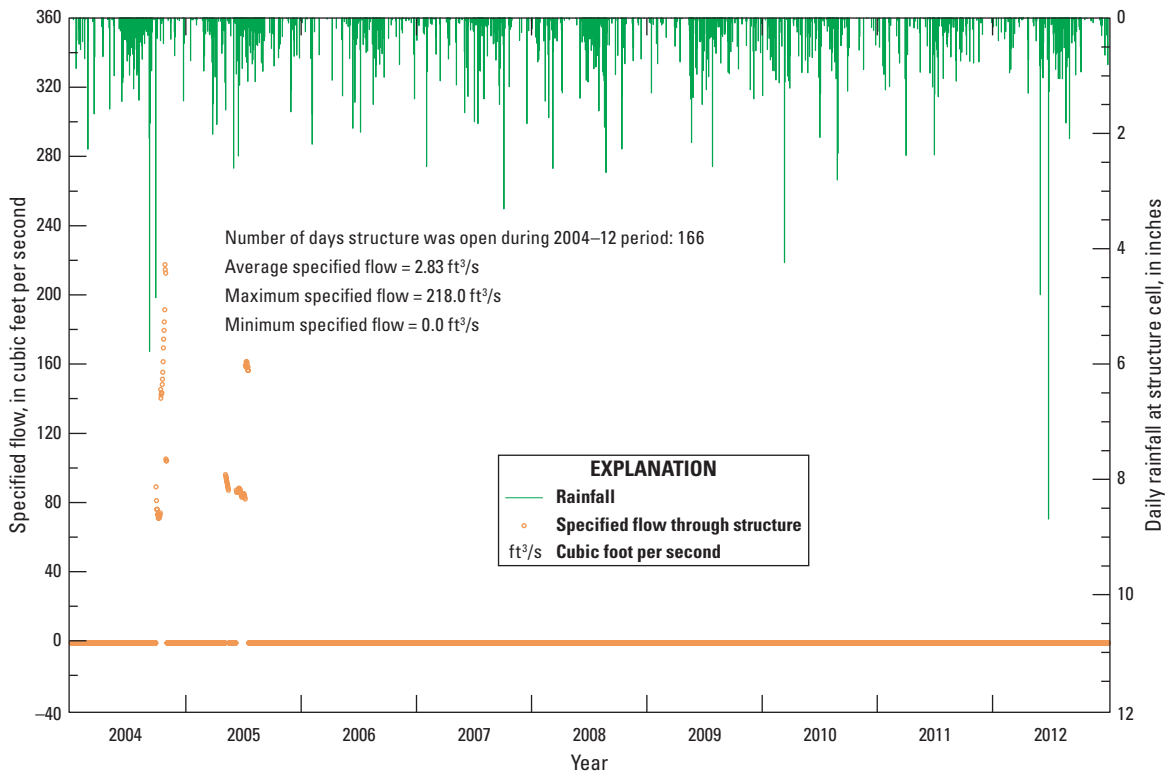

Figure 1.17 Specified flow through the S–353 structure and daily rainfall at structure cell, for the 2004–12 period.

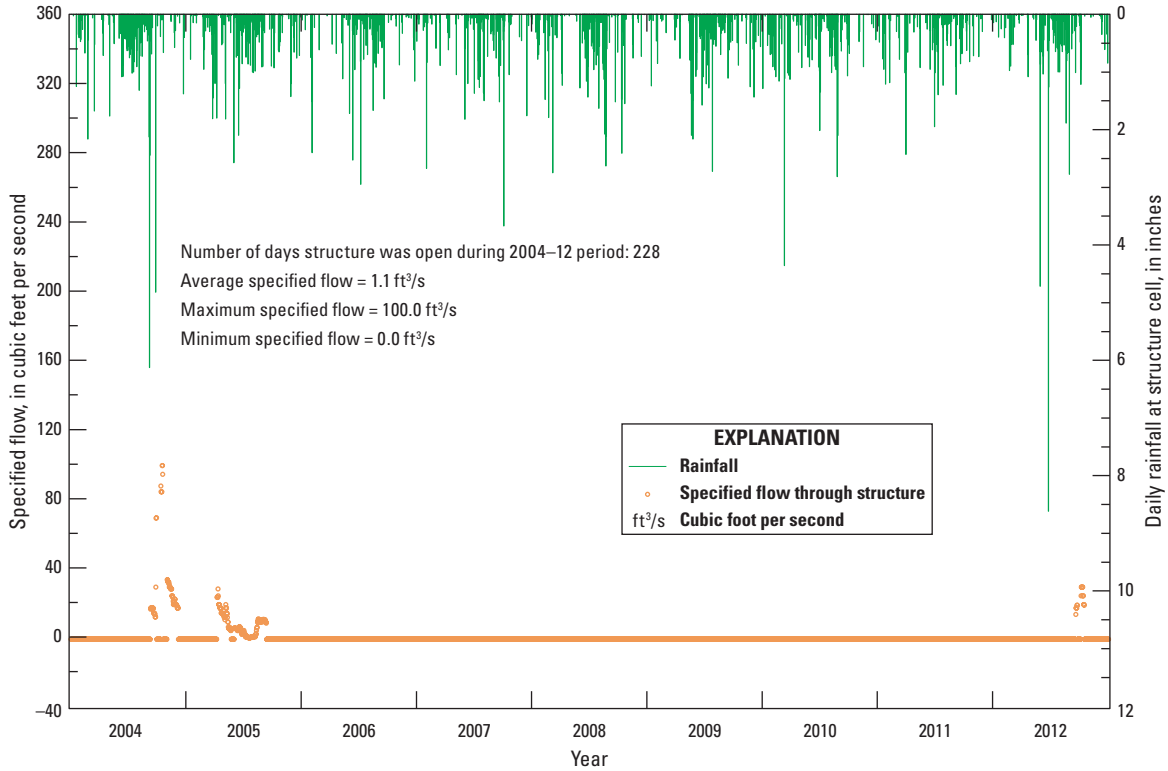

Figure 1.18 Specified flow through the Van Ness structure and daily rainfall at structure cell, for the 2004–12 period.

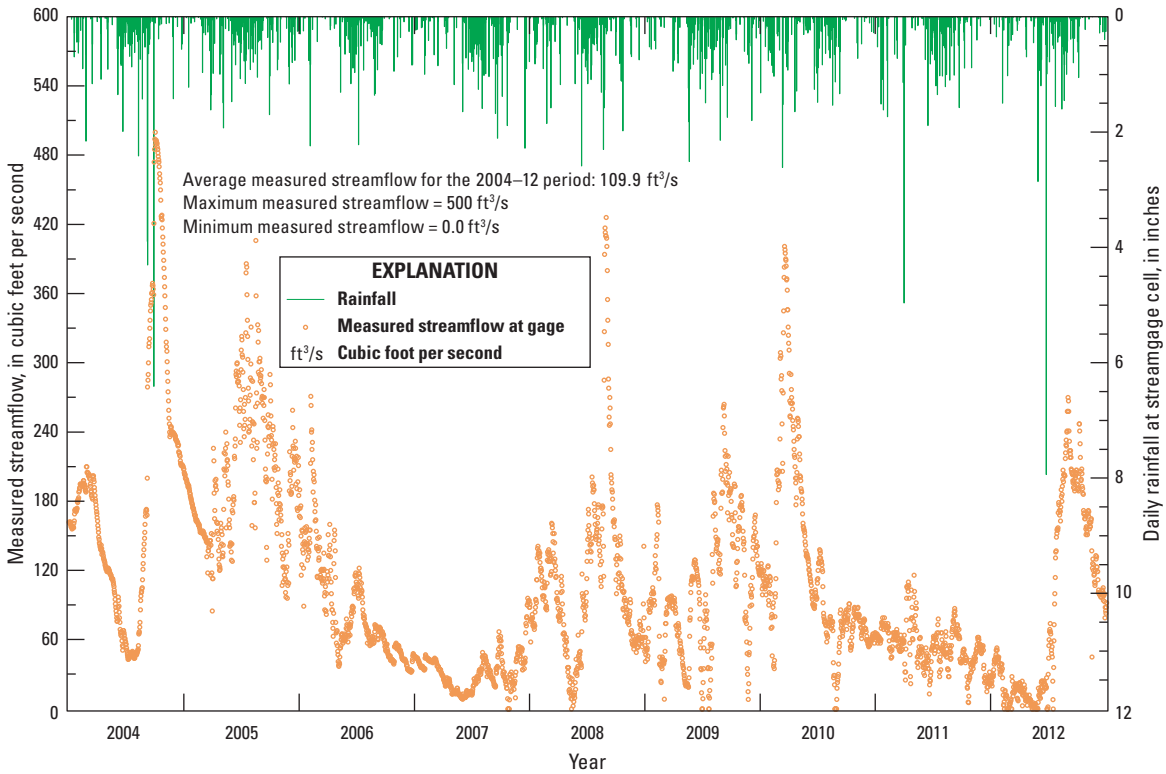

Figure 1.19 Measured flow at the Outlet River at Panacoochee Retreats streamflow-gaging station 02312700 and daily rainfall at streamgage, for the 2004–12 period.

Lake Panasoffkee is surrounded by areas of low land-surface altitude within the Tsala Apopka Plain physiographic region (figs. 3, 5). Many grid cells surrounding Lake Panasoffkee that represent areas of low land-surface altitude have relatively large simulated surface leakage rates from the surficial aquifer, because horizontal groundwater flow discharges to the surface in cells with low land-surface altitude. These areas are generally characterized by the presence of land-surface depressions. Cells with surface leakage do not consistently drain to a given lake or a stream, because the magnitude of the rainfall event determines whether the land-surface depressions are filled and what fraction of the runoff is drained to the nearest lake or stream. The need to identify cells draining surface leakage to Lake Panasoffkee was replaced in this model by calibrating the surface runoff to Lake Panasoffkee. The specified surface runoff to Lake Panasoffkee was calculated by minimizing the difference between measured and simulated lake stage using the stage-volume relation for the lake.

The streamflow routing Gum Springs Run and Rainbow River (segments 30 and 35 in fig. 1.3), was simplified by using measured streamflow at the Gum Springs near Holder gage (fig. 1.20; station 02312764, fig. 18) and measured streamflow at the Rainbow River at Dunnellon gage (fig. 1.21; station 02313100, fig. 18) to specify inflow as tabular flow files (Niswonger and Prudic, 2006). The average flow at station 02312764 was 88.6 ft^3/s per day during the 2004–12 period, with streamflow ranging from 5.1 to 520 ft^3/s (fig. 1.20). The average flow at station 02313100 was 594.3 ft^3/s per day during the 2004–12 period, with streamflow ranging from 391 to 831 ft^3/s (fig. 1.21). Surface runoff simulated downstream from these two streamflow-gaging stations was routed to the Withlacoochee River.

Rainfall, Infiltration, Evapotranspiration, Surface Leakage, and Net Recharge

The net recharge in the active flow model area was calculated by using the UZF1 Package of the MODFLOW-NWT code (Niswonger and others, 2006). Infiltration occurs whenever the water table is below land surface and the hydraulic conductivity of the topsoil exceeds the rainfall rate. Runoff occurs when the rainfall rate exceeds the hydraulic conductivity of the topsoil or when surface water is available and the water table is near land surface. The routing of infiltration through the unsaturated zone was calculated from rainfall by the UZF1 Package at each cell by using (1) the saturated vertical hydraulic conductivity of the unsaturated zone; (2) an initial soil water content of 0.07; (3) a residual soil water content of 0.07; (4) a Brooks-Corey exponent of 3.5; and (5) the simulated soil water content at each time step. The specified extinction soil water content was 0.07, making ET losses possible only when the soil water content exceeds 0.07.

Actual ET within the model was estimated by (1) varying the AET/RET ratios in table 2 by various calibration-defined percentages, (2) calculating the product of these revised ratios and the RET rates from the data obtained by Geostationary

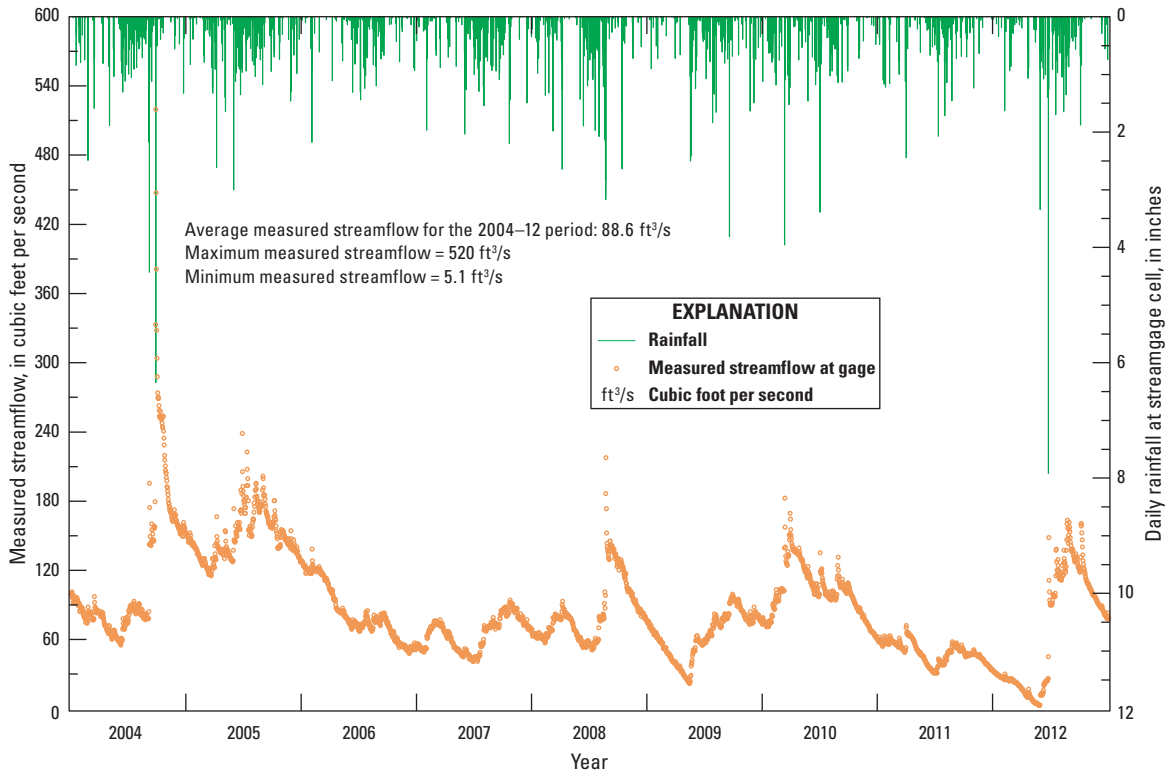

Figure 1.20 Measured flow at the Gum Springs near Holder streamflow-gaging station 02312764 and daily rainfall at streamgage, for the 2004–12 period.

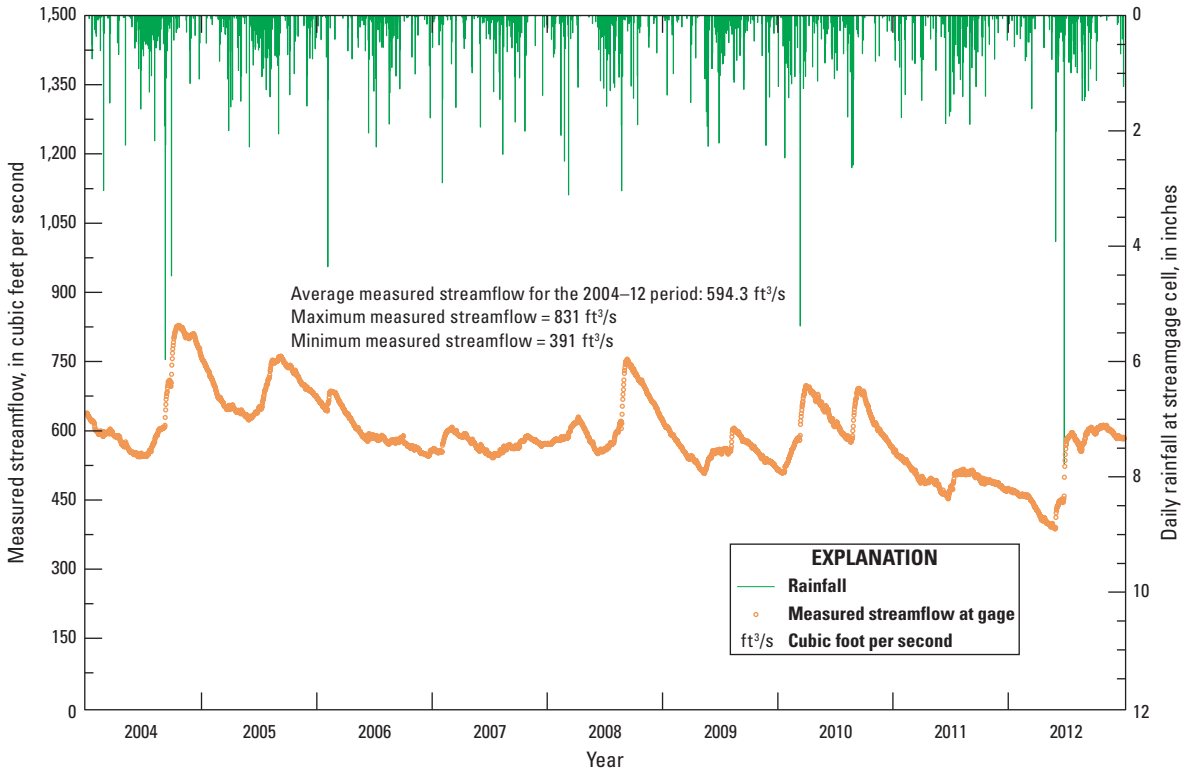

Figure 1.21 Measured flow at the Rainbow River at Dunnellon streamflow-gaging station 02313100 and daily rainfall at streamgage, for the 2004–12 period.

Operational Environmental Satellite (GOES), (3) using this product to calculate the evapotranspiration demand rates used in simulation of actual ET by the UZF1 Package (Niswonger and others, 2006), (4) simulating the annual total ET, and (5) repeating the previous four steps until the annual total ET was between the estimated ET rates by Sanford and Selnick (2013) and ET rates listed in table 3. The calibrated AET/RET ratios were calculated for all the land covers, except for lakes, listed in table 2. While the calibrated AET/RET rates for lakes were not changed from those rates listed in table 2, the calibrated AET/RET rates for the remaining five land covers (forest, grass, marsh, ridge, and urban in table 2) were calculated by increasing the AET/RET rates by 0.55 times the difference between unity and the AET/RET rates themselves.

Surface leakage is the surficial aquifer discharge to land surface that typically occurs in areas of land-surface depressions. Simulated surface leakage rates in 2004 for these areas indicate that rates are highest south of Lake Panasoffkee, along the downstream segments of the Withlacoochee River (fig. 1.22), along the Gulf of Mexico coastline, and in sections in the southeast corner of the model area. Surface leakage rates (groundwater discharges to land surface) are assigned to lakes or streams using the delineation of the subbasins that drain to these same lakes and streams. If a cell does not drain to a simulated stream or lake, the surface leakage that may occur at that cell is lost to ET; such cells are assigned a value of zero in the subbasin delineation. If a cell drains to a simulated stream or lake, a negative (lake) or positive (stream) integer is assigned in the subbasin delineation and the surface leakage that may occur in that cell is directed to the corresponding lake or stream, using the lake number or the stream segment.

Recharge and discharge areas in the Upper Floridan aquifer can be identified by the difference between the water-table altitude and the heads in the Upper Floridan aquifer. With a few exceptions—including a buffer zone a few miles wide extending from the coastline to the east, an area east of Lake Panasoffkee, and some areas along the Withlacoochee River—water-table altitudes are higher than the Upper Floridan aquifer heads, indicating the Upper Floridan aquifer is recharged by the surficial sands over a large part of the study area. Most of the Tsala Apopka Lake Basin recharges the surficial aquifer or infiltrates from land surface through the vadose zone to the Upper Floridan aquifer.

The simulated net recharge to the water table is the sum of recharge to the unsaturated zone (positive), groundwater ET (negative), and surface leakage (negative). Recharge to the unsaturated zone is the difference between infiltration and ET in the unsaturated zone. The unsaturated zone affects recharge because of ET, relations between flux and soil water content, internal drainage, travel times through the unsaturated zone, and the thickness of the unsaturated zone that changes with a falling or rising water table. Because of unsaturated-zone storage, the sum of recharge to the unsaturated zone is less than the sum of infiltration and ET during wet periods and is greater during dry periods (table 1.6). The average net recharge rate for the active flow model area for the 2004–12 period was about 10.3 inches per year (in/yr), ranging from 3.8 inches (in.) during 2006 to 14.2 in. during 2005. The net recharge rates for 2004 were positive over most of the central areas of the Tsala Apopka Lake Basin (fig. 1.23) and about 86 percent of the model area, extending over 3,440 mi^2 of the 4,003 mi^2 where the surficial aquifer is active. Discharge occurs along the coastline, in sections south and northeast of Lake Panasoffkee, and sections in the southeastern part of the active flow model area (fig. 1.23). Recharge rates are highest at deep lake cells in the Tsala Apopka Lake Basin and are the result of water being available for leakage for longer periods of time than shallow lake cells or marshes. Leakage rates for 2004 from lakes are presented as simulated net recharge for 2004 for the entire active flow model area (fig. 1.23); areas with the highest discharge in 2004 in the active flow model area indicate areas with the highest simulated surface leakage.

Groundwater Flow Across General-Head Boundary Cells

GHB cells were simulated at certain lateral boundary cells where the estimated potentiometric surface map for the Upper Floridan aquifer indicated that some flow exchange was occurring between the model area and adjacent areas (fig. 12). Conductance at these general-head boundary cells was calculated from the calibrated hydraulic conductivity at these cells, the thickness of the layer, and grid-cell size. GHB cells were also used for the surficial aquifer cells overlying the GHB cells in the Upper Floridan aquifer.

Average annual simulated flows through the GHB cells in the surficial aquifer were 0.12 in/yr entering the model area for the 2004–12 period after averaging annual flows using area-based weights from layers 1 and 2 where the surficial aquifer is active (table 1.7). Flow entering the model area in the surficial aquifer was greater where this aquifer overlies the Upper Floridan aquifer than the flow entering the model area where the surficial aquifer overlies the upper confining unit. Simulated total flow leaving the model area through the GHB boundary cells in the surficial aquifer was about four times lower than the simulated total flow leaving through the GHB cells in the Upper Floridan aquifer, which over the 2004–12 period averaged about 0.5 in/yr (table 1.7). Total annual flows through all GHB cells in the Upper Floridan aquifer ranged from 1.95 in/yr entering the model area in 2004 to 1.71 in/yr leaving the model area in 2011 (table 1.7). Flows through the GHB cells in 2004 ranged from about 0.12 in/yr (40 ft^3/s) leaving the model area along the southwest boundary to 0.29 in/yr (96 ft^3/s) entering the model area east of the cells having the largest outflow. Most of the flow in the Upper Floridan aquifer leaving the model area was simulated offshore along the western boundary and along sections of the northern and southern boundaries (fig. 1.24). Flow entering the Upper Floridan aquifer in the model area was simulated along sections of the eastern, northern, and southern boundaries (fig. 1.24). Flow leaving the model area through spring cells is documented in the Surface-Water and Groundwater Flow Budgets section.

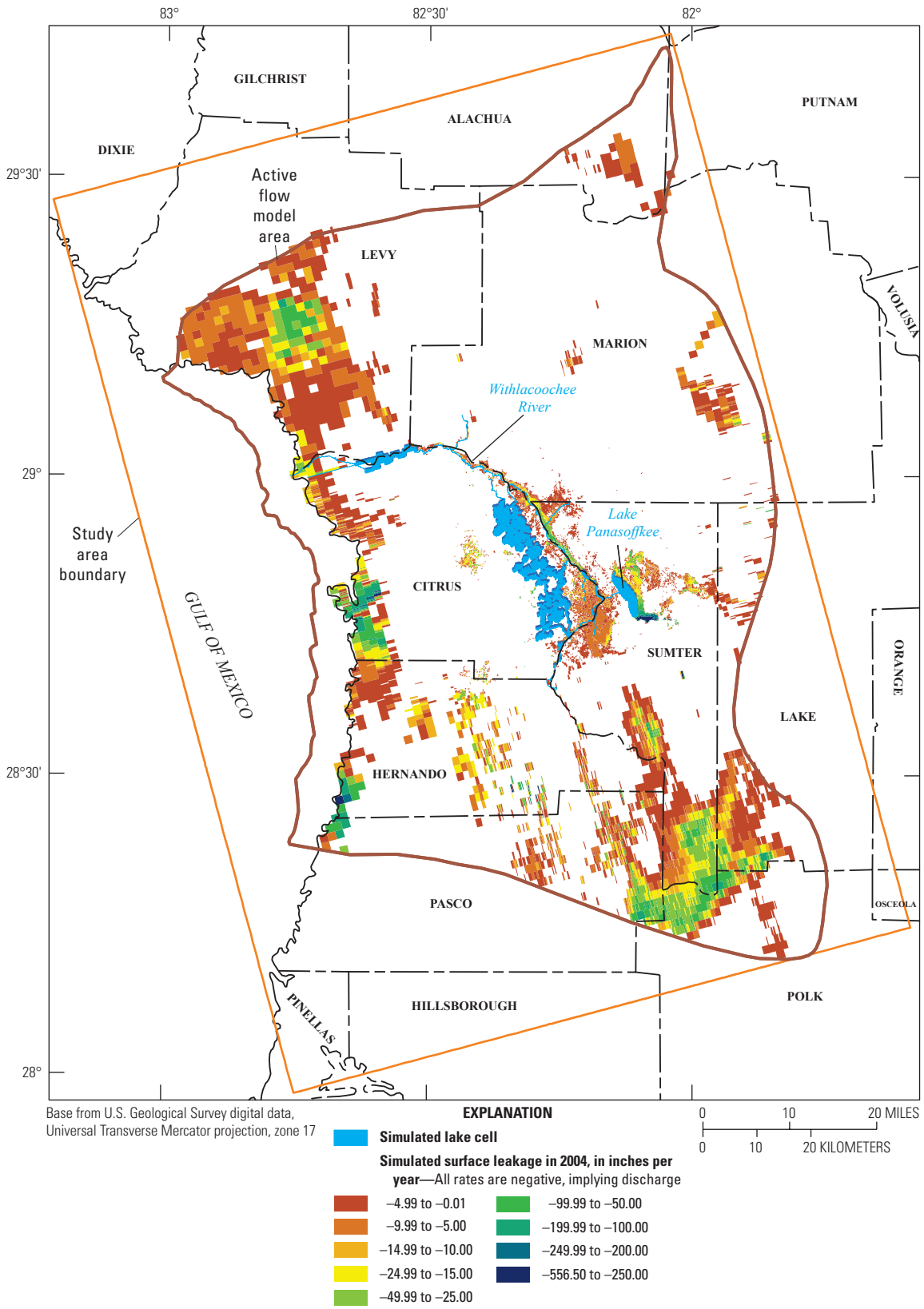

Figure 1.22 Simulated surface leakage rates for 2004.

Table 1.6. Simulated evapotranspiration, infiltration, recharge in the unsaturated flow zone, surface leakage, and net recharge rates in the surficial aquifer from the calibrated groundwater flow model.

[All rates are areal averages over active cells that are overlain by the unsaturated zone. All rates are in inches per year. UZET, evapotranspiration losses in the unsaturated zone; GWET, evapotranspiration losses in groundwater; UZINF, infiltration in the unsaturated zone; UZRCH, recharge to the water table from the unsaturated zone; UZSURFL, surface leakage; NETRECH, net recharge to the surficial aquifer, equal to UZRCH+GWET+UZSURFL; LKET, simulated lake evaporation scaled over active cells area; TOTET, total simulated evapotranspiration, equal to UZET+GWET+UZSURFL+LKET; Ave, average value per year for the 2004 to 2012 period]

Year	UZET	GWET	UZINF	UZRCH	UZSURFL	NETRECH	LKET	TOTET
2004	-22.02	-7.89	46.35	21.78	-4.13	9.76	-0.60	-34.64
2005	-24.31	-10.11	53.69	28.93	-4.60	14.23	-0.64	-39.66
2006	-22.00	-7.04	34.39	12.48	-1.68	3.76	-0.46	-31.18
2007	-25.48	-5.09	41.17	16.36	-1.43	9.84	-0.28	-32.28
2008	-22.74	-6.88	44.03	22.39	-2.26	13.24	-0.42	-32.30
2009	-23.12	-7.11	45.71	21.75	-2.35	12.29	-0.43	-33.00
2010	-22.24	-8.93	43.16	22.23	-3.18	10.12	-0.55	-34.90
2011	-23.23	-6.75	40.97	17.70	-2.04	8.90	-0.52	-32.54
2012	-22.36	-6.29	42.92	19.90	-2.66	10.96	-0.52	-31.83
Ave	**-23.05**	**-7.34**	**43.60**	**20.39**	**-2.70**	**10.34**	**-0.49**	**-33.59**

Spatial Distribution of Initial Water Levels

To generate the initial water levels for January 2004 for the transient 2004–12 surface-water and groundwater flow model, a steady-state approximation for January 2004 hydrologic conditions was made. The simulated steady-state head-distribution was used as the initial condition for the transient model. Boundary conditions for the steady-state run are based on average hydrologic conditions in the active flow model area in January 2004. The LAK7, SFR2, and UZF1 Packages used in the transient model were not used in the steady-state run because these packages, which contain implicitly transient formulations, are not suited for steady-state conditions. In the steady-state run, constant-head cells replaced the lake cells simulated in the LAK7 Package using the vertical hydraulic conductivity from the calibrated lakebed leakance for the lakes. The River (RIV) Package was substituted for the SFR2 Package by using the calibrated parameters for the stream segments and reaches. The Recharge and Evapotranspiration Packages were substituted for the UZF1 Package by using the calibrated parameters for the unsaturated zone to calculate average recharge rates for January 2004. The calibrated hydraulic parameters (discussed in the next section) provided the data needed for the steady-state run. This model-derived set of initial conditions eliminated the effects of head interpolation over large areas where only a few measured heads were available. Measured heads in the Upper Floridan aquifer during January 2004 remained nearly constant, minimizing the error introduced by the steady-state approximation for January 2004 hydrologic conditions. The range of values for the simulated initial water-table altitude for January 2004 hydrologic conditions was very similar to the range of values for heads in the Upper Floridan aquifer (figs. 1.25, 1.26).

There is some error associated with the assumption of steady-state conditions for January 2004, because actual conditions were transient and influenced by antecedent hydrologic conditions. Different initial water levels could lead to different simulated heads and flows at later times. To assess the effect the initial water levels had on the simulated head solution, forward runs of the 9-year transient model were done with two different sets of initial water levels to determine the time at which simulated heads in both runs became nearly equal. The first set of initial heads was that derived from the steady-state head distribution representing January 2004 conditions, described earlier. The second set of initial heads was generated by adding 1 ft, in each active cell and in all layers, to the steady-state head distribution representing January 2004 conditions. Comparison of results from the 9-year transient model runs with the two sets of initial conditions showed that by June 2004, the maximum absolute value in head difference was 0.4 ft in layer 2 and 0.2 ft in layer 3. By October 2004, the maximum head difference in layer 2 was 0.2 ft and 0.1 ft in layer 3. The time required for the two different initial head distributions to have negligible effects in the head solution was calculated to be less than 1 year after simulation began.

Calibrated Hydraulic Parameters

The horizontal and vertical hydraulic conductivities of the surficial aquifer and upper confining unit (where present) and the horizontal hydraulic conductivity of the Upper Floridan aquifer in the flow model area were calibrated using

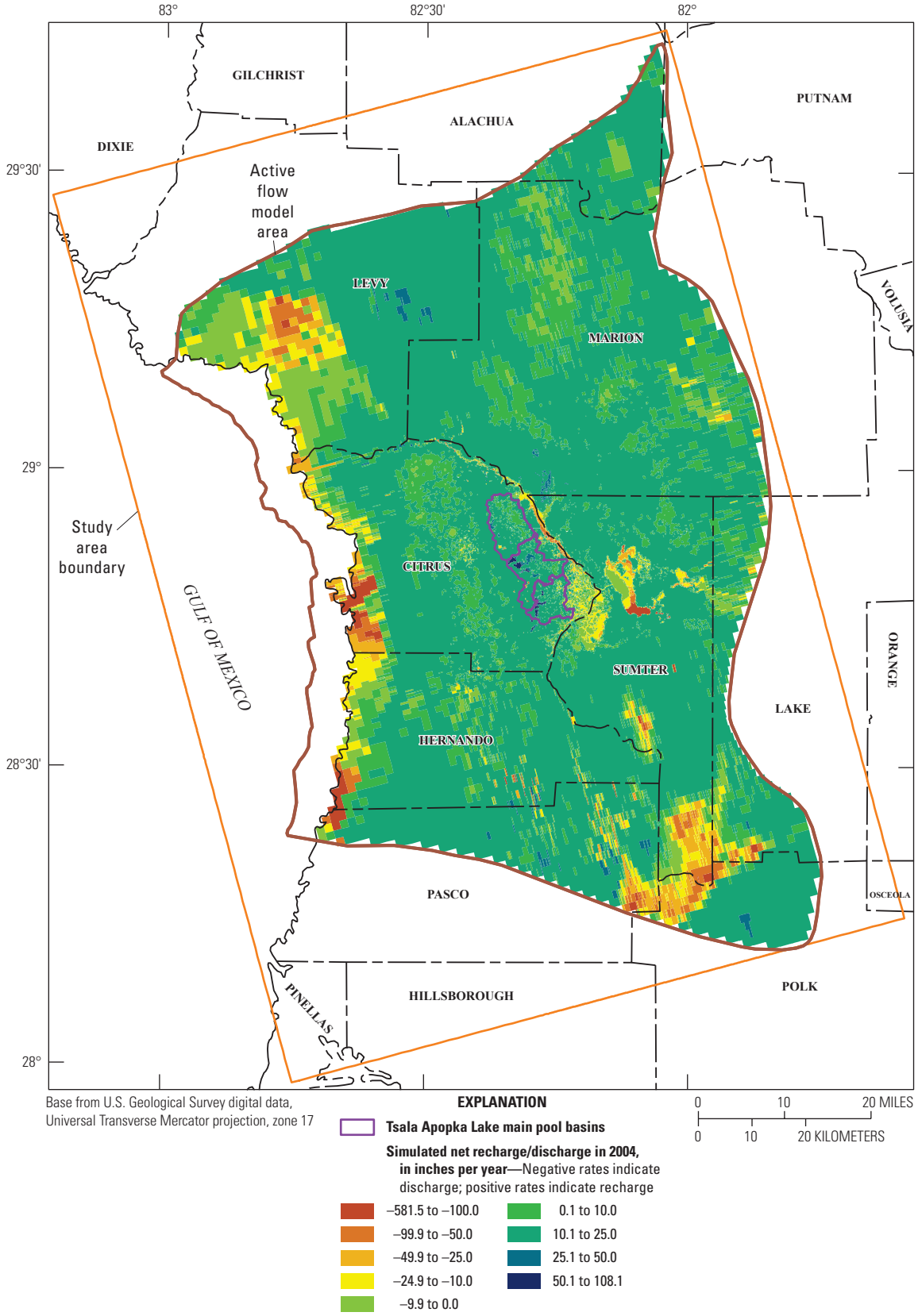

Figure 1.23 Simulated net recharge rates for 2004.

Table 1.7. Total annual flows through the lateral model boundaries simulated as general-head boundary cells.

[All rates are in inches per year. Negative values indicate flow leaving the active flow model area; positive values indicate flow entering the active flow model area. GHBL1, GHBL2, GHBL3, total lateral flow through lateral model boundary cells in layers 1, 2, and 3, respectively; Ave, average annual flow through lateral boundaries for the 2004 to 2012 period]

Year	GHBL1	GHBL2	GHBL3
2004	0.15	0.13	1.95
2005	0.12	0.10	0.84
2006	0.13	0.10	-0.68
2007	0.14	0.11	-1.14
2008	0.15	0.10	-0.95
2009	0.16	0.11	-1.05
2010	0.14	0.10	-1.14
2011	0.17	0.11	-1.71
2012	0.17	0.13	-0.31
Ave	**0.15**	**0.11**	**-0.47**

pilot points, spatial interpolation using a semivariogram, and inverse modeling (Doherty and Hunt, 2010). Other parameters could be calibrated without spatial interpolations, namely vertical anisotropy in the Upper Floridan aquifer, specific yield of the surficial aquifer, specific storage of the upper confining unit and Upper Floridan aquifer, lakebed leakances of each of the 15 simulated lakes, and streambed hydraulic conductivity for each segment. These calibrated parameters are presented in the next section.

Manning's roughness coefficient, the hydraulic conductivity of the land surface used to partition rainfall into surface runoff and infiltration, and the saturated vertical hydraulic conductivity of the unsaturated zone were not included in the inverse modeling calibration because of the intrinsic difficulties associated with their implementation in automated schemes. Manning's roughness coefficient was set equal to 0.06 for stream segments 5 to 16, 22, 37 to 40, and 43 (spillways) and to 0.05 for all other segments on the basis of streamflow matching. Changes in simulated streamflow caused by changes in Manning's roughness coefficients resulted in streamflow changes of less than 0.1 ft^3/s.

The hydraulic conductivity at land surface (SURFK) is specified per grid cell to calculate the surface runoff generated from a rainfall rate that exceeds the maximum infiltration rate (fig. 1.27). All rainfall below the maximum infiltration rate becomes infiltration that is subject to ET losses in the unsaturated zone and also the water table if that surface is within the extinction depth. SURFK values ranging from 0.08 to 0.13 foot per day (ft/d) were assigned to the topsoil to represent maximum infiltration rates ranging from 0.96 to 1.56 inches per day (in/d), based on physiographic region (figs. 3, 1.27). For example, cells in Brooksville Ridge, Dunnellon Gap, Lake Upland, and Northern Highlands were assigned a SURFK value of 0.11 ft/d (figs. 3, 1.27). The saturated vertical hydraulic conductivity for the unsaturated zone (VKS) was assigned values of 10, 15, 20, 30, and 50 ft/d, also based on the physiographic region (fig. 1.28). These values were determined manually by modifying VKS to simulate reasonable rates of recharge to the surficial aquifer that reduced the head residuals in both the surficial and Upper Floridan aquifers. Infiltration was routed through the unsaturated zone at all cells in the active flow model area.

Calibrated Hydraulic Conductivity

Calibrated horizontal hydraulic conductivity in the surficial aquifer areas that overlie the upper confining unit (KH1, layer 1) ranged from 0.1 to 85 ft/d (fig. 1.29). The highest KH1 values were simulated near the northeast lateral boundary of the model, whereas the lowest KH1 values were simulated near the central part of the southern lateral boundary. The calibrated vertical hydraulic conductivity in the surficial aquifer areas that overlie the upper confining unit (KV1, layer 1) ranged from 0.01 to 0.78 ft/d (fig. 1.30). The highest KV1 values were simulated near the central part of the eastern lateral boundary of the model and near the southwest section of the model area. The KV1 values of 0.11 to 0.20 ft/d, although scattered in layer 1, were the most prevalent values, which established the hydraulic connection between layers 1 and 2 wherever the surficial aquifer overlies the upper confining unit.

The calibrated horizontal hydraulic conductivity in layer 2 (KH2), in areas where the surficial aquifer overlies the Upper Floridan aquifer, and the upper confining unit where this unit is present, ranged from 0.2 to 120 ft/d; values were highest in the central and southern parts of the model area and lowest in extensive areas in the northeast and southwest parts of the active flow model areas (fig. 1.31). The transition of KH2 from the surficial aquifer to the upper confining unit was smoothed by interpolation using the variogram shown in equation 1.1. The calibrated vertical hydraulic conductivity in layer 2 (KV2) mainly determines the leakage to the Upper Floridan aquifer. KV2 ranged from 0.01 to 8.8 ft/d; the most prevalent simulated values were from 0.01 to 0.1 ft/d (fig. 1.32).

The calibrated horizontal hydraulic conductivity in the Upper Floridan aquifer (KH3, layer 3) ranged from 7.5 to 35,710 ft/d; the higher KH3 values coincide with areas of low hydraulic gradients, whereas the lower values coincide with areas of high hydraulic gradients (figs. 1.9, 1.33). Areas near large Upper Floridan aquifer springs (numbers 5, 7–11, 25, 43, 46, 56–58, and 81–82, fig. 13) are characterized by high levels of limestone dissolution, reflected as large KH3 simulated values (fig. 1.33). The simulated transmissivity in the Upper Floridan aquifer near these large springs generally exceeds 10 million square feet per day (ft^2/d) (fig. 1.34). The anisotropy ratio for the horizontal to vertical hydraulic conductivity of the Upper Floridan aquifer was assumed to be the same for all of layer 3. The calibrated value of this anisotropy was about 67, which indicates that the vertical hydraulic conductivity can become quite large, particularly near the springs.

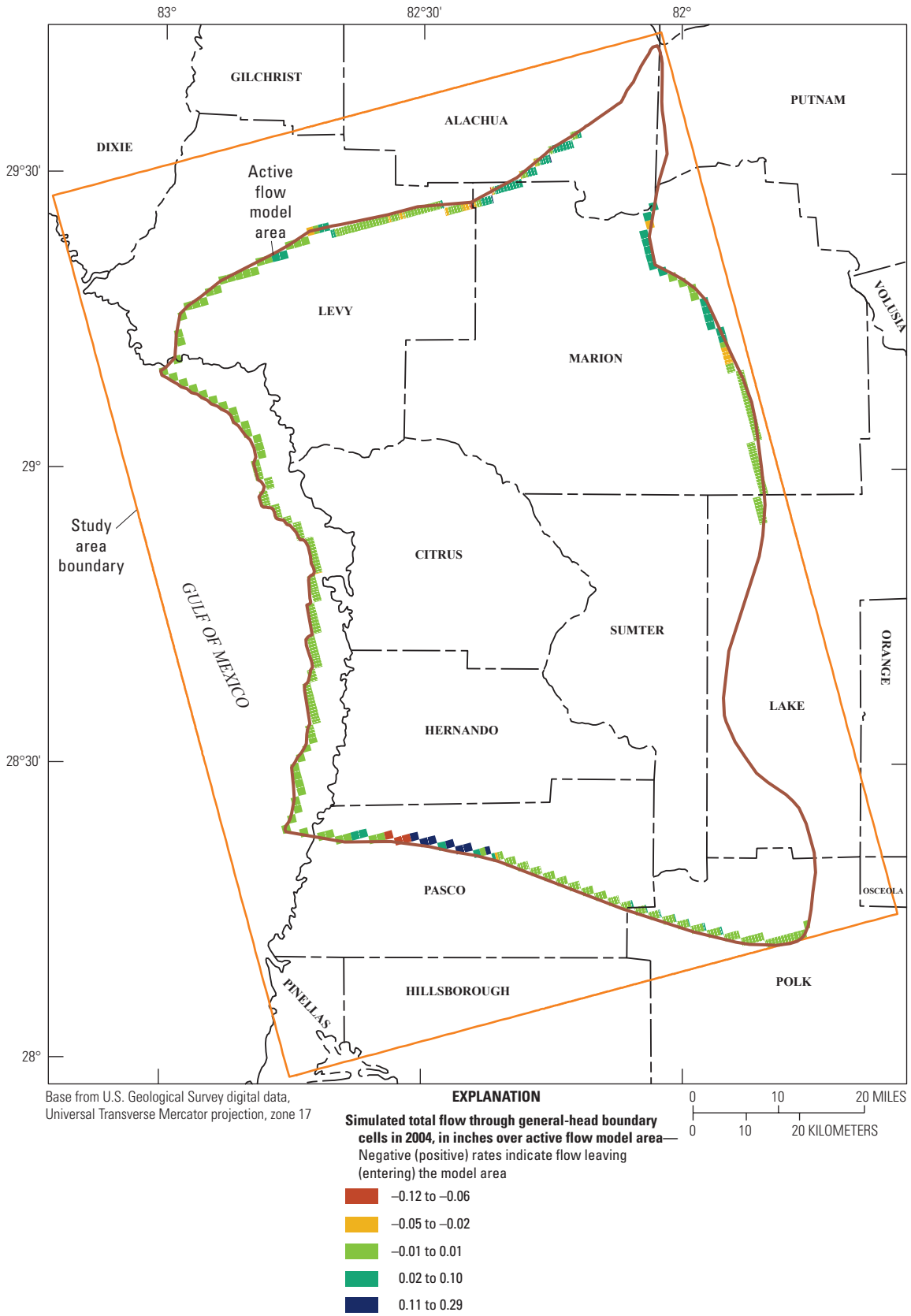

Figure 1.24 Average 2004 flow entering (positive) or leaving (negative) the active flow model area through the general-head boundary cells in the Upper Floridan aquifer.

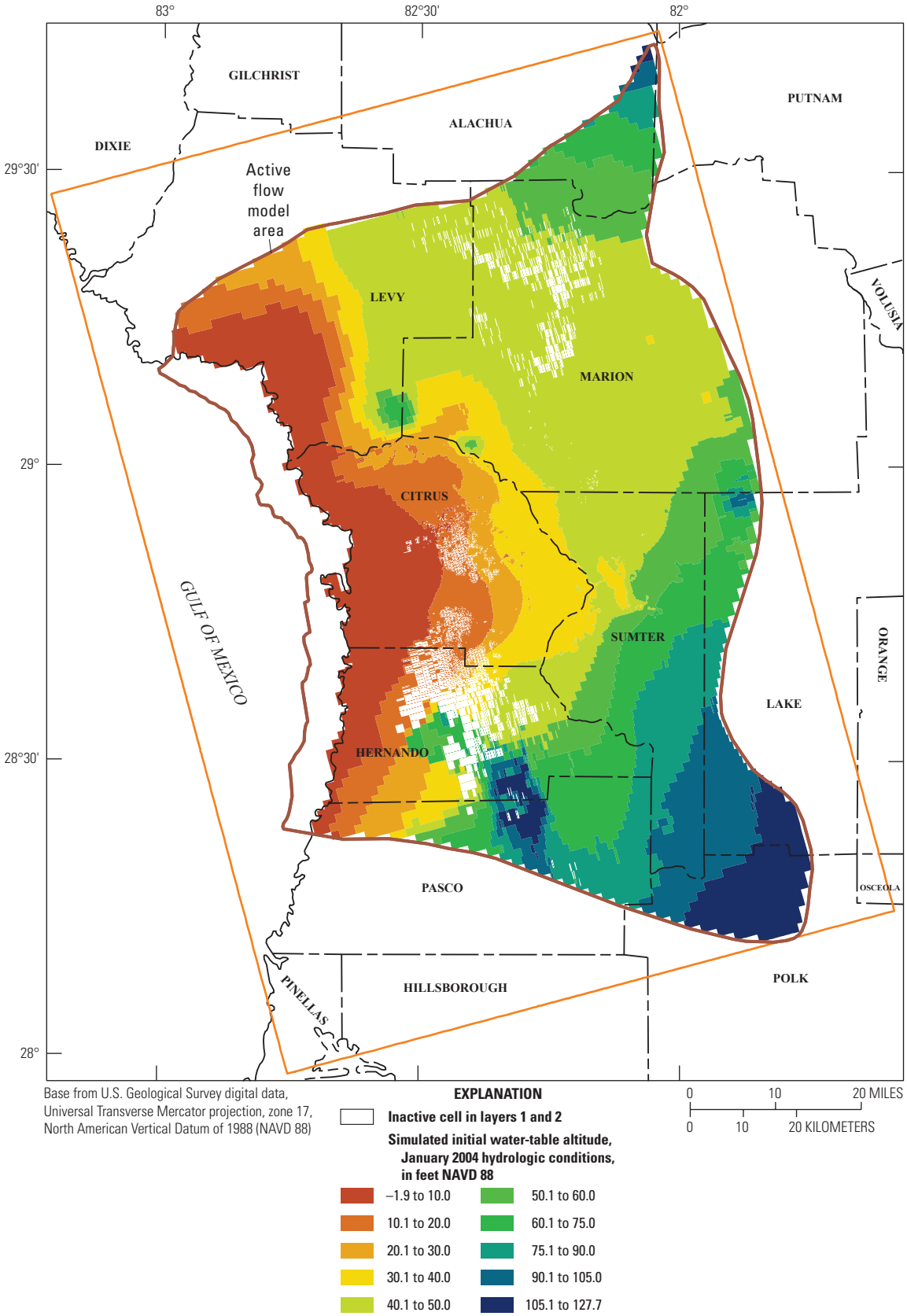

Figure 1.25 Simulated water-table altitude in the model area, January 2004 hydrologic conditions.

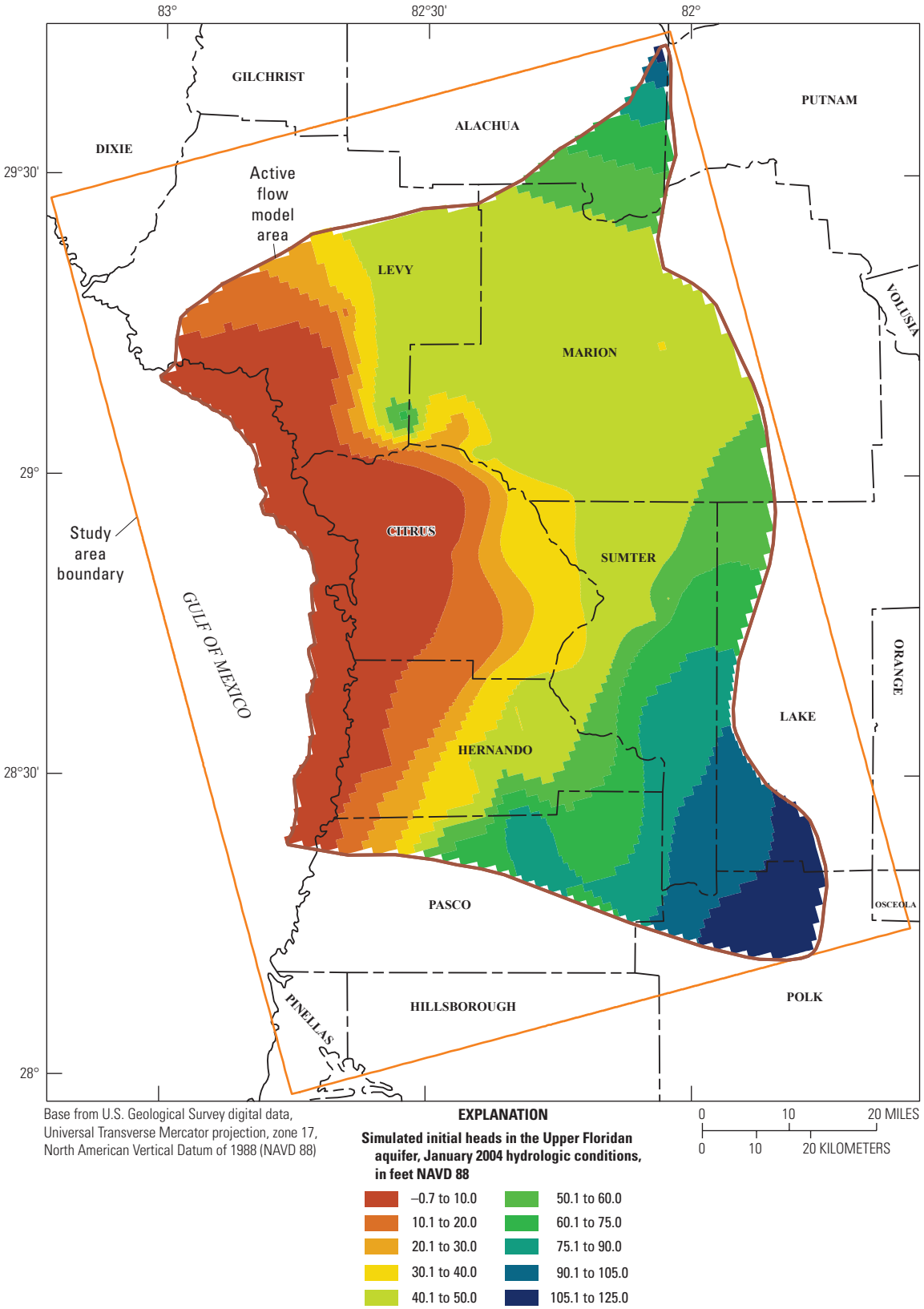

Figure 1.26 Simulated altitude of the potentiometric surface of the Upper Floridan aquifer in the model area, January 2004 hydrologic conditions.

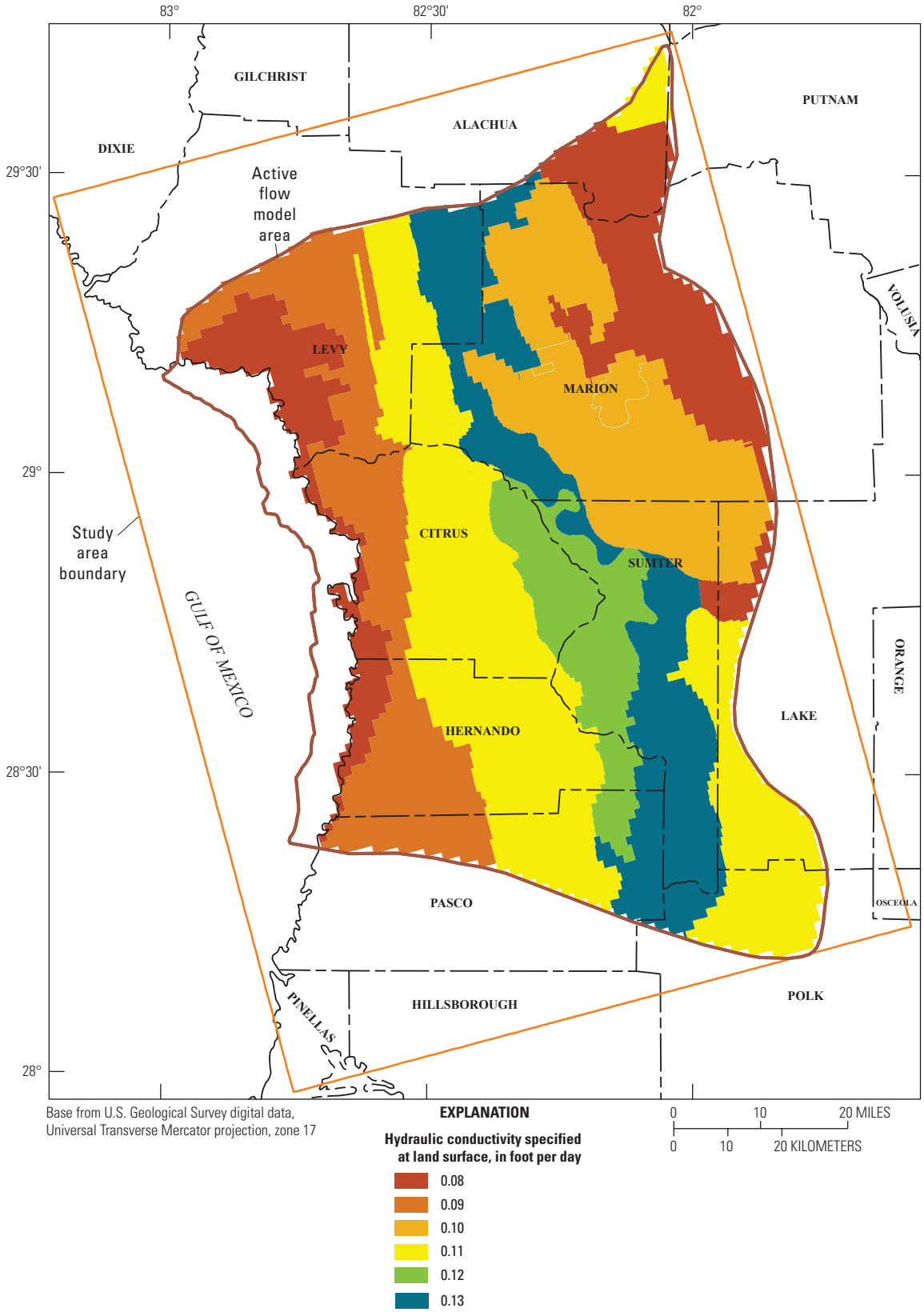

Figure 1.27 Hydraulic conductivity at land surface used to partition rainfall into surface runoff and infiltration.

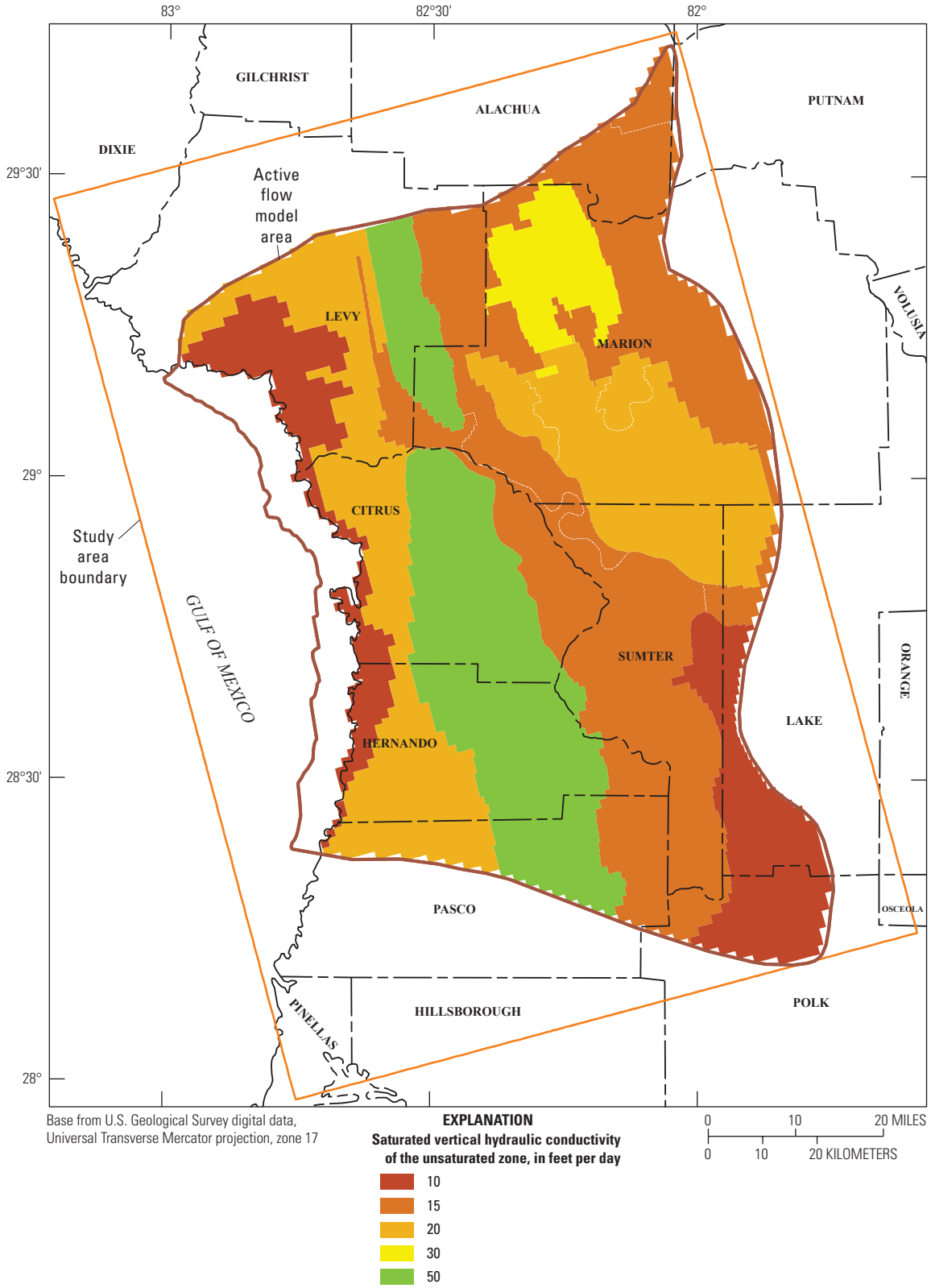

Figure 1.28 Saturated vertical hydraulic conductivity of the unsaturated zone.

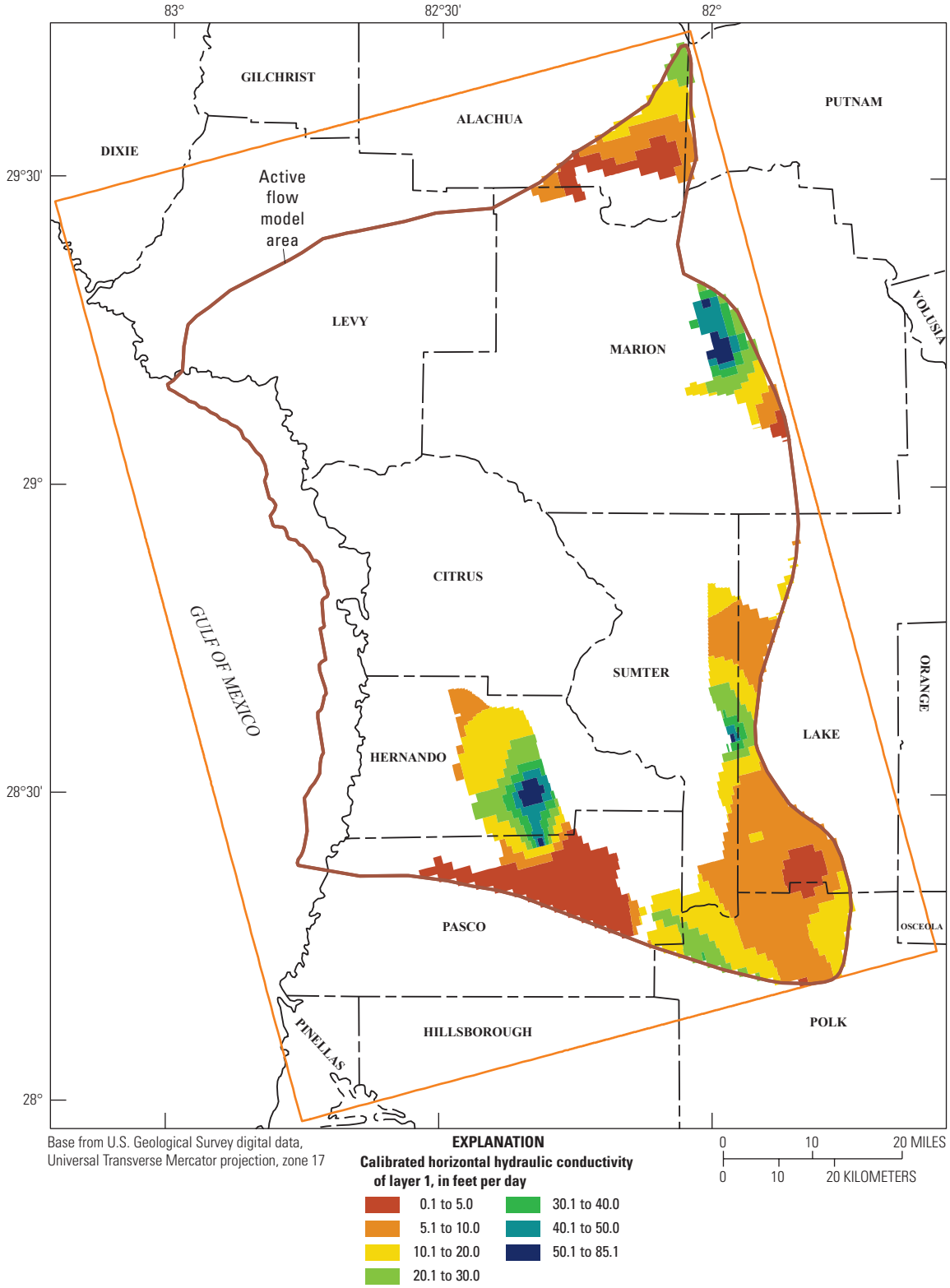

Figure 1.29 Calibrated horizontal hydraulic conductivity in areas where the surficial aquifer overlies the upper confining unit.

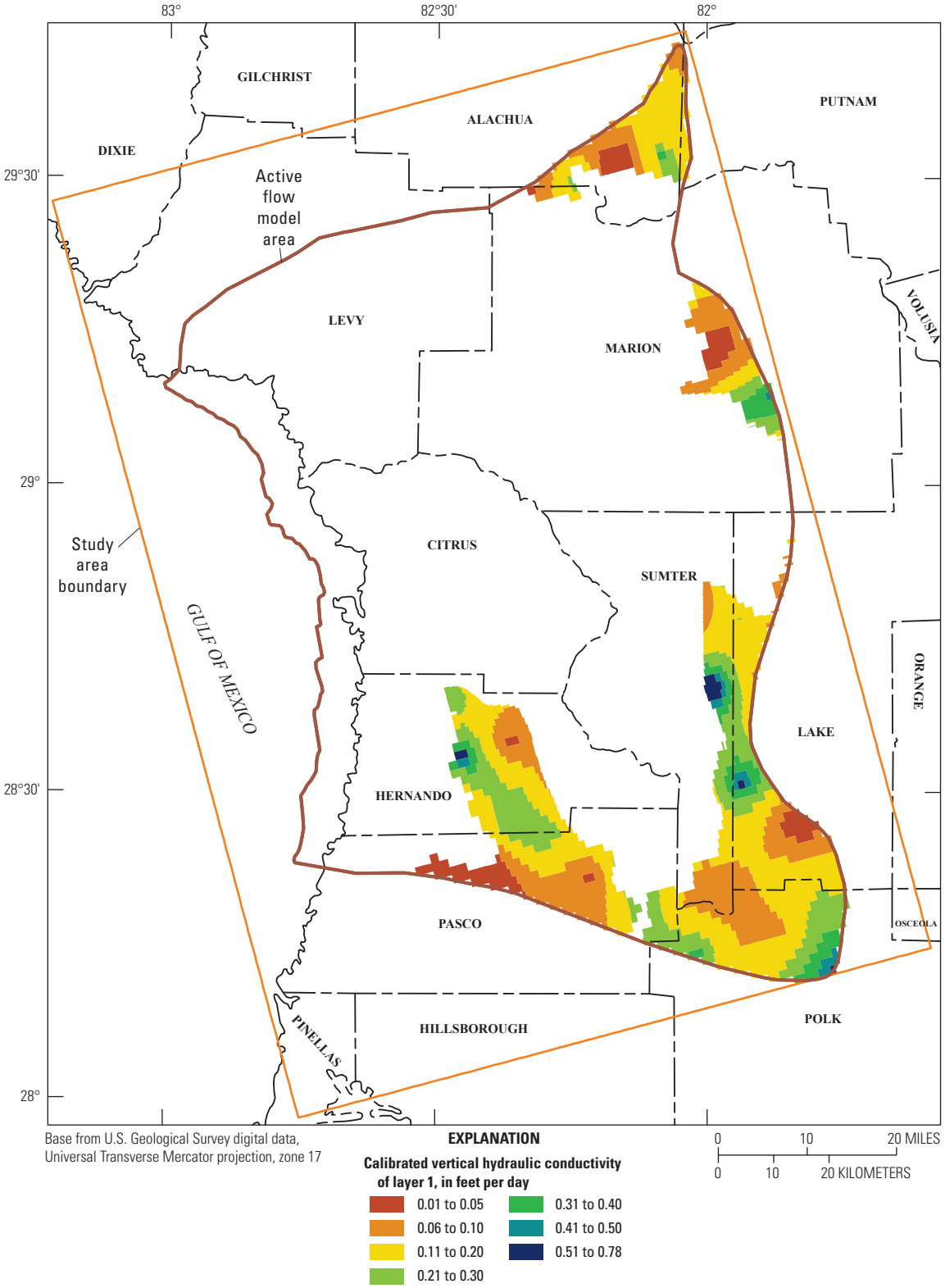

Figure 1.30 Calibrated vertical hydraulic conductivity in areas where the surficial aquifer overlies the upper confining unit.

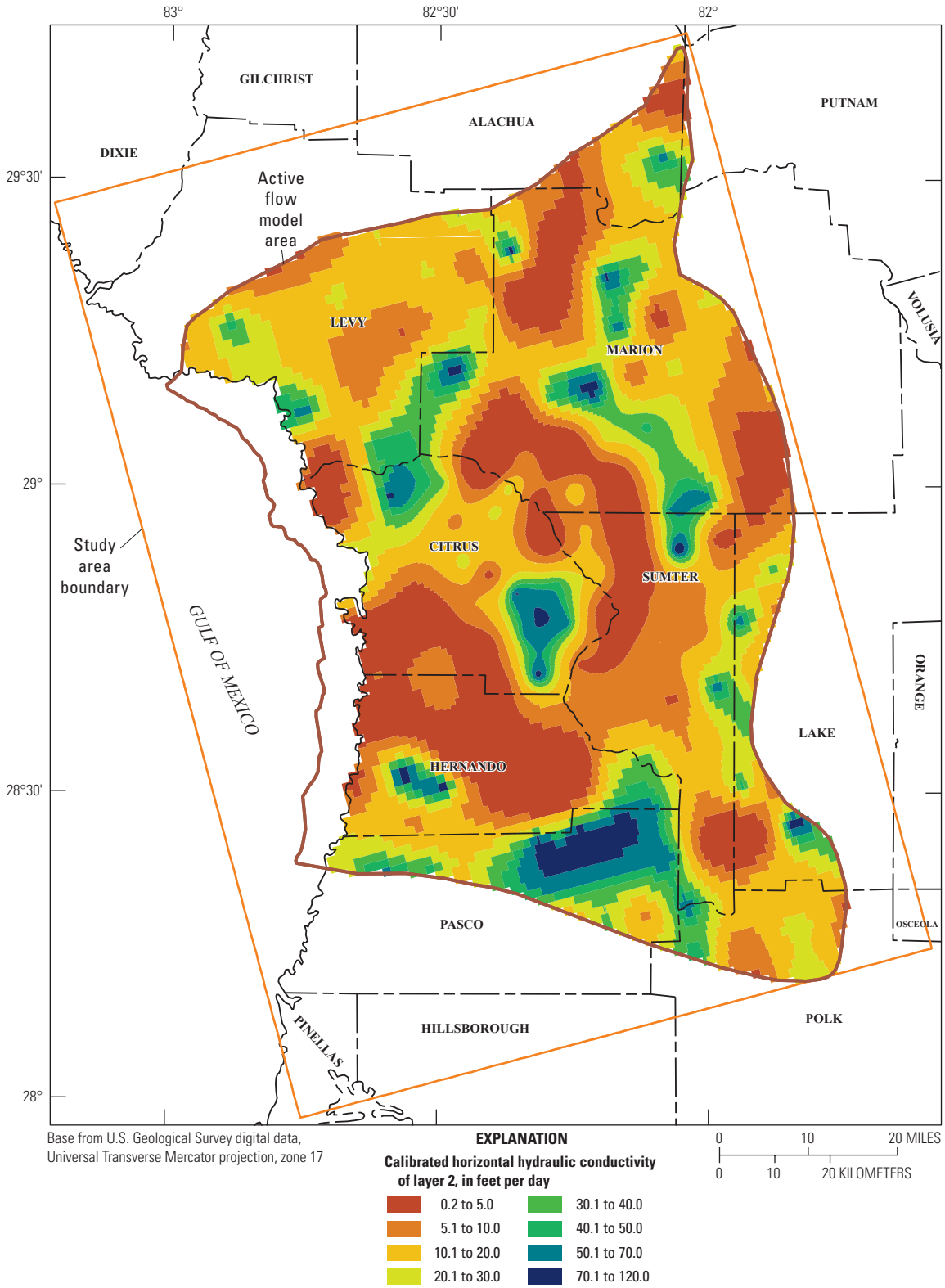

Figure 1.31 Calibrated horizontal hydraulic conductivity in areas where the upper confining unit present and where the surficial aquifer overlies the Upper Floridan aquifer.

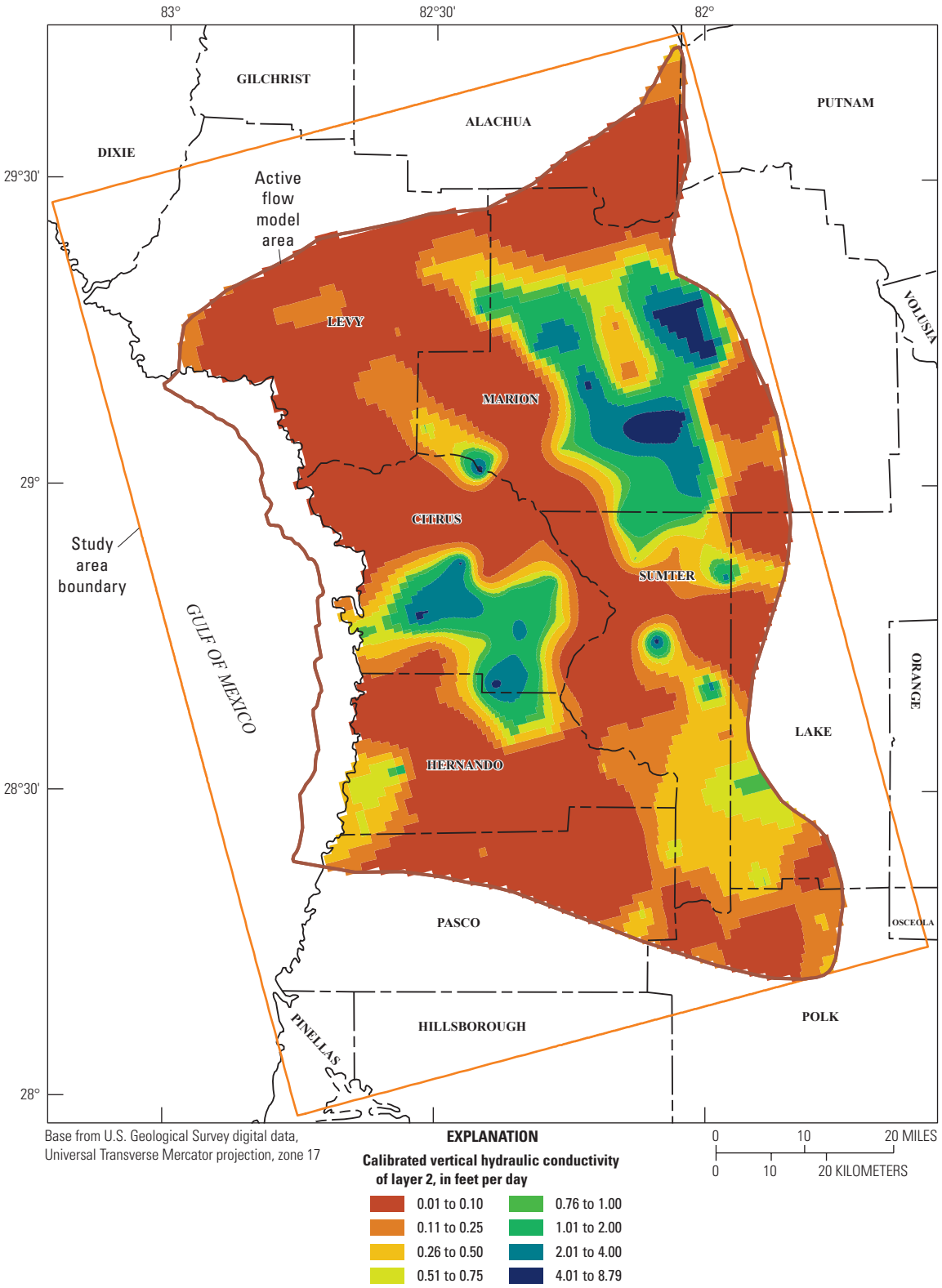

Figure 1.32 Calibrated vertical hydraulic conductivity in areas where the upper confining unit is present and where the surficial aquifer overlies the Upper Floridan aquifer.

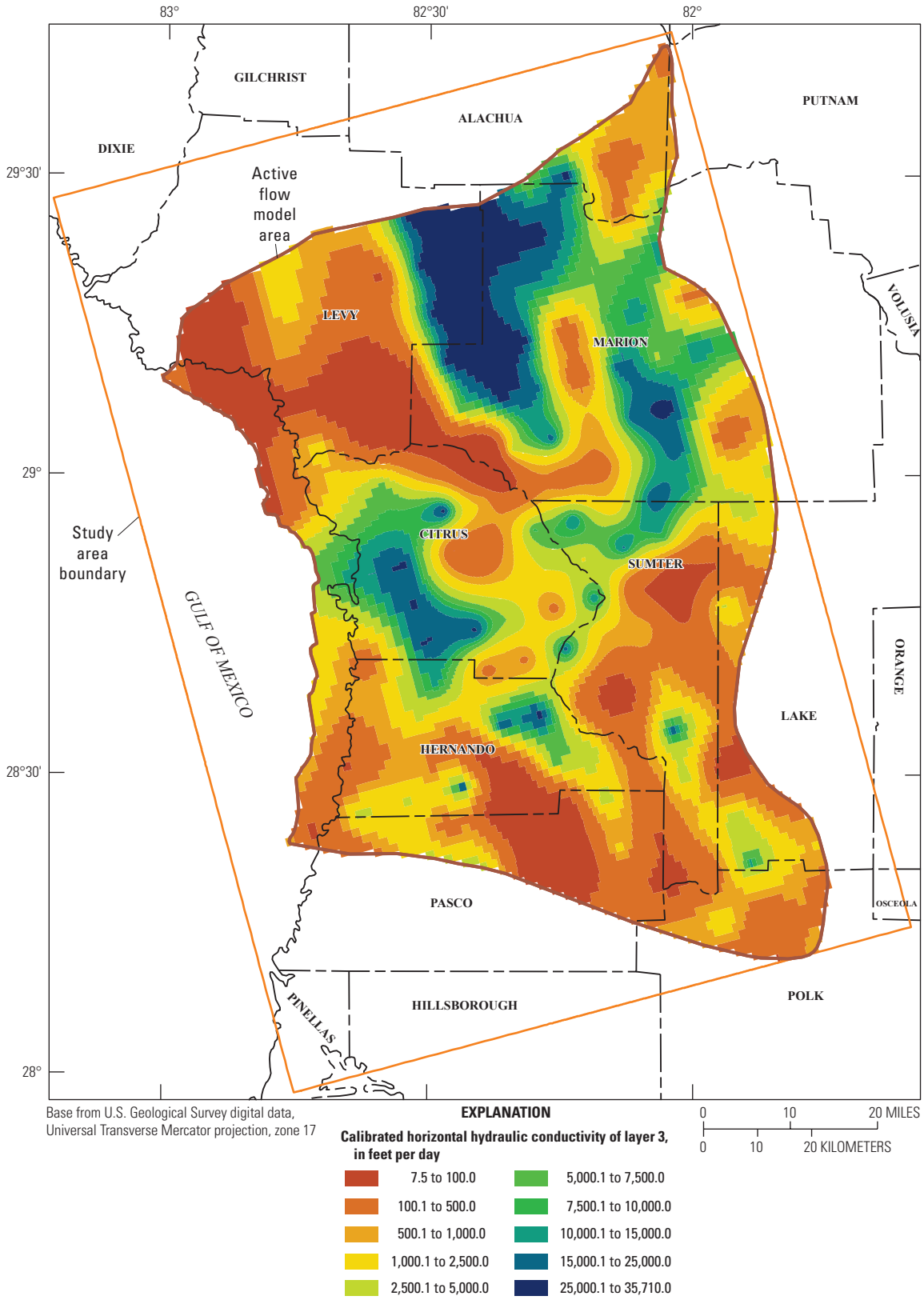

Figure 1.33 Calibrated horizontal hydraulic conductivity of model layer 3.

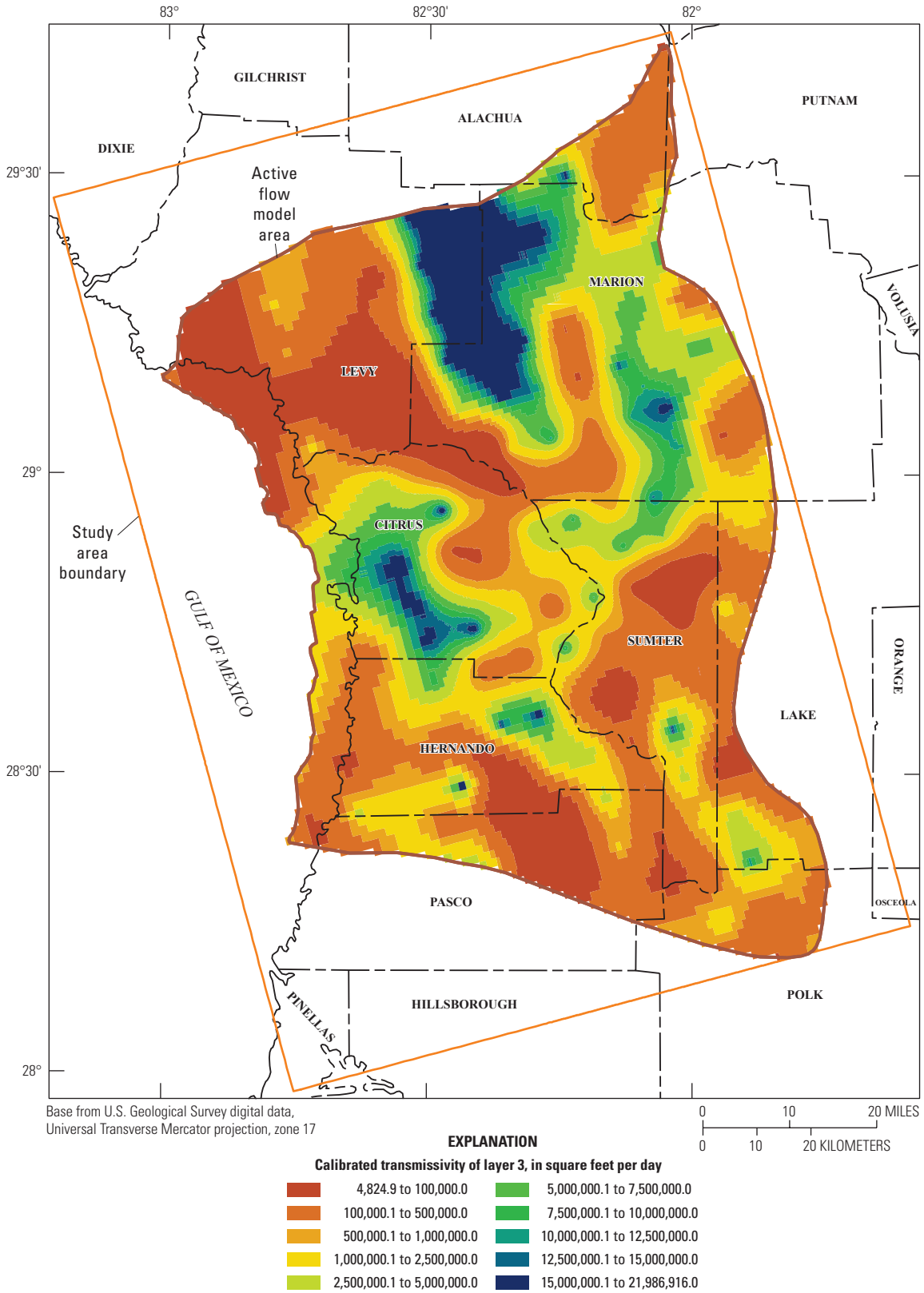

Figure 1.34 Calibrated transmissivity of model layer 3.

Calibrated Specific Yield and Specific Storage

A calibrated common value of 0.22 for specific yield was used for layer 1, where the surficial aquifer overlies the upper confining unit, and for layer 2, where the surficial aquifer overlies the Upper Floridan aquifer. The specific storage of layer 2, where the upper confining unit exists, and the specific storage of layer 3, the Upper Floridan aquifer, were each simulated using one value for each layer. The calibrated specific storages for the upper confining unit and Upper Floridan aquifer were 7.22×10^{-7} ft^{-1} and 6.30×10^{-7} ft^{-1}, respectively. These two calibrated specific storage values are consistent with the compressibility of water and that of a fractured rock aquifer matrix presented by Domenico (1972). Average thicknesses of the upper confining unit and Upper Floridan aquifer, where these are active, are 30 and 623 ft, respectively; average calibrated storage coefficients of the upper confining unit and Upper Floridan aquifer were 2.17×10^{-5} and 3.92×10^{-4}.

Calibrated Lakebed Leakance

The lack of data for measured lakebed leakance led to the assumption of no spatial variation in leakance within each lake, with each lake's leakance calibrated separately from others. The highest leakance was simulated for the Floral City pool (lake 8 in table 1.8) and the lowest leakance was simulated for Bonnet Lake (lake 4 in table 1.8, fig. 2). The hydraulic connection between the surficial aquifer and the lakes is determined by the lakebed leakance, the difference between pool stage and water-table altitude, and the thickness of the lakebed. With all other determining parameters being equal, the calibrated leakances indicate that the Floral City pool has the highest hydraulic connection with the surficial aquifer.

Table 1.8. Calibrated lakebed leakance values for all simulated lakes.

Lake number	Lakebed leakance (day^{-1})
1	2.000E-03
2	2.000E-03
3	2.000E-03
4	1.500E-03
5	2.000E-03
6	2.000E-03
7	2.000E-03
8	2.500E-03
9	2.000E-03
10	2.300E-03
11	3.000E-03
12	3.000E-03
13	2.000E-03
14	2.000E-03
15	2.000E-03

Calibrated Streamflow Routing Parameters

The calibrated parameters in the Streamflow Routing Package (SFR2 in MODFLOW-NWT) were the vertical hydraulic conductivity of the streambed (STRMBDKV, table 1.9). These parameters were assigned to each reach of each stream segment. The hydraulic connection between the surficial aquifer and the streams is determined by the vertical hydraulic conductivity of the streambed, the difference between the stream stage and water-table altitude, and the thickness of the streambed. The calibrated STRMBDKV values were higher for the downstream segments of the Withlacoochee River (segments 23 to 25, 29 to 36 in fig. 1.3, table 1.9) than for the upstream segments (1 to 4 in fig. 1.3, table 1.9). As the streambed slope at lake outlets without water-control structures is increased, the lake stage is depleted. The vertical hydraulic conductivity of the streambed, varied to decrease streamflow differences between measured and simulated, ranged from 0.0089 to 0.011 ft/d (table 1.9).

Model Fit

PEST (Doherty, 2013a, 2013b) was used to reduce the weighted objective function (eq. 1.2) until the goals listed in the Calibration Targets section were met. The calibration targets were satisfied after a series of iterations that required updating the lower and upper bounds of the parameters until reasonable parameter values were obtained.

The model performance is evaluated in this section in terms of the calculated mean error (ME) and the root mean square error (RMSE) from sets of n simulated (si) and measured (mi) groundwater heads, lake stages, streamflows, and spring flows. Each observation category was calculated separately for the corresponding values of n and analyzed. The ME and RMSE were calculated from

$$\mathrm{ME} = \frac{\sum_{i=1}^{n}\left(s_i - m_i\right)}{n} \quad \text{and} \quad \mathrm{RMSE} = \left[\frac{\sum_{i=1}^{n}\left(s_i - m_i\right)^2}{n}\right]^{1/2} . \qquad (1.4)$$

Simulated Lake Stages

Stage was measured at six lakes and the ME for each lake was less than or equal to 0.25 ft in absolute value (table 1.10), satisfying the calibration target for lake stage. These six lakes were the Floral City, Inverness, and Hernando pools in the Tsala Apopka Lake Basin, Lake Panasoffkee, the pool on the upstream side of the Wysong structure, and Lake Rousseau (table 1.3). The simulated stage hydrographs for these six lakes (figs. 1.35 to 1.40)

Table 1.9. Calibrated water-surface slope and vertical hydraulic conductivity of the streambeds for each stream segment.

[Segment, stream segment or set of segments; STRMBDKV, vertical hydraulic conductivity assigned to the streambed of all reaches in the stream segment, in feet per day]

Segment	STRMBDKV
1	8.904E-03
2	1.043E-02
3	1.023E-02
4	9.929E-03
5	9.394E-03
6	9.092E-03
7	1.002E-02
8	8.876E-03
9–16	0.000E+00
17	1.082E-02
18	9.583E-03
19	9.280E-03
20	9.635E-03
21	9.153E-03
22, 37, 39	0.000E+00
23	9.938E-03
24	1.054E-02
25	9.746E-03
26	1.045E-02
27	9.594E-03
28	8.961E-03
29	1.083E-02
30	9.429E-03
31	1.060E-02
32	1.054E-02
33	9.932E-03
34	1.056E-02
35	1.002E-02
36	1.111E-02
38	9.776E-03
40	1.086E-02
41	1.082E-02
42	1.082E-02
43	9.153E-03

reflect the sum of inflows and outflows occurring at each lake. Increases and decreases in simulated pool stages occurring for short periods of time are the net result of inflows (from large rainfall events) or outflows through the water-control structures. Steady decreases in simulated pool stages over long time periods are the result of downward leakage through the lakebed, evapotranspiration, and low rainfall conditions.

Table 1.10. Statistics of simulated lake stage residuals.

[LAKENO, lake number for which measured stages were available; NUM, number of daily measured stages made from 2004 to 2012; ME, mean error, in feet; RMSE, root mean square error, in feet; AVSTMEA and AVSTSIM, average measured and simulated stage for the 2004–12 period respectively. All stages are in feet above the North American Vertical Datum of 1988 (NAVD 88). There are 3,288 days in the 2004–12 period]

LAKENO	NUM	ME	RMSE	AVSTMEA	AVSTSIM
8	3,288	0.25	0.79	38.35	38.60
9	3,288	0.23	1.06	36.62	36.85
10	3,288	-0.09	0.85	35.43	35.34
12	3,288	-0.03	0.15	38.05	38.02
13	3,264	0.15	0.35	37.19	37.34
15	3,288	0.09	0.14	26.68	26.77

The simulated pool stages were overestimated by almost 2 ft during the second half of 2012 at Floral City pool, Wysong structure, and Lake Rousseau; during the second half of 2011 at the Inverness pool, and during the first half of 2012 at the Hernando pool (figs. 1.35 to 1.37; figs. 1.39 and 1.40). The large pool stage residuals during 2012 may be explained by the estimated spatial distribution of rainfall. Results of several model runs that arbitrarily decreased rainfall in the main pools of the Tsala Apopka Lake Basin, while keeping all other parameters unchanged, showed the model is highly sensitive to rainfall input. Limitations in surface runoff routing or simulated head differentials between the lake water surface and water table that were too high or low could have also affected simulated lake stages.

Simulated Groundwater Levels

Average water-level residuals (simulated minus measured) at surficial aquifer wells (fig. 1.41) and at Upper Floridan aquifer wells (fig. 1.42) were calculated by running the calibrated model for the 2004–12 period. The calculated standard deviation, σ, from the average 219 water-level residuals was 3.48 ft. The water-level residual intervals [-0.75σ, 0.75σ], [-1.5σ, 1.5σ], and [-2.25σ, 2.25σ] presented in the Calibration Targets section became intervals [–2.61, 2.61], [–5.22, 5.22], and [–7.83, 7.83] in feet for the water-level residuals. Of the wells in the surficial and Upper Floridan aquifers, the ME for 69 percent of the wells was within ±2.61 ft, the ME for 88 percent of the wells was within ±5.22 ft, and the ME for 95 percent of the wells was within ±7.83 ft (table 1.11). The overall RMSE was 3.48 ft and the overall ME was 0.05 ft (table 1.11). The range of average water-level measurements was 162.69 ft, making the ratio of standard deviation to the range of water-level measurements equal to 0.02.

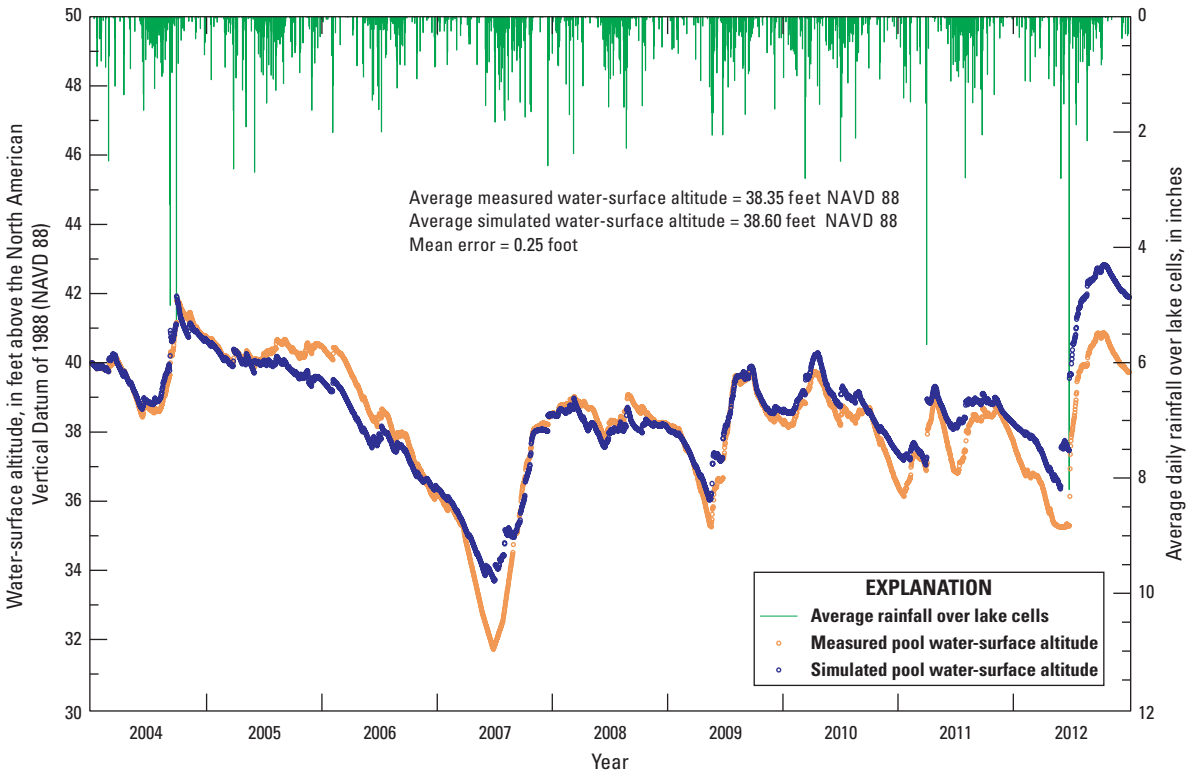

Figure 1.35 Measured and simulated stages at Floral City pool and average daily rainfall over lake cells, for the 2004–12 period.

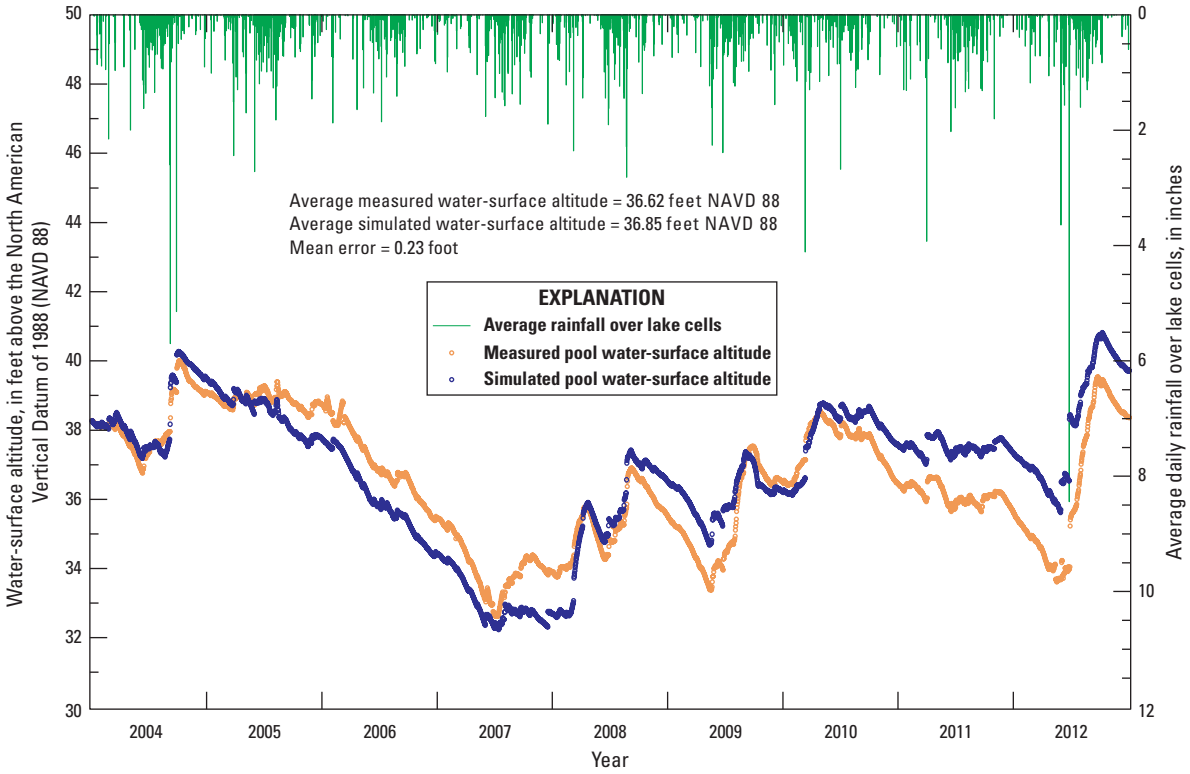

Figure 1.36 Measured and simulated stages at Inverness pool and average daily rainfall over lake cells, for the 2004–12 period.

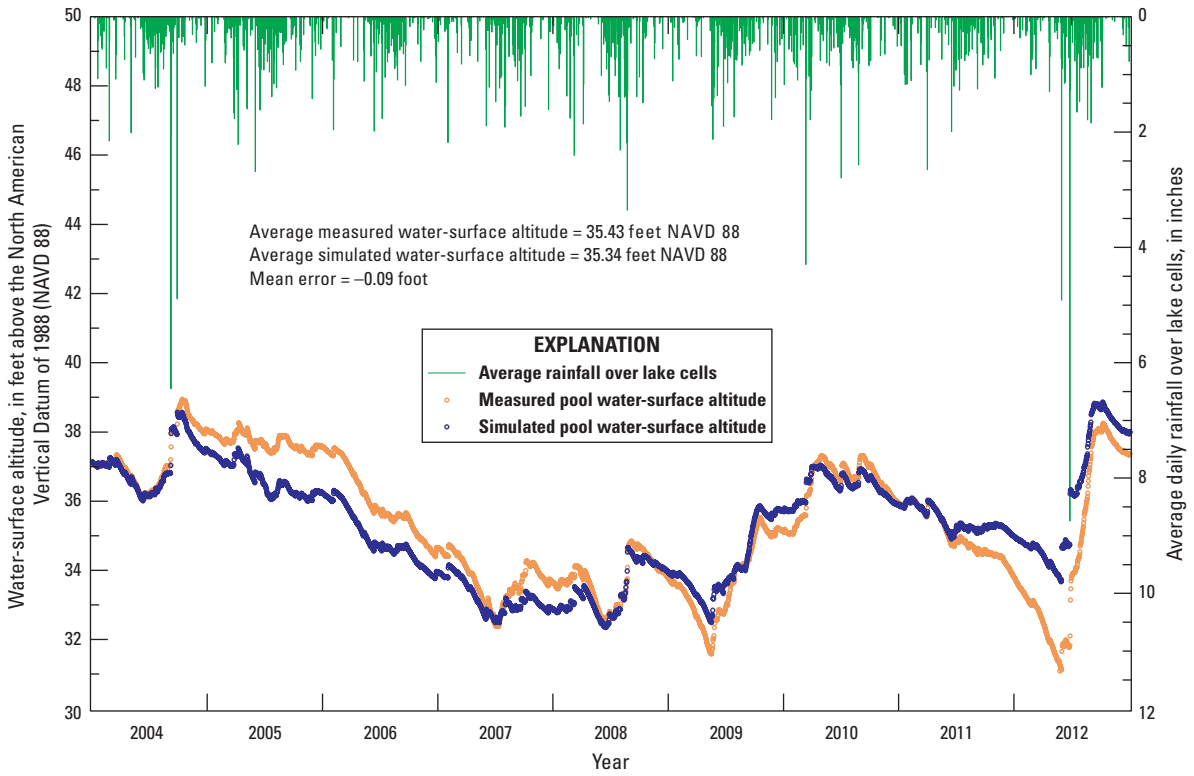

Figure 1.37 Measured and simulated stages at Hernando pool and average daily rainfall over lake cells, for the 2004–12 period.

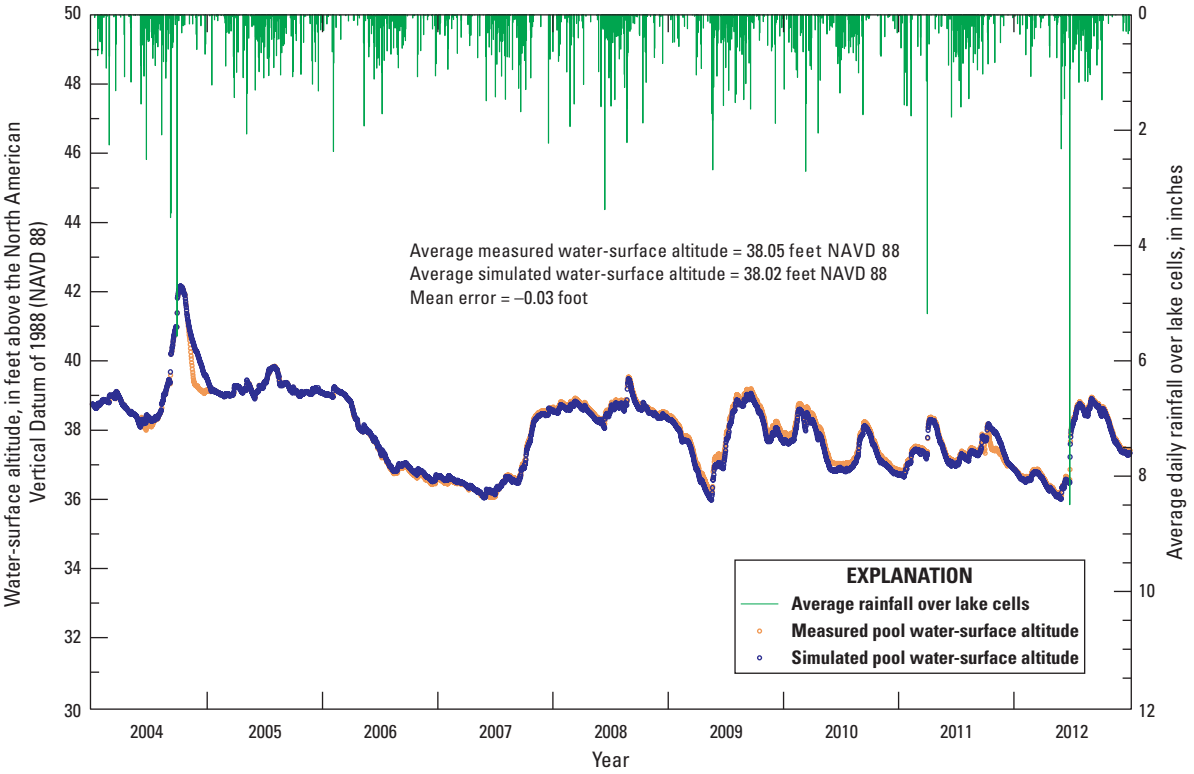

Figure 1.38 Measured and simulated stages at Lake Panasoffkee and average daily rainfall over lake cells, for the 2004–12 period.

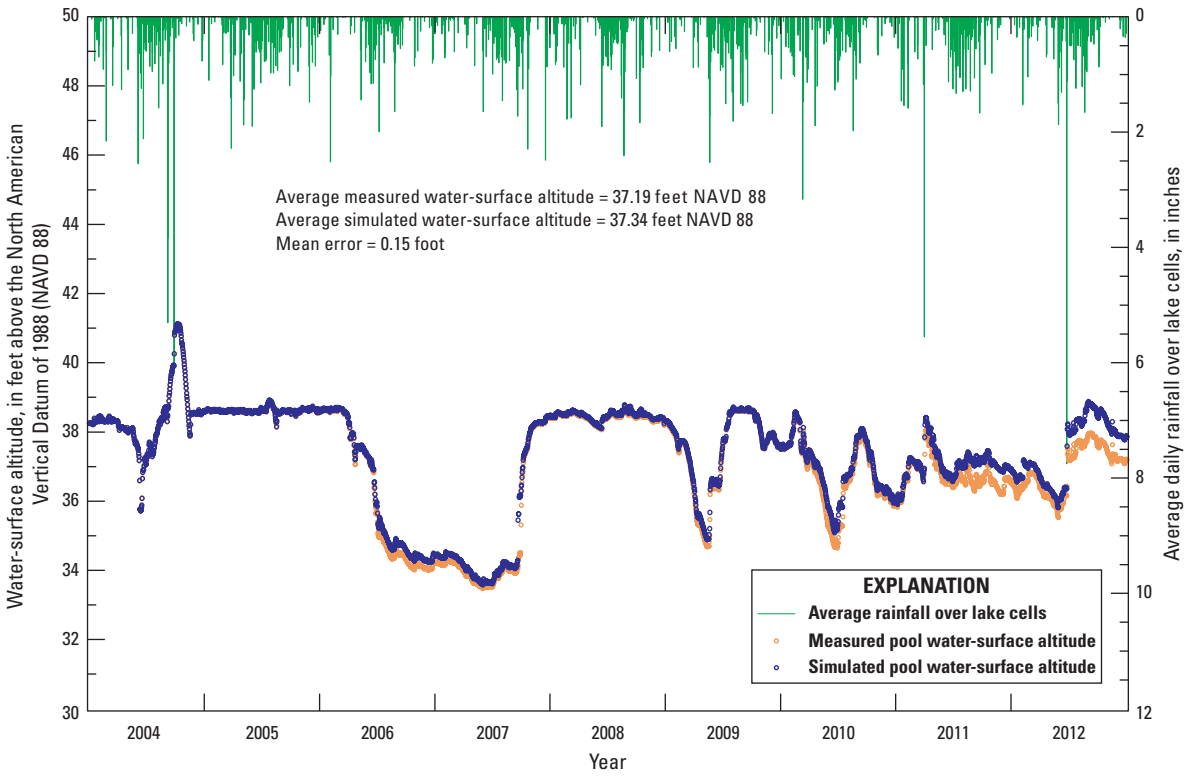

Figure 1.39 Measured and simulated stages at Wysong structure and average daily rainfall over lake cells, for the 2004–12 period.

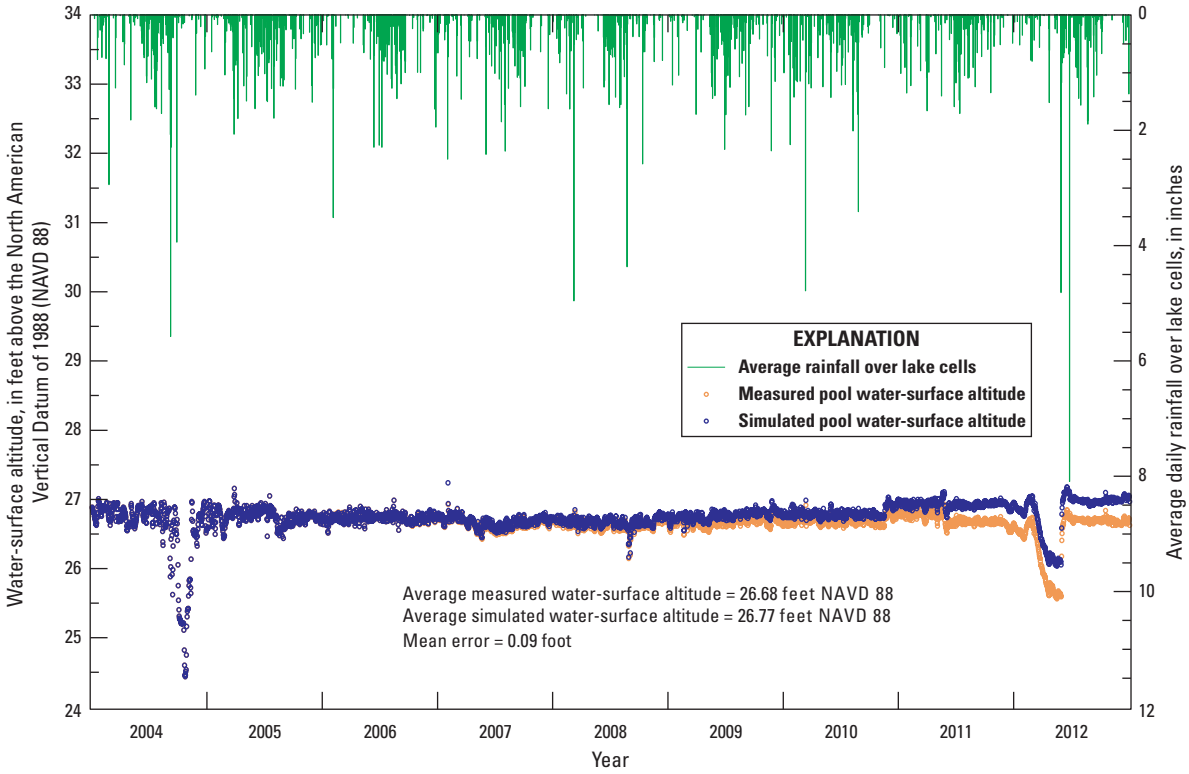

Figure 1.40 Measured and simulated stages at Lake Rousseau Dam and average daily rainfall over lake cells, for the 2004–12 period.

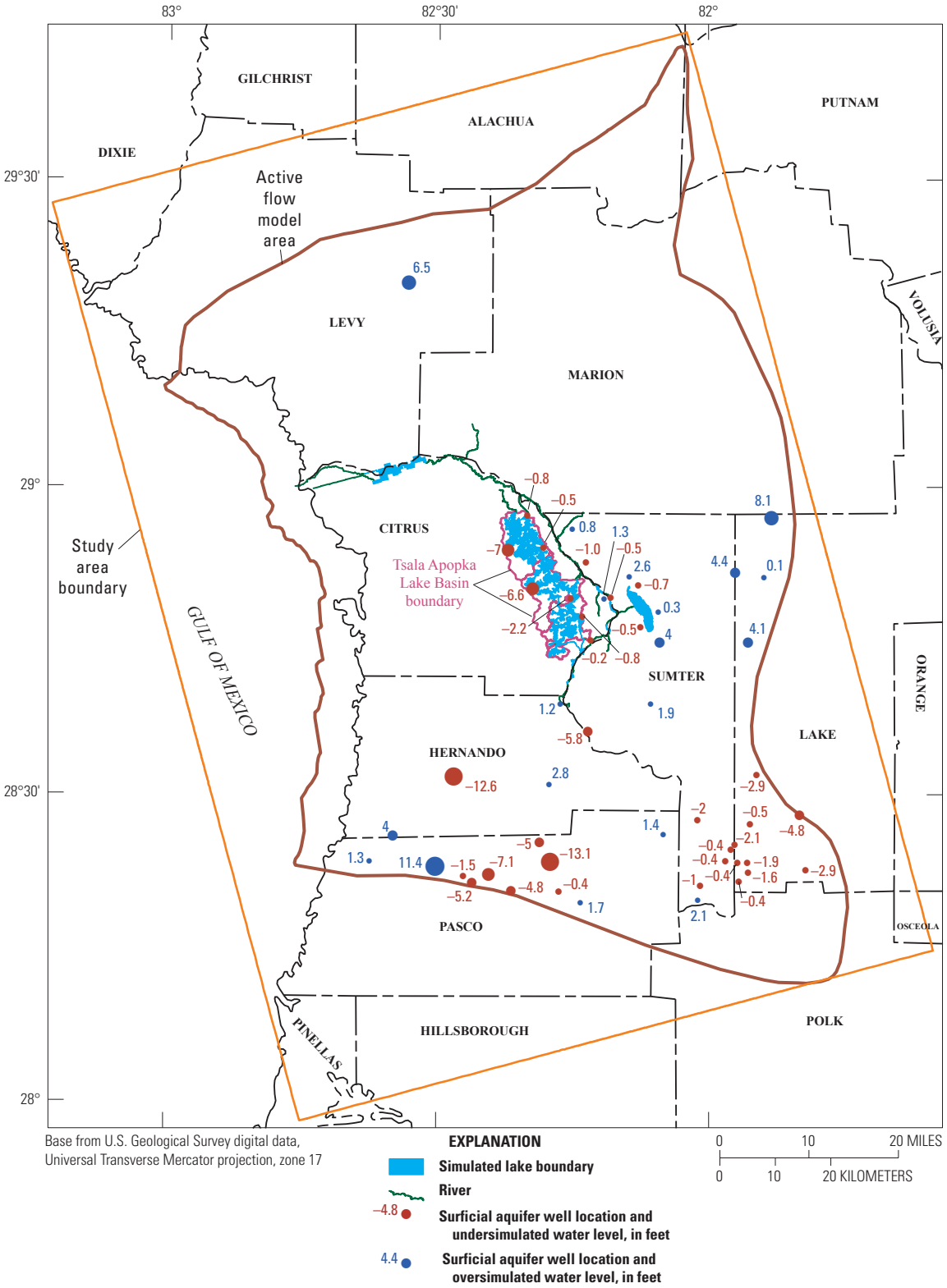

Figure 1.41 Average water level residuals at surficial aquifer wells, calculated from daily measured and simulated water levels from 2004 to 2012.

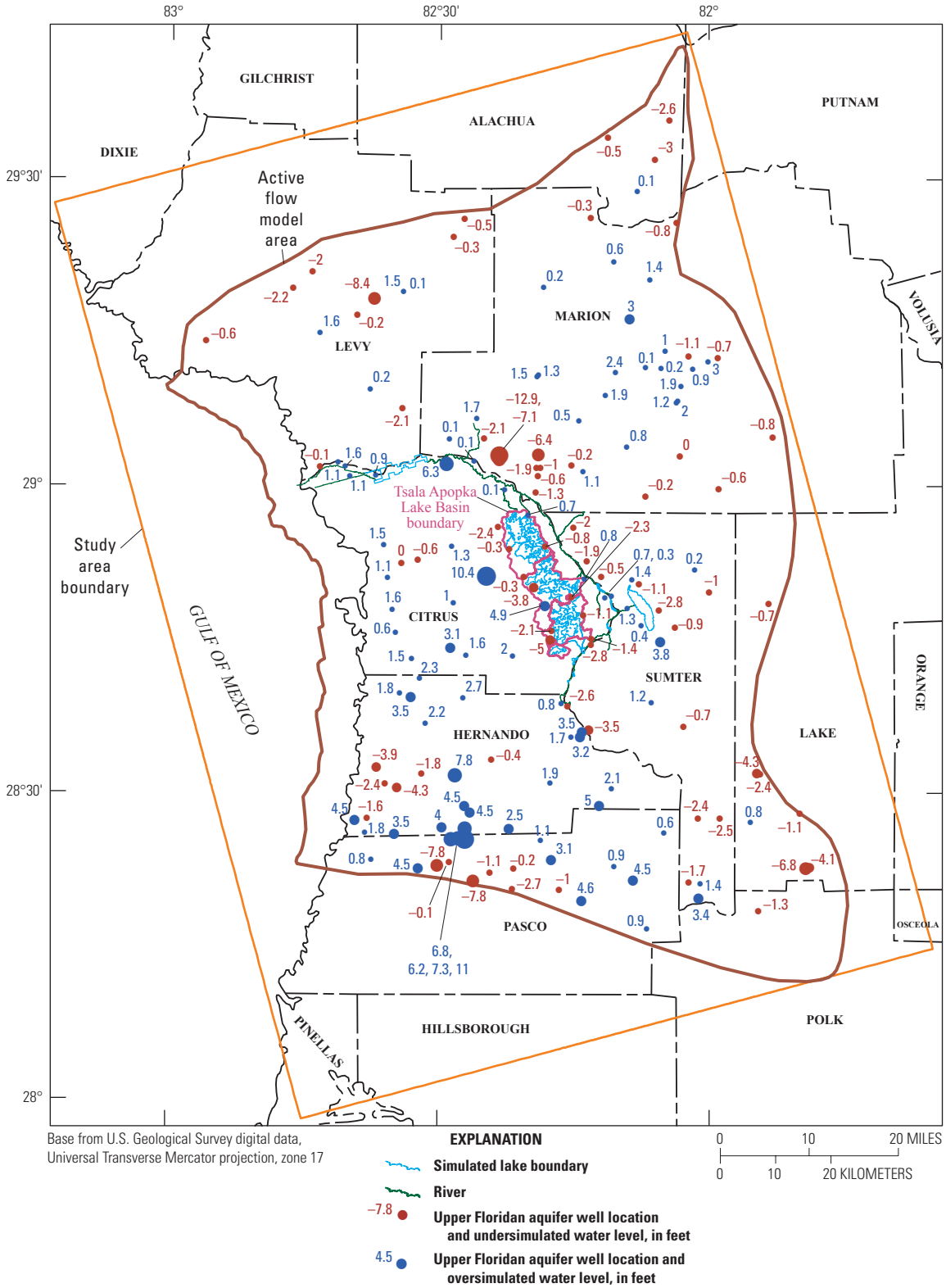

Figure 1.42 Average head residuals at Upper Floridan aquifer wells, calculated from daily measured and simulated heads from 2004 to 2012.

Table 1.11. Statistics of simulated head residuals for the surficial and Upper Floridan aquifers.

[Interval, range of values of ME; ME, average mean residual for the 2004–12 period. Intervals are based on the standard deviation of simulated head residuals, σ = 3.48 ft; SAW, number of surficial aquifer wells with ME within given Interval; UFW, number of Upper Floridan aquifer wells with ME within given Interval; TOTW, total of surficial and Upper Floridan aquifer wells with ME within given interval; SIMP, simulated percentage of wells in interval from total number of wells; EXPP, expected percentage of wells in interval from normal distribution; <, less than; >, greater than; Total, total number of wells; NA, not applicable; OME, overall mean error, in feet; ORMSE, overall root mean square error, in feet]

Interval	SAW	UFW	TOTW	SIMP	EXPP
ME < -2.25 σ	2	2	4	1.83	1.22
[-2.25 σ , -1.5 σ)	4	5	9	4.11	5.46
[-1.5 σ , -0.75 σ)	6	13	19	8.68	15.98
[-0.75 σ , 0.75 σ]	31	119	150	68.49	54.68
(0.75 σ , 1.5 σ]	6	20	26	11.87	15.98
(1.5 σ , 2.25 σ]	1	6	7	3.20	5.46
ME > 2.25 σ	2	2	4	1.83	1.22
Total	**52**	**167**	**219**	**100.00**	**100.00**
OME	-0.72	0.28	0.05	NA	NA
ORMSE	4.35	3.17	3.48	NA	NA

The largest negative head residual in the Upper Floridan aquifer was in southwest Marion County at well 23264, whereas the largest positive head residual was in north-central Pasco County at well 20481 (figs. 1.7, 1.42, table 1.4). Well 23264 is close to Rainbow Springs (numbers 7 to 11 in fig. 13, table 1.5). The steep hydraulic gradients in the potentiometric surface of the Upper Floridan aquifer in southwest Marion County (fig. 1.9) are explained by the large changes in hydraulic conductivity, and such gradients would require a high numerical grid resolution to reduce residuals further. Two small potentiometric highs on either side of Rainbow Springs are difficult to simulate accurately with the coarse grid-scale resolution.

Upper Floridan aquifer wells were spatially distributed throughout the model area more uniformly than the surficial aquifer wells (figs. 1.41, 1.42). The lack of wells in the surficial aquifer limits the areal extent of the calibration of head gradients between the surficial and Upper Floridan aquifers, most likely because the surficial sands are unsaturated. Large positive Upper Floridan aquifer head residuals in Hernando County and negative surficial aquifer water-level residuals in Hernando and Pasco Counties indicate the inability to represent the large hydraulic gradients between the surficial and Upper Floridan aquifers measured in this southwest corner of the model area. These large residuals are located in an area where the surficial aquifer transitions from an area where the Upper Floridan aquifer is confined by the upper confining unit in central Hernando County to an area where the Upper Floridan aquifer is unconfined in west-central Hernando County (fig. 1.30). The numerical grid used to develop the flow model has the coarsest numerical resolution near the four corners of the model (fig. 1.1), including the southwest corner of the model where these large residuals are present. The average simulated water level in the surficial aquifer in well 20582 in central Hernando County (fig. 1.6) over the 2004–12 period was about 57.7 ft; the average measured water level was 70.3 ft, yielding a negative residual of -12.6 ft (fig. 1.41). The simulated head in the Upper Floridan aquifer in well 20581 in central Hernando County (fig. 1.7) was about 26 ft; the average measured head was about 18.2, yielding a residual of 7.8 ft (fig. 1.42). The average simulated head difference between the surficial and Upper Floridan aquifers at these two wells, located less than 25 ft from each other (table 1.4), was 31.7 ft, compared to an average measured head difference of about 52 ft. One reason for these simulated differences may be that the numerical grid used to develop the model would need to have a higher resolution in the southwest corner of the model to increase the simulated hydraulic gradient between the two aquifers. Local heterogeneities cannot be captured at a regional scale, and the approximated nature of the conceptual flow model has uncertainty in all parameters; model error is the result of that approximation.

The simulation of the vertical hydraulic gradients between the surficial aquifer and the Upper Floridan aquifer in the active flow model area indicated the presence of a small downward hydraulic gradient near wells having measured water-table altitudes and Upper Floridan aquifer heads. Surficial aquifer well 23021 and Upper Floridan aquifer well 23032 are in northwest Sumter County (figs. 1.6, 1.7), and because of their proximity to each other, water levels from these two wells provide the necessary data to estimate a small downward hydraulic gradient between the two aquifers. The simulated water levels at these two wells also indicate a small downward hydraulic gradient between the two aquifers from 2004 to 2012, (figs. 1.43, 1.44). Surficial aquifer well 23503 and Upper Floridan aquifer well 23500 are in southeast Citrus County, near the Sumter-Citrus County line (figs. 1.6, 1.7), and average measured and simulated water levels in the surficial aquifer are slightly higher than those

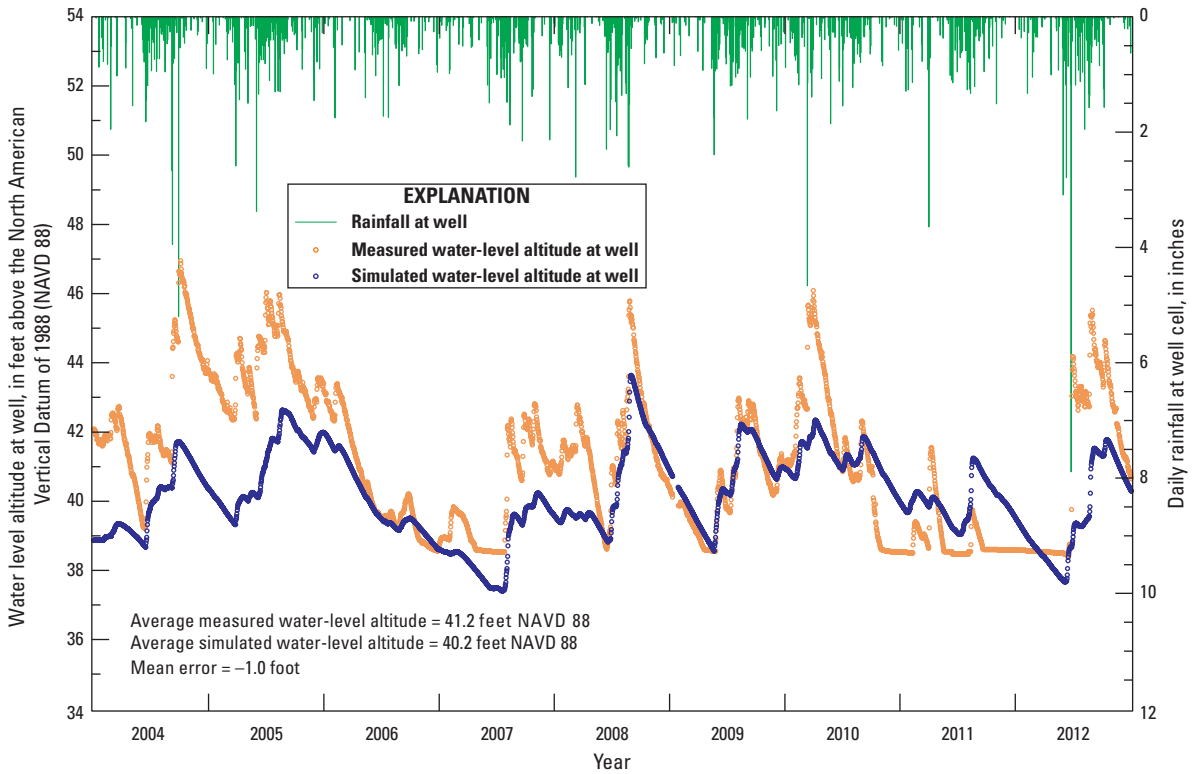

Figure 1.43 Measured and simulated heads at ROMP 112 surficial aquifer well (23021 in fig. 1.6), and daily rainfall at well, for the 2004–12 period.

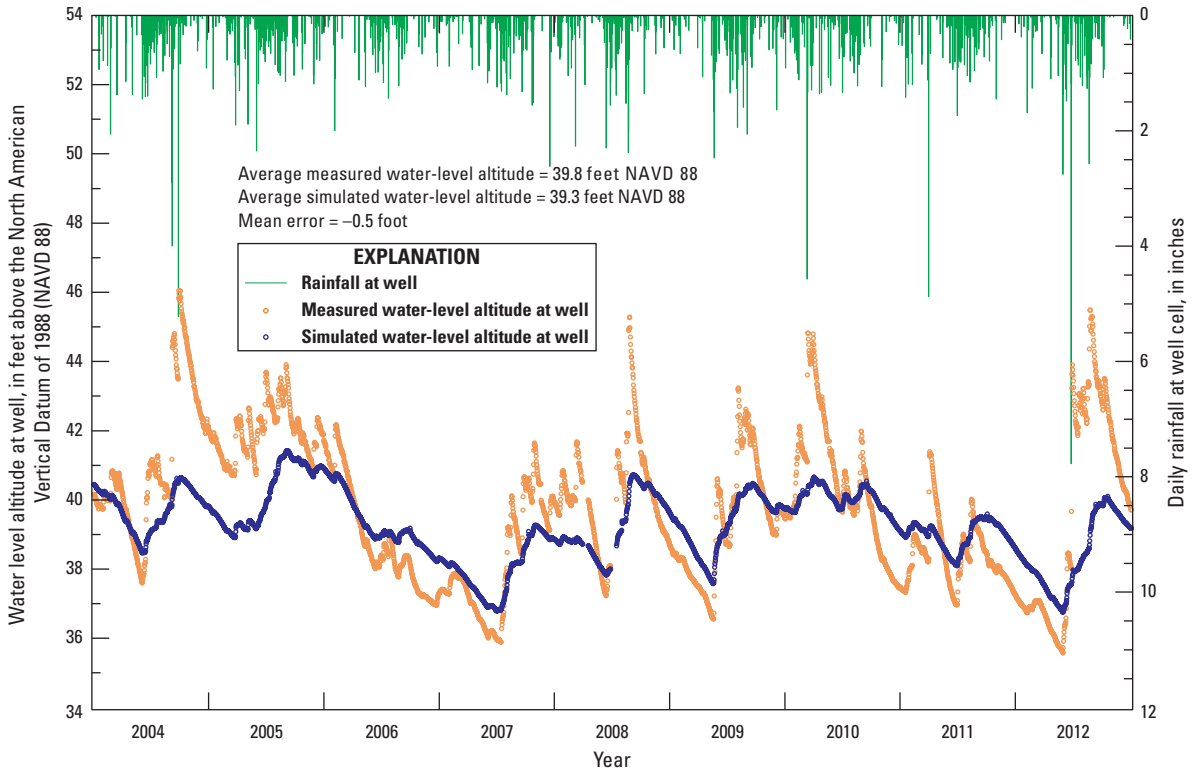

Figure 1.44 Measured and simulated heads at Sumter 13 JC 59 Upper Floridan aquifer well (23032 in fig. 1.7), and daily rainfall at well, for the 2004–12 period.

in the Upper Floridan aquifer (figs. 1.45, 1.46). Northwest of these two wells, surficial aquifer well 759564 and Upper Floridan aquifer well 759565 are inside the Floral City pool basin (figs. 1.6, 1.7). Average measured and simulated water levels at these two wells are slightly higher in the surficial aquifer than the heads in Upper Floridan aquifer (figs. 1.47, 1.48). The simulation of small vertical hydraulic gradients at nested wells (one tapping the surficial aquifer and another tapping the Upper Floridan aquifer) in the Tsala Apopka Lake Basin is a key requirement, in addition to the calibrated lakebed leakances, to correctly represent the leakage between the lakes and the underlying aquifers.

Simulated Spring Flows

The specified spring pool altitudes were held constant for 86 of the 91 simulated springs, with only 5 springs having sufficiently variable pool altitudes to warrant simulation. Spring number 5 (Silver Springs, table 1.5, fig. 13) was simulated with a time-varying spring pool altitude, because vegetation in the spring run impedes flow, which in turn causes the stage along the spring run to fluctuate. In addition, coastal springs 43, 46, and 57–58 (table 1.5, fig. 13) were simulated with a specified spring pool altitude that varied with time to represent tidal effects on the spring pools. Springs having variable pool altitudes were adjusted based on recorded changes in Upper Floridan aquifer heads at wells located closest to the coastal springs.

The majority of the simulated spring groups (70 of 82, table 1.12) had only one spring flow measurement or estimate; however, the springs that had continuous flow records yielded 62 percent (1,583 ft^3/s) of the total spring flow (2,565 ft^3/s) in the model area. All estimates were obtained from the Northern District Model (HydroGeoLogic, 2013). Mean errors calculated for springs having more than 20 flow measurements (table 1.12) ranged from -6.1 to 6.1 percent (table 1.12). These residuals meet the simulated spring flow calibration targets when the magnitude of the measured spring flows are considered. Mean errors calculated for first magnitude springs, having more than 20 flow measurements, ranged from -6.1 to 1.1 percent (table 1.12). Average simulated spring flow, over the stress periods when spring flows were measured, was 2,447 ft^3/s, or 95 percent of the total spring flow.

Peaks in simulated and measured spring flow occurred at similar times, as shown in the Silver Springs hydrograph (fig. 1.49), largely because of time-varying spring-pool-altitude input that has the same variations as the spring run stage. The simulated flow hydrograph of Rainbow Springs is characterized by several underestimated measured flow peaks during large rainfall events (fig. 1.50). This could be due to including surface runoff as part of the measured spring flow in the Rainbow Springs Run (fig. 1), because the contribution of the surface runoff component to streamflow increases as the magnitude of the rainfall event increases. This effect is also evident in the simulated flow hydrograph for Gum Springs (fig. 1.51), which reflects simulated spring flow having a smoother gradient after large rainfall events than measured spring flow. Measured spring flow was calculated using a simple constant ratio of three quarters of total streamflow as groundwater flow and one quarter as surface flow based on a base-flow separation technique of measured flow data.

The spring flows of Homosassa, SE Fork Homosassa, and Chassahowitzka Springs (spring numbers 43, 46, and 57–58, fig. 13) were simulated using a spring pool altitude that fluctuated daily to weekly because of tides. The residuals at these three springs, which had a large number of daily measured flows, met the calibration target goals for simulated spring flows (table 1.12, figs. 1.52 to 1.54). These three sets of simulated and measured hydrographs are characterized by daily to weekly flow fluctuations, which are typical of tidal effects on spring flows.

The agreement between simulated and measured spring flows at Weeki Wachee Springs (spring numbers 81–82, fig. 13) is indicated by most of the hydrograph peaks (fig. 1.55). Spring flow hydrograph peaks at Weeki Wachee were only underestimated for the two largest rainfall events that occurred during the 2004–12 period. This underestimation of spring flow at Weeki Wachee may be explained by the underestimation of heads in the Upper Floridan aquifer in west-central Hernando County (figs. 1.42, 1.55).

Simulated Streamflows and Stream Stages

Simulated streamflows and stream stages were calibrated according to the average ME in flow and stage criteria previously established for streamflows and stages in the Calibration Targets section. The streamflow-gaging station at Withlacoochee River near Pineola (station 02312598, fig. 18) is the first station downstream from Withlacoochee River at Nobleton (station 02312558, fig. 18), where boundary flow conditions in the streamflow routing were specified. The simulated flow residuals at the Withlacoochee River near Pineola and at the Withlacoochee River near Floral City streamflow-gaging stations were the highest at hydrograph peaks that coincided with the highest rainfall rates (figs. 1.56, 1.57, table 1.13). Simulated flow residuals at these two streamflow-gaging stations were lower during drier periods.

The simulated flow at the Outlet River at Panacoochee Retreats streamflow-gaging station (number 02312700, fig. 18) was determined from a water balance of inflows such as tributaries to Lake Panasoffkee, estimated surface runoff, and upward leakage from the Upper Floridan aquifer through the surficial aquifer, and the outflow to Outlet River from Lake Panasoffkee. The agreement between simulated and measured stages at Lake Panasoffkee (fig. 1.38) was also determined by the water balance of inflows and outflows at the lake. Both simulated and measured streamflow hydrographs indicate a time delay of several days between hyetograph peaks and streamflow hydrographs peaks at the Outlet River at Panacoochee Retreats station (fig. 1.58). The simulated streamflow hydrograph for the Withlacoochee River at Wysong structure (station 02312720, fig. 18) is the result of matching the simulated and measured stages at the Wysong structure as closely as possible (figs. 1.39, 1.59).

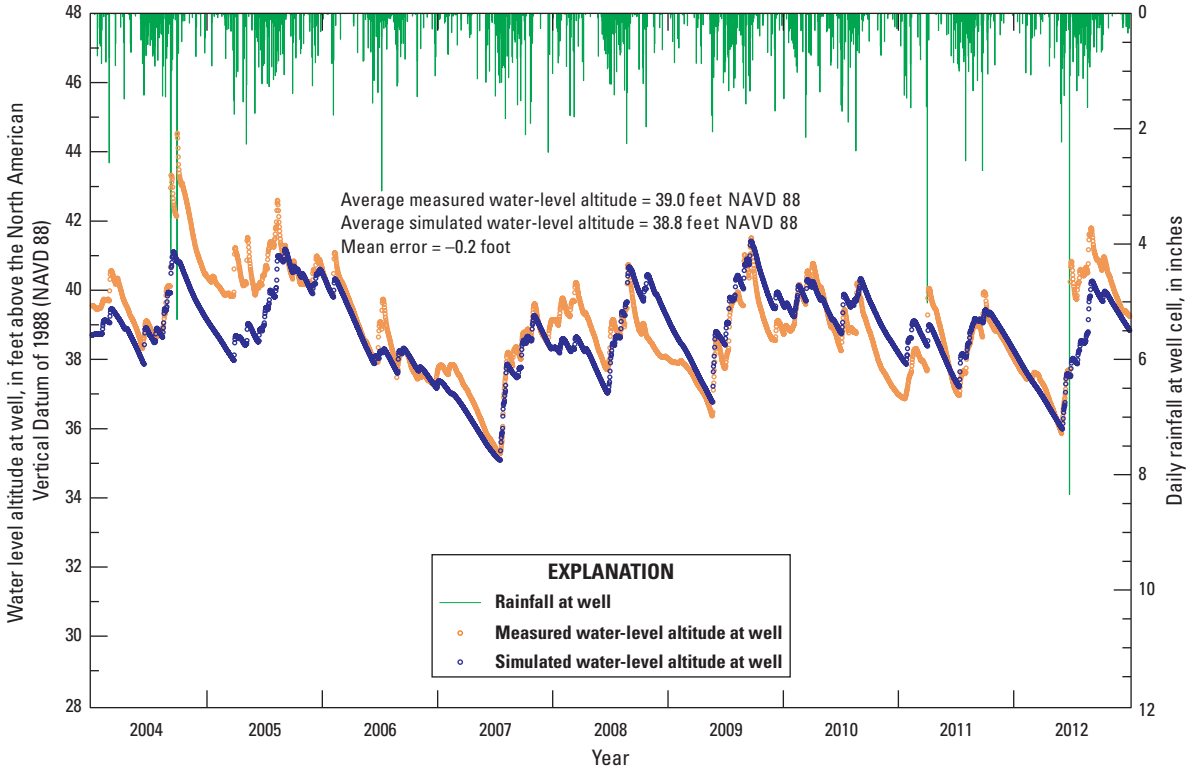

Figure 1.45 Measured and simulated heads at ROMP 110 surficial aquifer well (23503 in fig. 1.6), and daily rainfall at well, for the 2004–12 period.

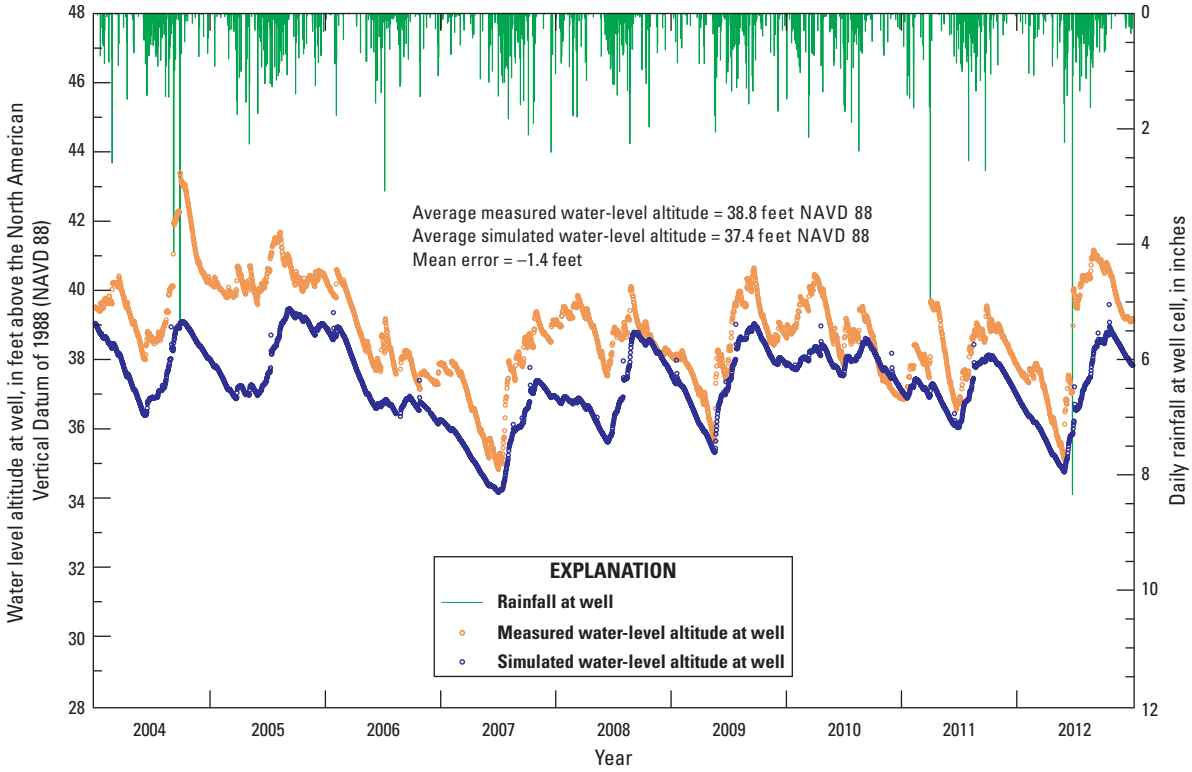

Figure 1.46 Measured and simulated heads at ROMP 110 Upper Floridan aquifer well (23500 in fig. 1.7), and daily rainfall at well, for the 2004–12 period.

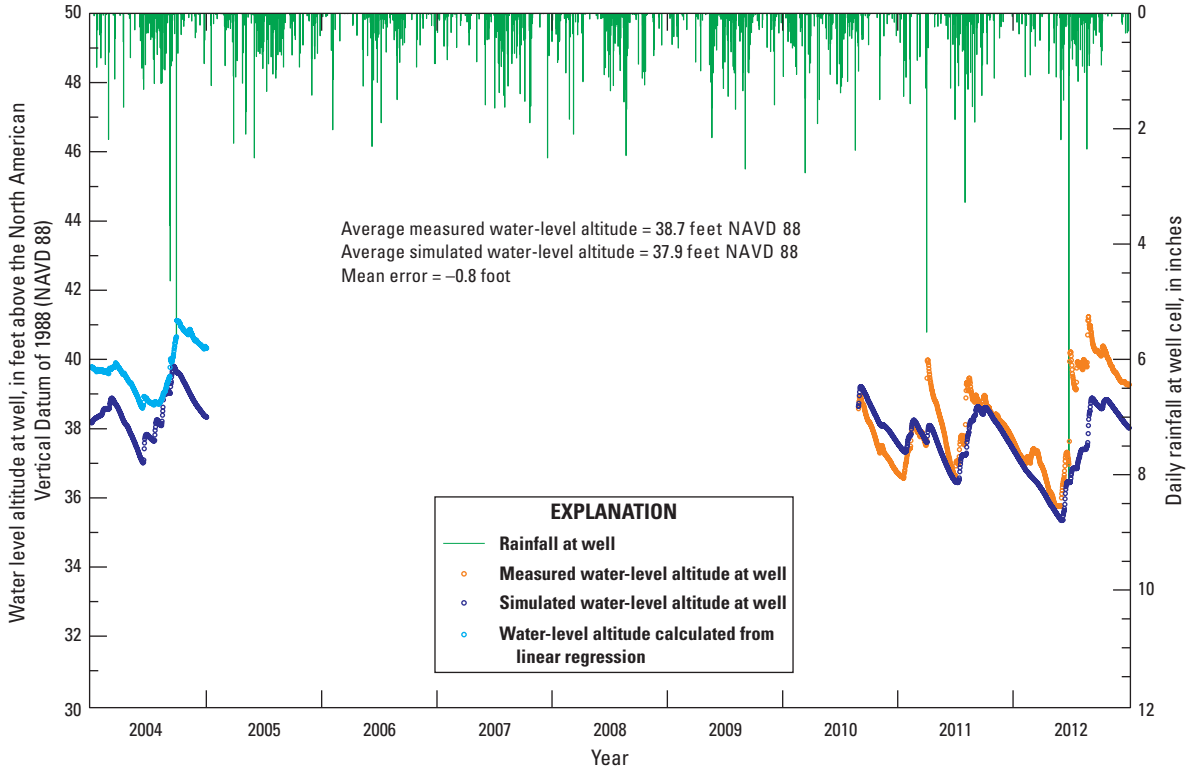

Figure 1.47 Measured and simulated heads at Tsala Apopka Lake 4 surficial aquifer well (759564 in fig. 1.6), and daily rainfall at well, for the 2004–12 period.

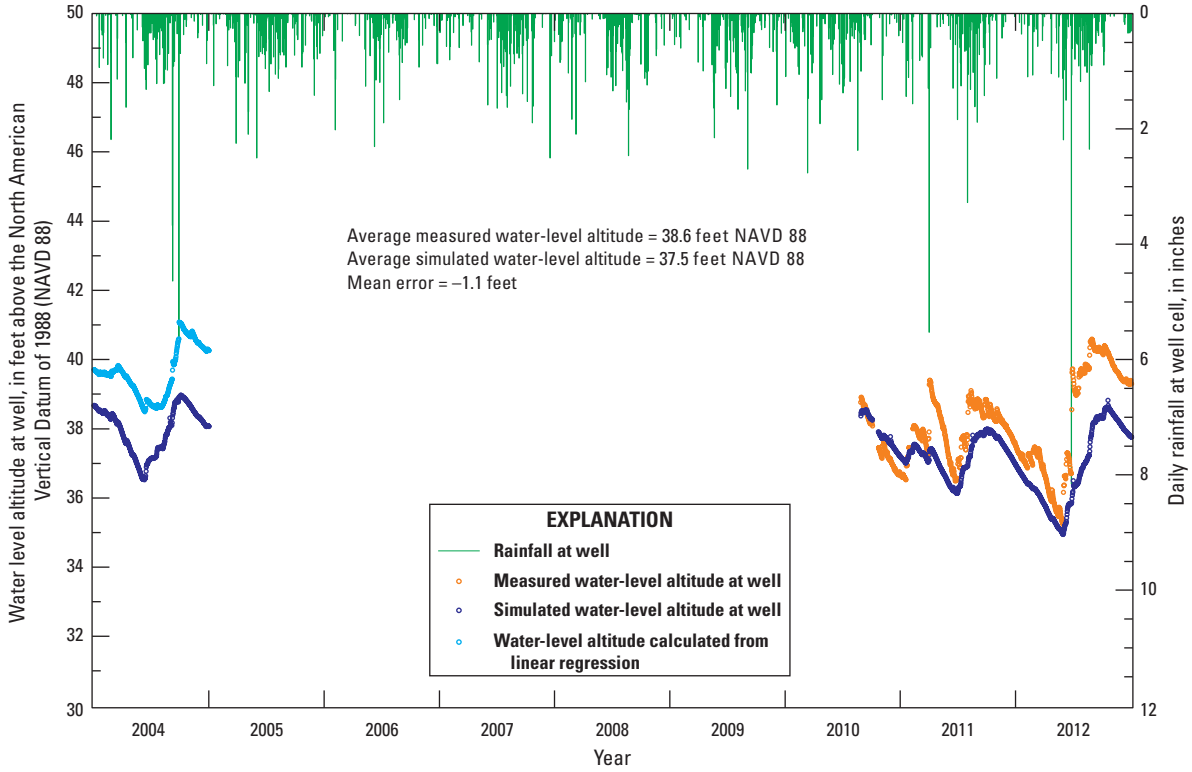

Figure 1.48 Measured and simulated heads at Tsala Apopka Lake 4 Upper Floridan aquifer well (759565 in fig. 1.7), and daily rainfall at well, for the 2004–12 period.

Table 1.12. Statistics of simulated spring flow residuals calculated from measured spring flows.

[GRPNO, group number of spring names listed in table 1.5; AVMFL, average measured spring flow from 2004 to 2012; AVSFL, average simulated spring flow for stress periods when flow was measured; ME, mean error calculated as simulated minus measured spring flows; RMSE, root mean square error between simulated and measured spring flows; PERCENT, percentage of error in simulated spring flow, negative if measured flow is larger than simulated and positive if vice versa; NUM, number of measured or estimated spring flows; 1 indicates there was only one estimated spring flow for the 2004–12 period. NA, not applicable; All flows are in cubic feet per second]

Spring group name	GRPNO	AVMFL	AVSFL	ME	RMSE	PERCENT	NUM
Magnesia Springs	1	5.0	5.4	0.4	0.4	8.0	1
Wekiva Spring	2	45.0	33.0	-12.0	12.0	-26.7	1
Big King Spring	3	5.0	2.8	-2.2	2.2	-44.0	1
Little King Spring	4	0.5	0.6	0.1	0.1	20.0	1
Silver Springs near Ocala	5	524.3	492.2	-32.1	42.3	-6.1	3,288
Coastie Spring	6	5.0	4.2	-0.8	0.8	-16.0	1
Rainbow Springs	7	594.3	597.9	3.6	46.1	0.6	3,288
Bubbling Spring	8	5.0	6.2	1.2	1.2	24.0	1
Indian Creek Spring #3, #4	9	5.0	5.6	0.6	0.6	12.0	1
Indian Creek Spring #1, #2	10	5.0	4.1	-0.9	0.9	-18.0	1
Lost Springs	11	5.0	4.2	-0.8	0.8	-16.0	1
Wilson Head Spring	12	2.0	2.8	0.8	0.8	40.0	1
Millers Creek Spring	13	2.0	1.4	-0.6	0.6	-30.0	1
Citrus-Blue Spring	14	5.0	5.2	0.2	0.2	4.0	1
Little Spring, Charles Fish House, Cedar Spring	15	6.9	6.3	-0.6	8.0	-8.7	11
Birds Underwater Spring, Pool Springs, Catfish Spring	16	5.0	4.1	-0.9	0.9	-18.0	1
Magnolia Circle Spring	17	3.0	2.4	-0.6	0.6	-20.0	1
Hunters, Jurassic, Petes Pier Springs Complex	18	5.0	4.2	-0.8	0.8	-16.0	1
Moray Springs Complex	19	2.0	1.6	-0.4	0.4	-20.0	1
Buzzard Island Spring (Citrus), Paradise Isles Complex	20	5.0	4.2	-0.8	0.8	-16.0	1
Crystal River Spring Group, Manatee Sanctuary Spring	21	475.0	434.1	-40.9	40.9	-8.6	1
Idiots Delight #1, #2, #3, Three Sisters Springs #1, #2, #3	22	15.0	12.4	-2.6	2.6	-17.3	1
Parker Island Springs, Banana Island Springs North	23	5.0	4.2	-0.8	0.8	-16.0	1
Banana Island Springs Complex, FWS Spring Complex	24	5.0	4.7	-0.3	0.3	-6.0	1
Tarpon Hole Spring, Hole #2, Mary Spring, Art Spring	25	5.0	4.3	-0.7	0.7	-14.0	1
Lightbourns Ledge	26	3.0	2.3	-0.7	0.7	-23.3	1
Daves Quest Springs Complex	27	3.0	2.2	-0.8	0.8	-26.7	1
Wynn Court Springs Complex, Black Spring	28	3.0	2.3	-0.7	0.7	-23.3	1
Golfview Boathouse Spring	29	3.0	2.2	-0.8	0.8	-26.7	1
Sids Spring, Garys Grotto	30	3.0	2.4	-0.6	0.6	-20.0	1
Gum Springs	31	64.1	68.0	3.9	11.0	6.1	3,288
Halls River Head Spring	32	102.0	85.3	-16.7	16.7	-16.4	1
Halls River #1 Spring	33	11.4	12.1	0.7	1.8	6.1	242
Bear Spring (Citrus)	34	5.0	4.0	-1.0	1.0	-20.0	1
Alligator Spring (Citrus), Banana Spring	35	5.0	4.0	-1.0	1.0	-20.0	1
Homosassa #1, #2, #3 Spring, Blue Hole Spring (Citrus)	36	83.1	84.2	1.1	5.4	1.3	3,140
Pumphouse Spring	37	5.0	4.8	-0.2	0.2	-4.0	1
Trotter Main Spring	38	5.0	4.0	-1.0	1.0	-20.0	1
SE Fork Head Spring Homosassa	39	58.1	59.4	1.3	7.4	2.2	3,166

Table 1.12. Statistics of simulated spring flow residuals calculated from measured spring flows.—Continued

[GRPNO, group number of spring names listed in table 1.5; AVMFL, average measured spring flow from 2004 to 2012; AVSFL, average simulated spring flow for stress periods when flow was measured; ME, mean error calculated as simulated minus measured spring flows; RMSE, root mean square error between simulated and measured spring flows; PERCENT, percentage of error in simulated spring flow, negative if measured flow is larger than simulated and positive if vice versa; NUM, number of measured or estimated spring flows; 1 indicates there was only one estimated spring flow for the 2004–12 period. NA, not applicable; All flows are in cubic feet per second]

Spring group name	GRPNO	AVMFL	AVSFL	ME	RMSE	PERCENT	NUM
Bluebird Springs	40	5.0	4.5	-0.5	0.5	-10.0	1
Otter Creek Spring	41	5.0	3.6	-1.4	1.4	-28.0	1
Hidden River Head Spring, #2, #6 Spring	42	7.0	7.0	0.0	0.0	0.0	1
Hidden River Spring #7, #8	43	4.0	2.8	-1.2	1.2	-30.0	1
Henry Green Spring	44	5.0	4.6	-0.4	0.4	-8.0	1
A. Wayne Lee Spring	45	5.0	5.2	0.2	0.2	4.0	1
Ruth and Potters Creek Spring	46	11.0	10.5	-0.5	3.2	-4.5	1,082
Salt Creek Head Spring (Citrus)	47	0.4	0.3	-0.1	0.1	-25.0	1
Lettuce Creek Spring	48	4.0	3.8	-0.2	0.2	-5.0	1
Crab Creek Spring	49	35.0	33.8	-1.2	1.2	-3.4	1
Chassahowitzka Springs	50	59.6	57.7	-1.9	23.1	-3.2	2,917
Johnson Creek HeadSpring	51	3.0	2.1	-0.9	0.9	-30.0	1
Baird Spring, #2, #3, #4	52	3.0	2.8	-0.2	0.2	-6.7	1
Ryles Spring	53	8.0	6.9	-1.1	1.1	-13.8	1
Beteejay and Rita Marie Spring	54	7.0	7.1	0.1	0.1	1.4	1
Blue Run	55	5.0	5.9	0.9	0.9	18.0	1
Blind Spring, Hernando Unnamed #7	56	20.0	17.5	-2.5	2.5	-12.5	1
Fenney Spring	57	6.9	5.0	-1.9	8.1	-27.5	11
Canal 485A Spring 2	58	5.0	4.6	-0.4	0.4	-8.0	1
Canal 485 Spring 5 and Canal 485A Spring 1B	59	5.0	4.6	-0.4	0.4	-8.0	1
Sumter-Blue Spring	60	3.0	1.6	-1.4	1.4	-46.7	1
Shady Brook Spring 3	61	2.0	1.5	-0.5	0.5	-25.0	1
Big Hole Spring (Dead Spring)	62	5.0	4.3	-0.7	0.7	-14.0	1
Buford #2 (Hernando)	63	3.0	4.0	1.0	1.0	33.3	1
Buford HeadSpring (Hernando)	64	3.0	3.8	0.8	0.8	26.7	1
Shady Brook Spring 4	65	2.0	1.7	-0.3	0.3	-15.0	1
Belton's Millpond Spring Group	66	6.9	6.7	-0.2	5.8	-2.9	186
Bugg Spring	67	9.0	8.5	-0.5	0.5	-5.6	1
Mud and Wilderness Spring	68	5.0	5.9	0.9	0.9	18.0	1
Hernando - Salt Spring	69	22.0	20.1	-1.9	1.9	-8.6	1
Hospital Hole Spring	70	5.0	3.8	-1.2	1.2	-24.0	1
Jenkins Creek Spring	71	5.0	7.1	2.1	2.1	42.0	1
Weeki Preserve Spring	72	10.0	13.2	3.2	3.2	32.0	1
Weeki Wachee Springs	73	156.7	158.5	1.8	11.5	1.1	3,283
Jewfish Hole	74	4.0	4.4	0.4	0.4	10.0	1
Boat Spring	75	0.4	0.7	0.3	0.3	75.0	1
Magnolia Spring and Gator Spring, Bobhill Spring	76	1.0	1.6	0.6	0.6	60.0	1
Double Keyhole Spring	77	3.0	3.5	0.5	0.5	16.7	1
Cedar Island Spring (Pasco)	78	3.0	3.1	0.1	0.1	3.3	1
Horseshoe Spring	79	8.0	8.4	0.4	0.4	5.0	1
Isabella Spring	80	4.0	4.6	0.6	0.6	15.0	1
Riverdale Spring	81	5.0	3.4	-1.6	1.6	-32.0	1
Dobes Hole Spring	82	1.0	1.2	0.2	0.2	20.0	1
Total	**NA**	**2,564.6**	**2,447.2**	**-117.4**	**NA**	**NA**	**23,972**

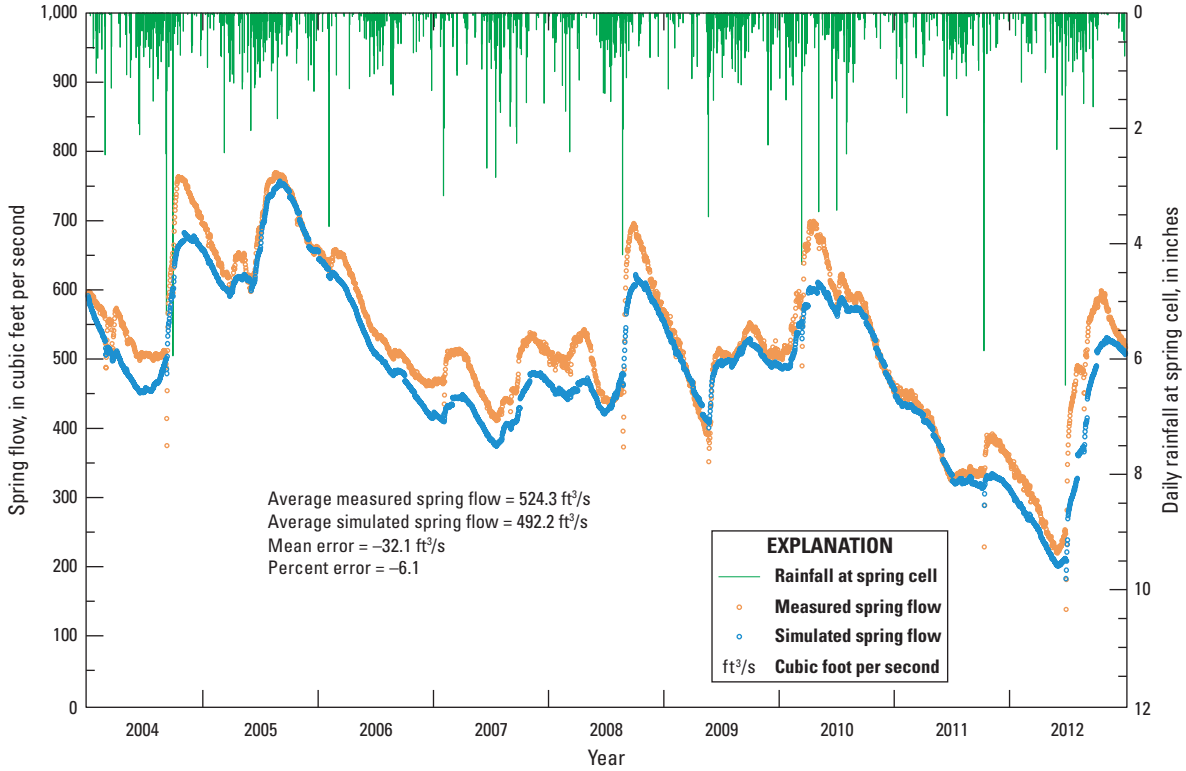

Figure 1.49 Measured and simulated flows of Silver Springs, and daily rainfall at spring cell, for the 2004–12 period.

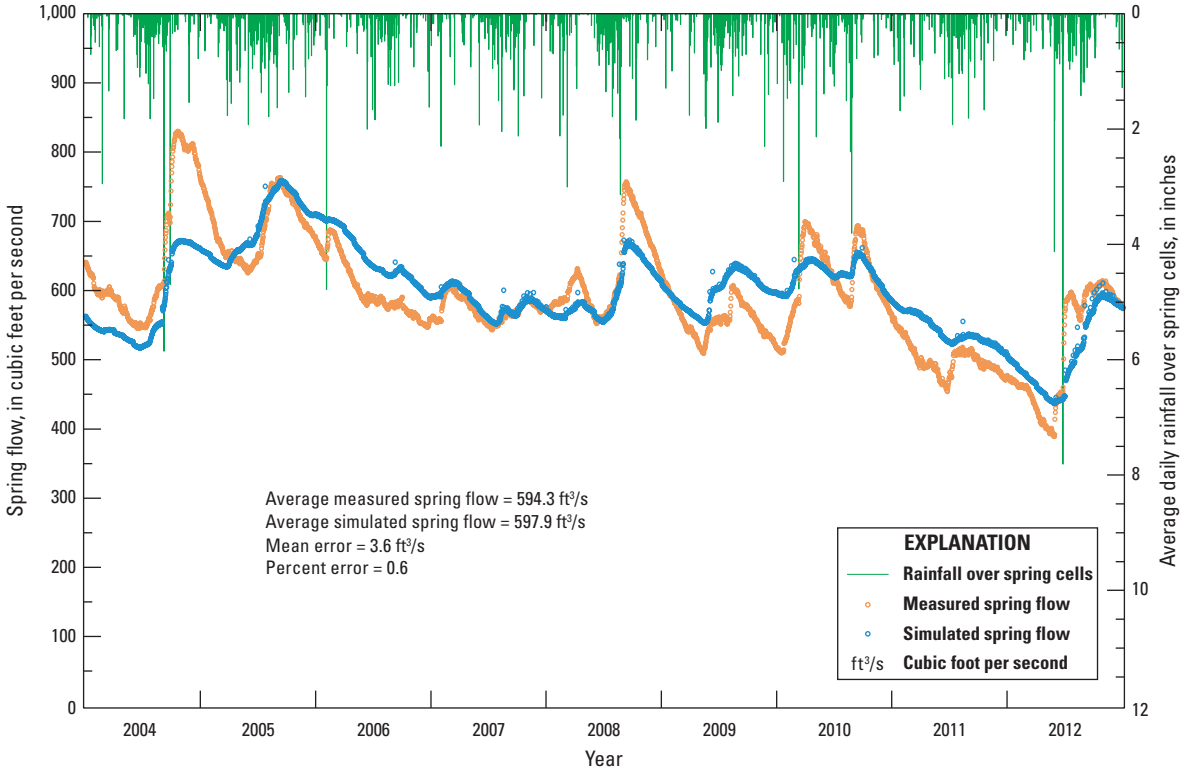

Figure 1.50 Measured and simulated flows of Rainbow Springs, and average daily rainfall over spring cells, for the 2004–12 period.

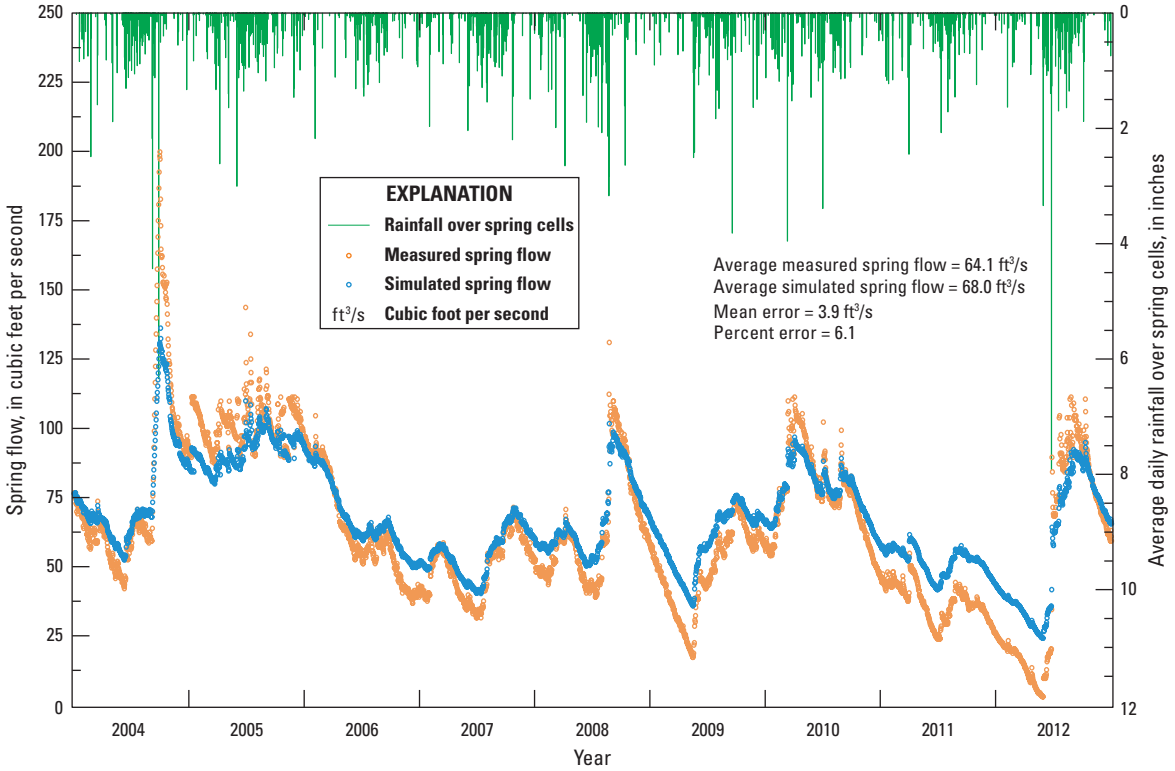

Figure 1.51 Measured and simulated flows of Gum Springs, and average daily rainfall over spring cells, for the 2004–12 period.

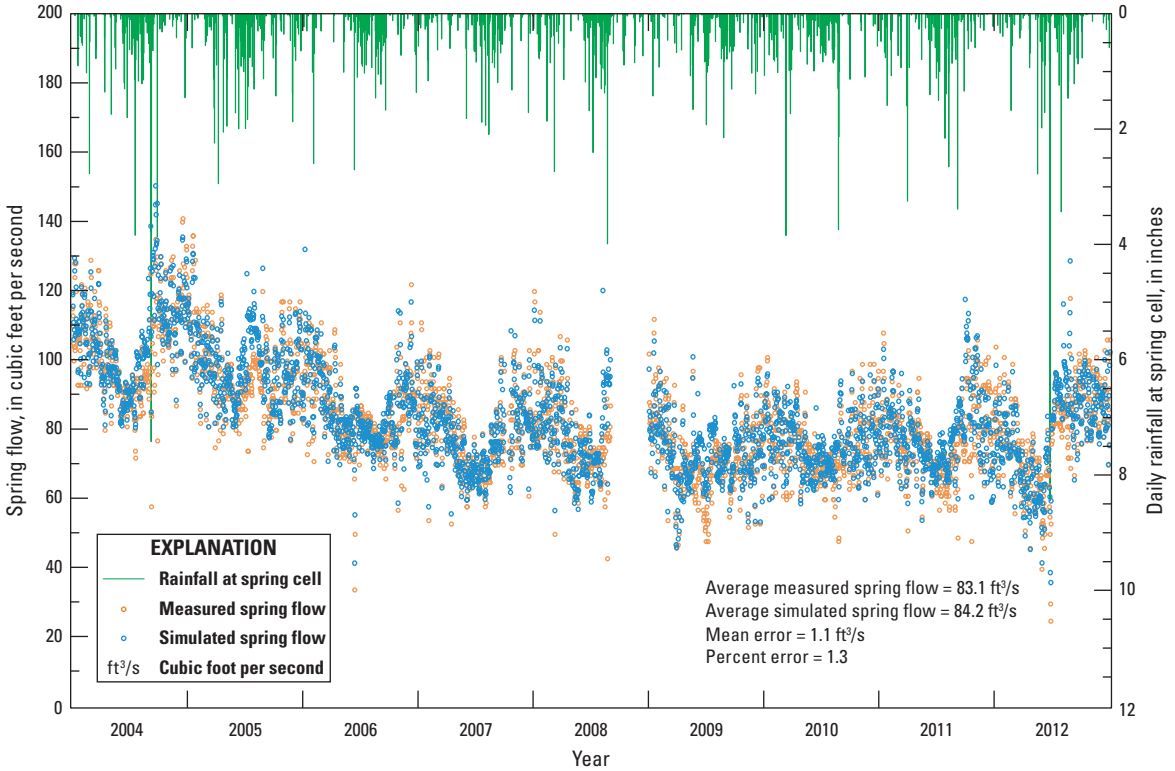

Figure 1.52 Measured and simulated flows of Homosassa Springs, and daily rainfall at spring cell, for the 2004–12 period.

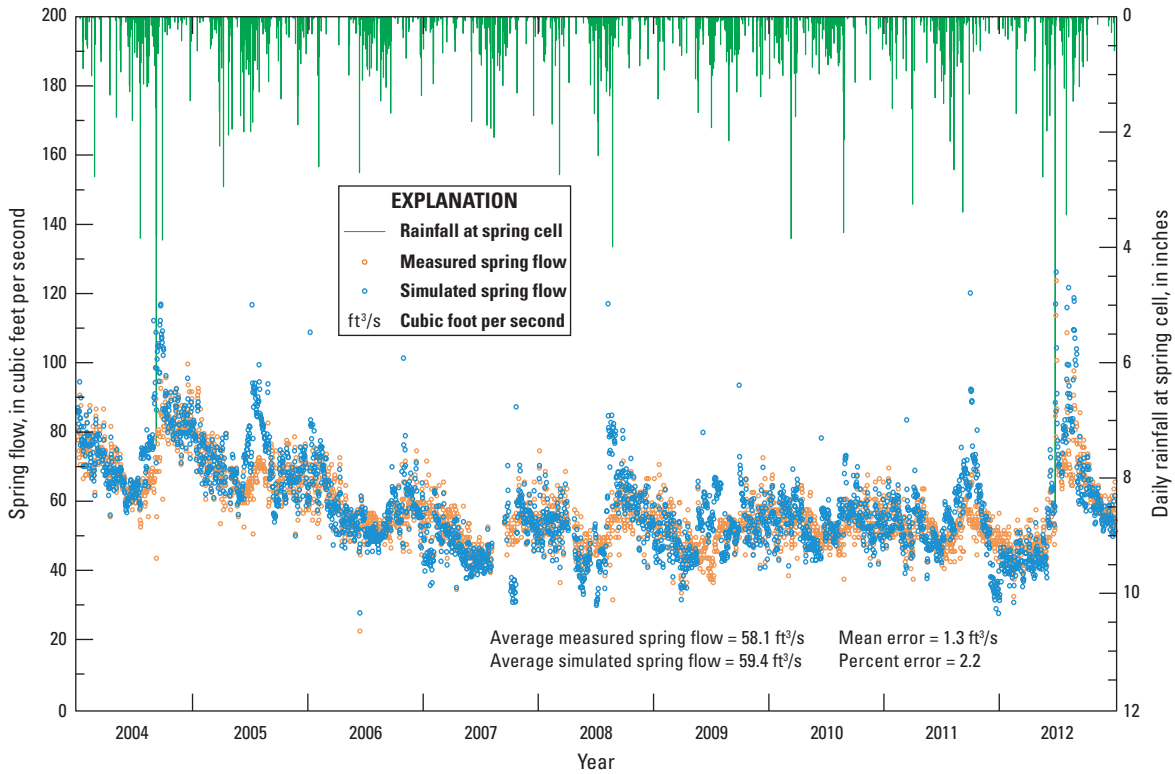

Figure 1.53 Measured and simulated spring flows of SE Fork Homosassa Springs, and daily rainfall at spring cell, for the 2004–12 period.

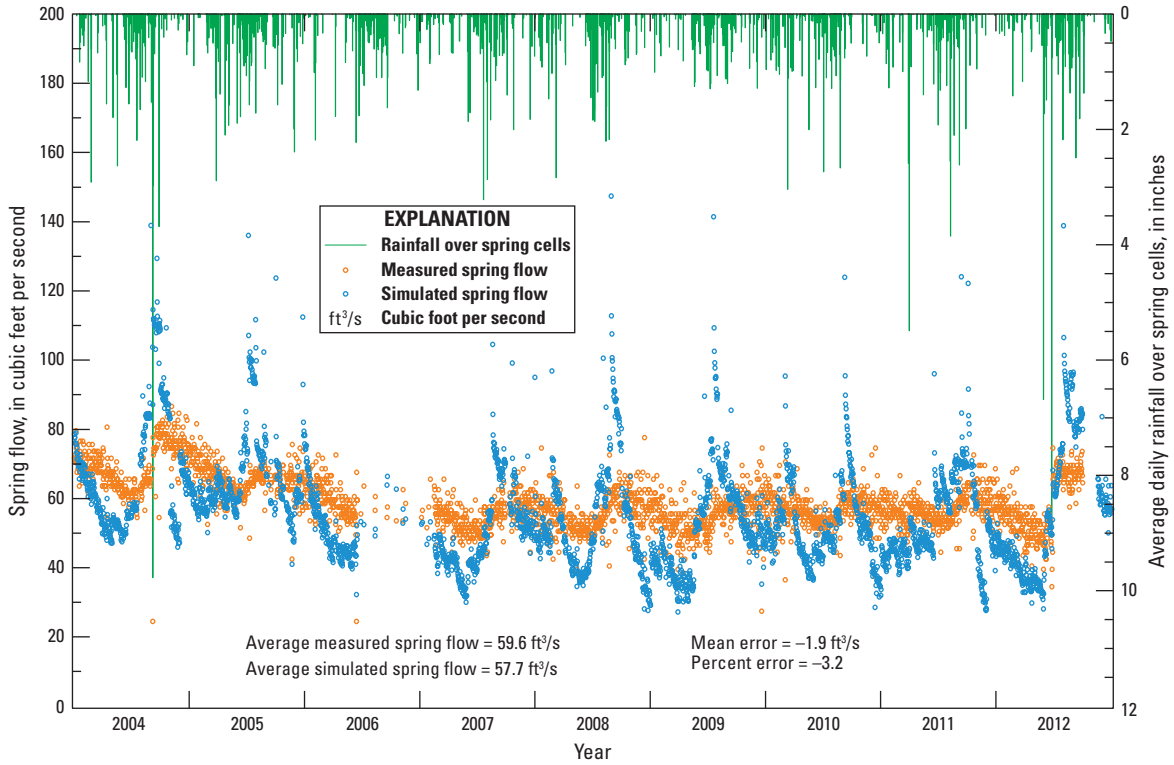

Figure 1.54 Measured and simulated spring flows of Chassahowitzka Springs, and average daily rainfall over spring cells, for the 2004–12 period.

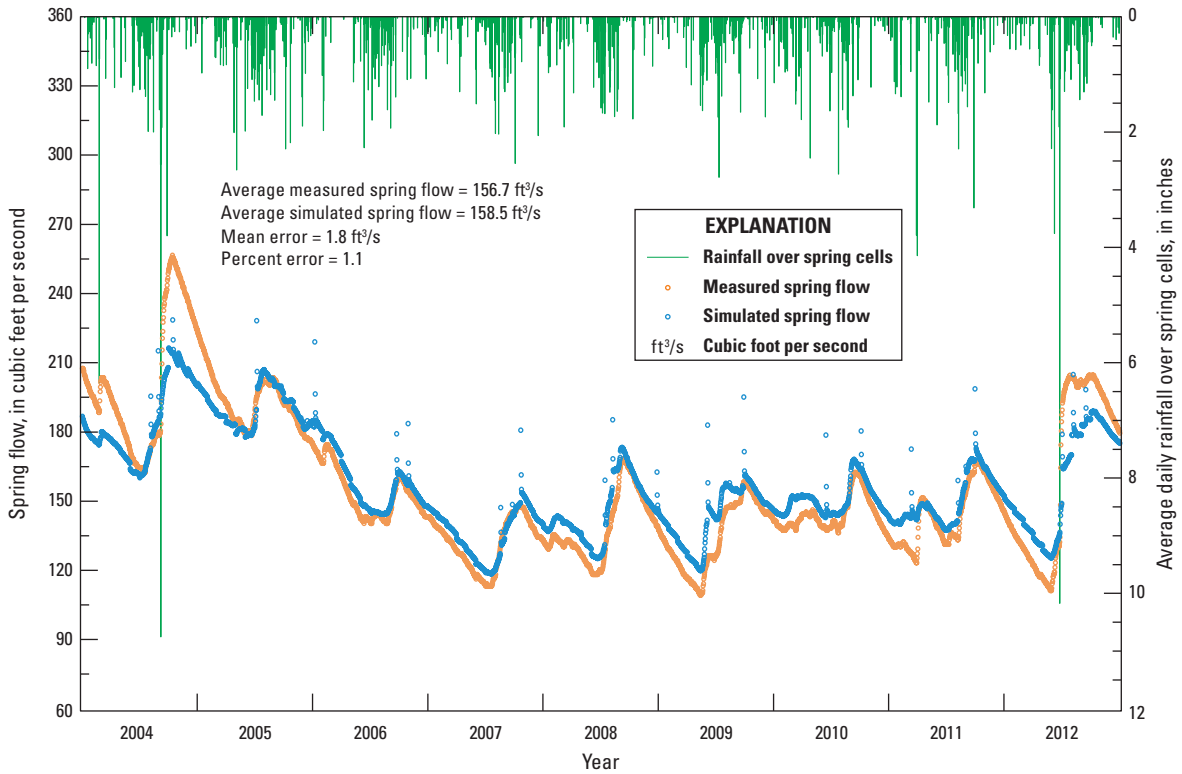

Figure 1.55 Measured and simulated spring flows of Weeki Wachee Springs, and average daily rainfall over spring cells, for the 2004–12 period.

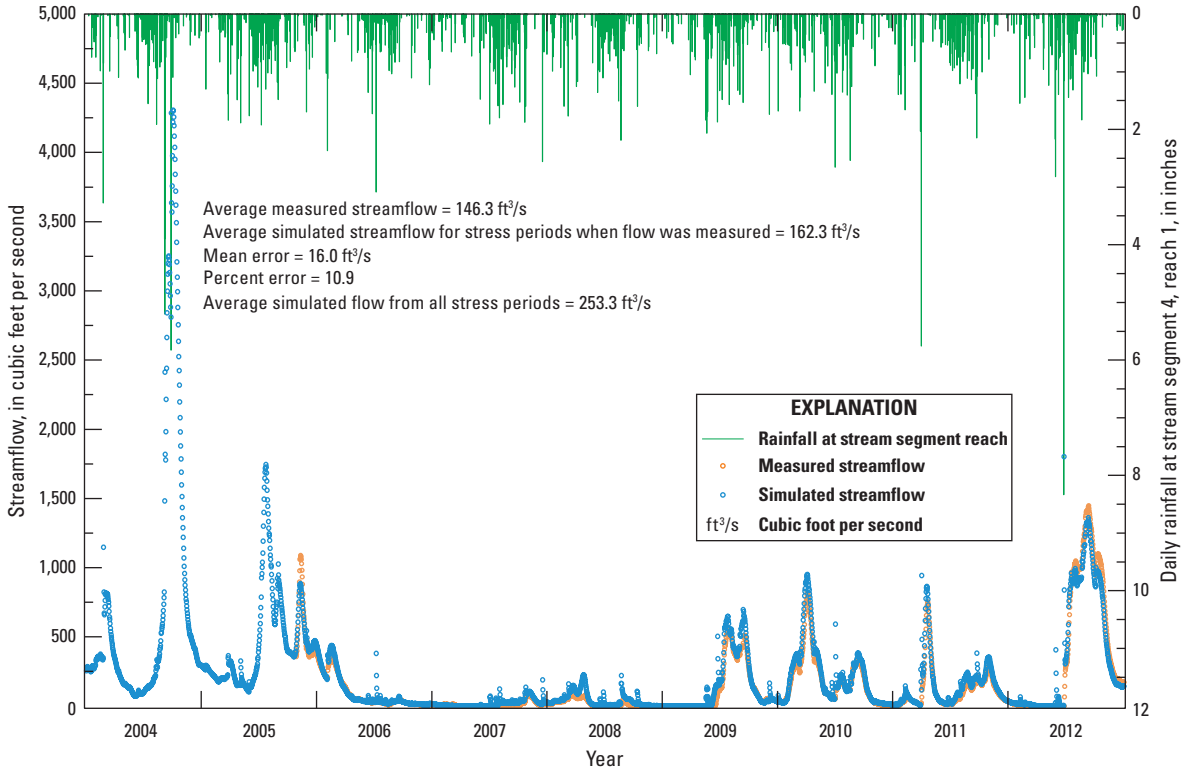

Figure 1.56 Measured and simulated flows at streamflow-gaging station number 02312598, Withlacoochee River near Pineola, and daily rainfall at streamgage, for the 2004–12 period.

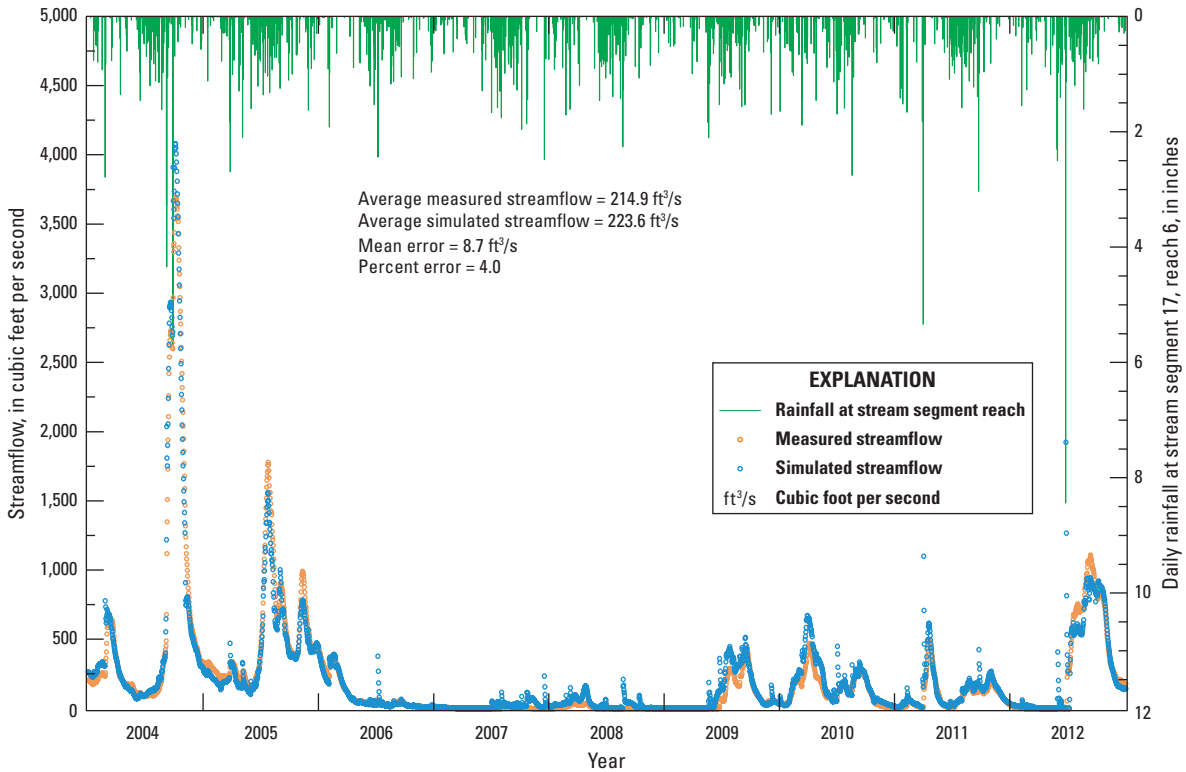

Figure 1.57. Measured and simulated flows at streamflow-gaging station number 02312600, Withlacoochee River near Floral City, and daily rainfall at streamgage, for the 2004–12 period.

The Withlacoochee River near Rutland and the Withlacoochee River near Inverness (stations 02312722 and 02312762, fig. 18) are the first two streamflow-gaging stations downstream from the Wysong structure, and simulated streamflow at both stations depends substantially on the simulated flow through the structure. The simulated streamflow hydrographs for both stations are similar to those for measured streamflow (figs. 1.60, 1.61). The time delay between the simulated and measured streamflow hydrograph peaks for these two streamflow-gaging stations is also observed at stations upstream of the Wysong structure (figs. 1.60, 1.61).

The simulation of streamflow along the spring runs in the model was accomplished in two steps. The first step was to simulate the spring flow using the GHB Package. The second step was to assign the simulated spring flow as lateral surface runoff along the stream segment representing the spring run to add the groundwater flow component to the surface-water flow component. Gum and Rainbow Springs (spring numbers 7–11 and 35–38, fig. 13) were springs for which the simulated spring flows were specified as surface runoff applied to segments 30 and 35, respectively (fig. 1.3). A comparison of simulated and measured streamflows at the two streamflow-gaging stations in these two segments (stations 02312764 and 02313100, fig. 18) indicates that some measured streamflow hydrograph peaks are underestimated (figs. 1.62, 1.63).

A comparison of measured and simulated streamflows at the Withlacoochee River near Holder (station 02313000, fig. 18) shows dispersed but numerous occurrences where simulated streamflows were overestimated (fig. 1.64). These overestimations by the model, which occurred during and shortly after days when rainfall was at least 2 in., result from the way the UZF1 Package (Niswonger and others, 2006) distributes the calculated surface runoff for every stress period. Surface runoff and groundwater discharge to land surface, calculated by UZF1, are applied in the same stress period directly to the stream segment or lake indicated by the subbasin delineation. Given that this model uses daily stress periods, the simulated hydrograph peaks may be overestimated because actual surface runoff may take more than one day to arrive at the stream segment and land-surface depressions are not filled up before surface runoff is discharged to the stream segment to which a cell drains. This model limitation also explains why the gradient of the simulated streamflow is steeper than that of the measured streamflow.

Simulated flows leaving Lake Rousseau through the Inglis Dam (station 02313230, fig. 18) and through the Inglis Bypass Spillway (station 02313250, fig. 18) were calibrated as a combined flow. Specified flows through the Inglis Dam were maintained as close as possible to the measured flows (fig. 1.65), because the Inglis Dam water-control structure was open in 777 days while the Inglis Bypass Spillway was open in all 3,288 days during the 2004–12 period. Lake Rousseau stage was calibrated by simulating flow through the Inglis Bypass Spillway (fig. 1.66) to minimize the stage residuals through trial and error. The dispersed but numerous large simulated flow residuals through the Inglis Bypass Spillway (fig. 1.66) are a result of the same type of residuals at the Withlacoochee River near Holder (station 02313000, fig. 18).

Table 1.13. Statistics of simulated streamflow residuals from measured streamflows.

[GAGEID, stream gage number. All stream stages are in feet above the North American Vertical Datum of 1988 (NAVD 88). All flows are in cubic feet per second. AVMST, AVMFL, average measured stream stage and streamflow from 2004 to 2012; AVSST, AVSFL, average simulated stream stage and streamflow from 2004 to 2012; MEST, MEFL, mean error in stream stage and streamflow from 2004 to 2012; RMSEST, RMSEFL, root mean square error in stream stage and streamflow; PERCST, PERCFL, average percentage residual in stream stage and streamflow from 2004 to 2012, negative if measured stage or flow is larger than simulated and positive if vice versa; NUMST, NUMFL, number of days in 2004 to 2012 with measured stream stage or measured streamflow; WR, Withlacoochee River]

Surface-water station name	GAGEID	AVMST	AVSST	MEST	RMSEST	PERCST	NUMST
WR at Nobleton	02312558	38.72	38.69	-0.03	0.79	-0.08	3,214
WR near Pineola	02312598	38.58	38.59	0.01	0.73	0.03	3,288
WR near Floral City	02312600	38.41	38.42	0.01	0.86	0.03	3,266
Outlet River at Panacoochee Retreats	02312700	37.68	37.61	-0.07	0.90	-0.19	2,907
WR above Wysong structure	02312719	37.19	37.20	0.01	1.42	0.03	3,264
WR near Rutland	02312722	33.98	33.96	-0.02	0.75	-0.06	3,279
WR near Inverness	02312762	33.53	33.46	-0.07	0.72	-0.21	3,207
Gum Springs near Holder	02312764	40.00	40.04	0.04	0.35	0.10	3,268
WR near Holder	02313000	28.40	28.35	-0.05	0.94	-0.18	3,216
Rainbow River at Dunnellon	02313100	27.27	27.31	0.04	0.33	0.15	2,824
WR at Dunnellon	02313200	27.13	27.13	0.00	1.37	0.00	3,252
WR below Inglis Dam	02313231	0.29	0.31	0.02	1.03	6.90	3,288

Surface-water station name	GAGEID	AVMFL	AVSFL	MEFL	RMSEFL	PERCFL	NUMFL
WR at Nobleton	02312558	244.87	245.04	0.17	2.04	0.07	3,228
WR near Pineola	02312598	146.32	162.30	15.98	66.33	10.92	2,623
WR near Floral City	02312600	214.88	223.58	8.70	90.29	4.05	3,288
Outlet River at Panacoochee Retreats	02312700	109.94	106.86	-3.08	14.53	-2.80	3,288
WR at Wysong structure	02312720	358.23	345.76	-12.47	187.23	-3.48	3,288
WR near Rutland	02312722	256.23	239.94	-16.29	131.12	-6.36	2,649
WR near Inverness	02312762	417.35	358.92	-58.43	260.44	-14.00	3,288
Gum Springs near Holder	02312764	88.56	76.89	-11.67	19.84	-13.18	3,288
WR near Holder	02313000	555.65	455.80	-99.85	409.69	-17.97	3,288
Rainbow River at Dunnellon	02313100	594.31	618.08	23.77	70.22	4.00	3,288
WR at Inglis Dam	02313230	232.96	195.57	-37.39	225.45	-16.05	3,288
WR Bypass Spillway	02313250	901.26	900.05	-1.21	663.58	-0.13	3,286

Surface Water and Groundwater Flow Budgets

Volumetric inflow and outflow rates, simulated in the Tsala Apopka Lake pools and lakes within the model area, were computed to quantify the contributions by each component of the surface water and groundwater flow system (table 1.14). Most of the simulated groundwater flow at the three main Tsala Apopka Lake pools, the pool on the upstream side of the Wysong structure, and at Lake Rousseau, is downward flow from leakage into the surficial aquifer and underlying Upper Floridan aquifer. In contrast, groundwater flow at Lake Panasoffkee is mostly upward from the Upper Floridan aquifer (table 1.14). These results indicate that a transition in the vertical direction of groundwater flow occurs somewhere between Lake Panasoffkee and the Tsala Apopka Lake main pools. The heads in the Upper Floridan aquifer east of Lake Panasoffkee are higher than the lake stage, and the transition zone is present when the heads in the Upper Floridan aquifer are lower than the water levels in the surficial aquifer and (or) in the Tsala Apopka Lake pools.

Recharge to the unsaturated zone minus groundwater ET loss and surface leakage to land surface depressions is the total recharge/discharge to the surficial aquifer (table 1.15). Total recharge was calculated using cell-by-cell flow data in the unsaturated flow zone and groundwater flow data. These flows were generated for the 9-year surface-water and groundwater

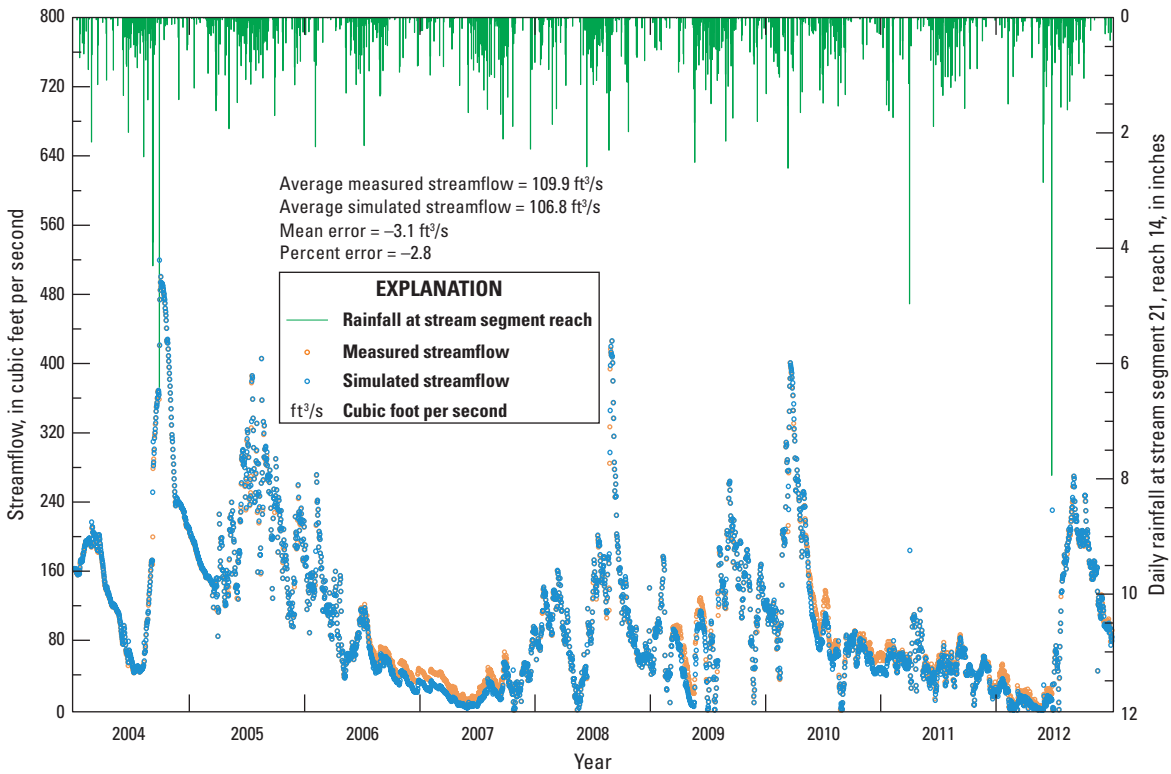

Figure 1.58 Measured and simulated flows at streamflow-gaging station number 02312700, Outlet River at Panacoochee Retreats, and daily rainfall at streamgage, for the 2004–12 period.

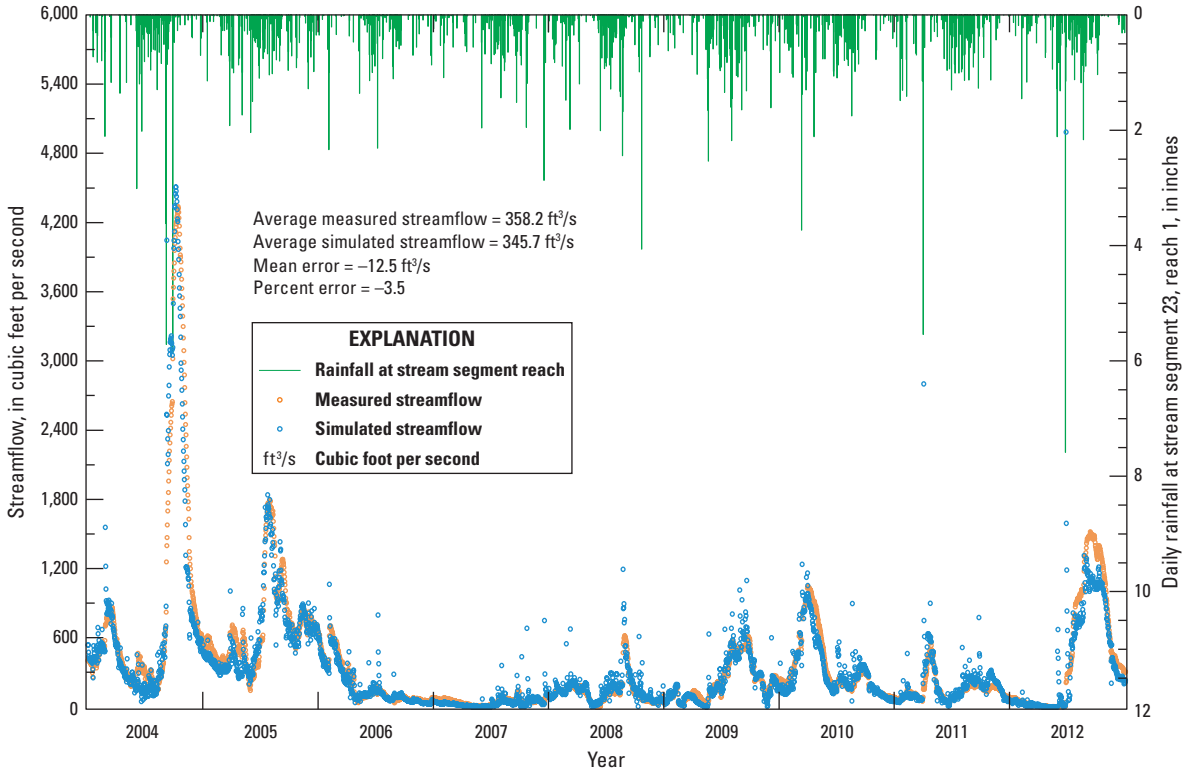

Figure 1.59 Measured and simulated flows at streamflow-gaging station number 02312720, Withlacoochee River at Wysong structure, and daily rainfall at streamgage, for the 2004–12 period.

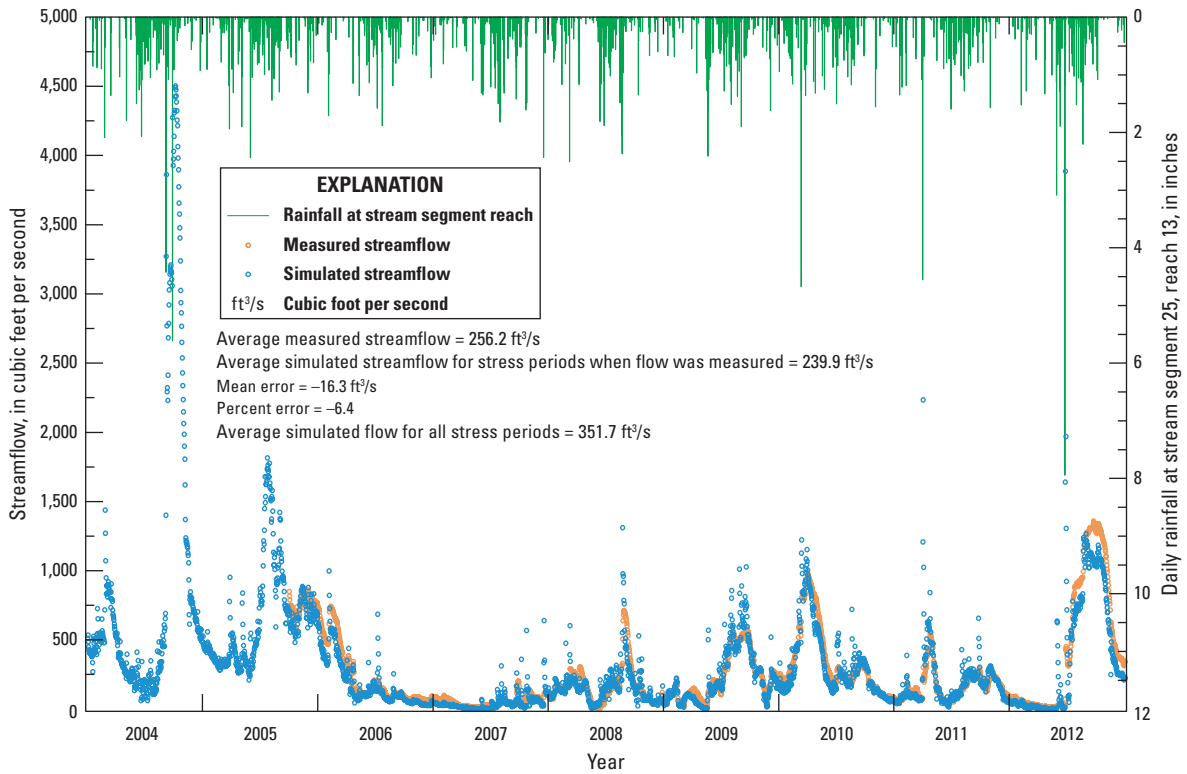

Figure 1.60 Measured and simulated flows at streamflow-gaging station number 02312722, Withlacoochee River near Rutland, and daily rainfall at streamgage, for the 2004–12 period.

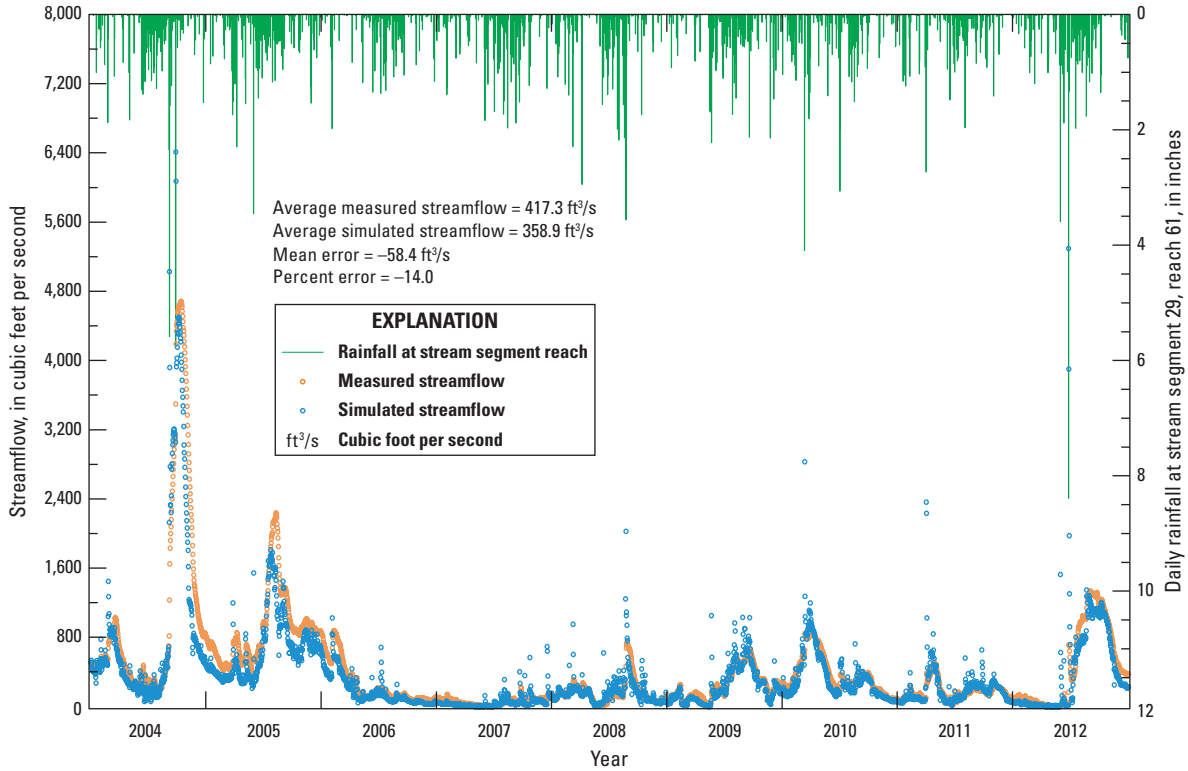

Figure 1.61 Measured and simulated flows at streamflow-gaging station number 02312762, Withlacoochee River near Inverness, and daily rainfall at streamgage, for the 2004–12 period.

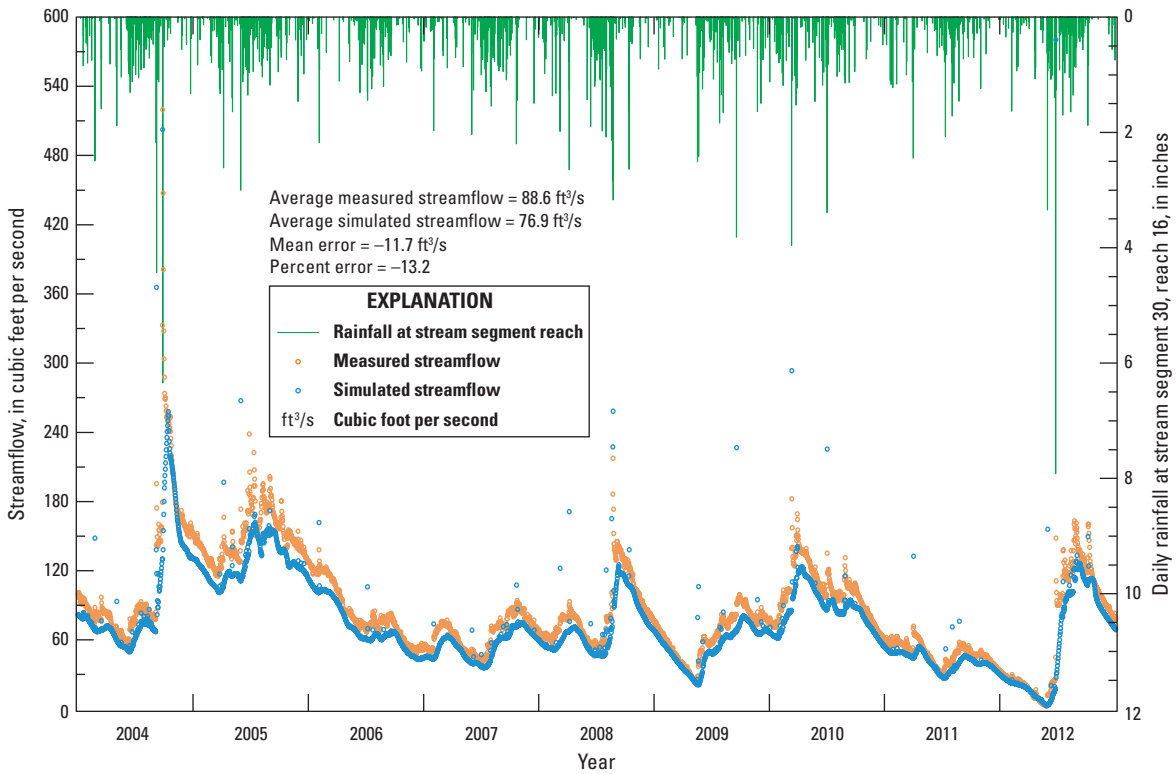

Figure 1.62 Measured and simulated flows at streamflow-gaging station number 02312764, Gum Springs near Holder, and daily rainfall at streamgage, for the 2004–12 period.

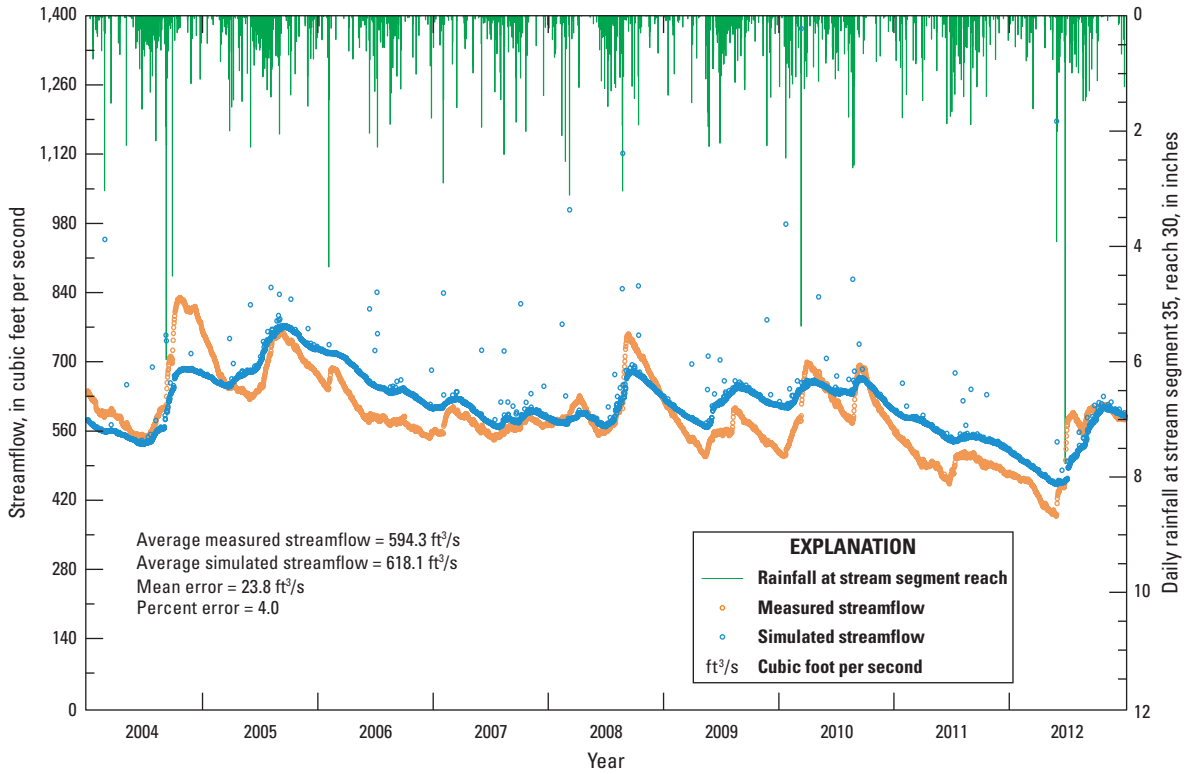

Figure 1.63 Measured and simulated flows at streamflow-gaging station number 02313100, Rainbow River at Dunnellon, and daily rainfall at streamgage, for the 2004–12 period.

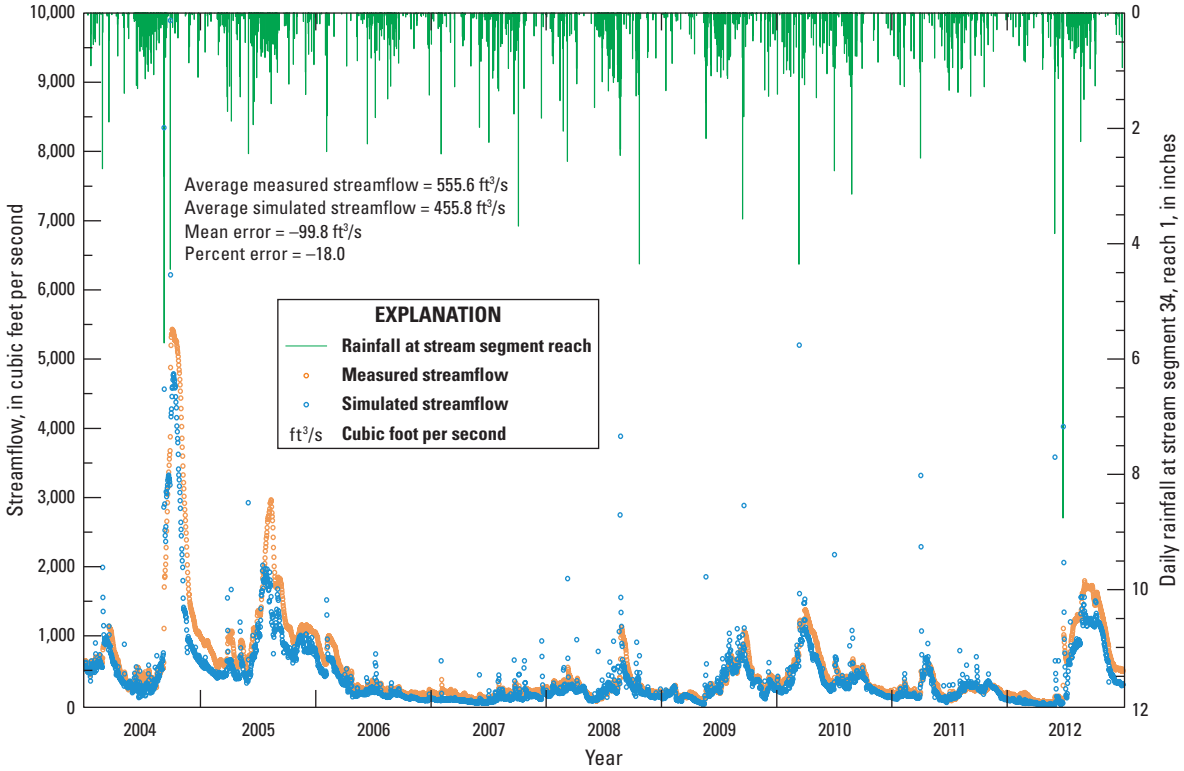

Figure 1.64 Measured and simulated flows at streamflow-gaging station number 02313000, Withlacoochee River near Holder, and daily rainfall at streamgage, for the 2004–12 period.

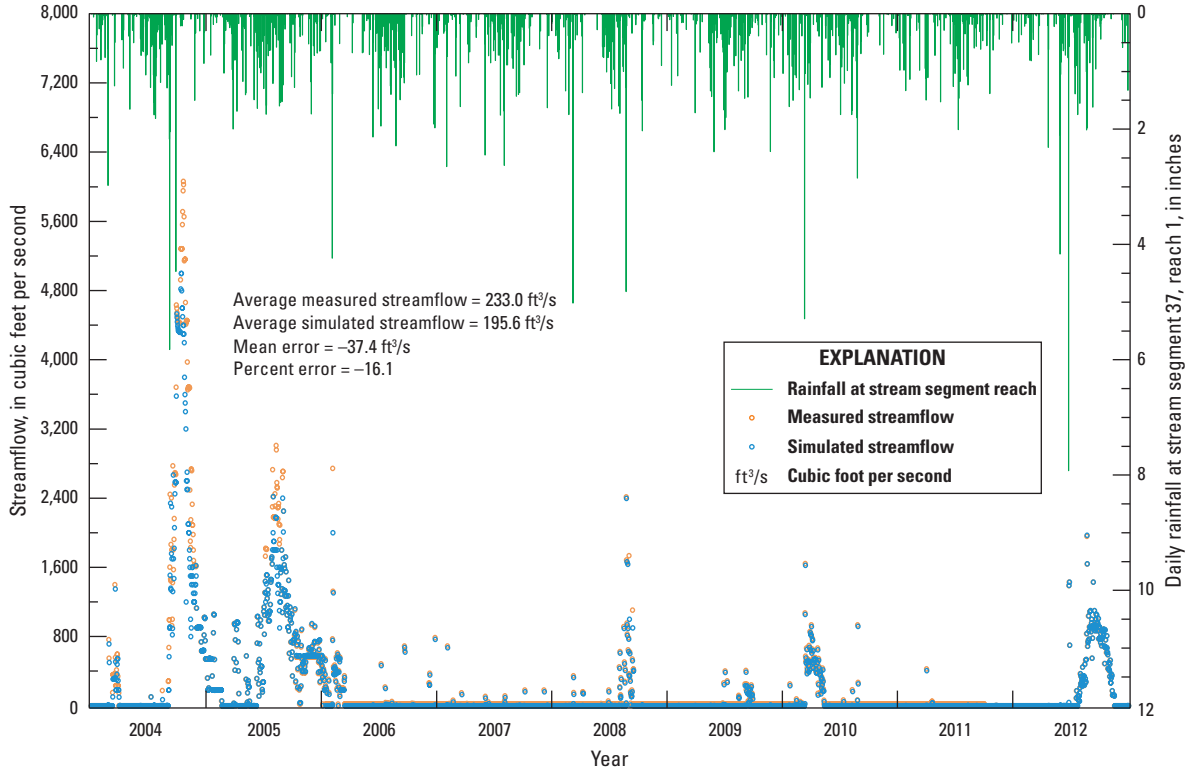

Figure 1.65 Measured and simulated flows at streamflow-gaging station number 02313230, Withlacoochee River at Inglis Dam, and daily rainfall at streamgage, for the 2004–12 period.

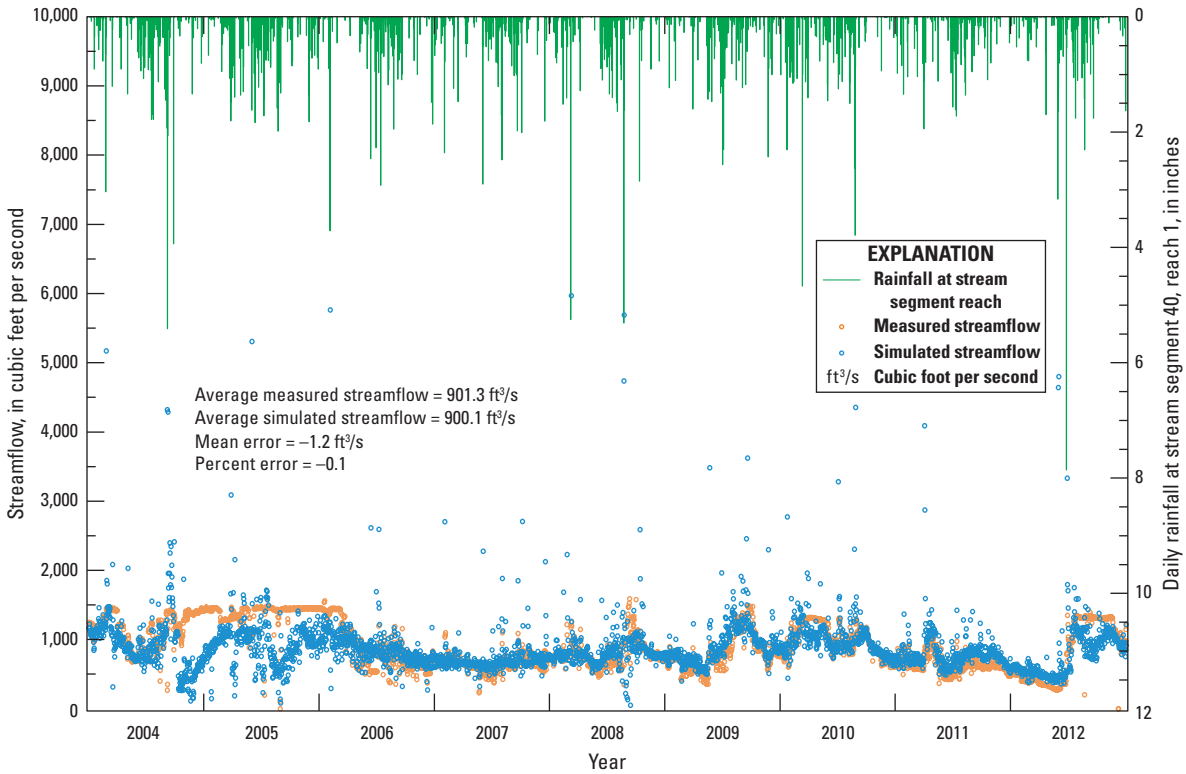

Figure 1.66 Measured and simulated flows at streamflow-gaging station number 02313250, Withlacoochee River Bypass Spillway, and daily rainfall at streamgage, for the 2004–12 period.

transient flow simulation. Simulated net recharge rates to the surficial aquifer cells underlain by the upper confining unit had an overall average of 8.0 in/yr for the 2004–12 simulation period (table 1.15). The net recharge rates in the surficial aquifer cells underlain by the Upper Floridan aquifer had an overall average of 11.3 in/yr (table 1.16). Annual average recharge to the surficial aquifer ranged from 3.8 to 14.2 in/yr, with an overall annual average of 10.3 in/yr (table 1.6). The sum of infiltration and ET rates in the unsaturated zone is not necessarily equal to the recharge routed to the surficial aquifer (UZINF1 plus UZET1 is not equal to UZRCH1 [table 1.15], and UZINF2 plus UZET2 is not equal to UZRCH2 [table 1.16]). Sometimes, not all infiltration from a given year is routed to the surficial aquifer by the end of that year, or some infiltration from one year is routed as recharge to the surficial aquifer during the following year because of water storage in the unsaturated zone.

The average net downward leakage rate, for the 2004–12 period, to the Upper Floridan aquifer (layer 3) from either the surficial aquifer or upper confining unit exceeded, in magnitude, the average total flow from Upper Floridan aquifer springs (FLOW3 is greater than the absolute value of DRAIN3 in table 1.16). There were no substantial changes in storage in the Upper Floridan aquifer during the simulation period, implying that the net downward leakage rate to the Upper Floridan aquifer is nearly equal to the sum of groundwater withdrawals, spring flow, and flow through the lateral boundaries (table 1.16).

A water budget for the entire flow model area, including all layers, is calculated by considering inflows and outflows, from 2004 to 2012, in a newly defined control volume, namely one that includes from land surface to the Upper Floridan aquifer. The largest component of the water budget for the model area is rainfall, with an annual average of 51.7 in/yr from 2004 to 2012 (table 1.17). Total ET, which includes ET in the unsaturated zone, in groundwater, in lakes and streams, and surface leakage to consider the water evaporated in land depressions, was 33.6 in/yr (table 1.17) or 65 percent of rainfall. The simulated fraction of rainfall lost to ET agrees well with estimates for Citrus County by Sanford and Selnick (2013), where they estimated the fraction to range between 0.6 and 0.69. Total annual surface runoff simulated at active cells that do not drain to a simulated lake or stream was the largest during 2004 and 2012, years when several large rainfall events from hurricanes and storms occurred in the model area. In comparison, the average annual surface runoff not drained to a simulated lake or stream was larger than the average annual simulated spring flow for the model area (table 1.17).

Discussion

The hydraulic properties of the surficial aquifer and of the underlying Upper Floridan aquifer within the Tsala Apopka Lake Basin, together with the lakebed leakance of the three main Tsala Apopka Lake pools, are the calibrated

Table 1.14. Simulated annual total inflows and outflows in several lakes in the model area, from 2004 to 2012.

[All linear volumetric flow rates are total annual rates, in inches per year. Lake areas were used to convert simulated output in cubic feet per day to inches per year. RAIN, rainfall into the lake, averaged over lake cells; EVAP, evapotranspiration loss simulated in the lake, averaged over lake cells; LKROFF, surface-water runoff into the lake from reverse flow through the flow-control structure; UZFROFF, simulated surface runoff into the lake as calculated by UZF1 Package; GWIN, groundwater inflow to the lake from the surficial aquifer; GWOUT, groundwater flow out of the lake into the surficial aquifer; SWIN, simulated surface-water inflow into the lake or calculated from water balance for Lake Panasoffkee; SWOUT, surface-water outflow from the lake into a stream or channel; NETFLOW, total net flow for the lake for the year, with a negative (or positive) value indicating a flow loss (or gain), respectively. Ave, average rate for the 2004 to 2012 simulation period]

Floral City pool									
Year	**RAIN**	**EVAP**	**LKROFF**	**UZFROFF**	**GWIN**	**GWOUT**	**SWIN**	**SWOUT**	**NETFLOW**
2004	55.46	54.98	0.00	17.92	0.00	23.28	51.03	38.91	7.24
2005	54.93	57.06	0.00	6.66	0.00	22.82	6.90	4.60	-15.99
2006	37.65	63.65	0.00	3.37	0.00	10.49	0.79	0.00	-32.33
2007	51.61	61.45	0.00	5.14	0.01	5.90	11.55	0.00	0.96
2008	49.78	59.93	0.00	5.84	0.00	10.50	29.74	24.98	-10.05
2009	52.00	60.14	0.00	4.21	0.00	11.81	58.68	43.07	-0.13
2010	48.54	59.52	0.00	6.52	0.00	14.55	65.21	55.90	-9.70
2011	52.63	60.39	0.00	10.85	0.00	11.98	45.25	32.47	3.89
2012	55.87	56.80	0.00	15.56	0.00	26.24	144.88	86.41	46.86
Ave	**50.94**	**59.32**	**0.00**	**8.45**	**0.00**	**15.29**	**46.00**	**31.82**	**-1.03**

Inverness pool									
Year	**RAIN**	**EVAP**	**LKROFF**	**UZFROFF**	**GWIN**	**GWOUT**	**SWIN**	**SWOUT**	**NETFLOW**
2004	58.39	54.28	0.00	16.57	0.00	22.48	34.65	17.84	15.01
2005	56.94	56.38	0.00	5.88	0.12	20.84	4.09	12.78	-22.97
2006	36.57	62.92	0.00	2.14	0.05	10.05	0.00	0.00	-34.21
2007	44.70	60.91	0.00	2.76	0.18	4.53	0.00	0.00	-17.80
2008	52.98	59.44	0.00	7.89	0.18	7.89	22.24	0.00	15.96
2009	48.66	59.77	0.00	3.76	0.08	9.36	38.36	28.21	-6.48
2010	48.69	59.00	0.00	6.16	0.03	17.64	49.78	14.72	13.30
2011	48.92	60.05	0.00	6.50	0.00	16.97	28.92	11.08	-3.76
2012	57.38	56.75	0.00	15.08	0.00	23.25	76.95	41.01	28.40
Ave	**50.36**	**58.83**	**0.00**	**7.42**	**0.07**	**14.78**	**28.33**	**13.96**	**-1.39**

Hernando pool									
Year	**RAIN**	**EVAP**	**LKROFF**	**UZFROFF**	**GWIN**	**GWOUT**	**SWIN**	**SWOUT**	**NETFLOW**
2004	57.37	53.82	9.66	9.63	0.00	11.46	11.86	20.28	2.96
2005	58.92	55.75	0.00	3.33	0.17	8.45	7.68	20.26	-14.36
2006	38.38	62.35	0.00	1.66	0.04	4.54	0.00	0.00	-26.81
2007	46.90	60.50	0.00	2.73	0.01	2.69	0.00	0.02	-13.57
2008	58.39	58.73	0.00	6.77	0.32	2.31	0.00	0.00	4.44
2009	53.04	59.41	0.00	2.62	0.17	3.32	18.75	0.00	11.85
2010	52.11	58.16	0.00	5.37	0.01	7.51	9.78	0.00	1.60
2011	43.58	59.27	0.00	1.96	0.01	5.90	7.36	0.00	-12.26
2012	61.17	56.22	0.00	10.93	0.00	9.54	26.80	1.27	31.87
Ave	**52.21**	**58.25**	**1.07**	**5.00**	**0.08**	**6.19**	**9.14**	**4.65**	**-1.59**

Table 1.14. Simulated annual inflows and outflows in the main pools and lakes of the model area, from 2004 to 2012.—Continued

[All linear volumetric flow rates are total annual rates, in inches per year. Drainage areas of lakes or pools were used to convert simulated output in cubic feet per day to inches per year. RAIN, rainfall into the pool or lake, averaged over pool or lake cells; EVAP, evapotranspiration loss simulated in the pool or lake, averaged over pool or lake cells; LKROFF, surface-water runoff into the pool or lake from reverse flow through the flow-control structure; UZFROFF, simulated surface runoff into the pool or lake as calculated by UZF1 Package; GWIN, groundwater inflow to the pool or lake from the surficial aquifer; GWOUT, groundwater flow out of the pool or lake into the surficial aquifer; SWIN, surface-water inflow into the pool or lake or as calculated from water balance; SWOUT, surface-water outflow from the pool or lake into a stream or channel; NETFLOW, total net flow for the pool or lake for the year, with a negative (or positive) value indicating a flow loss (or gain), respectively. Ave, average rate for the 2004 to 2012 simulation period]

Lake Panasoffkee									
Year	**RAIN**	**EVAP**	**LKROFF**	**UZFROFF**	**GWIN**	**GWOUT**	**SWIN**	**SWOUT**	**NETFLOW**
2004	54.73	52.73	0.00	0.00	5.69	0.44	509.75	507.92	9.08
2005	52.72	54.52	0.00	0.00	6.29	0.00	527.23	540.37	-8.65
2006	37.10	60.83	0.00	0.00	8.51	0.00	204.42	219.03	-29.83
2007	44.43	58.77	0.00	0.00	8.03	0.00	97.17	63.08	27.78
2008	53.85	57.07	0.00	0.00	6.26	0.01	294.32	301.44	-4.09
2009	52.47	58.04	0.00	0.00	8.56	0.00	252.32	264.55	-9.24
2010	44.60	56.79	0.00	0.00	10.25	0.00	303.08	312.40	-11.26
2011	47.31	57.44	0.00	0.00	8.86	0.00	139.08	133.97	3.84
2012	50.19	54.56	0.00	0.00	8.04	0.00	223.87	221.30	6.24
Ave	**48.60**	**56.75**	**0.00**	**0.00**	**7.83**	**0.05**	**283.47**	**284.90**	**-1.79**

Wysong structure									
Year	**RAIN**	**EVAP**	**LKROFF**	**UZFROFF**	**GWIN**	**GWOUT**	**SWIN**	**SWOUT**	**NETFLOW**
2004	57.83	43.63	0.00	15.59	0.01	0.08	3,633.75	3,656.47	7.00
2005	53.16	45.60	0.00	7.20	0.01	0.06	2,559.93	2,573.86	0.78
2006	34.73	50.70	0.00	2.38	0.12	0.02	700.58	713.59	-26.50
2007	43.58	48.81	0.00	3.29	0.12	0.01	191.92	179.38	10.71
2008	49.96	47.48	0.00	7.56	0.00	0.08	616.48	628.78	-2.34
2009	49.86	48.25	0.00	6.50	0.04	0.03	887.74	903.24	-7.38
2010	46.55	47.13	0.00	7.35	0.08	0.01	1,255.08	1,270.67	-8.75
2011	48.22	47.68	0.00	5.80	0.04	0.02	739.28	742.44	3.20
2012	47.57	45.18	0.00	7.70	0.01	0.05	1,576.54	1,581.22	5.37
Ave	**47.94**	**47.16**	**0.00**	**7.04**	**0.05**	**0.04**	**1,351.26**	**1,361.07**	**-1.99**

Lake Rousseau									
Year	**RAIN**	**EVAP**	**LKROFF**	**UZFROFF**	**GWIN**	**GWOUT**	**SWIN**	**SWOUT**	**NETFLOW**
2004	61.95	53.98	0.00	14.08	0.00	3.90	1,396.64	1,410.71	4.08
2005	64.22	55.98	0.00	5.97	0.00	4.10	1,253.73	1,257.94	5.90
2006	50.97	62.20	0.00	7.83	0.00	4.18	762.80	762.77	-7.55
2007	51.91	60.96	0.00	6.86	0.00	4.21	588.75	588.55	-6.20
2008	57.18	58.42	0.00	11.27	0.00	4.22	738.66	745.40	-0.93
2009	51.64	59.00	0.00	5.81	0.00	4.29	756.99	756.22	-5.07
2010	57.75	57.66	0.00	10.56	0.00	4.29	901.85	907.36	0.85
2011	43.33	59.07	0.00	3.09	0.00	4.43	653.71	647.05	-10.42
2012	55.11	56.20	0.00	13.82	0.00	4.36	865.80	875.16	-0.99
Ave	**54.90**	**58.16**	**0.00**	**8.81**	**0.00**	**4.22**	**879.88**	**883.46**	**-2.26**

Table 1.15. Simulated annual inflows and outflows in the surficial aquifer underlain by the upper confining unit, layer 1, from 2004 to 2012.

[All linear volumetric flow rates are total annual rates in inches per year, averaged over active cells in layer 1, 2004 to 2012. Negative (or positive) rates indicate flows leaving (or entering) the unsaturated flow zone or surficial aquifer. STOR1, amount of water from storage to/from the surficial aquifer; GHB1, net flow through the lateral boundaries of the surficial aquifer; UZET1, evapotranspiration loss rate in the unsaturated flow zone overlying the surficial aquifer in layer 1; UZINF1, infiltration rate, from rainfall rates, in the unsaturated flow zone overlying layer 1; GWET1, evapotranspiration loss rate in the surficial aquifer; UZRCH1, routed recharge to the unsaturated zone; SULEAK1, surface leakage occurring at land surface depressions; FLOW1, net downward flow to the upper confining unit; RECH1, recharge rate to the surficial aquifer, equal to UZRCH1+SULEAK1+GWET1; Ave, average for the 2004 to 2012 simulation period. Water balance in the surficial aquifer is established by the equation STOR1+GHB1+GWET1+UZRCH1+SULEAK1+FLOW1=0]

Year	STOR1	GHB1	UZET1	UZINF1	GWET1	UZRCH1	SULEAK1	FLOW1	RECH1
2004	1.96	0.15	-20.48	47.93	-12.68	25.95	-5.57	-9.81	7.70
2005	-1.03	0.12	-23.50	51.59	-13.32	27.96	-4.89	-8.84	9.75
2006	7.73	0.13	-21.87	32.93	-9.15	10.70	-0.80	-8.61	0.75
2007	1.64	0.14	-25.74	39.74	-6.61	14.56	-0.71	-9.02	7.24
2008	-1.52	0.15	-23.55	42.44	-8.34	19.91	-1.08	-9.12	10.49
2009	-2.15	0.16	-23.22	46.42	-9.20	22.47	-1.58	-9.70	11.69
2010	1.29	0.14	-22.55	42.23	-11.11	20.86	-2.42	-8.76	7.33
2011	0.39	0.17	-22.67	40.60	-8.76	18.07	-1.65	-8.22	7.66
2012	-1.94	0.17	-21.94	43.48	-8.53	20.80	-2.52	-7.98	9.75
Ave	**0.71**	**0.15**	**-22.84**	**43.04**	**-9.74**	**20.14**	**-2.36**	**-8.90**	**8.04**

parameters that largely determine pool stages, aquifer water levels, and the mostly downward flow from the pools. These hydraulic properties have been documented in previous simulation results (HydroGeoLogic, 2013), and the results presented herein were calibrated using measured water levels and measured flows through structures within the Tsala Apopka Lake Basin. Measured groundwater-level data inside the Tsala Apopka Lake Basin are available only after 2011, precluding a thorough calibration to hydrologic conditions before 2011. An attempt was made to estimate water-level data for 2004 hydrologic conditions using 2011 and 2012 measured groundwater data and linear regression. Although the regression coefficients generated for each day of 2004 were all greater than 0.97, small errors in estimated water levels at wells within the Tsala Apopka Lake Basin could result in large residuals after 2004, particularly when hydrologic conditions after 2004 were substantially different from average 2004 conditions.

Further calibration of hydraulic parameters at pilot points in the immediate vicinity of the Tsala Apopka Lake Basin was required to reduce residuals at nested surficial and Upper Floridan aquifer wells near the Tsala Apopka Lake Basin area. Parameters that had been calibrated to 2004 conditions in the Tsala Apopka Lake Basin had to be changed to further reduce pool stage residuals by (1) increasing hydraulic conductivity to decrease simulated heads in the Upper Floridan aquifer, and (2) increasing lakebed leakances to increase downward leakage.

Calibration of simulated recharge rates was achieved by routing infiltration in the unsaturated zone at deep water-table cells with saturated vertical hydraulic conductivity values that were updated through manual calibration. The time that infiltration takes to arrive to deep water-table cells can be estimated at sites where there are measured water levels at surficial aquifer wells. At these sites, the calibrated value of VKS was obtained by systematically reducing the residuals in surficial aquifer well levels. The infiltration routing through the unsaturated flow zone was performed at all water-table cells, and such simulation substantially increased the running times during calibration.

Model Sensitivity

The model calibration was performed using the highly parametrized inversion techniques in PEST. An integral part of the calibration process was the calculation of composite sensitivities for each model parameter. Composite parameter sensitivities, which help identify sensitive model parameters (Doherty, 2013a), are normalized to allow comparison of each parameter's contribution during each iteration to minimize the objective function defined by equation 1.3. The most sensitive parameters are the specific yield of the surficial aquifer, the horizontal hydraulic conductivity values in the Upper Floridan aquifer at several pilot points, and the vertical hydraulic conductivity of the surficial aquifer and upper confining unit at the pilot point of row 360 and column 70 (fig. 1.4, table 1.18). Most of the remaining parameters having high composite normalized sensitivities were pilot points in the Upper Floridan aquifer. These composite normalized sensitivities reflect the spatial distribution of measured heads in the surficial aquifer, and a more spatially even distribution of measured heads in the surficial aquifer would certainly have provided a somewhat different set of sensitivity values.

Table 1.16. Simulated annual inflows and outflows in layer 2 and the Upper Floridan aquifer (layer 3), from 2004 to 2012.

[All linear volumetric flow rates are total annual rates, in inches per year, averaged over all active cells in layer 2 or Upper Floridan aquifer (layer 3). STOR2, STOR3, flow rates from storage to/from layer 2 and the Upper Floridan aquifer, respectively; GHB2, GHB3, net flow through the lateral boundaries of layer 2 and the Upper Floridan aquifer, respectively; STRM2, seepage from the surficial aquifer to the streams; LKSEEP2, seepage from the lakes to the surficial aquifer; UZET2, evapotranspiration loss rate in the unsaturated zone overlying the surficial aquifer in layer 2; UZINF2, infiltration rate, from rainfall rates, in the unsaturated flow zone overlying layer 2; GWET2, groundwater loss to evapotranspiration in layer 2; UZRCH2, UZRCH3, routed recharge through the unsaturated zone to the surficial aquifer and to the Upper Floridan aquifer, respectively; SULEAK2, SULEAK3, surface leakage occurring at land surface depressions from surficial aquifer and Upper Floridan aquifer, respectively; FLOW2, FLOW3, net downward flow to layer 2 and the Upper Floridan aquifer, respectively; RECH2, recharge rate to the surficial aquifer, equal to UZRCH2 + SULEAK2 + GWET2; water balance in the surficial aquifer is established by the equation STOR2+GHB2+STRM2+LKSEEP2+GWET2+UZRCH2+SULEAK2+FLOW2=0. Ave, average for the 2004 to 2012 simulation period; GWW3, groundwater withdrawals from the Upper Floridan aquifer; DRAIN3, total spring flow leaving the Upper Floridan aquifer. Negative values indicate outflows, whereas positive values indicate inflows. Water balance in the Upper Floridan aquifer is calculated from the equation STOR3+GWW3+DRAIN3+GHB3+FLOW3=0]

Layer 2											
Year	**STOR2**	**GHB2**	**STRM2**	**LKSEEP2**	**UZET2**	**UZINF2**	**GWET2**	**UZRCH2**	**SULEAK2**	**FLOW2**	**RECH2**
2004	-1.98	0.13	-0.01	0.17	-22.54	45.82	-6.27	20.37	-3.41	-9.00	10.69
2005	-4.70	0.10	-0.01	0.15	-24.59	54.40	-9.02	29.26	-4.27	-11.51	15.97
2006	7.06	0.10	-0.01	0.08	-22.05	34.88	-6.32	13.08	-1.79	-12.20	4.97
2007	0.45	0.11	-0.02	0.05	-25.39	41.65	-4.57	16.97	-1.53	-11.46	10.87
2008	-2.46	0.10	-0.01	0.06	-22.46	44.57	-6.39	23.23	-2.49	-12.04	14.35
2009	-0.92	0.11	-0.02	0.07	-23.08	45.47	-6.40	21.50	-2.37	-11.97	12.73
2010	1.15	0.10	-0.01	0.11	-22.13	43.48	-8.19	22.70	-3.23	-12.63	11.28
2011	2.38	0.11	-0.01	0.10	-23.42	41.09	-6.07	17.57	-2.03	-12.05	9.47
2012	-2.14	0.13	-0.01	0.16	-22.50	42.73	-5.53	19.60	-2.41	-9.80	11.66
Ave	**-0.13**	**0.11**	**-0.01**	**0.11**	**-23.13**	**43.79**	**-6.53**	**20.48**	**-2.61**	**-11.41**	**11.33**

Upper Floridan aquifer (layer 3)							
Year	**STOR3**	**GWW3**	**DRAIN3**	**GHB3**	**FLOW3**	**UZRCH3**	**SULEAK3**
2004	0.00	-1.03	-8.07	1.95	6.66	0.66	-0.17
2005	0.00	-0.99	-9.14	0.84	8.52	0.94	-0.17
2006	0.02	-1.19	-7.82	-0.68	9.03	0.78	-0.14
2007	0.00	-1.12	-6.82	-1.14	8.48	0.71	-0.11
2008	0.00	-1.07	-7.64	-0.94	8.91	0.87	-0.13
2009	0.00	-1.05	-7.52	-1.06	8.86	0.95	-0.18
2010	0.00	-0.96	-8.06	-1.14	9.35	0.97	-0.16
2011	0.00	-0.89	-6.86	-1.72	8.92	0.66	-0.11
2012	-0.01	-0.91	-6.82	-0.31	7.26	1.01	-0.22
Ave	**0.00**	**-1.02**	**-7.64**	**-0.47**	**8.44**	**0.84**	**-0.15**

Table 1.17. Simulated annual inflows and outflows in the model area, from 2004 to 2012.

[All linear volumetric flow rates are total annual rates, in inches per year, averaged over all active cells in the model area. RAIN, total annual rainfall over land surface areas that are active in the flow model; STOR, combined flow rates from storage to/from the model layers; GWW3, groundwater withdrawals from the Upper Floridan aquifer; DRAIN3, total spring flow from the Upper Floridan aquifer; GHB, net flow through the lateral boundaries of the model layers; STRM_I, sum of stream flow specified as inflow at stream segment 1, reach 1, specified runoff along stream segment 30 (fig. 1.3) equal to the simulated flow from Gum Springs, and specified runoff along stream segment 35 (fig. 1.3) equal to the simulated flow from Rainbow Springs; STRM_O, sum of simulated stream flows leaving the model area through stream segments 33, 38, 40, and 42 (fig. 1.3); SURFLEAK, surface leakage occurring at land surface depressions from the model layers; ET, sum of evapotranspiration loss rate in the unsaturated zone, groundwater, and lakes; RUNOFF, surface runoff simulated at active grid cells that do not drain to a simulated lake or stream; Ave, average for the 2004 to 2012 simulation period. Negative values indicate outflows, whereas positive values indicate inflows. Water balance in the model area is calculated from the equation RAIN+STOR+GWW3+DRAIN3+GHB+STRM_I+STRM_O+SURFLEAK+ET+RUNOFF=0]

Year	RAIN	STOR	GWW3	DRAIN3	GHB	STRM_I	STRM_O	SURFLEAK	ET	RUNOFF
2004	59.47	-0.98	-1.03	-8.07	2.09	4.57	-5.81	-4.13	-30.51	-15.59
2005	59.34	-3.77	-0.99	-9.14	0.95	4.14	-5.15	-4.60	-35.06	-5.71
2006	38.25	7.25	-1.19	-7.82	-0.57	2.67	-3.11	-1.68	-29.50	-4.30
2007	47.70	0.75	-1.12	-6.82	-1.02	2.15	-2.40	-1.43	-30.85	-6.96
2008	54.43	-2.22	-1.07	-7.64	-0.83	2.33	-3.07	-2.26	-30.04	-9.63
2009	52.18	-1.23	-1.05	-7.52	-0.94	2.60	-3.08	-2.35	-30.65	-7.96
2010	51.01	1.19	-0.96	-8.06	-1.03	3.01	-3.73	-3.18	-31.72	-6.52
2011	47.78	1.88	-0.89	-6.86	-1.59	2.38	-2.61	-2.04	-30.50	-7.54
2012	55.48	-2.10	-0.91	-6.82	-0.17	3.05	-3.61	-2.66	-29.17	-13.10
Ave	**51.74**	**0.08**	**-1.02**	**-7.64**	**-0.35**	**2.99**	**-3.62**	**-2.70**	**-30.89**	**-8.59**

Table 1.18. Calibrated parameters with the highest composite normalized sensitivities in the surface-water/groundwater flow model, calculated using stage, head, spring-flow, and streamflow observations from hydrologic conditions of 2004.

[Group, parameter group name; ROW_COL, row and column grid number; SENS, dimensionless composite normalized sensitivity; upw, parameter group used in the upstream weighting package input file, including specific yield sy1, specific storage ss, and the ratio of horizontal to vertical hydraulic conductivity vka; kh1, kh2, kh3, horizontal hydraulic conductivity of layers 1, 2, and 3, respectively; kz1, kz2, vertical hydraulic conductivity of layers 1 and 2, respectively; stkz, vertical hydraulic conductivity of stream segment; lkbd, lakebed leakance; NA, parameter is either valid for the entire layer or for all cells forming the segment or lake]

Group	Parameter	ROW_COL	SENS	Group	Parameter	ROW_COL	SENS
upw	sy1	NA	0.017014	kh3	kh3_32_363	32_363	0.001654
kh3	kh3_38_120	38_120	0.014111	kh3	kh3_220_30	220_30	0.001625
kz2	kz2_360_70	360_70	0.012828	kh3	kh3_170_369	170_369	0.001613
kh3	kh3_360_120	360_120	0.011705	kh2	kh2_366_170	366_170	0.001613
kz1	kz1_360_70	360_70	0.011691	kh2	kh2_170_320	170_320	0.001608
kh3	kh3_354_70	354_70	0.011683	kh2	kh2_70_120	70_120	0.001435
kh3	kh3_358_38	358_38	0.011653	kz1	kz1_354_270	354_270	0.001429
kh3	kh3_38_357	38_357	0.010934	kh3	kh3_32_30	32_30	0.001425
upw	vka_ufa	NA	0.008381	kz2	kz2_120_369	120_369	0.001396
kh1	kh1_360_70	360_70	0.008377	kh3	kh3_348_17	348_17	0.001290
kz2	kz2_358_38	358_38	0.008353	kh3	kh3_354_320	354_320	0.001287
kh2	kh2_360_70	360_70	0.008327	kh3	kh3_360_170	360_170	0.001264
kh1	kh1_360_120	360_120	0.008324	kz2	kz2_366_320	366_320	0.001241
kh3	kh3_38_363	38_363	0.003934	kh3	kh3_120_23	120_23	0.001237
kh3	kh3_348_23	348_23	0.003793	kh3	kh3_270_220	270_220	0.001224
kh3	kh3_32_357	32_357	0.003273	upw	ss_ufa	NA	0.001179
kh3	kh3_38_170	38_170	0.002604	stkz	stkzseg31	NA	0.001096
kh3	kh3_58_143	58_143	0.001789	lkbd	lkbd14	NA	0.001025
kh3	kh3_354_23	354_23	0.001768	stkz	stkzseg30	NA	0.001017

References Cited in Appendix 1

Doherty, J., 2008, Groundwater data utilities: Brisbane, Australia, Watermark Numerical Computing.

Doherty, J., 2013a, PEST, Model-independent parameter estimation—User manual (8th ed., with minor revisions): Brisbane, Australia, Watermark Numerical Computing.

Doherty, J., 2013b, Addendum to the PEST manual: Brisbane, Australia, Watermark Numerical Computing.

Doherty, J.E., and Hunt, R.J., 2010, Approaches to highly parameterized inversion—A guide to using PEST for groundwater model calibration: Scientific Investigations Report 2010–5169, 59 p.

Domenico, P.A., 1972, Concepts and models in groundwater hydrology: New York, New York, McGraw-Hill, 405 p.

HydroGeoLogic, 2013, Northern District Groundwater Flow Model, v 4.0: Brooksville, Southwest Florida Water Management District, St Johns Water Management District, Marion County, and the Withlacoochee River Water Supply Authority, 755 p.

Kuniansky, E.L., Gomez-Gomez, F., and Torres-Gonzalez, S., 2003, Effects of aquifer development and changes in irrigation practices on ground-water availability in the Santa Isabel area, Puerto Rico: U.S. Geological Survey Water-Resources Investigations Report 03–4303, 56 p.

McBride, W.S., Metz, P.A., Ryan, P.J., Fulkerson, Mark, and Downing, H.C., 2017, Groundwater levels, geochemistry, and water budget of the Tsala Apopka Lake system, west-central Florida, 2004–12: U.S. Geological Survey Scientific Investigations Report 2017–5132, 100 p., https://doi.org/10.3133/sir20175132.

Merritt, M.L., and Konikow, L.F., 2000, Documentation of a computer program to simulate lake-aquifer interaction using the MODFLOW ground-water flow model and the MOC3D solute-transport model: U.S. Geological Survey Water-Resources Investigations Report 00–4167, 146 p.

Niswonger, R.G., Panday, Sorab, and Ibaraki, Motomu, 2011, MODFLOW-NWT, A Newton formulation for MODFLOW-2005: U.S. Geological Survey Techniques and Methods, book 6, chap. A37, 44 p., accessed June 8, 2016, at http://water.usgs.gov/ogw/modflow-nwt/.

Niswonger, R.G., and Prudic, D.E., 2006, Documentation of the Streamflow-Routing (SFR2) Package to include unsaturated flow beneath streams—A modification to SFR1: U.S. Geological Survey Techniques and Methods, book 6, chap. A13, 48 p.

Niswonger, R.G., Prudic, D.E., and Regan, S., 2006, Documentation of the Unsaturated-Zone Flow (UZF1) Package for modeling unsaturated flow between the land surface and the water table with MODFLOW-2005: U.S. Geological Survey Techniques and Methods, book 6, chap. A19, 62 p.

Prudic, D.E., and Niswonger, R.G., 2006, Revisions to the U.S. Geological Survey's MODFLOW Lake Package for simulation of groundwater interactions with lakes: American Geophysical Union Fall Meeting Abstract, December 2006.

Sanford, W.E., and Selnick, D.L., 2013, Estimation of evapotranspiration across the conterminous United States using a regression with climate and land-cover data: Journal of the American Water Resources Association (JAWRA), v. 49, no. 1, p. 217–230, https://doi.org/10.1111/jawr.12010.

Shah, N., Nachabe, M., and Ross, M., 2007, Extinction depth and evapotranspiration from ground water under land covers: Ground Water, v. 45, no. 3, p. 329–338.

Snyder, J.P., 1983, Map projections used by the U.S. Geological Survey: U.S. Geological Survey Bulletin B–1532, 313 p.

Prepared by the Lafayette Publishing Service Center

For more information about this publication, contact
Director, Caribbean-Florida Water Science Center
U.S. Geological Survey
4446 Pet Lane, Suite 108
Lutz, FL 33559
(813) 498-5000

For additional information visit
https://www2.usgs.gov/water/caribbeanflorida/index.html

Sepúlveda and others—**Effects of Surface-Water and Groundwater Inflows and Outflows on Tsala Apopka Lake Basin Hydrology**—Scientific Investigations Report 2018–5055

ISSN 2328-0328 (online)
https://doi.org/10.3133/sir20185055